This handbook marks the first formal publication of a long-lived and highly-esteemed reference in the Air Force Weather community; it is a new publication, derived from the legacy Field Operating Agency Technical Note 98/002, *Meteorological Techniques,* and supersedes all existing iterations of the legacy document. The transition from informal tech note to formal Air Force Handbook will enable the Air Force to host it in the same location as other 15-series publications, allow for more frequent updates, and will ensure appropriate review and approval of the processes and procedures contained in the document. The handbook, when used with relevant data and additional Air Force guidance, provides general guidance for effective meteorological techniques for a variety of parameters. It is not a substitute for sound judgement and situationally relevant meteorological reasoning. Refer recommended changes and questions about this publication to the Office of Primary Responsibility listed above using the Air Force Form 847, *Recommendation for Change of Publication*; route AF Forms 847 from the field through the appropriate chain of command. Ensure that all records created as a result of processes prescribed in this publication are maintained in accordance with Air Force Manual 33-363, *Management of Records*, and disposed of in accordance with Air Force Records Information Management System Records Disposition Schedule. The use of the name or mark of any specific manufacturer, commercial product, commodity, or service in this publication does not imply endorsement by the Air Force.

SUMMARY OF CHANGES

The document has been substantially revised and should be completely reviewed. The legacy 98/002 tech note has been updated several times over the twenty years since its initial publication,

and this Handbook was created based upon the 2012 tech note revision as a starting point. While the table of contents and list of topics will be familiar to anyone who has used the legacy technical note, numerous techniques were updated to reflect advanced processes and procedures, and many illustrations and figures were modernized with improved graphics and pictures.

Chapter 1

SURFACE WEATHER ELEMENTS

1.1. Visibility.   The American Meteorological Society defines visibility as "The greatest distance in a given direction at which it is just possible to see and identify with the unaided eye, (1) in the daytime, a prominent dark object against the sky at the horizon, or (2) at night, a known, preferably unfocused, moderately intense light source." Forecasting visibility is a challenge due to the difficulty in predicting the complicated behavior of "dry" and "moist" (both liquid and solid) airborne particles that obstruct or reduce visual range. Basic overviews of dry obstructions (lithometeors) and moist obstructions (hydrometeors) are provided below, followed by more concentrated analyses of individual obstructions.

1.1.1. Dry Obstructions (Lithometeors).   A lithometeor is the general term for particles suspended in a dry atmosphere; these include haze, smoke, dust, and sand.

1.1.1.1. *Haze.* Haze is an accumulation of very fine dust or salt particles in the atmosphere; it does not block light, but instead causes light rays to scatter. Haze particles produce a bluish color when viewed against a dark background, but look yellowish when viewed against a lighter background. This light-scattering phenomenon (called Mie scattering) also causes the visual ranges within a uniformly dense layer of haze to vary depending on whether the observer is looking into the sun or away from it. Typically, haze occurs under a stable atmospheric layer and significantly effects visibility. In general, industrial areas and coastal areas are most conducive to haze formation.

1.1.1.2. *Smoke.* Smoke is usually more localized than other visibility restrictions. Accurate visibility forecasts depend on detailed knowledge of the local terrain, surface wind patterns, and smoke sources (including schedules of operation of smoke generating activities).

1.1.1.3. *Blowing Dust and Sand.* Windblown particles such as blowing dust and sand can cause serious local restrictions to visibility, often reducing visibility to near zero. The critical wind speed for lifting dust and sand varies according to vegetation, soil type, and soil moisture. Specific forecasting rules vary by station and time of year; local references and procedures should document the wind speeds, directions, and surface moisture conditions in which visibility restrictions are most likely to occur.
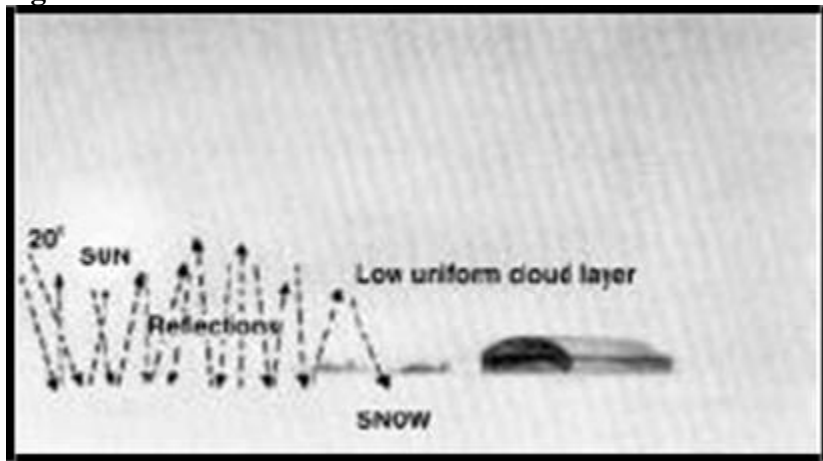
1.1.2. Moist Obstructions (Hydrometeors). Condensation or sublimation of atmospheric water vapor produces a hydrometeor. These particles form either in the free atmosphere or at the earth's surface, and include frozen water lifted by the wind. Hydrometeors that cause surface visibility reductions generally fall into two categories:

1.1.2.1. *Precipitation.* Precipitation refers to all forms of water particles, both liquid and solid, which fall from the atmosphere and reach the ground; these include: liquid precipitation (drizzle and rain), freezing precipitation (freezing drizzle and freezing rain), and solid (frozen) precipitation (ice pellets, hail, snow, snow pellets, snow grains, and ice crystals).

1.1.2.2. *Suspended (Liquid or Solid) Water Particles.* Liquid or solid water particles that form and remain suspended in the air (damp haze, cloud, fog, ice fog, and mist), as well as liquid or solid water particles that are lifted by the wind from the earth's surface (drifting snow, blowing snow, blowing spray) cause restrictions to visibility. One of the more unusual causes of reduced visibility due to suspended water/ice particles is whiteout, while the most common cause is fog.

1.1.2.2.1. Whiteout Conditions. Whiteout is a visibility-restricting phenomenon that occurs when a uniformly overcast layer of clouds overlies a snow- or ice-covered surface. Most whiteouts occur when the cloud deck is relatively low and the sun angle is at about 20° above the horizon. Cloud layers break up and diffuse parallel rays from the sun so that they strike the snow surface from many angles (**Figure 1.1**). This diffused light reflects back and forth between the snow and clouds until the amount of light coming through the clouds equals the amount reflected off the snow, completely eliminating shadows. The result is a loss of depth perception and an inability to distinguish the boundary between the ground and the sky (i.e., there is no horizon). Low-level flights and landings in these conditions become very dangerous.

Figure 1.1. Whiteout Conditions.

1.1.2.2.2. Fog. Fog is often described as "a stratus cloud resting near the ground." Fog forms when the temperature and dew point of the air approach the same value, either through cooling of the air (producing advection, radiation, steam, or upslope fog) or by adding enough moisture to raise the dew point (frontal fog). When composed of ice crystals, it is called ice fog.

1.1.2.2.2.1. Advection Fog. Advection Fog forms due to moist air moving over a colder surface, and the resulting cooling of the near-surface air to below its dew-point temperature. Advection fog can occur over both water and land.

1.1.2.2.2.2. Radiation Fog. Also called ground or valley fog, this type of fog is produced by radiational cooling. Under stable nighttime conditions, long-wave radiation is emitted by, and cools, the ground, forming a temperature inversion. In turn, moist air near the ground cools to its dew point. Depending on the moisture content of the ground, moisture may evaporate into the air, raising the dew point of this stable layer, accelerating radiation fog formation.

1.1.2.2.2.3. Upslope Fog. Upslope fog occurs when sloping terrain lifts air, cooling it adiabatically to its dew point and saturation. Upslope fog may be viewed as either a stratus cloud or fog, depending on the point of reference of the observer. Upslope fog generally forms at higher elevations and builds downward into valleys. This fog can maintain itself at higher wind speeds because of increased lift and adiabatic cooling. Upslope winds more than 10 to 12 knots usually result in stratus rather than fog. The eastern slope of the Rocky Mountains is a prime location for this type of fog.

1.1.2.2.2.4. Frontal Fog. Associated with frontal zones and frontal passages, this type of fog can be divided into types: warm-front pre-frontal fog; cold-front post-frontal fog; and front-passage fog. Pre- and post-frontal fogs are caused by rain falling into cold stable air and raising the dew point. Frontal-passage fog can occur in a number of situations, such as when warm and cold air masses, each near saturation, are mixed by very light winds in the frontal zone. It can occur when relatively warm air is suddenly cooled over moist ground with the passage of a well-marked precipitation cold front. It can also occur during low-latitude summer, where evaporation of front-passage rain water cools the surface and overlying air enough to add sufficient moisture to form fog.

1.1.2.2.2.5. Ice Fog. Ice fog is composed of ice crystals rather than water droplets and forms in extremely cold, arctic air (–29°C (–20°F) and colder). Factors contributing to reduced visibility associated with ice fog are temperature, time of day, water vapor availability, and pollutants. Burning hydrocarbon fuels, steam vents, motor vehicle exhausts, and jet exhausts are major sources of water vapor and pollutants that help to produce ice fog. A strong low-level inversion contributes to ice fog formation by trappingand concentrating the moisture in a shallow layer. Once ice fog forms, it usually persists until the temperature rises or there is an air mass change.

1.1.2.2.2.6. Sublimation Fog. The Glossary of Meteorology defines sublimation as the "transition from solid directly to vapor." Ice crystals sublime under low humidity in below-freezing conditions. Sublimation fog occurs when ground frost sublimes at sunrise, increasing atmospheric moisture. This can cause a rapid onset of short-lived, shallow, foggy conditions reducing visibility to as low as 1/2 mile.

1.1.2.2.2.7. General Fog Forecasting Guidance:

1.1.2.2.2.7.1. Fog lifts to stratus when the lapse rate approaches dry adiabatic.

1.1.2.2.2.7.2. Marked downslope flow prevents fog formation.

1.1.2.2.2.7.3. The wetter the ground, the higher the probability of fog formation.

1.1.2.2.2.7.4. Atmospheric moisture tends to sublimate on snow, making fog formation, and maintenance less likely.

1.1.2.2.2.7.5. With sufficient radiational cooling (below freezing), fog can dissipate rapidly and form ground frost through the deposition process.

1.1.2.2.2.7.6. Rapid formation or clearing of clouds can be decisive in fog formation. Rapid clearing at night after precipitation is especially favorable for the formation of radiation fog.

1.1.2.2.2.7.7. The wind speed forecast is important because decreases may lead to the formation of radiation fog. Conversely, increases can prevent fog, dissipate radiation fog, or increase the severity of advection fog.

1.1.2.2.2.7.8. A combination advection-radiation fog is common at stations near warm water surfaces.

1.1.2.2.2.7.9. In areas with high concentrations of atmospheric pollutants, condensation into fog can begin before the relative humidity reaches 100%.

1.1.2.2.2.7.10. The visibility in fog depends on the amount of water vapor available to form droplets and on the size of the droplets formed. At locations with large amounts of combustion products in the air, dense fog can occur with a relatively small water vapor content.

1.1.2.2.2.7.11. After sunrise, the faster the ground temperature rises, the faster fog and stratus clouds dissipate.

1.1.2.2.2.7.12. Solar insolation often lifts radiation fog into thin, multiple layers of stratus clouds.

1.1.2.2.2.7.13. If solar heating persists, and no higher clouds block surface heating, radiation fog usually dissipates.

1.1.2.2.2.7.14. Solar heating may lift advection fog into a single layer of stratus clouds and eventually dissipate the fog if the insolation is sufficiently strong.

1.1.2.2.2.8. In summary, the following characteristics are important to consider when forecasting fog:

1.1.2.2.2.8.1. Synoptic situation, time of year, and station climatology.

1.1.2.2.2.8.2. Thermal (static) stability of the air, amount of cooling/moistening expected, wind strength, and dew-point depression.

1.1.2.2.2.8.3. Trajectory of the air over types of underlying surfaces (i.e., cooler surfaces, bodies of water).

1.1.2.2.2.8.4. Terrain, topography, and land surface characteristics.

1.1.3. Visibility Details.

1.1.3.1. Fog. Fog may develop or intensify when one or more of the following conditions are satisfied:

1.1.3.1.1. *Air at the surface is saturated or slightly supersaturated with respect to water in the presence of cloud condensation nuclei.* For fog to form, the air near the Earth's surface must be saturated, or nearly so, meaning that the temperature must equal the dew point (RH = 100%). In reality, because fog is simply a cloud that has formed at the surface, the surface air must be supersaturated for the fog to form. This wouldn't be possible if the air was perfectly pure with no particulates, but because the air near the surface has many particles of dust, soil, and other minerals, the air can become supersaturated (RH slightly greater than 100%), which allows visible cloud droplets to form. However, mixed-phase (freezing) fogs and ice fogs can develop even if the environment is slightly unsaturated with respect to liquid water (RH less than 100%). Mixed-phase fogs are composed of supercooled water droplets and ice crystals, while ice fog is composed entirely of ice crystals and usually occurs at very cold temperatures (less than -30°C). For the formation of these fogs, RH with respect to water will typically be between 99% and 99.9%, while RH with respect to ice may or may not be greater than 100%. The surface air can become saturated via the following mechanisms:

1.1.3.1.1.1. Temperature cooling to the dew point via cold air advection or radiational cooling.

1.1.3.1.1.2. Dew point increasing to the temperature via moisture advection or evapotranspiration from the earth's surface.

1.1.3.1.1.3. Precipitation very rapidly raises the dew point and cools the temperature so they eventually equal each other. This process is called "wet-bulbing", whereby precipitation falls through an unsaturated layer of air and the resultant evaporative cooling eventually lowers the temperature to the wet-bulb temperature, while at the same time the dew point increases as moisture is added to the layer.

1.1.3.1.1.4. Introduction of more fine particulates (ash, dust, etc.) into surface air that is already very moist, which allows supersaturation to more easily be achieved. This is akin to cloud seeding.

1.1.3.1.2. *A wet ground surface exists, such as a body of water, moist vegetation, or soil recently moistened by precipitation.* While not imperative for fog formation, a wet surface such as water or moist vegetation serves as a source of moisture for the planetary boundary layer (PBL). This moisture increases the dew point of the PBL and reduces the amount of cooling that is required for fog formation. A wet surface is especially important for radiation fog formation (discussed in greater detail below), which may not always have an advective source of surface moisture such as from an ocean or lake.

1.1.3.1.3. *Surface winds are less than 10 knots.* Advection fog is characterized by stronger surface winds than radiation fog, but in general surface winds greater than 10 knots are detrimental to fog formation because they make it difficult for saturation to be achieved by maintaining a well-mixed PBL and bringing in drier ambient air. When fog has already formed, however, the turbulence generated by surface winds less than 10 knots plays a pivotal role in the intensity and maintenance of the fog deck.

1.1.3.1.4. *Dry air with relative humidity less than 50% exists above the surface moist layer.* Dry air above the surface is primarily important for radiation fog development and evolution, but is also important for the transition of advection fog to radiation fog. Dry air above the surface to great heights aloft is indicative of clear skies that are conducive to radiative cooling of the earth's surface. This allows the temperature to cool to the dew point, which also creates a surface temperature inversion. At some point, if the surface temperature cools to the dew point temperature, the air becomes saturated and fog may form. When fog does form, dry air aloft allows the top of the fog deck to continue to cool via outgoing IR radiation, which reinforces the fog deck and often causes it to intensify. The presence of dry air aloft also has an impact on the thickness of the fog deck. For example, because the residual layer (RL) above the surface temperature inversion is usually dry adiabatic, winds within the RL will mix dry air above the inversion into the fog deck. This causes the intensity of the fog deck to fluctuate, but also causes it to deepen as turbulence develops within the fog deck. When the sun rises, dry air aloft permits maximum heating of the fog deck. Solar radiation is able to penetrate to some depth within the fog, which eventually causes it to lift and dissipate when IR cooling is no longer sufficient to maintain the fog.

1.1.3.1.5. *Moisture convergence is occurring, especially along coastlines or in areas of complex terrain.* Moisture convergence is a measure of the degree to which moist air (water vapor) is converging into a given area. It takes into account converging winds and the advection of moisture by these winds. Moisture convergence occurs along frontal boundaries, complex terrain, and coastlines where the transition from "smooth" water to land with higher friction causes winds to slow down and converge. Moisture convergence is one of the most important aspects of advection fog formation, since it's common along coastlines when a sea breeze is present and can quickly bring unsaturated air to saturation and keep it saturated as long as onshore flow is maintained. As such, it's the primary factor in coastal advection fog events, especially if other factors (e.g., subsidence, dry air aloft, etc.) are favorable.

1.1.3.1.6. *Precipitation falls into a slightly unsaturated layer, bringing surface relative humidity with respect to water to 100%, or slight supersaturation (relative humidity greater than 100%).* Light precipitation (drizzle, mist) often leads to fog formation in the presence of warm fronts, cold fronts, or other convergent boundaries. When light precipitation falls into an unsaturated layer of air, some of it evaporates which cools and moistens the unsaturated air. This simultaneously lowers the temperature and raises the dew point, making precipitation an ideal way to saturate a layer of air. If winds are light and all of the particulates in the air have not been washed to the surface by heavier rain, fog often forms.

1.1.3.1.7. *Warm air advection occurs within an existing temperature inversion above a surface moist layer.* Warm air advection (WAA) within the temperature inversion above the fog layer is important to fog duration. If WAA is occurring in the inversion, the inversion will be strengthened and will take longer to be mixed out by daytime heating and turbulent mixing. This will allow the foggy air to be trapped under the inversion for a longer period of time.

1.1.3.1.8. *The atmosphere is statically or conditionally stable.* Stability is one of the most important considerations when forecasting fog. Fog will rarely form in a statically or conditionally unstable PBL, because drier air from aloft is allowed to mix with moist surface air. In other words, the moist surface air is not isolated from the drier air aloft. Most fog events occur under a surface anticyclone (surface high pressure), which effectively holds water vapor at the surface and isolates the surface from the typical well-mixed layer above an inversion. Both temperature inversions and subsidence inversions suppress substantial vertical mixing, and allow shallow fog layers to develop.

1.1.3.1.9. *Surface dew points are high.* While not imperative for fog formation, a high surface dew point generally means that the surface will not need to cool as much to achieve saturation. In addition, a higher dew point means there is more moisture near the surface, which is important for potential fog thickness. Fogs that form in maritime environments with high dew points will generally be thicker than fogs that form where dew points are lower.

1.1.3.1.10. *Upslope flow is occurring.* Fog is very common upstream along mountain ranges where moist air impinges on the mountain barrier, is lifted, and condenses to form clouds along the mountain side. Upslope flow is basically moisture convergence along a mountain barrier or other area of complex terrain. If a moist flow pattern persists, then upslope fog can last for several days as moisture is continually lifted along the mountain-side and condenses to form fog.

1.1.3.1.10.1. The opposite is downslope (katabatic) flow, which results in compressional warming of descending air and often leads to fog dissipation during the daylight hours. There are cases, however, where this sinking air along the mountain side spreads out on top of colder air in the valley, reinforcing an existing fog deck by creating a temperature inversion that traps the valley moisture.

1.1.3.1.11. *There is snow cover and/or the ground is frozen.* Advection fog often occurs during the winter months when warm, moist air moves over snow covered and/or frozen ground. The surface air is cooled from below by the ground surface, which may bring the surface air to saturation, allowing fog to develop.

1.1.3.1.12. *There is cloud cover during the day and/or clear skies at night.* Cloud cover above a fog layer can cause the layer to remain in place or intensify during the day by absorbing solar radiation that would otherwise penetrate the fog layer and cause it to dissipate. During nighttime hours, however, the same clouds can cause the fog layer to slowly dissipate as the clouds emit down-welling IR radiation into the fog layer, which mitigates some of the cooling of the fog layer from below.

1.1.3.2. Specific Forecasting Guidance – Advection Fog: Advection fog is relatively shallow and accompanied by a surface-based inversion. The depth of this fog increases with increasing wind speed (though at wind speeds above 9 knots greater turbulent mixing usually causes advection fog to lift into a low stratus cloud deck). Other favorable conditions include:

1.1.3.2.1. Coastal areas where moist air is advected over water cooled by upwelling. During late afternoon, such fog banks may be advected inland by sea breezes or changing synoptic flow. These fogs usually dissipate over warmer land; if they persist through late afternoon, they can advect well inland after evening cooling and last until convection develops the following morning.

1.1.3.2.2. In winter, when warm, moist air flows over colder land. This is commonly seen over the southern or central United States and the coastal areas of Korea and Europe. Because the ground often cools by radiation cooling, fog in these areas is called advection-radiation fog, a combination of radiation and advection fogs.

1.1.3.2.3. Warm, moist air that is cooled to saturation as it moves over cold water forms *sea fog*. If the initial dew point is less than the coldest water temperature, sea fog formation is unlikely. In poleward-moving air, or in air that has previously traversed a warm ocean current, the dew point is usually higher than the cold water temperature. Sea fog dissipates if a change in wind direction carries the fog over a warmer surface. An increase in the wind speed can temporarily raise a surface fog into a stratus deck. Over very cold water, dense sea fog may persist even with high winds. The movement of sea fog onshore to warmer land leads to rapid dissipation. With heating from below, the fog lifts, forming a stratus deck. With further heating, this stratus layer changes into a stratocumulus cloud layer and eventually changes into convective clouds or dissipates entirely. Cooling after the heat of the day can cause sea fog to roll back in and restrict ceilings and visibility again.

1.1.3.3. Specific Forecasting Guidance – Radiation Fog: Radiation fog occurs in air with a high dew point. This condition ensures radiation cooling lowers the air temperature to the dew point. The first step in making a good radiation fog forecast is to accurately predict the nighttime minimum temperature. Additional factors include the following:

1.1.3.3.1. Air near the ground becomes saturated. When the ground surface is dry in the early evening, the dew- point temperature of the air may drop slightly during the night due to condensation of some water vapor as dew or frost.

1.1.3.3.2. In calm conditions, this type of fog is limited to a shallow layer near the ground; wind speeds of 3-7 knots bring more moist air in contact with the cool surface and cause the fog layer to thicken. A stronger breeze prevents formation of radiation fog due to mixing with drier air aloft.

1.1.3.3.3. Constant or increasing dew points with height in the lowest 200 to 300 feet, so that slight mixing increases the humidity.

1.1.3.3.4. Stable air mass with cloud cover during the day, clear skies at night, light winds, and moist air near the surface. These conditions often occur with a stationary, high-pressure area.

1.1.3.3.5. Relatively long period of radiational cooling, e.g., long nights and short days associated with late fall and winter in humid climates of the middle latitudes.

1.1.3.3.6. In nearly saturated air, light rainfall will trigger the formation of ground fog.

1.1.3.3.7. In valleys, radiation fog formation is enhanced due to cooling from cold air drainage. This cooled air can result in very dense fog.

1.1.3.3.8. In hilly or mountainous areas, an upper-level type of radiation fog—continental high inversion fog—forms in the winter with moist air underlying a subsiding anticyclone. A stratus deck often forms at the base of the subsidence inversion, then lowers. Since the subsiding air above the inversion is relatively clear and dry, air at the top of the cloud deck cools by long-wave radiational cooling, which intensifies the inversion and thickens the stratus layer. A persistent form of continental high inversion fog occurs in valleys affected by maritime polar air. The moist maritime air may become trapped in these valleys beneath a subsiding stagnant high-pressure cell for periods of two weeks or longer. Nocturnal long-wave radiational cooling of the maritime air in the valley causes stratus clouds to form for a few hours the first night after the air becomes trapped. These stratus clouds usually dissipate with surface heating the following day. On each successive night, the stratus cloud deck thickens and lasts longer into the next day. The presence of fallen snow adds moisture and reduces daytime warming, further intensifying the stratus and fog. In the absence of air mass changes, eventually the stratus clouds lower to the ground. The first indicator of formation of persistent continental high inversion fog is the presence of a well-established, stagnant high- pressure system at the surface and 700 mb level. In addition, a strong subsidence inversion separates very humid air from a dry air mass aloft over the area of interest. The weakening or movement of the high-pressure system and the approach of a surface front dissipates this type of fog.

1.1.3.3.9. Radiation fog sometimes forms about 100 feet (30 meters) above ground and builds downward. When this happens, surface temperature rises sharply. Similarly, an unexpected rise in surface temperature can indicate impending deterioration of visibility and ceiling due to fog.

1.1.3.3.10. Radiation fog dissipates from the edges toward the center. This area is not a favorable area for cumulus or thunderstorm development.

1.1.3.4. Specific Forecasting Guidance – Frontal Fog. Frontal fog forms from the evaporation of warm precipitation as it falls into drier, colder air in a frontal system.

1.1.3.4.1. Pre-frontal, or warm-frontal, fog (**Figure 1.2**) is the most common and often occurs over widespread areas ahead of warm fronts. Whenever the dew-point temperature of the overrunning warm airmass exceeds the wet-bulb temperature of the cold airmass it's replacing, fog or stratus form. Fog usually dissipates after frontal passage due to increasing temperatures and surface winds.

1.1.3.4.2. Post-frontal, or cold-frontal, fog (**Figure 1.3**) occurs less frequently than warm-frontal fog. Slow-moving, shallow-sloped cold fronts characterized by vertically decreasing winds through the frontal surface, produce persistent, widespread areas of fog and stratus clouds 150 to 250 miles behind the surface frontal position to at least the intersection of the frontal boundary with the 850 mb level. Strong turbulent mixing behind fast-moving cold fronts, characterized by vertically increasing winds through the frontal surface, often produce stratus clouds but no fog.

Figure 1.2. Pre-frontal fog associated with a warm front.
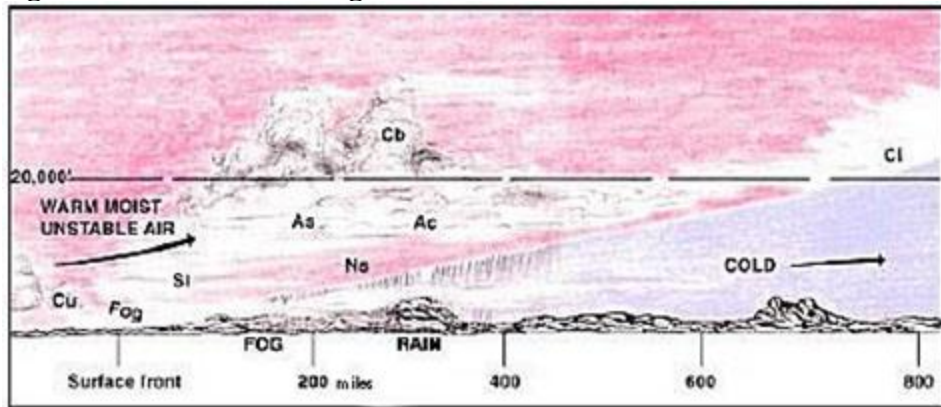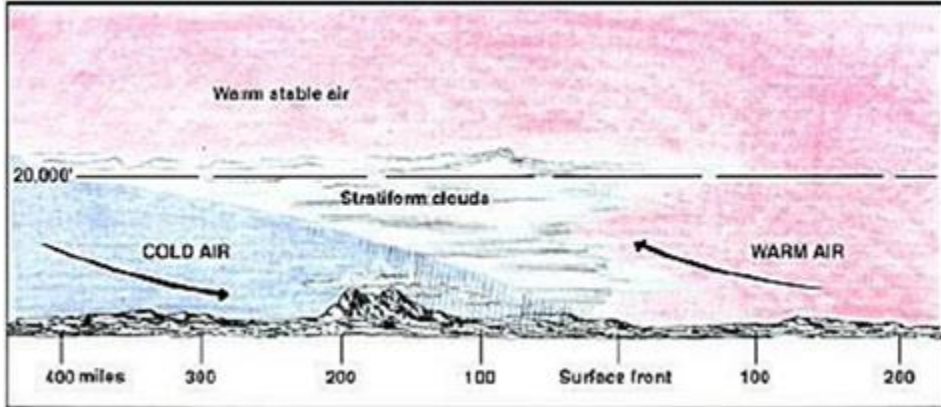
Figure 1.3. Post-frontal fog associated with a slow-moving cold front.

1.1.3.5. Snow and Blowing Snow. According to the AMS Glossary of Meteorology, blowing snow is snow lifted from the surface of the earth by the wind to a height of 2 meters (6 feet) or more, and blown about in such quantities that horizontal visibility is reduced to less than 7 statute miles. Blowing snow is encoded as BS in surface aviation weather observations and as BLSN as an obstruction to vision in METAR or SPECI observations. Blowing snow can be falling snow or snow that has already accumulated but is picked up by strong winds. Consider the following rules of thumb when forecasting visibility in snow or blowing snow:

1.1.3.5.1. Moderate, dry, and fluffy snowfall with wind speeds exceeding 15 knots usually reduces visibility in blowing snow.

1.1.3.5.2. Snow cover that has previously been subject to wind movement (either blowing or drifting) usually does not produce as severe a visibility restriction as new snow.

1.1.3.5.3. Snow cover that fell when temperatures were near freezing does not blow except in very strong winds.

1.1.3.5.4. The stronger the wind, the lower the visibility in blowing snow. The converse is also true; visibility usually improves with decreasing wind speed.

1.1.3.5.5. Loose snow becomes blowing snow at wind speeds of 10 to 15 knots or greater. Although any blowing snow restricts visibility, the amount of the visibility restriction depends on such factors as terrain, wind speed, snow depth, and composition.

1.1.3.5.6. Blowing snow is a greater hazard to flying operations in polar regions than in mid- latitudes because the colder snow is dry, fine and easily lifted.

1.1.3.5.7. Winds may raise the snow 1000 feet above the ground, lowering visibility. A frequent and sudden increase in surface winds in polar regions may cause the visibility to drop from unlimited to near zero within a few minutes.

1.1.3.5.8. Fresh snow blows or drifts at temperatures of –20°C (–4°F) or less. After 3 or more days of exposure to direct sunlight, snow forms a crust and does not readily drift or blow. The crust, however, is seldom uniform across a snowfield. Terrain undulations, shadows, and vegetation often retard the formation of the crust.

1.1.3.5.9. If additional snow falls onto snowpack that has already crusted, only the new snow blows or drifts.

1.1.3.5.10. Use **Table 1.1** as a guide to forecast visibility based on the intensity of snow. When forecasting more than one form of precipitation at a time, or when forecasting fog to occur with the precipitation, consider forecasting a lower visibility than shown in **Table 1.1**

Table 1.1. Visibility limits based on snowfall intensity.

Intensity	Visibility Limits (statute miles)
Light snow showers	Greater than ½ mile
Moderate snow showers	Greater than ¼ mile but less than ½ mile
Heavy snow showers	Less than ¼ mile

1.1.3.6. Haze. Research shows that the primary constituent of haze droplets over industrial areas, such as the central and eastern United States and parts of Asia, is sulfuric acid. In these areas, sulfur dioxide released from industry (such as oil refining and steel manufacturing) bonds with oxygen in oxidation reactions enhanced by sunlight and/or liquid water. These reactions result in the formation of sulfate aerosols, include sulfuric acid. Sulfate aerosols are hygroscopic (they absorb water from the environment), even at relative humidities as low as 70%, making them effective condensation nuclei. When the environment is supersaturated, sulfate aerosols grow large enough to be seen as clouds. When the humidity is low, however, they only grow to around a tenth of a micrometer in diameter, and remain suspended in the atmosphere to form haze. Haze usually occurs in the planetary boundary layer (PBL), which extends from the surface up to about 2 km on average, but can extend up to 500 mb in places like Southwest Asia. The top of the PBL is delineated by a temperature inversion and a cessation of vertical mixing, and this is typically the upper boundary of a haze layer. However, elevated layers of haze may also occur, such as in regions downstream from where particles have been lofted above the PBL by cumulus clouds. Elevated haze is also possible on the poleward side of fronts. Sulfate aerosols are chemically stable, and as such, settle very slowly. Therefore, in the absence of a cleansing mechanism such as precipitation, haze can persist for days. This is especially true when atmospheric conditions are stagnant, such as under a persistent area of high

pressure. Here, limited mixing, plenty of sun, and increasing boundary layer moisture create particularly favorable conditions for the formation of sulfate aerosols. Haze normally restricts visibility to 3 to 6 miles, and occasionally to less than 1 mile. It usually dissipates when the atmosphere becomes thermally unstable or wind speeds increase. This can occur with heating, advection, or turbulent mixing.

1.1.3.7. Dust Storms. Dust storms are a function of wind speed, wind direction and soil moisture content. After generating blowing dust upstream, wind speed becomes important in advection of the dust. Dust may be advected by winds aloft when surface winds are weak or calm. Duration of the advected dust is a function of the depth of the dust and the advecting wind speeds. Synoptic situations, such as cold frontal passages, may change both the wind direction and the probability of dust advecting into your area.

1.1.3.7.1. Dust Source Regions. Forecasting dust generation is more difficult than forecasting the advection of observed dust into the area; there are several key factors to keep in mind, including the following common dust source regions:

1.1.3.7.1.1. *Deserts.* Dust storms occur in regions with little vegetation and precipitation; these conditions are most prevalent in deserts, where rainfall is scarce. In general, dust is unlikely within 24 to 36 hours of a rainstorm, but rainstorms can lead to increased dust potential beyond 36 hours. Runoff after heavy rain carries soil particles picked up by erosion; once the water evaporates, these particles can be easily lofted.

1.1.3.7.1.2. *Agricultural areas.* Agricultural land that is fallow, recently tilled, or has a marginal growing climate is a potential source area for dust. The mechanical breaking of soil creates an environment rich in fine-grained soil that is picked up and moved by seasonal winds. This is commonly observed in northern Syria and Iraq.

1.1.3.7.1.3. *Coastal areas.* Dust plumes can be generated in advance of cold fronts moving across sandy or silty coastal regions.

1.1.3.7.1.4. *River flood plains (alluvial plains).* The flood plain of the Tigris and Euphrates Rivers in southern Iraq serves as the source region for many dust storms, particularly during shamal events - a northwesterly wind that blows over Iraq and the Persian Gulf states. Shamals are often strong during the day and decrease in strength at night.

1.1.3.7.1.5. *Dry lake beds.* Water in lakes erodes rocks and forms fine-grained soils. When lakes dry up, these soils inhibit plant growth and blow easily in strong winds.

1.1.3.7.2. Dust Lofting Mechanisms. After an appropriate source, the next key ingredient for dust storm generation is wind from the surface through the depth of the boundary layer strong enough to move and loft dust particles. **Table 1.2** shows threshold dust-lofting wind speeds for different desert environments. The first sand and dust particles that move are those from 0.08 to 1 mm in diameter; this occurs with wind speeds of 10 to 25 knots. In general, winds at the surface need to be 15 knots or greater to mobilize dust. Once a dust storm starts, it can maintain the same intensity even when wind speeds slow to below initiation levels, since the bond between dust particles and

the surface is already broken. Lofting of dust also requires turbulence in the boundary layer. Typically, wind shear creates the turbulence that lofts dust up and away from the surface. As a rule of thumb, if the wind at the surface is blowing 15 knots, the wind at 1000 feet) must be about 30 knots to keep the dust particles aloft. An unstable boundary layer, which favors vertical motions, is also necessary for dust lofting. With the lack of vegetation in dust-prone regions, the ground can experience extreme daytime heating, which creates an unstable boundary layer. As the amount of heating increases, the unstable layer deepens. In contrast, stable boundary layers suppress vertical motions and inhibit dust lofting. Diurnal effects also impact dust storm potential. Dry desert air has a wide diurnal temperature difference. Strong radiative cooling leads to rapid heat loss after sunset, resulting in a surface-based inversion, which may inhibit dust lofting. However, the formation of a surface-based inversion has little effect on dust that is already suspended higher in the atmosphere. Furthermore, if winds are sufficiently strong, they will inhibit the formation of an inversion or even remove one that has already formed. **Table 1.3** shows favorable parameters for dust storm generation in various scenarios.

Table 1.2. Threshold dust-lofting wind speeds for different desert environments.

Environment	Threshold Wind Speed
Fine to medium sand in dune-covered areas	10 to 15 mph (8.7 to 13 knots)
Sandy areas with poorly developed desert pavement	20 mph (17.4 knots)
Fine material, desert flats	20 to 25 mph (17.4 to 21.7 knots)
Alluvial fans and crusted salt flats (dry lake beds)	30 to 35 mph (26.1 to 30.4 knots)
Well-developed desert pavement	40 mph (36.8 knots)

Table 1.3. Favorable conditions for the generation and advection of dust.

Parameter or Condition	Favorable When
Location with respect to source region	Located downstream and in close proximity
Agricultural practices	Soil left unprotected
Previous dry years	Plant cover reduced
Wind speed	30 knots or greater
Wind direction	Significant dust source is upstream
Cold front	Passes through the area
Squall line	Passes through the area
Leeside trough	Deepening and increasing winds
Thunderstorm	Mature storm in local area or generates blowing dust upstream
Whirlwind	In local area
Time of day	1200 to 1900L
Surface dew point depression	10 C or greater

1.1.3.7.3. Dust Removal Mechanisms. Lofted dust eventually settles, but may travel half way around the globe before doing so. The three most common dust removal mechanisms are dispersion, advection, and entrainment in precipitation.

1.1.3.7.3.1. Dispersion. Dust plumes tend to fan out as they move downstream from their source regions; this is caused by dispersion. At the most basic level, the more air that entrains into a dust plume, the more the plume dilutes, spreads out, and disperses. Dispersion is primarily influenced by turbulence, which mixes ambient air with the dust plume. Any increase in turbulence increases the rate at which the plume disperses. There are three kinds of turbulence that act to disperse a plume - mechanical, caused by air flowing over features such as hills or buildings; shear, resulting from differences in wind speed and/or direction; and buoyancy, caused by parcels of air rising during the diurnal heating of the surface.

1.1.3.7.3.2. Advection. Advection moves dust away from its source; winds aloft may carry dust in a direction different from the wind direction at the surface. When predicting where a dust plume will travel, check the vertical wind profile. Dust that leaves the ground going one direction can rise to a level where it travels in an entirely different direction.

1.1.3.7.3.3. Entrainment in precipitation. Most dust particles are hygroscopic, or water-attracting. In fact, dust particles usually form the nucleus of precipitation. Because of this affinity to moisture, precipitation very effectively removes dust from the troposphere.

1.1.3.7.4. Dust storm types. Several types of dust storms, including shamal, frontal, and convective, are described below. The shamal is unique to the Middle East, but frontal and convective dust storms can be experienced in other arid regions, including the Southwestern United States.

1.1.3.7.4.1. Summer shamal. The term "shamal" comes from the Arabic word for "north," and describes a type of dust storm caused by prevailing north winds over the Arabian Peninsula, Iraq, and Kuwait. Typical sources for the dust lie between the Tigris and Euphrates rivers. The summer shamal, also known as the "Wind of 120 days," is nearly constant from June through September across Syria, Saudi Arabia, and Iraq. It is caused by convergence between the Southern Arabian Peninsula Monsoon Trough and the subtropical ridge that extends from the Mediterranean Sea into Iraq and the northern Arabian Peninsula. Additionally, cold air advection aloft causes steep lapse rates and increased instability. The end result is that updrafts keep dust particles suspended, sometimes at high altitudes. Due to the dry desert air and high rate of thermal radiation during the day, a nocturnal radiational inversion is established almost every night across Southwest Asia (SWA) as the desert floor cools. The inversion is usually quite shallow, extending up to 1000-2000 feet above ground level. Above the inversion, a nocturnal low-level jet (LLJ) stream is often established. When the inversion collapses or is mixed out during the ensuing daylight hours, the strong LLJ winds can reach the surface and are also a source of the summer shamal, as long as they exceed 15 knots. Summer shamal dust storms are typically 3000-8000 feet tall, but can extend up to 15,000-18,000 feet. Visibilities can go from unrestricted to zero within minutes and remain that way for 1-3 hours before slowly starting to increase. Dust storms can last from 1-10 days depending on the wind flow pattern and atmospheric stability profile, but 3 days is average.

1.1.3.7.4.2. Winter shamal. Many winter shamal dust storms are associated with passing cold fronts, which are classified as "frontal dust storms." A few, however, are caused as very cold air masses funnel south or southeastward from Turkey or Syria into the Tigris/Euphrates River Valley. These cold air masses maintain temperature and moisture continuity as they descend the Arabian Peninsula, creating a relatively sharp temperature gradient between the leading edge of the air mass and the surrounding air. Because the air mass is much colder than the surrounding air, it lifts the warmer and more buoyant ambient air, as well as dust if the ambient vertical temperature profile is conditionally unstable aloft. This physical mechanism, known as a density current, is the same mechanism that lofts dust when a thunderstorm downdraft reaches the surface, causing a haboob.

1.1.3.7.4.3. Frontal dust storms. The main difference between frontal dust storms and shamals is a matter of scale; shamals are localized, mesoscale phenomena, while frontal dust storms are caused by synoptic-scale systems whose winds carry sand particles over large distances. They accompany low pressure systems and associated frontal boundaries. The three major varieties are prefrontal, postfrontal, and shear-line.

1.1.3.7.4.3.1. Prefrontal. Prefrontal dust storms occur across much of SWA as low pressure systems move across the region. The polar front jet stream located behind a cold front and the subtropical jet stream located ahead of a cold front can converge into a single jet streak (or jet max) that translates to the surface in the left front quadrant. Ageostrophic circulations associated with the divergent (left-front and right-rear) quadrants of the jet streak also increase upward vertical velocities, which enhance the probability of dust lofting as well. Prefrontal winds are called the Sharqi in Iraq, the Kaus in Saudi Arabia, the Shlour in Syria and Lebanon, and the Khamsin in Egypt. Easterly to southerly prefrontal winds are favored for prefrontal dust storms in October and November, but such plumes will rarely be long-lived given their prefrontal nature. Wind speeds are 10-20 knots on average, although gusts of 25-30 knots do occur. Prefrontal dust storms can be difficult to detect in METSAT imagery because they are short-lived and often located over similarly shaded terrain. Cloud cover due to pre-cold frontal overrunning often obscures these types of dust storms from METSAT view.

1.1.3.7.4.3.2. Postfrontal. Postfrontal dust storms are associated with a dynamic weather feature (e.g., cold front); cloudiness associated with the cold front may mask the dust signature in METSAT imagery, but in most cases the dust "head" is the best indicator of the leading edge of the cold air. Given their stronger mechanical forcing, postfrontal dust storms usually reach greater heights than those associated with shamal winds. They typically reach 8,000-15,000 feet, but postfrontal dust has been observed up to jet stream level (~30,000 feet). Surface winds are 15-30 knots on average, but gusts of 40-50 knots may occur with very strong low pressure systems. Wind speed can be estimated by the thermal contrast across the front. A temperature change of 10°C corresponds to a maximum wind speed of 30 knots, with a 5 knot increase for every additional 5°C. There are two types of postfrontal dust storms: The

first type lasts 24-36 hours as a cold frontal system migrates across SWA. Dust moves across the Persian Gulf in 12-24 hours, and the cold front can reach the southern Arabian Peninsula in 48-72 hours. The second type lasts 3-5 days and occurs when a weaker cold front (typically in early autumn) stalls out and becomes stationary. Cyclogenesis occurs along the stationary boundary, with frontal waves moving to the east-northeast.

1.1.3.7.4.3.3. Shear line. These dust storms are common in winter along the Arabian Peninsula, Red Sea, and in the equatorial regions of Africa. Trade winds from the east converge with a polar high pressure system, resulting in a narrow band of accelerated flow. This creates enough turbulence to lift dust particles into the atmosphere. Being slightly warmer than the cool air, the dust is sometimes apparent on infrared satellite imagery. A similar situation is observed on the Arabian Sea when a cold front weakens across the India-Pakistan border. A shear line is produced, which can yield a rope cloud if sufficient moisture is present. Wind speeds are typically 10-25 knots, with gusts to 40 knots. Visibility typically remains 1-3 nautical miles.

1.1.3.7.4.4. Convective dust storms. Convective dust storms are very difficult to forecast, partially because they are typically a small-scale phenomenon (e.g., dust devils may be only tens of meters in width). Microbursts are particularly dangerous for aircraft, given the reduced visibility and unpredictable nature of high winds.

1.1.3.7.4.4.1. Dust devils. Dust devils occur throughout much of the world; they're created by strong surface heating under clear skies and light winds when the sun warms the air near the ground to temperatures well above those just above the surface layer. Once sufficient heating is achieved, a localized pocket of air quickly rises through the cooler air above it. Hot air rushes in to replace the rising air at the bottom of the developing vortex, intensifying the spinning effect. Once formed, the dust devil is a funnel-like chimney through which hot air moves both upwardly and circularly. The dust devil persists until the supply of warm, unstable air is broken or depleted. Dust devils are typically smaller and less intense than tornadoes, although the strongest dust devils can achieve the intensity of a weak tornado. Dust devil diameter is typically between 10 and 300 feet (3 to 90 meters), with an average height of 500 to 1000 feet (150 to 300 meters). Dust devils typically last only a few minutes, but may persist for up to an hour in optimal conditions.

1.1.3.7.4.4.2. Haboobs. A haboob is an intense dust storm generated by the convective outflow from a collapsing or ongoing thunderstorm, or from any collapsing cumuliform cloud of appreciable vertical extent. Haboobs are most frequent in the deserts of northern Africa, but they also occur in SWA and the southwestern United States. Because low-level air is so dry in desert environments, any precipitation that falls into it will quickly evaporate (or sublimate in the case of ice crystals). This cools the ambient air, making it negatively buoyant with a tendency to sink towards the surface. As long as the wet bulb potential temperature of the sinking air (downdraft) remains cooler than the potential temperature of the air at the surface by at least 4°C, that air will continue to the surface unimpeded and spread out in all directions, but with

a stronger component in the direction of the low-level winds. The air that reaches the surface is colder and therefore denser than the ambient environmental air, so the downdraft air will act like a wedge that rapidly lifts the positively buoyant warm air around it. While this is happening, any dry soil at the cold air/warm air interface has the potential to be lofted to great heights and propagate in the direction of the average cloud-bearing layer winds - this intense dust event is the haboob. The haboob environment is usually characterized by a surge of midlevel moisture, with a dry adiabatic lapse rate below that. Some elevated instability usually exists in the form of a "best lifted index" (the most unstable lifted index) less than 0. Haboobs usually travel an average of 60-90 miles, but can travel greater distances if the convective outflow is strong enough, the low-level winds are strong enough, and/or the vertical temperature profile is dry adiabatic over a large area. Most haboobs reach a height of 5000-8000 feet, but some can ascend to 10,000-14,000 feet. Peak winds in the haboob are approximately 95% greater than the speed of movement. Duration varies, but can reach up to six hours.

1.1.4. Visibility Forecasting Aids and Techniques – Fog.

1.1.4.1. AFW Ensemble Visibility Forecasts. Air Force Weather's ensemble products (the Global Ensemble Prediction Suite (GEPS) and the Mesoscale Ensemble Prediction Suite (MEPS) use statistical regression analyses of relative humidity, precipitable water, and surface wind speed to produce visibility probability products, available from the AFW-WEBS ensembles page at **https://weather.af.mil/confluence/display/AFWWEBSTBT/Ensembles+Main+Page**. Each ensemble produces probability products for visibilities less than five, three, and one statute miles.

1.1.4.2. Visibility Climatology. The 14th Weather Squadron (**https://climate.af.mil**) is the Air Force's climatology center, and operates and maintains a vast library of climatological data. For fog forecasting, their most useful products are wind stratified conditional climatologies (WSCC), surface climograms, and operational climatic data summaries (OCDS-II).
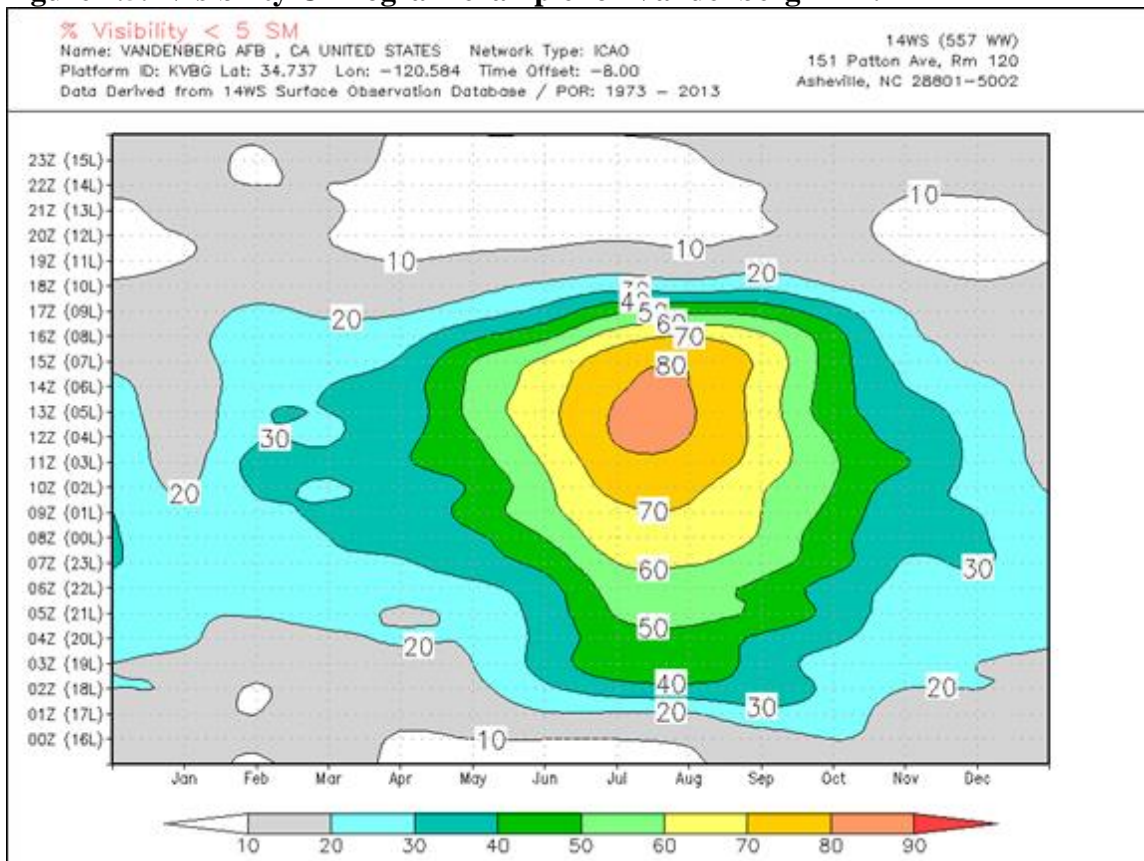
1.1.4.2.1. Wind Stratified Conditional Climatologies (WSCC). Given a set of initial conditions (month, time of day, wind direction, ceiling height, and visibility), WSCCs indicate the percentage likelihood that a particular visibility category will be observed at a future hour (**Figure 1.4**). The output can be used as a baseline for constructing fog forecasts in areas that are conducive to fog formation.

Figure 1.4. WSCC example.

							VISIBILITY						
13 FCST HRS	1	2	3	4	5	6	7	8	9	12	15	18	24
TIME	17Z	18Z	19Z	20Z	21Z	22Z	23Z	00Z	01Z	04Z	07Z	10Z	16Z
0.5 mi							1						
1 mi						1	1	1					
1.5 mi			1				1	1	2				
2 mi					1	1	1	1	1	1			1
3 mi		1	2	1		3	5	5	2	2	4	2	2
7 mi	8	21	25	30	39	47	55	57	55	32	32	35	36
Unlimited	92	78	72	69	61	48	37	36	39	66	64	63	61
OCCURRENCES	161	169	174	157	161	171	166	152	163	152	154	147	161

Total Initial Condition Observations: 335

1.1.4.2.2. Surface Climograms. A climogram is a two-dimensional view of the likelihood of an event's occurrence; many weather parameters are available, including fog. **Figure 1.5** is a surface climogram for Vandenberg AFB, showing the likelihood of visibility less than 5 statute miles for all hours of the day and all months of the year.

Figure 1.5. Visibility Climogram example for Vandenberg AFB.
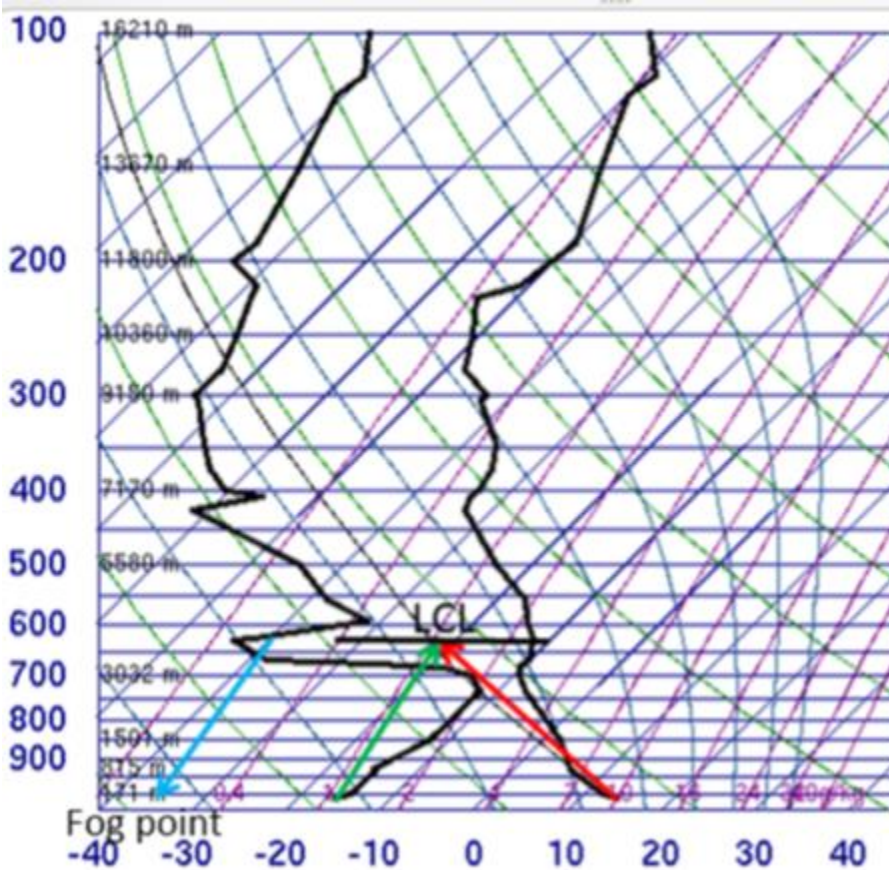
1.1.4.2.3. Operational Climatic Data Summaries (OCDS-II). The OCDS-II web application enables users to generate plots of fog frequency, stratified by time of day and month of the year, for a user-selected station (**Figure 1.6**).

Figure 1.6. OCDS-II example.

% FREQUENCY OF FOG

HOURS	JAN	FEB	MAR	APR	MAY	JUN	JUL	AUG	SEP	OCT	NOV	DEC	ANN
17-19 LST	20.4	22.2	16.2	7.8	10.1	7.5	3.9	6.4	13.4	10.1	6.6	25.8	13.0
20-22 LST	23.0	23.3	16.1	12.0	12.7	11.9	5.6	7.0	16.3	9.2	12.2	21.8	14.6
23-01 LST	29.1	22.0	21.4	16.6	13.0	17.3	13.3	20.1	28.5	15.5	14.3	25.8	20.1
02-04 LST	27.3	24.2	30.3	20.2	23.9	27.1	22.1	26.7	32.7	21.5	22.9	24.9	25.4
05-07 LST	25.5	27.6	35.4	24.7	22.8	21.2	28.2	32.4	35.5	22.4	24.2	30.6	27.7
08-10 LST	29.3	35.6	23.3	23.5	10.7	5.8	8.7	12.1	16.8	14.6	18.4	34.8	20.5
11-13 LST	21.6	25.9	13.2	15.0	6.8	5.8	0.6	4.7	4.9	7.4	12.5	22.9	12.6
14-16 LST	17.0	18.2	13.6	15.2	12.4	1.8	0.5	1.3	3.3	11.4	11.8	19.3	11.1
All Hours	24.4	25.2	21.8	17.1	14.4	13.0	11.5	15.1	20.3	14.4	15.7	26.1	18.5

* = No Data   T = Trace   # = Occurrences rounded to 0

1.1.4.3. Radiation Fog Point (FP). The radiation fog point is the temperature (in °C) at which radiation fog forms. To find the FP, first find the pressure level of the LCL. From the dew point at the LCL, follow an isohume (line of constant saturation mixing ratio) down to the surface; the temperature value where the isohume intersects the surface is the radiation fog point. For an example of this calculation, refer to **Figure 1.7** In the example, the LCL is at 630 mb, and the dew point at the LCL is -40°C. Following the isohume down to the surface from that dew point value, the FP is determined to be -36°C.

Figure 1.7. Radiation Fog Point example.

1.1.4.4. Radiation Fog Threat (FT). The radiation fog threat indicates the potential for radiation fog formation; it's calculated by subtracting the radiation fog point (see the previous section for details) from the 850 mb wet-bulb potential temperature (WBPT850). If not already known, WBPT850 is found by first finding the pressure level of the 850 mb LCL, and then lowering the parcel moist adiabatically to 1000 mb; the point at which the lowered parcel intersects the 1000 mb level is the WBPT850. Refer to **Table 1.4** to determine the likelihood of radiation fog formation.

Table 1.4. Fog threat thresholds, indicating likelihood of radiation fog formation.

Fog Threat Value	Likelihood of radiation fog formation
Greater than 3	Low
Between 0 and 3	Moderate
Less than 0	High

Fog Threat Value = WBPT850 – Fog Point

1.1.4.5. Radiation Fog Stability Index (FSI). The radiation fog stability index uses a representative 1200Z sounding to give the likelihood of radiation fog formation, and is defined in **Table 1.5**

Table 1.5. Fog Stability Index (FSI) thresholds, indicating likelihood of radiation fog formation.

FSI Value	Likelihood of radiation fog formation
Greater than 55	Low
Between 31 and 55	Moderate
Less than 31	High

$$FSI = 4T_{Sfc} - 2(T_{850} + Td_{Sfc}) + W_{850}$$

T_{Sfc} = Surface temperature in °C. T_{850} = 850 mb temperature in °C.
Td_{Sfc} = Surface dew point in °C. W_{850} = 850 mb wind speed in knots.

1.1.4.5.1. The FSI is indicative of radiation fog potential if there's strong static stability between the surface and 850 mb, as indicated by increasing temperatures with height in the layer.

1.1.4.5.2. FSI is also indicative of radiation fog potential if there's ample moisture in the layer, indicated by the surface dew point depression (i.e., the difference between the surface temperature and dew point).

1.1.4.5.3. Finally, FSI is also indicative of radiation fog potential if there are slow wind speeds at 850 mb, which aren't conducive to mixing drier ambient air into the fog layer.
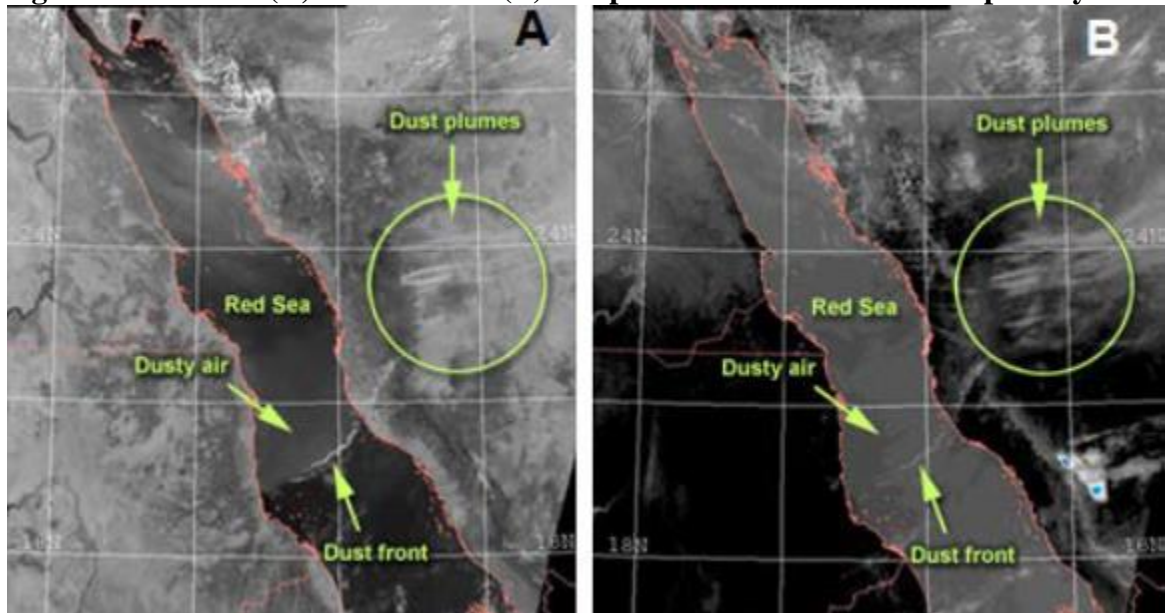
1.1.5. Visibility Forecasting Aids and Techniques – Dust.

1.1.5.1. AFW Ensemble blowing dust forecasts. The GEPS and MEPS produce blowing dust probability products, available on AFW-WEBS, for visibilities less than five, three, and one statute miles.

1.1.5.2. Satellite detection of dust. Satellite detection of dust is difficult, especially at night and in single channel imagery. Enhanced RGB satellite imagery and Aerosol Optical Depth (AOD) have somewhat eased these difficulties. Satellite animations (especially daytime visible imagery) can help identify the location of dust, since the movement of the dust plume makes it stand out against the stationary land surface. Animated infrared imagery can also be used to track dust over land during the day, since the dust contrasts against the hot land surface. Infrared imagery is not as useful at night, since the land cools and the contrast between the dust and land decreases.
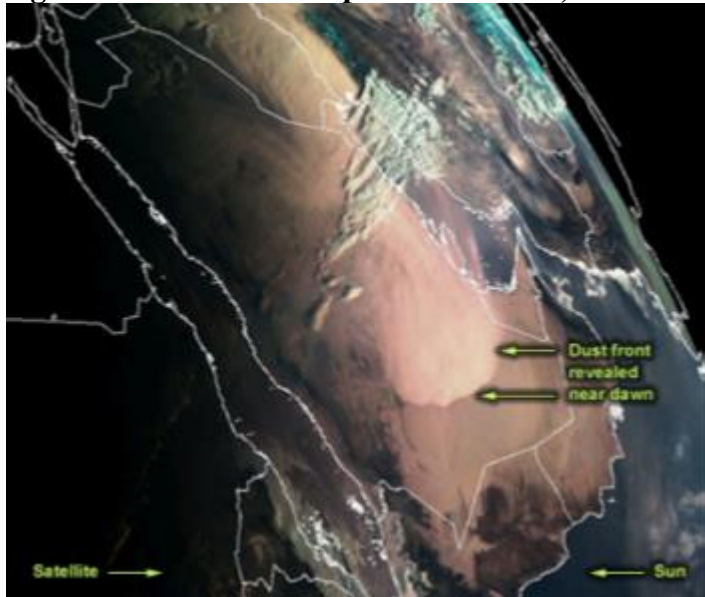
1.1.5.2.1. Daytime detection. In general, dust is easier to detect during the day than at night, although there are some differences depending on the time of day. **Figure 1.8** depicts visible (A) and infrared (B) Moderate Resolution Imaging Spectroradiometer (MODIS) images, respectively. In the visible image, dust is easily discernible over the Red Sea, but more difficult to observe over the adjoining land; in visible imagery, dust stands out over the dark water background, but blends in with the sandy land surface. The opposite is true in the infrared image; here, dust is clearly depicted over land, but not over the Red Sea. The dust over land is cooler than the underlying surface, and thus detectable on infrared imagery. Over the Red Sea, the thermal contrast is lessened, and the dust disappears.

Figure 1.8. Visible (A) and infrared (B) comparison of dust detection capability.
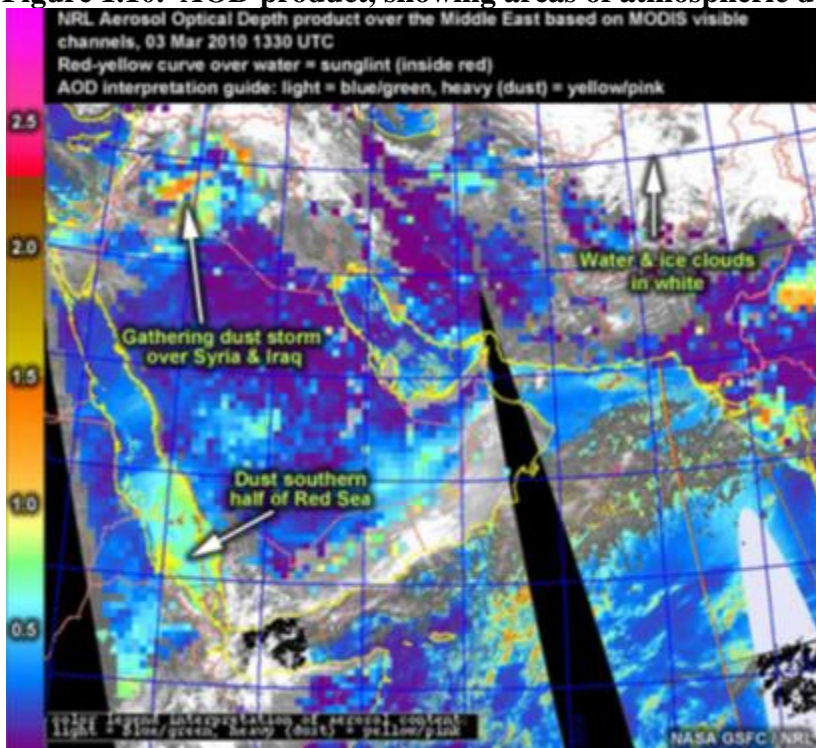
1.1.5.2.2. Sunrise and sunset detection. Dust detection in visible satellite imagery at sunrise and sunset varies from detection during the day. If a satellite is looking in the general direction of the sun and the dust, the forward scattering of dust particles heightens the reflection from dust. Conversely, if the satellite is looking away from the sun, backscattering occurs. Now, less solar energy is being reflected back to the satellite, reducing the ability to detect dust. An example of forward scattering is shown in **Figure 1.9**; a large dust cloud is seen progressing across the Arabian Peninsula at dawn. This dust plume would be difficult to detect in the middle of the day.

Figure 1.9. Sunrise dust plume detection, due to forward scattering.

1.1.5.2.3. Aerosol Optical Depth (AOD). AOD is a unit-less measure of the amount of light that airborne particles, such as dust, smoke, haze, and pollution, prevent from passing through a column of the atmosphere. AOD doesn't provide surface visibility estimates (since the dust detected could reside anywhere in the vertical column), but it can serve as a first-order indicator of potential reduced surface visibilities. **Figure 1.10** shows a sample AOD product over Southwest Asia, with warm colors indicating the presence of atmospheric dust.

Figure 1.10. AOD product, showing areas of atmospheric dust.

1.1.5.3. Surface Climograms. Climatology can aid in dust forecasting, the surface climogram product can provide a two-dimensional view of the likelihood of reduced visibility due to dust at any hour and month of the year (refer to **paragraph 1.1.4.2.2**. for details.)

1.1.5.4. Forecasting haboobs from ongoing thunderstorms. First, determine if elevated instability is present (represented by a "best lifted index" less than 0), then look for high mid-level moisture (e.g., high relative humidity between 700 and 500 mb) and steep (dry adiabatic) lapse rates between the surface and approximately 18,000 feet. If all these factors are present, find the strongest wind at any level aloft where the wet bulb potential temperature is less than the surface potential temperature by at least 4°C; this wind may be brought to the surface.

1.1.5.5. Forecasting haboobs from collapsing thunderstorms. Thunderstorm collapse is most likely after sunset when buoyancy diminishes. To determine haboob potential, first find the cloud base height of the thunderstorm. The higher it is (particularly greater than 10,000 feet), the weaker the potential haboob. Rapidly warming cloud tops in infrared satellite imagery are indicative of an imminent collapse.

1.1.5.6. Autumn dust storm forecast process.

1.1.5.6.1. *Determine the mission scenario.* Determine the time period of interest; you'll be interested in any dust events that may occur during this time period which may rapidly restrict visibility or negatively impact any missions scheduled or ongoing in your AOR.

1.1.5.6.2. *Examine thunderstorm and blowing dust climatology.* Refer to AFW-WEBS and the 14th Weather Squadron to determine the climatological likelihood of dust storms at your location.

1.1.5.6.3. *Examine a recent dust source region database.* Examine the most recent analysis of dust source regions; couple climatology data with historical dust source region information to determine where dust events are most likely to develop.

1.1.5.6.4. *Examine a recent soil moisture profile.* From AFW-WEBS, examine a 0.25 degree (25 km) resolution 0-10 cm soil moisture profile; locations shaded yellow, light orange, or brown are considered dry. Consult a chart of local soil types determine which soil is most likely to be lofted. Sandy soils drain easier than clay soils and will be more prone to dust lofting, although lofting potential depends strongly on particle size as well.

1.1.5.6.5. *Analyze the synoptic environment.* At the 200-300 mb level, look for long wave troughs and ridges, as well as jet maxima (or jet streaks). Note the magnitude of jet maxima and areas of divergence in the left front or right rear quadrants. At the 500 mb level, look for shortwave ridges and troughs embedded in the long wave pattern. Also look for areas of positive or negative vorticity advection, and take note of temperatures at 500 mb as indicators of warm or cold air aloft as well as dew points as indicators of dry air aloft. Soundings are also useful when diagnosing mid-level temperatures and moisture. At the 700 mb level, look for shortwave troughs and ridges, and examine dew points. 700 mb temperatures will also indicate any capping inversions that may prevent unimpeded upward vertical motions. At the 850 mb level, look for

high and low height centers, as well as the presence of a nocturnal low-level jet (LLJ) stream if nightfall is approaching. Also examine 850 mb dew points to determine the amount of low-level dry air present. Analyze the 925 mb level the same the 850 mb level, but key in on wind speeds; 925 mb wind speeds with a dry adiabatic layer often strengthen wind speeds at the surface and enhance dust lofting potential. In fact, the strongest wind anywhere in a dry adiabatic layer could come to the surface and contribute to downdraft strength. Finally, at the surface, analyze areas of high and low pressure and associated fronts, as well as areas of low-level convergence. Surface winds of at least 15 knots are usually needed to loft dust.

1.1.5.6.6. *Analyze observed or model forecast soundings.* Look for observed or forecast surface winds greater than or equal to 15 knots. In Iraq, north or northwest low-level winds are favorable for dust lofting because they are parallel to several dust source regions. Dry low-level air (from the surface up to somewhere in the 700-400 mb layer) is often conducive to momentum transfer from aloft that can enhance surface winds. Look for the presence (or lack of) a temperature inversion; dust will generally start to settle at the surface after dark once the nocturnal radiational inversion develops. An inversion also makes it difficult for dust to be lofted in the first place due to a shallow layer of stability that is not conducive to upward motion. The presence (or lack of) a dry adiabatic (or super-adiabatic) layer from the surface to some height aloft is a key indicator of dust lofting potential; the height of a dust plume can be approximated by the depth of the dry adiabatic layer. When the temperature becomes less than dry adiabatic, it's difficult for dust to continue being lofted to greater heights because the potential temperature starts to increase rather than remain constant. It's often important for winds within the dry adiabatic layer to be in-phase (i.e., coming from the same direction); this increases the probability that winds from aloft will be brought to the surface via momentum transfer. The strongest wind within a dry adiabatic layer may be able to come to the surface and contribute to non-convective or convective wind gusts, which will enhance dust lofting potential.

1.1.5.6.7. *Determine the type of dust storm (shamal, frontal, or convective) that's likely to occur, and make and verify your forecast.* Couple the knowledge gained from previous steps with knowledge of the different varieties of dust events that may occur; the general characteristics of the major dust storm types were detailed earlier in the chapter. Forecast if and when dust will be lofted, and when it will settle; the height of a dust plume can be approximated by the maximum height of the dry adiabatic layer in the environment in which the plume occurs, and dust settles at a rate of 1000 feet per hour once surface winds drop below 15 knots or an outflow boundary has passed. Verify your forecast using surface observations and METSAT data.

1.1.5.7. Summer shamal forecast process.

1.1.5.7.1. *Determine the mission scenario.* Determine the time period of interest; you'll be interested in any dust events that may occur during this time period which may rapidly restrict visibility or negatively impact any missions scheduled or ongoing in your AOR.

1.1.5.7.2. *Examine thunderstorm and blowing dust climatology.* Refer to AFW-WEBS and the 14th Weather Squadron to determine the climatological likelihood of dust storms at your location.

1.1.5.7.3. *Conduct sounding analysis.* Examine a morning sounding within or near dust source regions; note the strength of any inversions and determine if they will break due to turbulent mixing and/or daytime heating. Look for winds that are nearly unidirectional or in-phase through the portion of the troposphere where the lapse rate is dry adiabatic. Add 5-10 knots to low-level wind forecasts if winds are in-phase up to 700 mb (with a dry adiabatic lapse rate), and add 10-15 knots if winds are in-phase up to 500 mb (with a dry adiabatic lapse rate). Note that the strongest wind within the dry adiabatic layer may be able to be brought to the surface in the form of non-convective surface wind gusts. The height of an elevated dust layer can be approximated by determining where the lapse rate becomes less than dry adiabatic.

1.1.5.7.4. *Conduct surface analysis.* Look for surface wind speeds greater than or equal to 15 knots over relevant source regions; remember to add 5-15 knots to your surface wind speed forecast if winds are in-phase up to 700 mb or 500 mb and the layer is dry adiabatic. Also remember that the strongest wind speed within the dry adiabatic layer can be brought to the surface. Look for wind speeds at 1000 feet AGL (925 mb is a good approximation) greater than or equal to 26 knots over southern Iraq and greater than or equal to 30 knots over Bahrain.

1.1.5.7.5. *Conduct METSAT imagery analysis.* Use single channel or, preferably, multi-spectral imagery to determine the extent and location of any existing dust plumes.

1.1.5.7.6. *Make and verify your dust storm forecast.* Forecast the onset, duration, and persistence of any dust events in your area of responsibility during the proposed time period of mission execution (often in the 6-24 hour time period). Ensure you note any local rules of thumb about dust advection, as well as any geographic features such as small dust source regions, terrain, vegetation, and water sources. Note where precipitation has fallen in the past 48 hours; it'll be much more difficult for dust to be lofted in these areas than in areas with dry soil characteristics.

> 1.1.5.7.6.1. Verify your forecast by examining METSAT imagery during the mission window and from PIREPS, if available.

1.1.5.8. Haboob forecast process.

1.1.5.8.1. *Determine the mission scenario.* Determine the time period of interest; you'll be interested in any dust events that may occur during this time period which may rapidly restrict visibility or negatively impact any missions scheduled or ongoing in your AOR.

1.1.5.8.2. *Examine thunderstorm and blowing dust climatology.* Refer to AFW-WEBS and the 14th Weather Squadron to determine the climatological likelihood of dust storms at your location.

1.1.5.8.3. *Examine a recent dust source region database*. Examine the most recent analysis of dust source regions; couple climatology data with historical dust source region information to determine where dust events are most likely to develop. Areas where thunderstorms are most likely and that are located within or downstream of dust source regions have the highest climatological haboob potential.

1.1.5.8.4. *Conduct instability analysis.* Using either observed soundings or model data, determine if any elevated instability will be present for updraft development. If using observed soundings without model data, lift the Most Unstable (MU) parcel in the lowest 300 mb of the atmosphere dry adiabatically to its Lifting Condensation Level (LCL). Above the LCL, lift the parcel moist adiabatically to the top of the sounding. Calculated the Lifted Index (LI) by subtracting the temperature of the environment at 500 mb from the temperature of the parcel at 500 mb. A negative LI (less than -2) indicates that convection is possible later in the day. If using model data, examine forecast charts of the Best Lifted Index.

1.1.5.8.5. *Conduct mid-level moisture analysis.* Diagnose negatively buoyant downdraft potential by examining the contribution due to high water droplet and/or ice crystal concentration, as well as resultant precipitation. Using either observed soundings or model data, determine the maximum relative humidity (RH) in the 700 mb to 400 mb layer. Precipitation aloft is possible where RH is greater than 90% in the 700-400 mb layer. Water droplets falling into a deep, dry planetary boundary layer (PBL) will evaporate and cool the PBL; this is often seen as virga falling from high-based cumulus clouds. At temperatures below -5°C in the 700-400 mb moist layer, a percentage of water vapor will form as ice crystals, further cooling the PBL as they fall into it. Therefore, the higher the RH (greater than 90%) at temperatures below -5°C in the 700-400 mb layer, and the colder the temperatures, the stronger the potential downdraft. If using model data, examine 700 mb and 500 mb forecast charts that plot RH, or examine forecast sounding data in the 700-400 mb layer.

1.1.5.8.6. *Examine surface to 500 mb lapse rates.* Diagnose negatively buoyant downdraft potential by examining the contribution to downdraft strength due to cold temperatures aloft. Using observed soundings, determine the rate of environmental temperature decrease from the surface to 500 mb (approximately 18,000 feet, or 5.5 km). Subtract the environmental temperature at 500 mb from the surface temperature, and divide this temperature difference by 5.5 km to get an average lapse rate in the surface to 500 mb layer (units: °C/km). The steeper the environmental lapse rate (greater than 5°C/km, with 9.8°C/km optimal), the more negatively buoyant and stronger the potential downdraft. Dust is most easily lofted where the lapse rate within the PBL is dry adiabatic. The maximum height a dust plume can achieve is approximated by the height at which the environmental lapse rate ceases to be dry adiabatic (i.e., less than 9.8°C/km).

1.1.5.8.7. *Find the strongest wind aloft that could be brought to the surface.* If wet-bulb potential temperatures aloft are less than the potential temperature at the surface by at least 4°C, the strongest wind at any of those levels may be able to be brought to the surface, contributing to downdraft strength. Convective downdrafts that result in haboobs will remain negatively buoyant as long as this temperature differential is maintained; the 4°C difference is required because downdrafts may punch through a shallow layer that is somewhat stable to downward motion (i.e., where the wet bulb potential temperature is slightly greater than the surface potential temperature).

1.1.5.8.8. *Determine if the mission environment is conducive to haboobs.* Assess haboob potential based on the analyses conducted in the previous steps, and incorporate dust model data where applicable. With current technology, it's not possible to definitively forecast when and where individual haboobs will develop. But using this method, you can determine if the haboob threat in the mission area is minimal, slight, moderate, or high.

1.1.6. Visibility Forecasting Aids and Techniques.

1.1.6.1. Haze. The Air Force's GEPS and MEPS ensembles produce a Pollution Trapping Index (PTI), which determines the potential for reduced visibility due to haze – the PTI probability products are available from the ensembles main page on AFW-WEBS. Favorable values for pollution trapping are achieved when lapse rates are stable (negative) and winds are light. Under these conditions, pollutants such as sulfuric acid are likely to linger and thicken, producing haze. PTI is calculated using the lapse rate and wind, based on the following algorithm and interpreted according to **Table 1.6**.

Table 1.6. Interpretation of the GEPS and MEPS Pollution Trapping Index (PTI) index.

PTI Value	Pollution Trapping Potential
Greater than -40	Minimal
Greater than -30	Slight
Greater than -20	Moderate
Greater than -10	High

$$PTI = -1.0 \times (LAPSE + WIND^2)$$

LAPSE = Surface to 700 mb lapse rate in Kelvin/km (positive = unstable)
WIND = 10 meter surface wind (m/s)

1.1.6.2. Snow. The GEPS and MEPS produce two blowing snow products, available on AFW-WEBS: joint probability of wind gusts greater than or equal to 25 knots and six-hour snow accumulation greater than 0.1 inch, and joint probability of wind gusts greater than or equal to 35 knots and six-hour snow accumulation greater than one inch. Although these products don't directly indicate the probability of reduced visibility due to blowing snow, they do indicate the probability of strong winds and accumulating snow occurring concurrently, leading to reduced visibility.

1.1.7. Final thoughts on visibility forecasting. Experience plays an important role in visibility forecasting – consider the following:

1.1.7.1. Actual Prevailing Visibility. A drop in visibility (i.e., from 25 miles to 15 miles) could indicate a significant increase in low-level moisture that could go unnoticed in a 7+ mile report.

1.1.7.2. Sector Visibility. If sector visibility is significantly different from prevailing, it could mean something significant is occurring. For example, the lowering of sector visibility could mean a fog bank is forming or that dust is rising due to an increase in winds from a thunderstorm.

1.1.7.3. Obstructions to Visibility. Reports should include what is obstructing vision (i.e., fog, smoke, haze, etc.) as well as an estimated layer height top and/or base. For example, "visibility 10 miles in haze, top of haze layer approximately 1500 feet," includes haze as being the obstruction to vision and identifies the layer of haze.

1.1.7.4. Tops and Bases of Haze Layers. These are important because they may indicate the bases of inversions. Tops and bases of haze layers are usually difficult to estimate, but a definite top and/or base is sometimes detectable when looking towards the horizon. Determine the height by noting the orientation to higher terrain, trees, or buildings, if available. Pilot reports of haze tops and/or bases are also useful.

1.2. Precipitation. For precipitation to occur, two basic ingredients are necessary: moisture and a mechanism for lifting the air sufficiently to promote condensation. Lifting mechanisms include convection, orographic lifting, and frontal lifting. There are many techniques and methods available for forecasting precipitation.

1.2.1. Precipitation General Guidance.

1.2.1.1. Extrapolation. Extrapolation works best in short-period forecasting, especially when precipitation is occurring upstream of the station. First, outline   areas of continuous, intermittent and showery precipitation on an hourly or 3-hourly surface product. Use radar and satellite data to refine the surface chart depiction. Use different types of lines, shading, or symbols to distinguish the various types of precipitation. Next, compare the present area to several hourly (or 3-hourly) past positions. If the past motion is reasonably continuous, make extrapolations for several hours. (Note: Consider local effects that may block or slow the movement of the extrapolated area.)

1.2.1.2. Cloud Top Temperatures. The thickness of the cloud layer aloft and the temperatures in the upper levels of clouds are usually closely related to the type and intensity of precipitation observed at the surface, particularly in the mid- latitudes. Monitor satellite imagery to determine if cooling cloud tops are occurring (indicating upward vertical motion). In general, colder cloud tops correspond to a greater chance of precipitation.
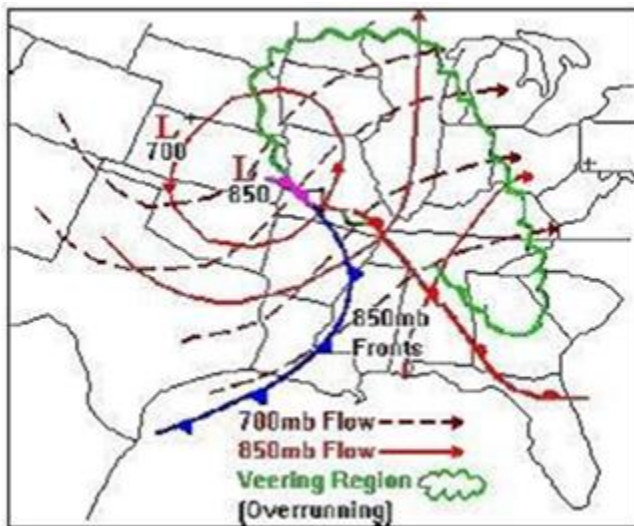
1.2.1.3. Dew Point Depression. An upper level dew point depression less than or equal to 2°C is a good predictor of both overcast skies and precipitation. Dew point spreads less than or equal to 2°C on the 850 and 700 mb forecast products are a good indication of potential precipitation, assuming there is also upward vertical motion.

1.2.1.4. Overrunning. Overrunning precipitation occurs in association with active warm fronts, stationary fronts and, to a lesser degree, with slow-moving cold fronts (**Figure 1.11**). Stratus is a by-product and generally results from the evaporation of relatively warm precipitation into cooler air. Use the 925 mb, 850 mb and 700 mb products to determine whether sufficient moisture and vertical motion are present to produce overrunning precipitation:

1.2.1.4.1. The 925 mb and 850 mb products reveal whether the wind flow is favorable for the advection of this moisture into the area.

1.2.1.4.2. The 700 mb product reveals if the thermal structure is adequate to produce overrunning precipitation. In general, overrunning requires warm-air advection and cyclonic curvature at 700 mb to produce significant precipitation. Therefore, the outer limits of overrunning precipitation are usually the 700 mb ridge line in advance of the system (beginning of precipitation) and behind the system where the wind changes from veering with height (warm- air advection) to backing with height (cold-air advection and the ending of precipitation).

Figure 1.11. Overrunning associated with a typical cyclone.

1.2.1.5. Drizzle Formation. The basic requirements for significant drizzle are:

1.2.1.5.1. A cloud layer or fog at least 2000 feet deep.

1.2.1.5.2. Cloud layer or fog must persist several hours to allow droplets time to form.

1.2.1.5.3. Sufficient upward vertical motion to maintain the cloud layer or fog.

1.2.1.5.4. A source of moisture to maintain the cloud or fog. Light drizzle can fall from radiation and sea fog without the help of upward vertical motions.

1.2.1.5.5. Identify areas of potential upward vertical motion by drawing streamlines on surface charts to locate and track local axes of confluence. Make a reasonable estimate of whether surface confluence is stronger or weaker than usual. Drizzle onset is faster and more likely with stronger confluence.

1.2.1.5.6. Upslope flow and/or sea breeze confluence can produce the weak upward vertical motion required for drizzle formation, without surface observations indicating local confluence. Similarly, persistent large-scale southerly flow naturally converges as it moves northward, and can also provide the required low-level upward motion. Finally, the lift associated with a nearby front can supply the upward motion to generate large areas of fog and stratus. In these instances, it's possible to extrapolate the onset of drizzle at your location from upstream stations. If surface temperatures are less than or equal to 0°C (32°F), forecast freezing drizzle.

1.2.2. Determining Precipitation Type.
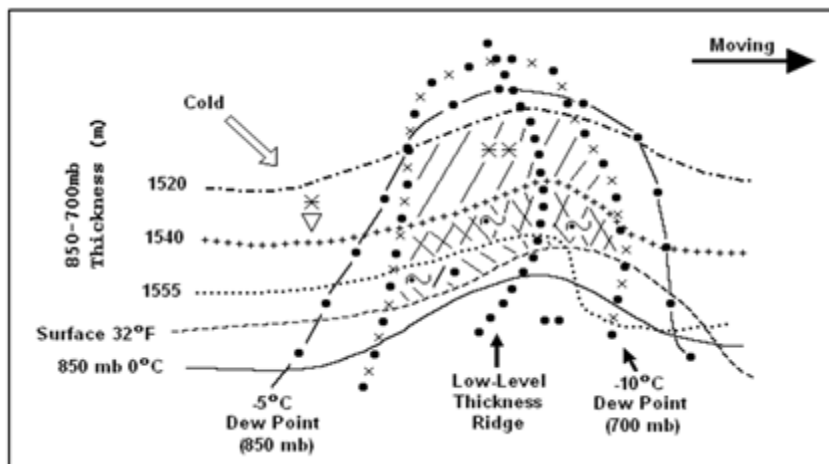
1.2.2.1. *Thickness.* Thickness (the vertical distance between two constant-pressure surfaces) is the most common predictor for precipitation type. Thickness is a function of temperature: the warmer the air, the thicker the layer. If the thickness of the layer is known, then the layer's mean temperature can be determined. The most used 1000-500 mb thickness value for forecasting precipitation type is the 540 (5400 meter) threshold. Another predictor is the 0°C 850 mb isotherm. A third predictor is the 850-700 mb, 1550-meter thickness line. Studies have shown that snow is rare when the 850-700 mb thickness is greater than 1550 meters, or the 1000-500-mb thickness is greater than 5440 meters.

1.2.2.1.1. Analyzing and Extrapolating Thickness Patterns – Method 1. This method requires that both the low- and mid-level thickness be calculated and plotted, but the precipitation analysis is rapid and straightforward. Using forecast charts, plot the following parameters:

1.2.2.1.1.1. Mid-level thickness (700 mb height minus the 850 mb height).

1.2.2.1.1.2. Low-level thickness (850 mb height minus the 1000 mb height).

1.2.2.1.1.3. 700 mb height contours.

1.2.2.1.1.4. 700 mb dew points.

1.2.2.1.1.5. 850 mb dew points.

1.2.2.1.1.6. The surface 0°C (32°F) isotherm.

1.2.2.1.1.7. The 850 mb 0°C (32°F) isotherm.

1.2.2.1.1.8. Analyze the mid-level thickness for the 1520- and 1540-meter contours and analyze for these dew points: –5°C (850 mb) and –10°C (700 mb). Forecast two or more inches of snow to occur in the area within these lines where precipitation is expected (see **Figure 1.12**). Analyze the mid-level thickness for the 1555-meter line. Forecast freezing precipitation to occur in the area between this line and the 1540-meter line and within the above dew-point lines, provided the surface temperature is below freezing. Find any areas of appropriate thickness but lacking sufficient moisture at either 850 mb or 700 mb. Be alert for any changes in the moisture pattern by advection or vertical motion. Expect only liquid precipitation on the warm side of the 850 mb 0°C (32°F) isotherm.

Figure 1.12. Method 1 – the plot shows where to expect different precipitation types.

1.2.2.1.2. Analyzing and Extrapolating Thickness Patterns – Method 2. This method requires extrapolation of analyzed thickness contours to their appropriate position at the valid time of the precipitation forecast. The following are general rules for this method of extrapolating thickness patterns:

1.2.2.1.2.1. Low-Level Thickness. Choose several 1000-to-850 mb thickness lines that give a good estimate of the thickness pattern; e.g., the 1300-, 1340-, or 1380-meter lines. Move each line in the direction of the wind at 3000 feet with 100 percent of that wind speed. The thickness ridge moves at the speed of the associated short wave. In a strongly baroclinic situation, it moves slightly to the left of the 500 mb flow at 50 percent of the wind speed. Since thickness patterns merely depict the large-scale mass distribution, take care to adjust for rapid changes at 500 mb. Compare the thickness analysis with the surface analysis to ensure a reasonable forecast product.

1.2.2.1.2.2. Mid-Level Thickness. Move the 1520- to 1540-meter band at 100 percent of the 8000-foot wind field. Consider continuity, the latest surface analysis, and other charts when developing a new thickness forecast chart.

1.2.2.1.2.3. Snowfall begins with the approach of a low-level thickness ridge after the passage of the 700 mb ridge line or the line of no 12-hour temperature change (the zero isallotherm) and with the approach of the low-level thickness ridge. Snowfall usually ends after the passage of the low-level thickness ridge and the 700 mb trough. Snowfall is heaviest 1 to 2 hours beforehand, and ends after the passage of the low-level thickness ridge and the 700 mb trough.

1.2.2.2. *Freezing Precipitation Indicators.*

1.2.2.2.1. Height of the Freezing Level. Forecasters often use the freezing level to determine the type of precipitation (see **Table 1.7**). The forecast is based on the assumption that the freezing level must be lower than 1200 feet above the surface for most of the precipitation reaching the ground to be snow. However, forecasters must understand the complex thermodynamic changes occurring in the low levels to correctly forecast winter precipitation situations. For example, the freezing level often lowers 500 to 1000 feet during first 1.5 hours after precipitation begins, due to evaporation or sublimation. When saturation occurs, these processes cease and freezing levels rise to their original heights within 3 hours. With strong warm air advection, the freezing level rises as much as a few thousand feet in a 6- to 8-hour period. The following methods account for both single or multiple freezing levels to forecast the type of precipitation expected at the surface. Each method considers the change of state of precipitation from liquid-to-solid or solid-to-liquid as it falls through the atmosphere.

Table 1.7. Probability of snowfall as a function of freezing level height.

Height of freezing level above ground	Probability precipitation will fall as snow
12 mb	90%
25 mb	70%
35 mb	50%
45 mb	30%
61 mb	10%

1.2.2.2.1.1. Single Freezing Level. If the freezing level equals or exceeds 1200 feet above ground level (AGL), forecast liquid precipitation. If the freezing level is less than or equal to 600 feet AGL, forecast solid precipitation. If the freezing level is between 600 and 1200 feet AGL, forecast mixed precipitation.

1.2.2.2.1.2. Multiple Freezing Levels. When there are multiple freezing levels, warm layers exist where the temperature is above freezing. The thickness of the warm and cold layers affects the precipitation type at the surface. If the warm layer is greater than 1200 feet thick and the cold layer closest to the surface is less than or equal to 1500 feet thick, forecast freezing rain. Conversely, if the warm layer is greater than 1200 feet thick and the cold layer closest to the surface is greater than 1500 feet thick, forecast ice pellets. Finally, if the warm layer is between 600 and 1200 feet thick, forecast ice pellets regardless of the height of the lower freezing level.

1.2.2.2.2. Forecasting Snow vs. Freezing Drizzle. This technique is based on the precipitation nucleation process, and applies to the continental United States, Europe, and the Pacific theater. The technique below assumes the atmosphere is below freezing through its entire depth, and the water droplets remain supercooled until surface contact.

1.2.2.2.2.1. Does a lower-level moist layer (below 700 mb) extend upward to where temperatures are –15°C? If not, then freezing drizzle is possible.

1.2.2.2.2.2. Is a mid-level dry layer (800 to 500 mb) present or forecast? If yes, freezing drizzle or a mixture of snow and freezing drizzle is possible.

1.2.2.2.2.3. Is the mid-level dry layer (dew point depression greater than or equal to 10°C) deeper than 5000 feet? If yes, precipitation may change to freezing drizzle, or a prolonged period of mixed snow and freezing drizzle is possible.

1.2.2.2.2.4. Is mid-level moisture increasing? If freezing drizzle is occurring and mid-level moisture is increasing, precipitation may change to all snow.

1.2.2.2.2.5. Is elevated convection occurring or forecast to occur? If yes, the mid-level dry layer may be eroded, causing snow instead of freezing drizzle.

1.2.3. Freezing Precipitation. Detailed descriptions of the three primary types of freezing precipitation are presented below.

1.2.3.1. Freezing rain. Freezing rain is rain that falls in liquid form but freezes upon contact with sub-freezing surfaces. In the majority of cases, rain must be supercooled (i.e., below freezing) before striking the surface. The two factors that exert the greatest influence on freezing rain potential are the depth and average temperature of the melting layer. **Figure 1.13** is a graphical summary of this relationship, and an example of how these factors are primary influences on ice pellet (or sleet) development as well. The figure shows that precipitation type will be ice pellets regardless of melting layer temperature when its depth is less than about 400 meters. Similarly, when the melting layer is greater than 4000 meters deep, precipitation type will almost always be freezing rain, regardless of the layer's average temperature. **Figure 1.14** is an example of a sounding environment in which freezing rain would be observed. Freezing rain will rarely be observed at surface temperatures colder than -10°C (14°F), since too many ice crystals are present for liquid (supercooled) water to remain the predominant hydrometeor type. In fact, most freezing rain events occur with surface temperatures between 0°C (32°F) and -5°C (23°F). Freezing rain usually occurs when the air is very moist (relative humidity [RH] with respect to water greater than 90%) from the surface through 700 mb and into the dendritic layer. This ensures that snowflakes will develop in the dendritic layer. These snowflakes may melt as they fall through the melting layer, becoming supercooled raindrops. The depth of the refreezing layer is also an important consideration, but less so than the above factors. The deeper the refreezing layer, the more likely that a liquid raindrop will become frozen again and reach the surface as sleet or snow rather than freezing rain. The RH within the melting layer must be considered as well. The lower the RH, the greater the distance required for complete melting of snowflakes aloft given the evaporative cooling component. A snowflake falling through a melting layer with 90% RH may take an additional 100 meters to melt than if that same layer was saturated (RH = 100%). Finally, the size and type of snowflakes falling into a melting layer play a role in the melting layer depth and average temperature required for complete snowflake melting. Larger snowflakes (those composed of stellar dendrites or sector plates, for example) require a larger melting layer depth and higher average temperature to melt completely before falling into the refreezing layer. **Figure 1.15** is a nomogram of precipitation type based on the 1000 mb wet bulb temperature (°C) and the 850 mb wet bulb temperature (°C), and **Figure 1.16** utilizes 1000 to 850 mb thickness (m) and 850 to 700 mb thickness (m) to estimate precipitation type.

Figure 1.13. Melting layer depth vs. mean layer temperature for freezing rain potential.
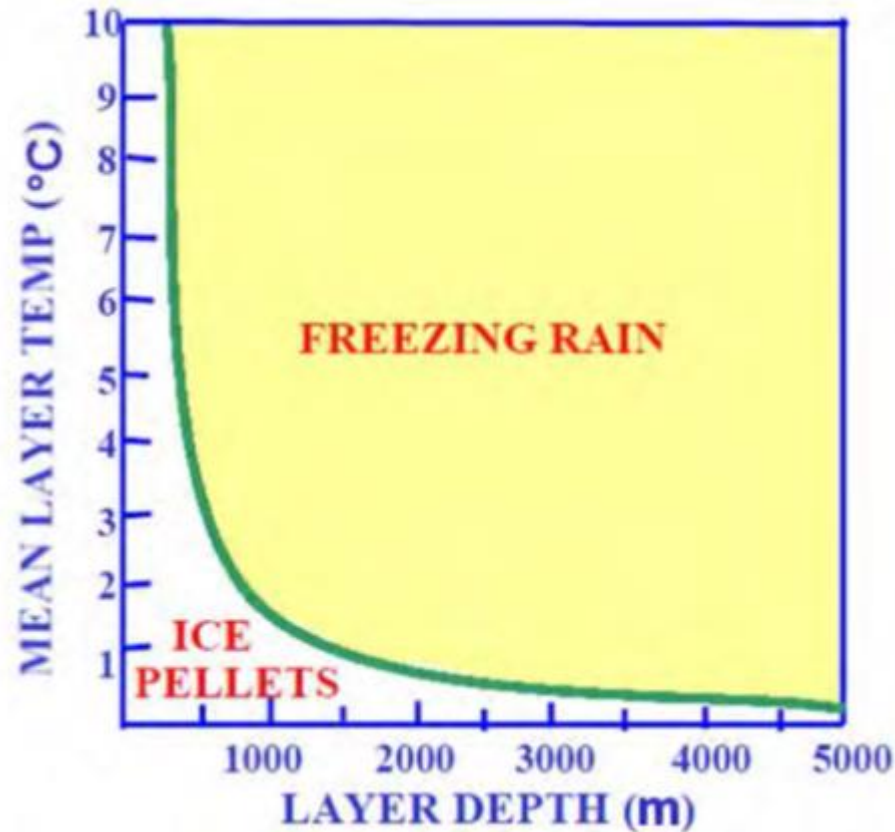
Figure 1.14. Typical freezing rain sounding. Note the depth and magnitude of the melting layer, as well as the moisture into the dendritic layer.
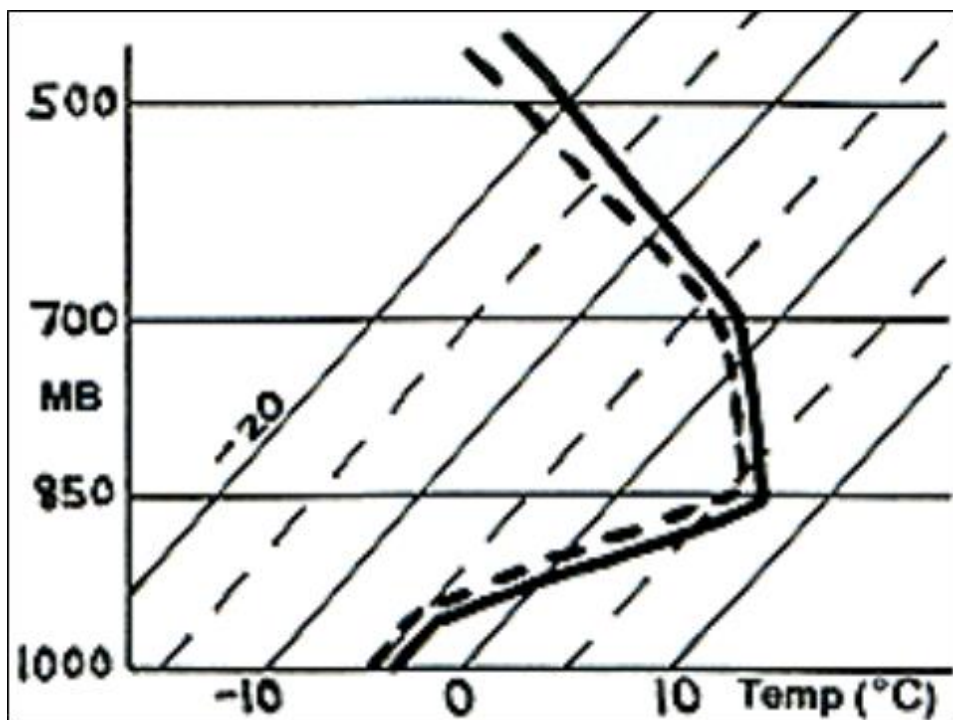
Figure 1.15. Precipitation type nomogram, based on 1000 mb and 850 mb wet bulb temperatures.
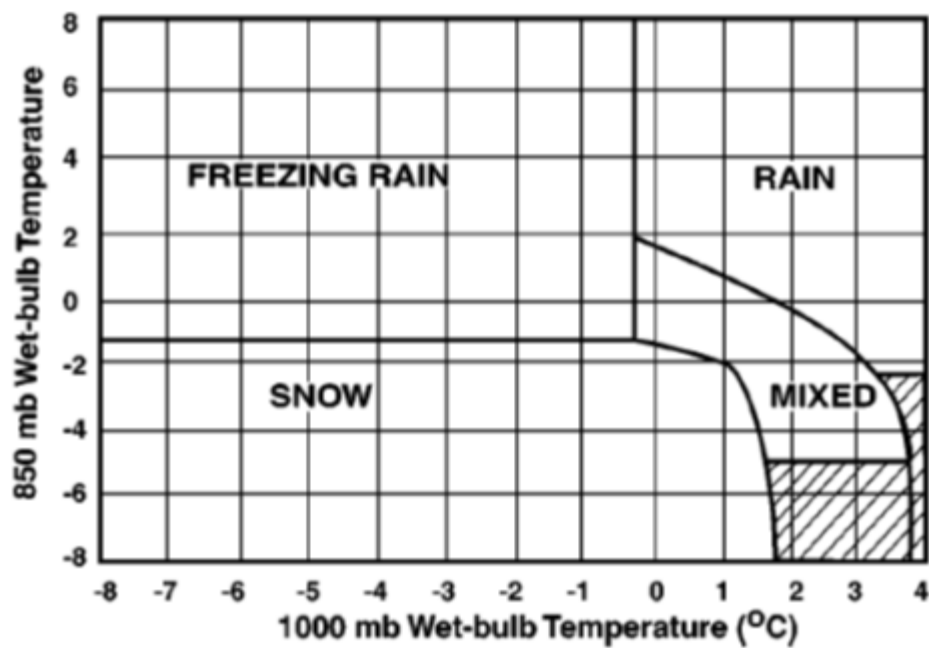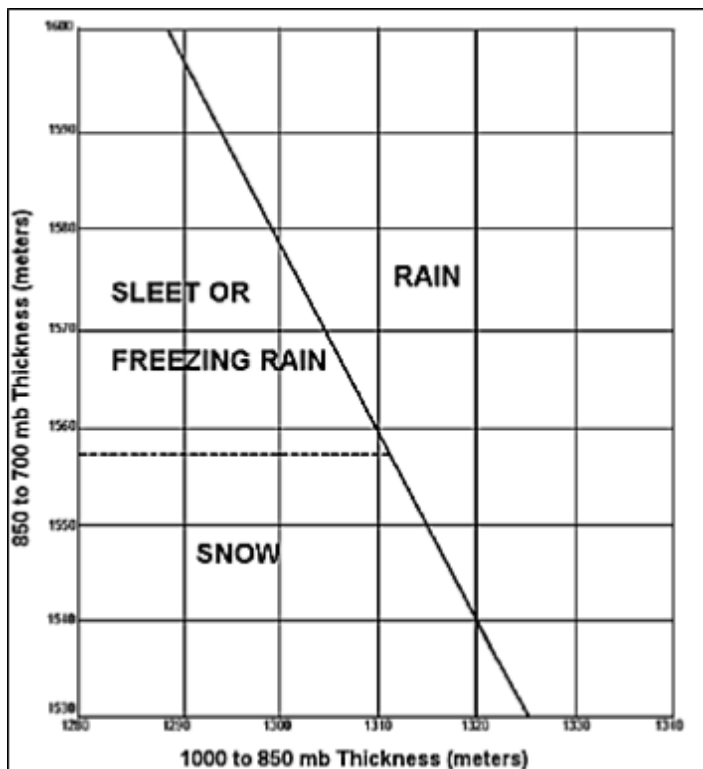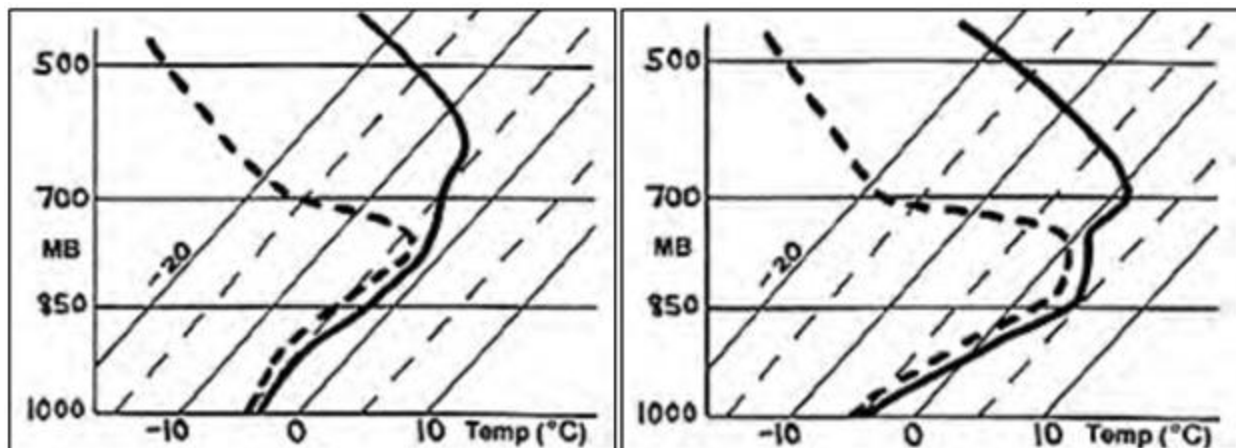
Figure 1.16. Precipitation type nomogram, based on 1000-850 mb and 850-700 mb thicknesses.

1.2.3.2. Freezing drizzle. Freezing drizzle is precipitation in the form of small, liquid water droplets that freeze upon contact with a surface that is colder than 0°C. Like freezing rain drops, freezing drizzle droplets must be supercooled (colder than 0°C) before reaching the surface. **Figure 1.17** shows examples of sounding environments in which freezing drizzle would be expected. Precipitation type will rarely be freezing drizzle if in-cloud and surface temperatures are below -10°C. Ice particles become much more common at temperatures colder than -10°C and tend to deplete small supercooled water droplets necessary for drizzle formation, so frozen precipitation such as light snow or even sleet become more likely when temperatures fall below -10°C. While freezing rain and sleet have deep moisture profiles with high RH extending into the -10°C to -20°C dendritic layer, the moisture associated with freezing drizzle is almost always found below 700 mb, with very dry air aloft. As is apparent in **Figure 1.17**, the entire moisture profile need not be below freezing for freezing drizzle to be observed at the surface. The top of the cloud can be above freezing as long as the surface layer is below freezing so the drizzle droplets that have developed become supercooled before they reach the surface. Freezing drizzle is less likely in desert or continental environments with copious amounts of dust that can serve as cloud condensation nuclei (CCN). A lack of CCN allows the distribution of small water droplets to be quite broad, increasing the efficiency of the collision-coalescence process by which water droplets develop, and making it easier for drizzle droplets to form. Therefore, freezing drizzle becomes much less likely when cloudy air is filled with CCN. Freezing drizzle almost always falls from stratiform clouds, and the stratiform cloud depth (or thickness) must be at least 200 meters for the microphysical processes to function efficiently. The deeper the stratiform cloud deck, the longer the freezing drizzle is likely to
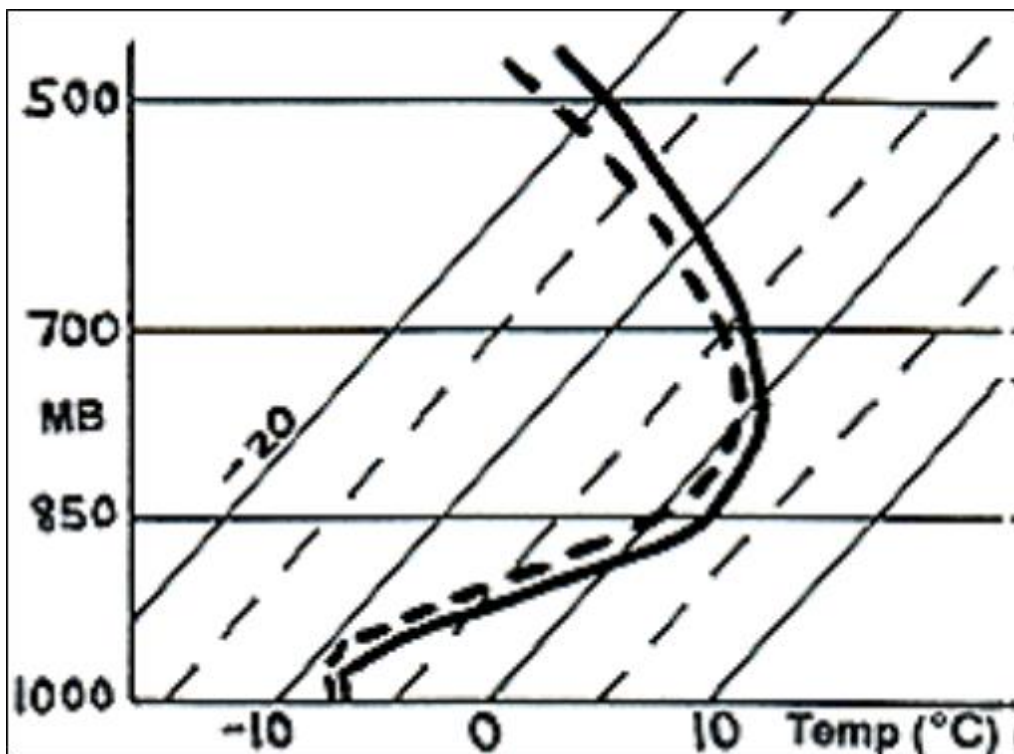
last, although the cloud deck can't be so deep as to be seeded by ice crystals that deplete supercooled water droplets. As with freezing rain and sleet, there must be a source of lift (i.e., vertical motion) for freezing drizzle to develop, but only weak vertical motion (5-10 cm/s) is required for drizzle as opposed to the stronger vertical motions that would be required for freezing rain or sleet. In the freezing drizzle sounding to the left in **Figure 1.17**, the moist layer extends up to 750 mb and is warmer than -6° C. In the freezing drizzle sounding on the right in **Figure 1.17**, an above-freezing cloud layer extends from 925 mb to 750 mb, but the surface-to-925 mb layer is below freezing, allowing some above-freezing droplets to become supercooled before impacting the sub-freezing surface.

Figure 1.17. Freezing drizzle soundings.

1.2.3.3. Sleet. Sleet (a.k.a. ice pellets) is precipitation in the form of transparent or translucent pieces of ice less than 5 millimeters (mm) in diameter. The two factors that exert the greatest influence on sleet potential are the depth and average temperature of the melting layer (refer back to **Figure 1.13** for a graphical summary of this relationship). Precipitation type will be sleet regardless of the melting layer temperature when its depth is less than about 400 meters. In this situation, ice particles that fall into the melting layer don't have enough time to melt because the layer is too shallow, or the mean temperature of the layer is too cold. Note in **Figure 1.13** that the distribution of mean melting layer temperatures and melting layer depth for sleet is much less than for freezing rain, an illustration of the rarity of sleet vs. freezing rain and snow. Sleet is often the "transition" precipitation between freezing rain and snow as the magnitude and depth of the melting layer diminishes or changes with temperature advection and microphysical processes. **Figure 1.18** is an idealized sounding environment in which sleet would be observed. The melting layer is relatively deep in this case, but barely above freezing. Also note that moisture extends into the dendritic layer. Unlike freezing drizzle and freezing rain, sleet can occur with surface temperatures well below freezing in an environment with a very strong temperature inversion. As with freezing rain, sleet requires saturated or near saturated conditions (RH greater than 90%) from the surface past 700 mb and into the dendritic layer. If the dendritic layer is not supersaturated with respect to ice (RH greater than 100%), ice crystals will not grow and none will be present to fall into the melting layer.

Figure 1.18. Idealized sleet sounding.

1.2.3.4. Factors affecting freezing precipitation. The following factors should also be considered when determining the potential for freezing precipitation:

1.2.3.4.1. Cloud Condensation Nuclei (CCN). CCN are particulates in the atmosphere such as dust, minerals, and even ice crystals around which cloud droplets develop (or nucleate). The air in the troposphere is never 100% pure with no CCN. If no CCN existed, it would be very difficult for clouds and precipitation to develop at all. The type, size, and distribution of CCN in a column of air are the most important considerations for precipitation type and intensity. While high concentrations and relatively large CCN are favorable for heavier freezing precipitation such as sleet and/or freezing rain, a lower concentration of CCN is necessary for freezing drizzle formation because the droplet size distribution is broadened, allowing efficient collision and coalescence (or "sticking together") to occur. Therefore, in regions of high CCN concentrations such as near deserts or other continental areas where dust, soil, and mineral particles are abundant, freezing rain and sleet are more likely than freezing drizzle on most occasions. This is why freezing drizzle often occurs when a shallow, cold air mass replaces a warmer one, pushing away the low-level CCN.

1.2.3.4.2. Cloud depth. Cloud depth is the thickness of a cloud from its base to its top. For cumuliform clouds, the cloud base is assumed to occur at the height of the lifting condensation level (LCL), derived from a surface-based parcel. The parcel is then lifted moist adiabatically from the LCL to the point where the parcel temperature equals or becomes colder than the actual temperature of the atmosphere. This is called the equilibrium level (EL). The EL is assumed to be the cumuliform cloud top, although strong updrafts may allow a portion of the cumuliform cloud to "overshoot" the EL.

The depth of the cloud is found by subtracting the height of the cloud top from the LCL height above the ground. Because stratiform clouds, which often produce freezing precipitation, rarely form due to vertical motions from positive buoyancy, their depth must be estimated differently. Stratiform cloud depth can be directly estimated from the moisture characteristics of the sounding. This is done by using varying values of the dew point depression (DD), which is the difference between the temperature and the dew point, from the surface to some point aloft where the DD thresholds are no longer satisfied. A smaller DD indicates a greater potential that clouds exist at a given level. In general, the larger the cloud depth, the heavier any freezing precipitation that develops will be. Freezing rain, sleet, and snow require much larger cloud depths than freezing drizzle. However, the duration of freezing drizzle correlates closely with the depth of the cloud from which it is falling. Freezing drizzle duration increases as cloud depth increases past 200 m, but this depends on other factors as well, such as temperature and CCN concentration. Freezing rain, sleet, and snow soundings often indicate saturated or near saturated conditions from the surface up to 500 mb (through the -10°C to -20°C dendritic layer), while freezing drizzle soundings may only be saturated from the surface up to 850 mb.

1.2.3.4.3. Ground temperature. The ground temperature can warm or cool the temperature of the lowest few centimeters of the atmosphere via a process called conduction, but other than that, has little influence on the character of falling precipitation. It does, however, exert an enormous influence on the character of precipitation once it hits the ground. Precipitation may fall as rain, but be characterized as freezing rain if the ground temperature is 0°C or less. On the other hand, liquid precipitation may be supercooled (i.e., below freezing) as it falls through a sub-freezing layer, but if the ground temperature is greater than 0°C, it will not freeze upon contact with the surface, and thus be characterized as rain. The character of sleet is largely unchanged by ground temperature, except for the fact that ice pellets will melt if the ground temperature is greater than 0°C. Freezing rain and freezing drizzle will have little impact on ground temperatures when they reach the surface. In other words, ground temperatures may decrease slightly given the colder temperature of the droplets, but no melting, evaporation, or sublimation will occur to cool the temperature enough to change precipitation type. In fact, freezing rain and freezing drizzle often slightly raise the temperature of a sub-freezing ground surface by the phase-change from liquid to ice, which is a warming process. This offsets any sensible cooling of the ground surface by the cold precipitation, leaving the ground temperature largely unchanged. Sleet, because of its frozen character as it hits the surface, can lower the ground temperature by melting, whereby heat is removed from the ground to melt the ice pellets. As a result, sleet can start to accumulate on a ground surface that is slightly above freezing to begin with, because it lowers the ground temperature via melting. The same concept applies for heavy snow.

1.2.3.4.4. Relative humidity. When examining low-level relative humidity, it is best to look at an observed or model forecast sounding. In general, because most freezing precipitation occurs when temperatures range from 4°C to -10°C, it's safe to assume that the primary types of hydrometeors are water droplets or supercooled water droplets. Some ice crystals will be present below 0°C, but don't become abundant until temperatures drop to -10°C or colder. As the temperature decreases, the RH necessary for freezing precipitation development also decreases. For temperatures 0°C and above, RH with respect to water must be 90% or greater for precipitation development. At temperatures colder than 0°C, precipitation can still develop when RH is as low as 75%, because some ice crystals will be present to serve as effective CCN. The deeper the layer of high RH, the more intense freezing precipitation will be. If the moist layer is shallow, any precipitation will be light and in the form of freezing drizzle. If the layer is deep and extends past 700 mb, however, heavier freezing precipitation such as sleet and freezing rain becomes likely.

1.2.3.4.5. Low-level wet bulb temperatures. The wet bulb temperature is the temperature to which air could be cooled solely via evaporation. In many cases, low-level wet bulb temperatures are more important than actual temperatures. There are typically many cases during a mid-latitude (e.g., SWA, CONUS) autumn when low-level temperatures are above freezing, but because the low-levels are so dry, the wet bulb temperatures are below freezing. This means that if precipitation starts to fall into the dry low-levels and evaporates, the temperature will start to cool toward the wet bulb temperature. At the same time, water vapor is added to the low-levels, which increases the dew point toward the wet bulb temperature as well. This process is known as "wet-bulbing", and is often observed during the cold season in the form of lowering cloud bases as precipitation falls into dry air and evaporates, melts, or sublimates.

1.2.3.4.6. Low-level wind profile. The direction and speed of the low-level winds impact the timing, intensity, and duration of freezing precipitation events. Low-level winds direct moisture into an area of responsibility (AOR), but they can also advect moisture out of it. The stronger the inflow winds and the higher the mixing ratios being advected into an AOR, the more intense freezing precipitation will be. The duration of freezing precipitation events is also impacted by the direction and magnitude of moisture advection. Freezing precipitation requires a continuous supply of moisture to last for long periods of time. Therefore, as long as moisture is advected into an AOR and other factors remain favorable (mainly lift), precipitation will likely continue. Consider upstream moisture diagnostics such as mixing ratios, dew points, relative humidity, and dew point depressions. For freezing precipitation in particular, low-level moisture (water vapor) needs to be advected into existing cloud-covered regions, so the supplied water vapor and resultant supercooled water droplets can be used for ice crystal growth aloft (when considering freezing rain and sleet potential). Freezing drizzle also requires a continuous source of moisture below 850 mb, although temperatures are usually warm enough in freezing drizzle-producing clouds that ice crystals need not be in abundant supply. When the supply of upstream moisture runs out and moisture is no longer advected into the AOR, the microphysical processes that act to create and maintain clouds and precipitation cease to function, allowing clouds and precipitation to dissipate. Note that a loss of midlevel moisture will cause snow,

freezing rain, and sleet to dissipate, while freezing drizzle dissipates only from a loss of low-level moisture.

1.2.3.4.7. Sources of lift. As with all types of precipitation, some source of lift is needed for freezing precipitation development. Air that is lifted cools and eventually condenses into tiny water droplets, which may collide with each other and coalesce into larger water droplets that can fall to the ground as precipitation. A common source of lift in freezing precipitation environments is large-scale divergence (speed and/or direction) aloft, often evident on 200 mb and 300 mb charts. Frontal lift (warm, cold, or stationary) and other sources of low-level convergence are also common; warm fronts and stationary fronts will usually be confined from the surface to below 850 mb, while strong cold fronts can sometimes extend up to 700 mb. Orographic lift near large hills or mountains can be another source; this is particularly problematic if moist low-level air is impinging on the mountain barrier and lifted. Freezing precipitation may persist for several hours if there is a continuous moisture feed and the air mass is stagnant against the mountain barrier. On rare occasions, convection may develop that produces large accumulations of sleet or freezing rain. This may occur in a conditionally unstable atmosphere where stronger vertical motions are favored. Thundersnow may also develop if air is rapidly cooled below freezing by melting and evaporation.

1.2.4. Snowfall. The following key parameters should be examined when determining if an environment is favorable for heavy snow:

1.2.4.1. Relative humidity within the dendritic layer. Snow production is most efficient in the dendritic layer (the layer of the atmosphere between approximately -10°C and -20°C where microphysical processes for ice and snow growth are most efficient). For complex reasons, liquid water droplets can exist when temperatures are as cold as -40°C. Therefore, when dealing with precipitation formation processes below freezing, both supercooled water droplets and ice crystals exist at the same time. In the real atmosphere, ice crystals remain relatively scarce until the temperature drops to -10°C. Between -10°C and -20°C, ice crystals and supercooled water droplets coexist, and when temperatures cool below -20°C, ice crystals rapidly outnumber supercooled water droplets. The -10°C to -20°C layer, or the dendritic layer, is where most ice crystal and snowflake formation occurs. However, for precipitation to develop in the dendritic layer, all or part of the layer must be supersaturated with respect to ice. This means that the RH with respect to ice crystals must be greater than 100%. RH with respect to water is the ratio of the actual amount of water vapor in the air to how much the air cold hold if it was saturated. This is the version of RH that is depicted on all forecast and observational charts, and is the version you're used to. RH with respect to ice, on the other hand, is the ratio of the actual amount of water vapor in the air to how much water vapor the air could hold in the presence of ice crystals. Below freezing, RH with respect to ice crystals will always be greater than RH with respect to liquid water. Therefore, air may be unsaturated with respect to water droplets (RH less than 100%), and supersaturated with respect to ice crystals (greater than 100%) at the same time. As a result, ice crystals are allowed to grow at the expense of supercooled water droplets because the liquid droplets evaporate (RH less than 100%) into water vapor that then deposits onto existing ice crystals. In general, when RH with respect to water is greater

than 90% at below freezing temperatures, the air will be supersaturated with respect to ice crystals.

1.2.4.2. Low-level temperatures. When examining low-level temperatures, use an observed or model forecast sounding. Focus on the temperature at the surface, 925 mb, 850 mb, and 700 mb; any above-freezing layers will be located between the surface and 700 mb. Precipitation type will be all snow if one or more of the following temperature factors are satisfied:

    1.2.4.2.1. The surface to 700 mb layer is entirely below freezing.

    1.2.4.2.2. The surface temperature may be above freezing (up to about 5°C/41°F) with precipitation remaining snow. However, whether or not precipitation reaches the surface as snow depends on the depth of the above freezing layer at the surface; the deeper the layer, the more time snowflakes have to melt before reaching the ground. Generally, for precipitation to reach the surface as snow, the above freezing layer should not be more than 1,000 feet thick.

    1.2.4.2.3. Wet bulb temperatures from 700 mb to the surface are well-below freezing, even when actual temperatures are above freezing. Precipitation that develops in the mid-levels will evaporate as it falls into an unsaturated layer of air, raising that layer's dew point while simultaneously cooling its temperature. This brings actual low-level temperatures closer to the low-level wet bulb temperatures, which are below freezing if snow will occur.
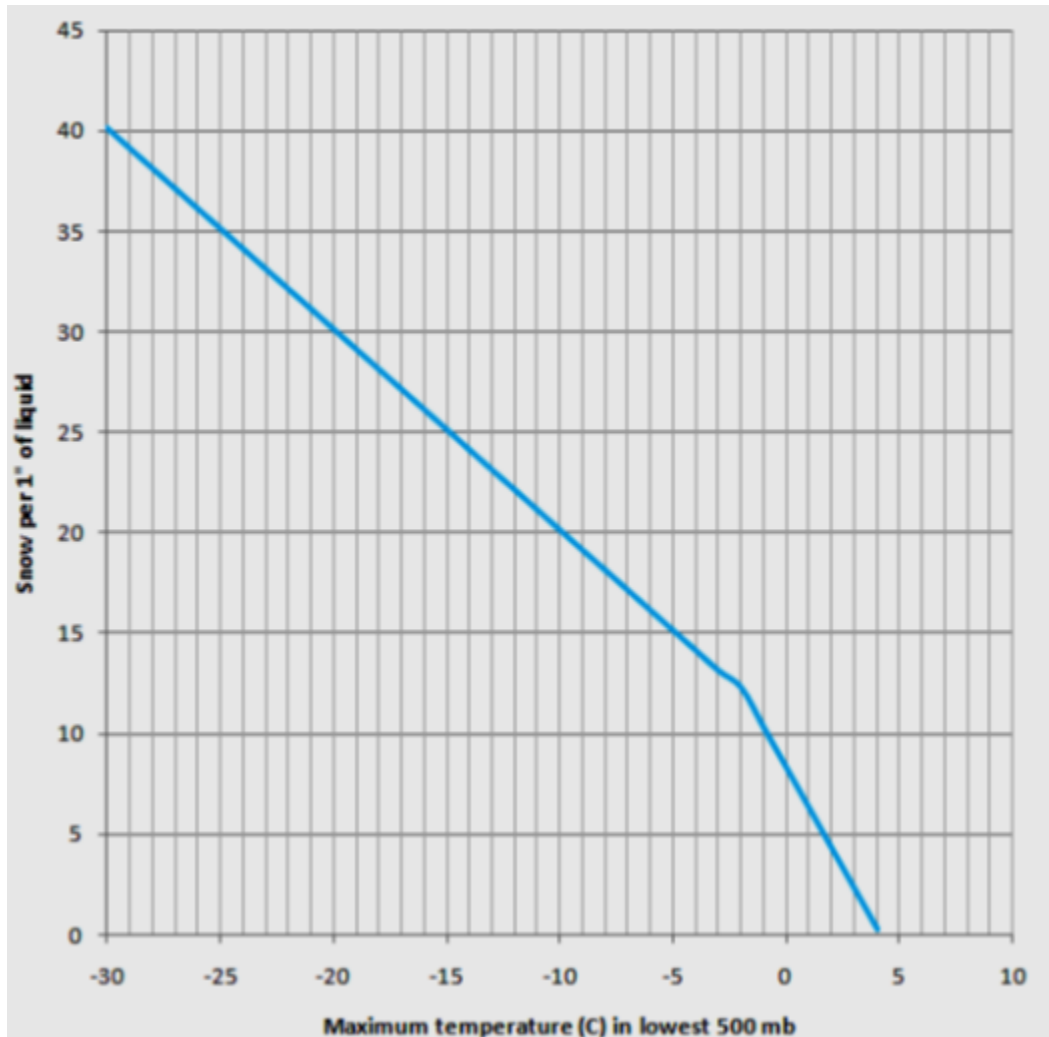
1.2.4.3. Low-level wet bulb temperatures. There are typically many cases during a mid-latitude season when the low-level temperatures are above freezing, but because the low-levels are so dry, the wet bulb temperatures are below freezing. This means that if precipitation starts to fall into the dry low-levels and evaporates, stealing heat from the ambient air, the temperature will start to cool toward the wet bulb temperature. At the same time, water vapor is being added to the low-levels, which increases the dew point toward the wet bulb temperature as well. If precipitation continues, at some point the temperature will have cooled, and the dew point will have warmed, to the wet bulb temperature, resulting in saturation (or supersaturation). This allows precipitation that was previously evaporating aloft to reach the surface. If the low-level wet bulb temperatures were below freezing, it's likely that the actual temperatures are now below freezing as well, allowing any precipitation to fall as snow. Therefore, when forecasting snow potential in an environment where precipitation type is challenging, the low-level wet bulb temperatures should always be considered. Watch for wet bulb temperatures below freezing, as well as layers of above-freezing low-level temperatures. The profile of wet bulb temperatures will likely match the appearance of the temperature/dew point profile once precipitation starts to fall aloft and ventures to the surface. Note that the wet bulb temperature concept neglects the other two physical processes that cool air: sublimation and melting. In cases of very heavy snow falling through a slightly unsaturated, above freezing layer of air near the surface, rapid melting of the large snowflakes will drop the temperature to or below freezing.

1.2.4.4. Upward vertical motion in the 700-500 mb layer. Most ice crystal and snowflake production occurs in the 700-500 mb layer; this is also where many of the complex microphysical processes involved in ice crystal growth occur. As with all forms of precipitation, for snow to develop, a source of lift is required. Unlike the spring and summertime, however, when low-level moisture is usually plentiful, that same moisture is lacking during the autumn and winter. In fact, the best moisture during the fall and winter is usually found in the mid-levels of the atmosphere, or between 700-500 mb. It follows that a source of lift below and within this layer is crucial for ice crystal and snow development. Lift within the 700-500 mb layer allows ice crystals to develop and grow by collecting supercooled water droplets (water droplets that exist below freezing) or via deposition of water vapor at the expense of supercooled water droplets. Without a continuous source of lift, not enough moisture would be available for precipitation (snow in this case) to continue. Hence, tracking the 700 and 500 mb lows is very important when developing a snow forecast, because they're proxies for how much lift may be ongoing in the 700-500 mb layer. In general, once the 500 mb and 700 mb lows move well to the east of an area of responsibility (AOR) in the Northern Hemisphere, lift starts to diminish and dry air is advected into the mid-levels, which effectively shuts off precipitation development processes.

1.2.4.5. Snow-to-Liquid Ratio (SLR). Snow-to-Liquid Ratio (SLR). SLR is the ratio of the amount of snow expected compared to an inch of liquid water; a 12-to-1 SLR means that one inch of liquid water would result in 12 inches of snow. SLR varies based on atmospheric conditions; the maximum temperature in the lowest 500 mb (MAXTEMP) of the atmosphere is the most significant variable in determining the SLR, as it has the most impact on snow density (**Figure 1.19**). Important factors to remember about SLR are:

1.2.4.5.1. Snow isn't observed when MAXTEMP exceeds 4°C (39°F).

1.2.4.5.2. As MAXTEMP decreases, SLR increases, because snow density decreases.

1.2.4.5.3. SLR decreases faster when MAXTEMP becomes warmer than -2°C, or around 28°F, because snow density increases at a greater rate as MAXTEMP warms beyond this point.

Figure 1.19. MAXTEMP and SLR relationship.

1.2.4.6. Low and mid-level winds. Wind speed and direction from the surface to 400 mb are important considerations for snow formation. For snow to continue developing inside a cloud, it must have a continuous supply of moisture. It's especially important for moisture to be ingested into the dendritic layer so ice crystals can continue to develop and grow, but moisture advection into the low-levels is also very important because this eventually supplies supercooled water droplets to the dendritic layer. Therefore, winds must be directed from a source of low- and mid-level moisture. Snow will usually start to dissipate when dry air advection occurs in the lower and middle atmosphere.

1.2.4.7. Precipitable water (PW). PW is a measure of the total amount of liquid water that would be present at the bottom of a cylinder if all the water in a column extending to the top of the atmosphere fell out as precipitation. PW is not a static parameter; it increases when water vapor is added to a column and decreases when it is removed. In addition, water vapor concentration generally decreases as pressure decreases with height, because sources of water vapor become scarcer and air expands with decreasing pressure. As such, a large percentage of a PW value will come from water vapor in the lower atmosphere. Higher values of PW mean more water vapor is present in the atmosphere for precipitation.

PW is an excellent diagnostic tool when determining heavy rain potential, but is also useful for forecasting snow amounts. In general, the higher the PW value, the more snow will fall. However, higher PW values are often coincident with warmer low-level temperatures as well, which decreases the SLR, resulting in smaller snow accumulations than one would expect. This will not be the case if moisture is confined to the low-levels while the dendritic layer is unsaturated. It's also important for vertical wind shear (VWS) within the cloud layer to be unidirectional and quite weak. This allows the clouds to remain upright, which promotes maximum efficiency of the microphysical processes involved in ice crystal and snowflake development.

1.2.4.8. Ground temperatures. The temperature of the soil or ground surface is of critical importance when forecasting snow amounts. Snow will take longer to start accumulating on warmer surfaces, which will reduce accumulations. Ground temperature varies with time of day and time of year. Cooler ground temperatures are generally realized after dark and during cold seasons. However, snow itself causes the surface to instantaneously cool via conduction and melting. As snowflakes hit the ground, sensible heat is transferred from the warmer ground to the colder snowflake. This causes the ground to cool. In addition, as the snowflake melts when it hits the warmer ground, the latent heat of fusion is absorbed by the snowflake, which further cools the ground. Heavy snowfall is best at reducing ground temperatures because the aforementioned processes are accelerated.

1.2.5. Precipitation Forecasting Aids and Techniques – Freezing Precipitation.

1.2.5.1. Precipitation type and wet bulb temperature nomogram. Refer to **Figure 1.15** for a quick-reference likelihood of freezing precipitation based on a comparison of the 1000 mb and 850 mb wet bulb temperatures.

1.2.5.2. Precipitation type and atmospheric thickness nomogram. Refer to **Figure 1.16** for a quick-reference likelihood of freezing precipitation based on a comparison of the 1000-850 mb and 850-700 mb thickness levels.

1.2.5.3. AFW ensemble freezing precipitation probability forecasts. Air Force Weather's GEPS and MEPS ensembles use algorithms based on CCN temperature, energy required to melt snow to rain, and model outputs of precipitation, temperature, relative humidity, and incoming shortwave radiation to produce freezing precipitation probability charts – they're available from the ensembles main page on AFW-WEBS.

1.2.5.4. Dual-polarization radar and freezing precipitation. Dual-polarization radar provides a number of benefits in a winter weather setting. The base data variables and the Hydrometeor Classification (HC) product aid in distinguishing between liquid and frozen precipitation. Also, the Melting Layer (ML) product helps forecasters determine the timing of the transition from one precipitation type to another. An important caveat to remember is that dual-polarization products are only valid at the height of the radar beam; precipitation type may be vastly different at the surface than at beam level. Always use the dual-polarization products in combination with an understanding of the atmospheric thermodynamic profile for the given situation. The following procedure, derived from a 2011 study, demonstrates a step-by-step process for determining precipitation type based on whether or not a melting layer is detected in the dual-polarization products.

1.2.5.4.1. If a melting layer is detected:

1.2.5.4.1.1. Determine if there is refreezing near the radar. This can be achieved through analysis of the Correlation Coefficient (CC) field. Areas of noisy CC near the radar site may be indicative of refreezing and sleet at or near the surface.

1.2.5.4.1.2. If refreezing is not evident based on radar imagery, use a sounding to examine the temperature profile below the melting layer. If there is a refreezing layer with temperatures at or below -6°C and thickness greater than 2500 feet, sleet is likely at the surface. If not, rain or freezing rain should be expected at the surface, depending on whether the surface temperature is above or below freezing.

1.2.5.4.2. If a melting layer is not detected, the entire temperature profile is below freezing. Use a sounding to determine if the atmosphere is saturated at temperatures colder than -10°C. If yes, forecast snow. If not, forecast freezing drizzle or drizzle, depending on surface temperatures.

1.2.5.4.3. Dry snow is represented in dual-polarization data by CC greater than 0.97 and ZDR around 0.5 dB. Wet snowflakes, which are melting or coated with water, have CC between 0.88 and 0.97, and Differential Reflectivity (ZDR) from 1 to 2 dB. Freezing drizzle and drizzle are characterized by CC of 0.98 or greater and ZDR close to, but slightly above, zero. The HC product can also be used to determine precipitation type. However, its output is valid only at beam height, and should be used with caution when determining precipitation type at the surface.

1.2.5.4.4. Transition precipitation types. The ML product can help determine the timing of the transition from one precipitation type to another. If the melting layer rings decrease in size and draw closer to the radar with time, the elevation of the melting layer is decreasing, and a transition from liquid to mixed or frozen precipitation may be imminent at the radar site. Gradients of CC or ZDR may also represent a transition between precipitation types. For example, if a gradient between uniform and noisy CC is advancing toward the radar, a transition from liquid to mixed precipitation could be forthcoming.

1.2.6. Precipitation Forecasting Aids and Techniques – Snow.

1.2.6.1. Estimating Rates/Accumulation Using Weather and Visibility. Estimates of snowfall rates can be determined from visibility measurements (**Table 1.8**). Snowfall rate is inversely proportional to prevailing visibility assuming falling snow is the predominant horizontal obscuration. Snow accumulation is dependent upon snowfall rate and storm duration. Snow falling at lower temperatures tends to compact and melt much less than snow falling near freezing. Keeping these factors in mind, the rainfall intensity and associated hourly rainfall can be roughly converted into an estimated snowfall intensity/hourly snowfall rate table. Under most circumstances when temperatures are below freezing throughout the entire sounding, the atmosphere will not have enough moisture or instability to generate exact equivalent rain-snow rates. **Table 1.8** assumes that the greater reduction of visibility is by falling snow rather than other precipitation types, fog, or blowing snow. Accumulations for each visibility category are over a temperature range from +1°C (greater than or equal to 34°F) for low end rates to less than or equal to -8°C (less than or equal to 10°F) for high end rates.

Table 1.8. Snowfall accumulation vs. surface visibility.

Visibility (miles)	Intensity	Accumulation (inches/hour)
Greater than 3	-SN	Less than 0.1
2-3		Less than 0.2
1 1/2		Less than 0.3
1 1/4		0.1 – 0.4
1		0.2 – 0.6
3/4		0.3 – 0.9
1/2	SN	0.6 – 1.4
1/4	+SN	1.0 – 2.2
1/8		1.5 – 3.4
Less than or equal to 1/16		2.5 – 5.0+

1.2.6.2. Garcia snowfall method. This method only considers the influence of mid-level moisture and moisture advection on snowfall amounts; instability, vertical motion, temperature, and other factors are not included.

1.2.6.2.1. Determine the forecast area of responsibility (AOR).

1.2.6.2.2. Find the isentropic surface that intersects the 750-700 mb layer, and determine the mixing ratio (g/kg) on that surface. If unable to find the isentropic surface, use the average mixing ratio between 750-700 mb from the nearest sounding.

1.2.6.2.3. Find an area upstream at 700 mb with the highest mixing ratio that could be advected into your AOR within 12 hours. In this area (or at this location), determine the average mixing ratio (g/kg) in the 750-700 mb layer.

1.2.6.2.4. Take the average of the mixing ratios of the location in your AOR and the upstream location and multiply it by 2 to get a maximum 12 hour snow amount forecast.

1.2.6.2.5. For example, assume a sounding location in your AOR has an average mixing ratio of 4 g/kg in the 750-700 mb layer. An upstream location at 700 mb has an average mixing ratio of 5 g/kg in the 750-700 mb layer that could be advected into your AOR. The average mixing ratio between these two locations is 4.5 g/kg. Multiplying this value by 2 gives a maximum 12 hour snow forecast of 9 inches in your AOR.

1.2.6.3. Cook snowfall method. This method uses 200 mb temperature advection as the sole proxy for snow amount forecasts, by assuming that WAA at that level is a reflection of the strength of lower atmospheric features that control snow development. This method is most reliable from late fall through early spring (October-March in the Northern Hemisphere); it shouldn't be used before October 15th or after March 10th.

1.2.6.3.1. Determine the forecast AOR.

1.2.6.3.2. On the most recent 200 mb chart, highlight the 11,760 and 11,640 meter height contours – snow will be located between these contours 80% of the time.

1.2.6.3.3. Find the current 200 mb temperature at a location in your AOR.

1.2.6.3.4. Find a location upstream of your AOR at 200 mb whose temperature could be advected into your AOR in the next 12-24 hours, and note the temperature at this location.

1.2.6.3.5. Calculate the difference between the 200 mb AOR temperature and the 200 mb upstream temperature; this will indicate whether there is warm air advection (WAA) or cold air advection (CAA) into your AOR.

1.2.6.3.6. Divide the temperature difference in half to obtain an average 24 hour snow amount forecast for your AOR.

1.2.6.3.7. If CAA is noted at 700 mb within 8 degrees upstream of your AOR at forecast time t = 0, divide the 200 mb temperature difference by 4 instead of 2 to get the average 24 hour snowfall amount.

1.2.6.3.8. For example, assume the 200 mb temperature at your location is -60°C, and the 200 mb temperature at the upstream location is -50°C. The difference between these values is 10°C. Dividing 10°C in half gives an average 24 hour snow amount forecast of 5 inches.

1.2.6.4. Precipitable Water (PW) snowfall method. This method accounts for both low-level and mid-level moisture, but does not delineate between the two. It assumes that PW remains constant during a snow event, which is never the case. PW is constantly increasing via moisture advection and decreasing via precipitation. It also assumes that all of the PW will precipitate out. This may be true in some cases, but in most cases the PW method will provide an upper limit on snowfall amounts.

1.2.6.4.1. Determine the forecast AOR, and find the most current representative sounding.

1.2.6.4.2. Find the PW value from the sounding.

1.2.6.4.3. Multiply the PW value by the expected Snow-to-Liquid Ratio (SLR, refer to **Figure 1.19**) to get a forecast snow amount for the next 12 hours.

1.2.6.4.4. For example, assume the PW value from the 00Z sounding is 0.6", and the SLR is 12:1. The resulting snow amount forecast for the next 12 hours would be 0.6 X 12 = 6 inches.

1.2.6.5. Numerical Weather Prediction snowfall products. AFW-WEBS provides a variety of GALWEM, GEPS and MEPS products for snowfall prediction; peruse the website to familiarize yourself with the types of products available.

1.2.7. Final thoughts on precipitation forecasting. The following tables are "rule of thumb" guides to determine precipitation type – they're not meant to be used by themselves, but can provide initial guidance on a variety of scenarios. Remember to always use additional tools before finalizing a forecast.

Table 1.9. General Rules of Thumb – Drizzle.

Drizzle Rules of Thumb
Most common with disorganized weather systems.
Often occurs with an inversion present.
Most often occurs on cool side (overrunning) of stationary fronts.
The air must be saturated from the surface to the 850 or 800 mb level.
Temperatures at cloud top should be -4° C or warmer.
Cloud bases must be less than 4,000 feet (under 1,000 feet best).
Cloud layer or fog layer must be between 2,000-6,000 feet thick (drizzle is rare when thickness is greater than 10,000 feet).
Cloud layer or fog layer must persist for several hours (allows droplets time to build).
Must be sufficient upward motion to maintain cloud layer or fog.
If drizzle occurs, there must be source of moisture to maintain the cloud or fog.

Table 1.10. General Rules of Thumb – Thickness Values and Precipitation Type.

1000-500 mb Thickness Value	Precipitation Type
5330 to 5520 meter band	Freezing Drizzle
5330 to 5440 meter band	Freezing Rain
5400 meter band	Threshold for Snow vs. Rain
5360 to 5400 meter band	Snow

Table 1.11. General Rules of Thumb – Freezing Precipitation.

Freezing Precipitation Rules of Thumb
Freezing rain is most likely at surface temperatures between 0° C and -5° C.
More than half of freezing rain cases occur at surface temperatures between 1.5° C and -1.5° C.
A majority of freezing drizzle cases occur at surface temperatures between -3° C and -5° C.
Freezing drizzle can occur at surface temperatures between -5° C and -10° C.

Table 1.12. General Rules of Thumb – Parameter Values and Precipitation Type.

Parameter	Value	Precipitation Type
Surface temperature	Greater than 40° F	Rain
	35° to 40° F	Mixed
	Less than 35° F	Snow
Surface dew point	Greater than 35° F	Rain
	25° to 35° F	Mixed
	Less than 25° F	Snow
850 mb temperature	Greater than 0° C	Rain
	-2° to 0° C	Mixed
	Less than -2° C	Snow
700 mb temperature	Greater than -5° C	Rain
	-5° to -9° C	Mixed
	Less than -9° C	Snow
500 mb temperature - poleward of 40° latitude or in mountainous regions	Greater than -25° C	Rain
	-25° to -29° C	Mixed
	Less than -29° C	Snow
500 mb temperature - equatorward of 40° latitude	Greater than -15° C	Rain
	-15° to -19° C	Mixed
	Less than -19° C	Snow
Low level (surface & 850 mb) temperatures below freezing	Upper level snow	Snow
	Upper level rain	Freezing rain

1.3. Surface Winds.   Accurate surface wind forecasting is an important task for a forecaster. Winds are important for safe launch and recovery of aircraft, and are vital for successful low-level flight, ground combat operations, and base resource protection activities. An accurate wind forecast is a vital pre-requisite for accurately forecasting most other weather elements.

1.3.1. Wind Basics.   This section reviews the basic atmospheric forces responsible for atmospheric winds, and describes how these forces combine. It then describes how these wind types are related to flow patterns around pressure systems.
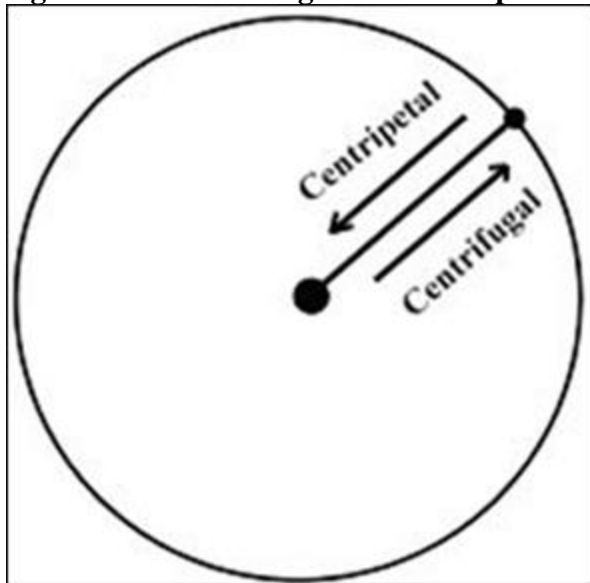
1.3.1.1. *Atmospheric Forces.*

1.3.1.1.1. Pressure Gradient Force. This force is responsible for winds in the atmosphere. It arises from spatial differences of atmospheric pressure, and acts to move air parcels from higher to lower pressure. The difference in the pressure between two points (over a given distance) is defined as the pressure gradient. The magnitude of the pressure gradient force is directly proportional to the strength of the pressure gradient. Tightly packed isobars indicate a strong gradient, and are associated with strong winds. In contrast, loosely packed isobars indicate a weak gradient, and are associated with weak winds.

1.3.1.1.2. Coriolis Force. The Coriolis force is the "apparent" force that causes any mass moving through the Earth's atmosphere to be deflected from its intended path. This force deflects winds to the right in the Northern Hemisphere and to the left in the Southern Hemisphere, due to the Earth's rotation. The Coriolis Force is inversely proportional to latitude; it is zero at the equator and increases to infinity at the poles.

1.3.1.1.3. Centrifugal and Centripetal Forces (**Figure 1.20**). The centrifugal force causes and an air parcel to move outward from the center of rotation; its strength is directionally proportional to the speed and radius of rotation. Centripetal force, equal in magnitude and opposite in direction to the centrifugal force, keeps the air parcel moving around a curved path (such as around curved height contours on a constant-pressure surface).

Figure 1.20. Centrifugal and Centripetal Forces.
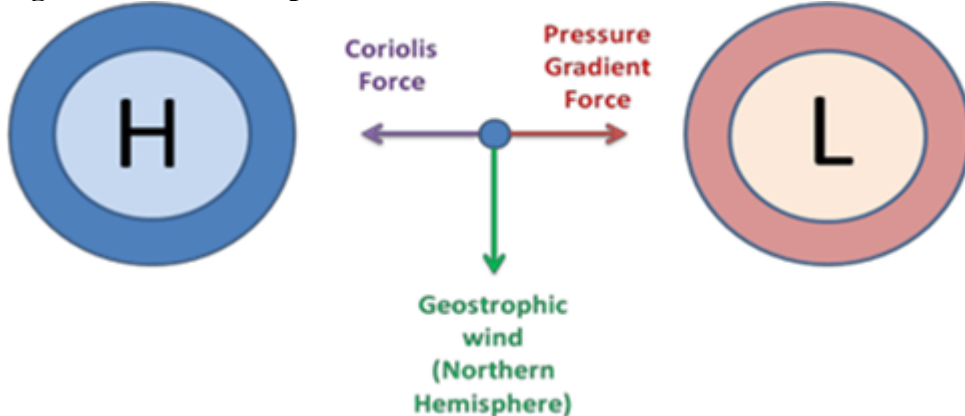
1.3.1.1.4. Frictional Force. Friction directly opposes and slows down the motion of a mass upon contact with another mass. The strength of the force depends on the nature of the contact surface. The more irregular the contact surface, the greater the frictional force. Friction always acts opposite to the direction of motion. With an increase in friction, the wind velocity decreases. This force slows the wind within the boundary layer; the resulting surface wind is about 2/3 of the geostrophic or gradient wind. Friction also causes winds to flow across isobars from high to low pressure (i.e., out of highs and into lows). It may cause the wind to blow at angles up to 50° across isobars over rugged terrain and 10° across isobars over water. The effects of friction usually reach to about 1,500 feet above ground level (AGL) over smooth terrain and as much as 6,000 feet AGL over mountainous terrain (i.e., up to the "Friction Level", also called the geostrophic wind level or gradient wind level).

1.3.1.2. *Wind Types.*
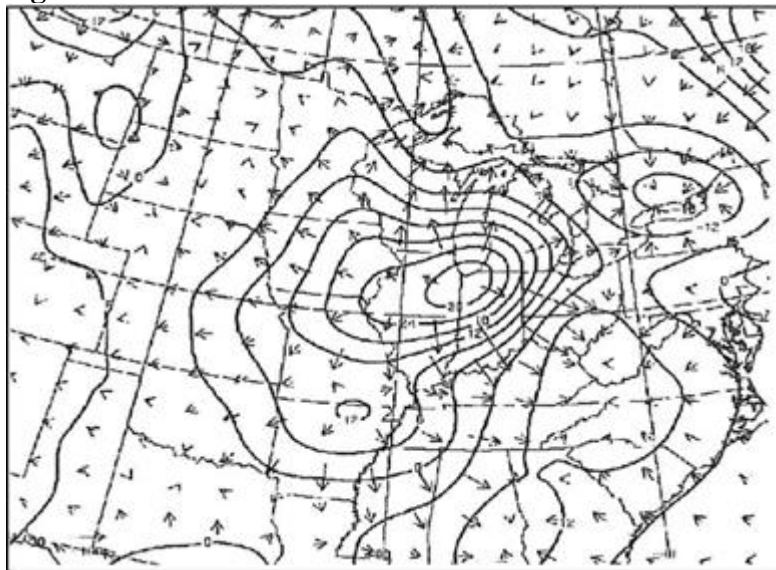
1.3.1.2.1. Geostrophic Wind (**Figure 1.21**). The geostrophic wind results from the balance between the pressure gradient and the Coriolis Force, and blows at right angles to the pressure gradient (and parallel to isobars). The geostrophic wind gives a good approximation of the actual wind when both friction and isobaric curvature are small.

Figure 1.21. Geostrophic Wind.

1.3.1.2.2. Gradient Wind. The gradient wind is airflow resulting when the pressure gradient force and the centrifugal force exactly balance the Coriolis force; it's essentially the same as the geostrophic wind, except that it blows parallel to curved isobars rather than straight isobars. In the middle latitudes, this wind is a better approximation of the actual wind speed than the geostrophic wind speed.

1.3.1.2.3. Isallobaric Wind. Isallobaric winds result from changes in pressure over time, and flow perpendicular to isallobaric contours (from an isallobaric high to an isallobaric low) as depicted by the wind vectors in **Figure 1.22** Geostrophic and gradient wind speeds should be adjusted for the isallobaric flow to get a better estimate of the actual winds. Although the gradient wind (adjusted for the effects of friction) is a good estimate of the actual wind when the pressure is unchanging, it is not always accurate when the pressure rapidly changes.

Figure 1.22. Isallobaric Wind.

1.3.1.2.4. Thermal Wind. The thermal wind does not "blow" like the geostrophic wind or the gradient wind; it's simply the difference between geostrophic winds at two different heights or pressures, considering both magnitude and direction. If a horizontal temperature gradient exists (i.e., a change in temperature over some distance), pressure or height surfaces tilt with increasing altitude (i.e., thicknesses are higher where temperatures are warmer). The magnitude of the geostrophic wind is proportional to the tilt of these surfaces. This means that the geostrophic wind changes with altitude when a horizontal temperature gradient exists in the lower atmosphere. This is the fundamental statement of the thermal wind relationship. The polar front jet (PFJ) stream in both Hemispheres exists because of the thermal wind relationship. On average, a horizontal (north-south) temperature gradient exists in the lower atmosphere between 30° and 60° N/S latitude, with warmer temperatures equatorward and cooler temperatures poleward. This results in increasing winds with height in both hemispheres that are maximized above the strongest temperature gradient, commonly called the polar front. The maximum in wind speeds above the polar front is the PFJ. Note that in the Northern Hemisphere, the PFJ blows from west to east because height surfaces tilt downward from south to north or from higher thicknesses to the south toward lower thickness in the north. In this case, the PFJ blows in the same direction as the thermal wind, which parallels thickness contours.

1.3.1.2.5. Cyclostrophic Wind. The cyclostrophic wind is flow that results when the PGF is exactly balanced by an apparent centrifugal force (when flow is considered in a rotating coordinate system). It is only applicable for mesoscale and microscale phenomena where the CF can largely be neglected, such as tornadoes, waterspouts, and dust devils.

1.3.1.2.6. Actual Wind. The actual wind is the true, observed wind, resulting from the combination of the previously described winds and forces.

1.3.1.3. *Flow around pressure systems.* Winds generally blow from higher toward lower pressure; the flow is clockwise out of highs and counterclockwise into lows in the Northern Hemisphere. The direction of the flow is reversed in the Southern Hemisphere; winds flow counterclockwise out of highs and clockwise into lows. Buys-Ballot's Law is useful for identifying the general location of highs and lows by observation alone: in the Northern Hemisphere, if you stand with the surface wind to your back and turn 30° clockwise, a low is to the left, and a high is to the right. In the Southern Hemisphere, with your back to the wind, turn 30° counterclockwise and the low is to the right, and the high is to the left.

1.3.2. General Tools for Forecasting Surface Winds.

1.3.2.1. *Climatology.* Consult climatology during your initial preparations, to identify prevailing winds for the location and time of interest. The climatological winds will account for meso- and micro-scale local phenomena such as land and sea breezes and thermal lows. Variations from the climatological winds are often the result of migratory weather systems such as lows, highs, and fronts.

1.3.2.2. *Topography.* Local terrain features can have an important effect on both the direction and speed of surface winds. Frictional effects due to rough terrain can slow wind speeds and change their direction, while mountains upstream may delay or block winds or trigger strong downslope winds.

1.3.2.3. *Trends.* If the air mass and pressure systems affecting the area of interest are not expected to change, use persistence for short-term forecasting. This is especially true in tropical locations, where conditions remain much the same from day to day. In these locations, diurnal variations in winds usually dominate. Trend charts are excellent tools to track and forecast these "persistent" winds.

1.3.2.4. *Wind Profiles.* Wind profiles include data from Skew-T diagrams, wind profilers, meteograms, and WSR-88D VAD wind profiles. These vertical profiles show the winds in a small cross-section of the atmosphere, but also represent the winds over a much larger horizontal area. The low-level jet can often be seen on vertical wind profiles. To utilize wind profile data, read the wind values off the profile display, determine the temperature profile from a current Skew-T or upper air product, and follow the rules in the previous sections on geostrophic and gradient winds.

1.3.2.5. *Satellite Imagery.* Low-level cloud patterns from satellite imagery are valuable in forecasting surface winds, especially in data-sparse oceanic areas (remember that winds at cloud level may be higher than at the surface.) The best images to use are high-resolution visible and infrared images; study the terrain in the area of interest and determine the type and shape of clouds, then use the following guidance:

1.3.2.5.1. Open-cell cumulus. These type of clouds are associated with straight-line or cyclonic flow; they're called "open-cell" since the lines of clouds trace the cell borders, leaving the center of the cell cloud-free (refer to the top of **Figure 1.23**). The shape of open-cell cumulus clouds gives an indication of the low-level winds in the region, as shown in **Figure 1.24**.

1.3.2.5.2. Closed-cell stratocumulus. These clouds are associated with anticyclonic flow and relatively light wind speeds less than 20 knots; they're called "closed-cell" since the cells have cloudy centers with clearing around the edges of the cells (see the bottom of **Figure 1.23**). Wind direction is difficult to determine from observation of these clouds.

Figure 1.23. Comparison of open-cell cumulus (top of image) and closed-cell stratocumulus (bottom of image).
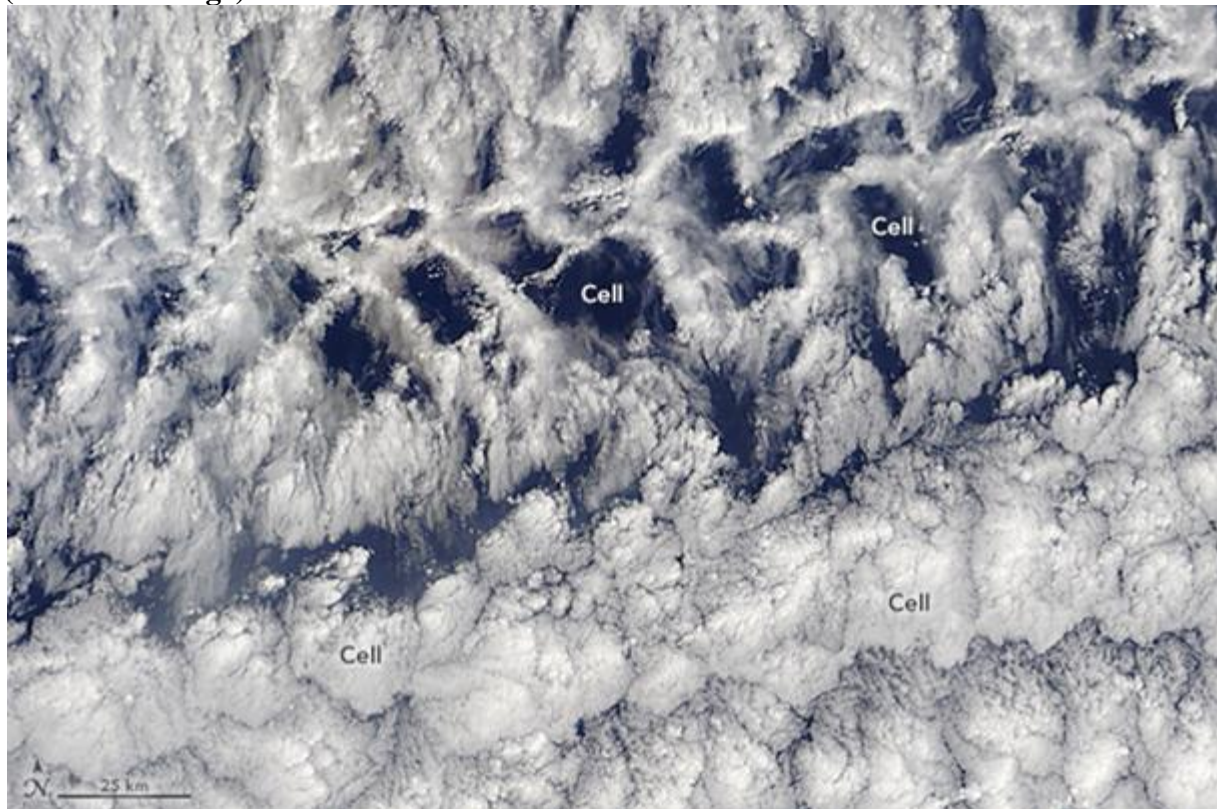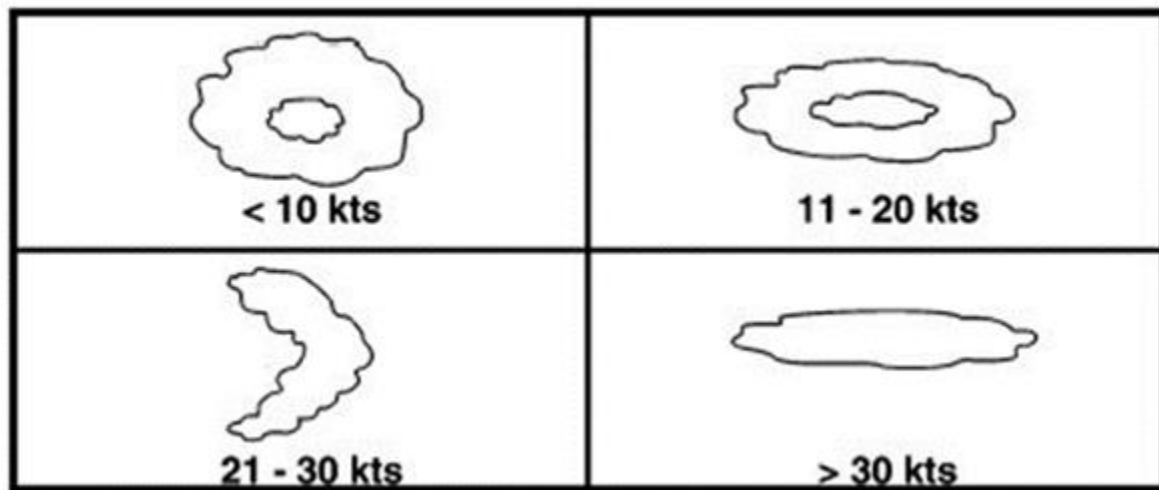
Figure 1.24. Open-cell cumulus shapes, based on wind speed.

1.3.2.5.3. Stratocumulus lines. These clouds are normally seen off southern or eastern coastlines or over large lakes; they occur with any type of flow (straight-line, cyclonic, or anticyclonic). Winds blow nearly parallel to the cloud lines, and the smaller the cloud elements, the stronger the winds. Visible separation between cloud elements indicates speeds greater than 20 knots. **Figure 1.25** shows an example of these clouds over the Alaskan Peninsula.

Figure 1.25. Stratocumulus lines over the Alaskan Peninsula.

1.3.2.5.4. Cumulus lines or streets. Similar to the stratocumulus version, these lines form mainly in tropical and subtropical environments. Winds blow virtually parallel to the lines or streets.

1.3.2.5.5. Smoke, ash, and dust. These vectors may be found at various levels in the atmosphere, and will advect along the prevailing wind trajectory with sharp boundaries near the point of origin upstream, and diffuse boundaries downstream.

1.3.2.5.6. Lee-side clearing. If lee-side clearing is evident on satellite imagery, it's an indicator of winds crossing a mountain ridgeline at an angle greater than 45°.

1.3.2.5.7. Lakes in the summertime. During the warmer months, cumulus clouds will dissipate as them move from warmer ground over cooler lakes. Cloud-free areas will occur just downstream of lakes, as the cooler lake air is advected over the downstream land region, before clouds start developing.

1.3.2.5.8. Lakes in the wintertime. During the colder months, colder, drier air moving over an unfrozen lake will form stratocumulus lines downstream, over the lake and the land. A cloud-free region often exists on the upstream side of the water body.

1.3.2.5.9. Ice packs on large lakes and seas. Persistent winds will push ice away from the upstream shoreline, and pack it tightly against the downstream shoreline.

1.3.2.5.10. Bow waves, plume clouds, and Von Karman vortices. Bow waves are usually found in front of an obstacle to the wind flow (such as an island), and plume clouds and Von Karman vortices are found downstream of wind flow obstacles (**Figure 1.26**).

Figure 1.26. Von Karman vortices downstream of Madiera, off the western African coast.

1.3.2.6. *Elevation Effects.* A decrease of air pressure and density, along with a decrease of friction with increasing elevation, result in an average wind speed increase of roughly 1 to 2 knots for every 2000 feet above sea level. **Table 1.13** shows the increase in wind speed with elevation at specific temperatures. After making wind forecasts using other tools, adjust wind speeds for elevation using this table.

Table 1.13. Elevation, Temperature, and Wind Speed Adjustments.

Elevation (feet)	Temperature °C (°F)	35 knot Surface Winds	50 knot Surface Winds
0	10 (50)	35	50
2000	7 (44)	36	52
4000	4 (38)	37	54
6000	0 (32)	39	56
8000	-3 (26)	40	58
10000	-7 (20)	41	59
12000	-10 (14)	42	61
14000	-13 (8)	43	64

1.3.2.7. *Local Wind Effects.* After using the general techniques outlined in the previous sections, forecasters should fine-tune their wind forecasts based on local effects, such as the following:

1.3.2.7.1. Drainage winds. These winds occur at night, during strong cooling conditions and a very weak pressure gradient. Since cooler air is heavier than warmer air, it sinks to lower elevations in sloping terrain. Drainage winds require only a very shallow terrain slope, and have occurred with elevation changes as little as 200 feet. Wind speeds rarely exceed 2 or 3 knots, and they frequently occur when the forecast area is under a surface ridge of high pressure.

1.3.2.7.2. Mountain breeze. This breeze is simply a stronger case of drainage wind, occurring in areas of higher elevation differential (such as mountainous region). At night, radiation cools the mountainside air. As the cooler air becomes denser, it sinks toward the lower elevations and collects in the valleys. Mountain breeze speeds may reach 11 to 13 knots, and the cooler air may settle in and become several hundred feet thick in the valley.

1.3.2.7.3. Fall wind. This cold wind typically originates in snow-covered mountains under high pressure. The air on the snow-covered mountains is cooled enough to remain colder than the valley air, despite adiabatic warming upon descent. Near the edges of the mountains, the cold air flows rapidly through terrain gaps and settles down to the valley below. Fall winds usually begin once high pressure is established over the region for several days, and channeled fall winds have reached persistent speeds of 100 knots in the most extreme cases. Temperatures in the lower elevations may drop more than 11°C (20°F) when the breeze sets in.
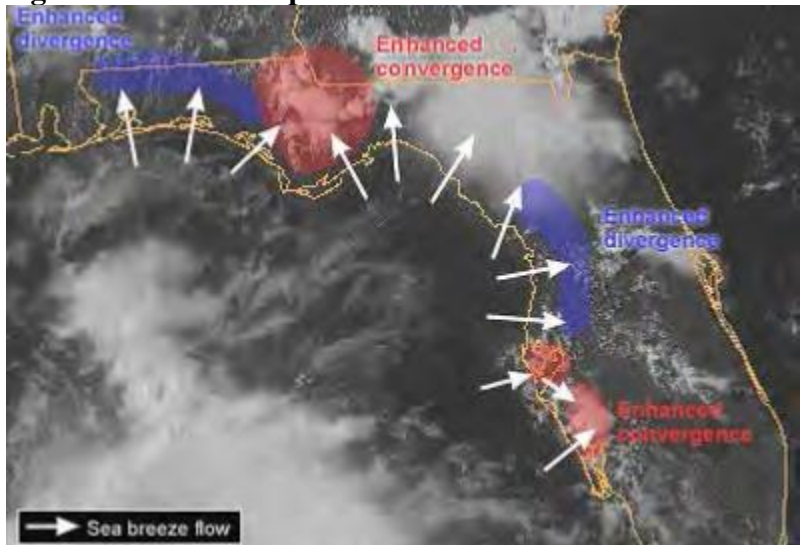
1.3.2.7.4. Valley breeze. These winds flow in the opposite direction of the mountain breeze described above; they develop during the day as the mountain slopes rapidly become heated by the sun (more quickly than the protected valleys). Air from the valley then "slides" upward to replace the buoyant, heated air rising from the mountain slopes. Valley breezes averages about 13 knots, and the stronger the heating, the stronger the wind. Early afternoon, is the most favorable time for the strongest winds. Optimal conditions for valley breeze development are clear skies and a weak synoptic pressure gradient.

1.3.2.7.5. Foehn (Chinook) wind. This warm wind flows down the lee side of mountains. The wind forms when moist air is forced to ascend on the windward side of a mountain, and then descends on the leeward side. As the air rises on the windward side, it expands and cools at the relatively slow moist adiabatic cooling rate. The moisture in the air condenses into clouds, and eventually precipitates out. As the now dry air descends on the leeward side, it is compressed and heated relatively quickly at the dry adiabatic heating rate. The result is a very strong, warm, and dry downslope wind. Chinook winds begin when strong winds aloft flow perpendicular to a mountain range. A leeside trough may form, further forcing the air downslope. Look for clouds and precipitation on the windward side of the mountain range, ending suddenly at or near the ridgeline in a "Foehn wall." Conditions associated with mountain-wave turbulence may also cause Chinooks; lenticular clouds usually associated with mountain-wave turbulence may also indicate this phenomenon. Temperatures may rise as much as 28°C (50°F) in a few minutes at the base of the mountains, and melting snow cover can cause flash flooding.

1.3.2.7.6. Land and sea breezes. Land and sea breezes occur throughout the year in the tropics, but mainly during the spring to autumn months at mid-latitudes. At these times of year, weak synoptic-scale flow and clear skies promote strong daytime heating of the land surface, leading to the development of a sea breeze circulation. Sea breeze development typically initiates 3 to 4 hours after sunrise, or when the land temperature exceeds the adjacent water temperature by an average of 6 to 10°F. The strength of the breeze is proportional to the magnitude of the land/sea temperature difference. This temperature gradient is referred to as the "sea breeze front." Weak onshore synoptic flow favors sea breeze development and penetration, while offshore flow limits or even prevents sea breeze development. This developmental phase is characterized by fair weather, although cumulus formation should be expected. As the day progresses, the pressure gradient between land and sea increases as solar heating lowers the pressure over land relative to that over water. The tightening pressure gradient leads to surface winds between 10 and 20 knots through a vertical depth of about 500 feet. The entire sea breeze circulation typically tops out between 1,500 and 3,000 feet above the surface at mid-latitudes, but occasionally reaches 13,000 feet above the surface in the tropics. The sea breeze is strongest and penetrates farthest inland (35 to 45 miles is not unusual) during the afternoon hours. Cumulus clouds are common along the sea breeze front, with shower and thunderstorm development possible when conditions are unstable. Areas of enhanced lift where the sea breeze front interacts with other surface features, such as outflow boundaries and convergence lines, are particularly favorable for thunderstorm development. By late afternoon and early evening, the land begins to cool, weakening the temperature and pressure gradients. The sea breeze circulation diminishes and eventually ceases one or two hours after sunset. As the land cools and becomes colder than the ocean surface, the process reverses itself with the formation of a seaward-directed land breeze. The land breeze is typically weaker than the sea breeze, and peaks shortly before sunrise. Sea and land breezes can be modified by the factors outlined below:

1.3.2.7.6.1. Coastline shape. The shape of the coastline may enhance or diminish the convergence associated with the sea breeze. Onshore flow along a concave coastline (such as a bay) becomes divergent, which inhibits lift along the sea breeze front. The opposite is true for a convex coastline (such as a cape or point), where onshore flow enhances convergence and convective development. These effects are illustrated in **Figure 1.27**.

Figure 1.27. The shape of the coastline determines sea breeze divergence or convergence.

1.3.2.7.6.2. Ambient wind flow. The direction of the ambient synoptic flow may enhance, limit, or even prevent sea breeze development. If the ambient flow is in the same direction as the sea breeze, the sea breeze will be stronger and will penetrate farther inland. If the ambient flow is opposite the direction of the sea breeze, inland penetration will be limited or even precluded. Occasionally, the ambient flow is parallel to the coastline, and thus perpendicular to the sea breeze. If this is the case, the sea breeze may still occur, but at an angle to the coastline.

1.3.2.7.6.3. Temperature inversions. When a temperature inversion develops, heating is typically limited to a shallow layer near the surface. This tends to reduce the strength of the sea breeze. In fact, a deep layer of modest heating may result in a stronger sea breeze than a shallow layer of robust heating. An inversion may also inhibit upward development along the sea breeze, and thus prevent thunderstorm development. The inversion also traps low-level moisture and inhibits the decay of morning fog and stratus, leading to reduced daytime heating and a weaker sea breeze.

1.3.2.7.6.4. Topography. Mountains and valleys affect the sea breeze in several ways. Mountain-valley circulations may enhance or lead to early development of the sea breeze. Enhanced afternoon heating in valleys may also locally strengthen the sea breeze. Finally, convergence/interactions between mountain and valley breezes and the sea breeze often result in shower and thunderstorm development.

1.3.3. Severe non-convective winds. Severe non-convective winds are possible when one or more of the following conditions are satisfied:

1.3.3.1. *Lapse rates below 700 mb are greater than 5 degrees Celsius per kilometer (°C/km), with lapse rates greater than or equal to 8°C/km optimal.* Steep low-level lapse rates (greater than 5°C/km) are important for the optimal transfer of momentum (i.e., winds) from the upper atmosphere to the lower atmosphere. Momentum transfer is maximized when lapse rates from the surface to approximately 18,000 feet (500 mb) are dry adiabatic (9.8°C/km) or super adiabatic (greater than 9.8°C/km). Strong negative buoyancy is promoted, which allows mass from aloft to come to the surface unimpeded as long as the negative buoyancy is maintained. Negative buoyancy is promoted by warm air at the surface and cold air aloft. Cold air is denser than warm air and will have a tendency to sink, which is necessary for winds aloft to reach the surface. Therefore, cold air vs. warm air at the surface promotes efficient momentum transfer down to the surface.

1.3.3.2. *The maximum wind is greater than 50 knots in the layer aloft where the wet bulb potential temperature (theta-w) is less than the surface potential temperature + 4°C.* Wet bulb potential temperature (theta-w) is the temperature a parcel of air would have if it was expanded upward to its LCL and then compressed downward moist adiabatically to 1000 mb. A parcel that is brought to its LCL from some pressure level has been cooled to saturation, or where it can no longer hold more water before precipitating. Once the LCL has been reached, the parcel can be lowered moist adiabatically to the original pressure level to determine how cold the parcel would get solely via evaporation of the moisture it contained at its LCL. This is the parcel's wet bulb temperature. The drier the air, the lower the wet bulb temperature. We can compare the wet bulb temperature to temperatures below the original pressure level by lowering the parcel from its wet bulb temperature to 1000 mb, which yields theta-w. Now that the parcel has cooled as much as possible via evaporation and has been compressed to 1000 mb, we can compare theta-w with low-level potential temperatures, most notably that of the surface. The wind from every level aloft where theta-w is less than the surface potential temperature +4°C may be able to come to the surface via momentum transfer because that air is denser than the air it is falling into. The +4°C caveat is incorporated because winds with downward momentum can penetrate a shallow cool layer at the surface where theta-w may be equal to or slightly greater than the surface potential temperature.

1.3.3.3. *The planetary boundary layer (PBL) extends from the surface to at least 850 mb, or 5,000 feet above ground level (AGL).* The PBL is the layer of the atmosphere where the effects of friction on air flow cannot be neglected. Large turbulent fluxes of heat and momentum occur that also alter wind flow. The PBL (or friction layer) extends from the surface up to about 2 km on average, but can extend up to 500 mb, or 18,000 feet, in places like Southwest Asia (SWA). In general, the deeper the PBL, the stronger surface wind speeds will be, because strong winds from aloft are able to come to the surface via momentum transfer. In a deep PBL, turbulent mixing has homogenized the air, or mixed warm air with cool air and dry air with moist air. The result is that the temperature and moisture characteristics of the PBL are quite uniform, and this situation is optimal for momentum transport from aloft to the surface depending on the wind, temperature, and moisture characteristics of the upper level air. A deep, well-mixed PBL is also characterized by steep lapse rates (near 9.8°C/km). In desert regions like SWA where a deep layer of dry air is common, dry adiabatic lapse rates can extend up to 18,000 feet (500 mb), making these areas prone to non-convective and convective wind gusts at the surface.

1.3.3.4. *The local pressure change (or tendency) is strongly positive or negative, with a change of at least plus or minus 2 mb in 3 hours.* The actual wind has two components: the geostrophic wind and the ageostrophic wind. When discussing the influence of local pressure tendencies on non-convective winds, the focus is on the ageostrophic component of the total wind. The ageostrophic wind itself has two components: the isallobaric wind and the inertial-advective wind. The isallobaric wind is caused by the time rate of change of acceleration induced by the pressure gradient force. In other words, it is proportional to the magnitude of local pressure tendencies, and "blows" toward lower pressure tendencies (or toward falling pressure, not just toward lower pressure). The inertial-advective wind is caused by the advection of the wind by itself. In this case, we're only concerned with the isallobaric wind. The stronger the local pressure tendencies, the stronger the isallobaric wind, and the stronger the isallobaric wind, which is a component of the actual wind, the stronger the actual wind. Therefore, it is safe to assume that non-convective wind speeds will be enhanced in areas of rapidly falling or rising pressure.

1.3.3.5. *A strong surface pressure gradient exists, indicated by tightly packed isobars on a surface chart.* The pressure gradient is the change in pressure over a given distance. For our purposes, only the horizontal pressure gradient will be considered. However, in cases of convective weather, the vertical pressure gradient must be considered as well. The stronger the surface pressure gradient, the stronger the resultant surface wind speeds. A strong surface pressure gradient is characterized by tightly packed isobars (or contours of constant pressure) across a location. For reference, a strong pressure gradient aloft is characterized by tightly packed isohypses, or contours of constant geopotential height. To calculate the surface pressure gradient, use the following steps:

1.3.3.5.1. Find a representative surface chart or forecast surface chart with isobars contoured.

1.3.3.5.2. Draw a 6° latitude/6° longitude circle (diameter of approximately 660 km in the mid-latitudes) with the forecast location at the center.

1.3.3.5.3. Determine the surface pressure of the northernmost, southernmost, easternmost, and westernmost points along the perimeter of the circle.

1.3.3.5.4. The north-south pressure gradient is the difference between the surface pressure at the northernmost point and the southernmost point, divided by 660 km. The units of the result will be millibars per kilometer (mb/km). For an example, suppose the pressure at point p-north is 1005 mb, and the pressure at point p-south is 1020 mb. The difference is -15 mb. Dividing this by 660 km yields a north-south pressure gradient of -0.02 mb/km. Note that this pressure gradient is pointing from north to south (in the negative direction), or from low to high pressure. This is opposite the pressure gradient force, which acts from high to low pressure and forces winds in that direction.

1.3.3.5.5. The east-west pressure gradient is the difference between the surface pressure at the easternmost point and the westernmost point, divided by 660 km. The units are again mb/km. For an example, suppose the pressure at point p-east is 1020 mb, and the pressure at point p-west is 990 mb. The difference is +30 mb. Dividing this by 660 km yields an east-west pressure gradient of +0.045 mb/km. Note that this pressure gradient is pointing from west to east (in the positive direction), also from low to high pressure.

1.3.3.5.6. To find the magnitude of the horizontal pressure gradient, you must then use the Pythagorean Theorem: (-0.02 mb/km)^2 + (0.045 mb/km)^2] = 0.049 mb/km.

1.3.3.6. *The vertical wind shear profile is unidirectional, or in-phase from the surface to at least 500 mb.* Winds originating from a cold air mass will generally be stronger than winds originating from a warm air mass, because the "cold wind" will be denser and have more momentum going forward. This is why post-cold frontal winds are generally stronger than post-warm frontal winds. In addition, the orientation of the wind with respect to complex terrain impacts how fast the wind will be when it reaches your AOR. Winds oriented perpendicular to complex terrain will be blocked by the terrain and tend to slow down at the surface, while winds oriented parallel to complex terrain will accelerate through canyons or valleys due to the Bernoulli effect. Note that flow that is perpendicular to complex terrain will often result in clouds and precipitation on the upslope portion of the terrain, and possible upper level turbulence downstream. In addition, winds that are unidirectional, or in-phase, at levels aloft will be able to come to the surface via momentum transfer more efficiently than winds that are from different directions. This is especially true when the wet bulb potential temperature aloft is less than the surface potential temperature, plus 4°C.

1.3.4. Wind Forecasting Aids and Techniques – Crosswinds. A crosswind is the wind component directed perpendicular to a runway. Winds parallel to a runway have zero crosswind component, regardless of speed, while winds perpendicular to the runway have a crosswind component equal to their actual wind speeds (use the maximum sustained wind or gust, whichever is greater). Crosswind component values are calculated by first determining the absolute (positive) difference in degrees between the direction of the runway heading and the direction (magnetic) of the actual wind (e.g., runway orientation is 030°/210°; wind direction is 090°). Difference off runway is 60° (90°- 30° = 60°). Then, use **Table 1.14** to relate this direction difference to the actual wind speed to find the crosswind component.

Table 1.14. Crosswind Component Table.

Speed (knots)	Angle between wind direction and heading (degrees)								
	10	20	30	40	50	60	70	80	90
5	1	2	3	3	4	4	5	5	5
10	2	3	5	6	8	9	9	10	10
15	3	5	8	10	11	13	14	15	15
20	3	7	10	13	15	17	19	20	20
25	4	9	13	16	19	22	23	25	25
30	5	10	15	19	23	26	28	30	30
35	6	12	18	22	27	30	33	34	35
40	7	14	20	26	31	35	38	39	40
45	8	15	23	29	34	39	42	44	45
50	9	17	25	32	38	43	47	49	50
55	10	19	28	35	42	48	52	54	55
60	10	21	30	39	46	52	56	59	60
65	11	22	33	42	50	56	61	64	65
70	12	24	35	45	54	61	66	69	70
75	13	26	38	48	57	65	70	74	75
80	14	27	40	51	61	69	75	79	80
85	15	29	43	55	65	74	80	84	85
90	16	31	45	58	69	78	85	89	90
95	16	32	48	61	73	82	89	94	95

1.3.5. Wind Forecasting Aids and Techniques – Low-level wind shear. Wind shear is a change in wind direction, wind speed, or both along a given spatial direction (a horizontal or vertical distance). The strongest wind shears are associated with abrupt changes in wind direction and/or speed over a short distance; wind shear is often associated with fronts, inversions, and thunderstorms. The radar VAD wind profile and other velocity products, combined with surface observations and rawinsonde data, can help identify areas of low-level wind shear. Low-level wind shear is particularly hazardous to aviation operations: it occurs so close to the surface that pilots often do not have enough time to compensate for its effects. The decision tree in **Table 1.15** can be used to determine the potential for low-level wind shear, but the conditions are not all inclusive and local effects (e.g., mountain waves, local terrain) are not addressed. The vector wind difference discussed in step 10 is obtained from **Table 1.16**, using the following method:

Table 1.15. Low-level wind shear decision flowchart.

Step	Item	Decision
1	Are thunderstorms forecast or observed within 10 NM?	If yes, forecast LLWS. If no, go to step 2.
2	Is there a low-level jet below 2000 feet?	If yes, forecast LLWS. If no, go to step 3.
3	Is the sustained surface wind speed 30 knots or greater?	If yes, forecast LLWS. If no, go to step 4.
4	Is the surface wind speed 10 knots or greater?	If yes, go to step 5. If no, go to step 6.
5	Is the difference between the gradient wind speed (2000 feet) and 2X the surface wind speed 20 knots or greater?	If yes, forecast LLWS. If no, go to step 9.
6	Is there an inversion or isothermal layer below 2000 feet?	If yes, go to step 7. If no, go to step 8.
7	Is the value of the vector difference between the gradient wind (2000 feet) and the surface wind 30 knots or greater?	If yes, forecast LLWS. If no, go to step 9.
8	Is the value of the vector difference between the gradient wind (2000 feet) and the surface wind 35 knots or greater?	If yes, forecast LLWS. If no, go to step 9.
9	Is a surface front present or forecast to be in the area?	If yes, go to step 10. If no, go to step 13.
10	Is the vector difference across the front equal to or greater than 20 knots over 50 NM (see **Table 1.16**)?	If yes, forecast LLWS. If no, go to step 11.
11	Is the temperature gradient across the front 5° C (10° F) or more per 50 NM?	If yes, forecast LLWS. If no, go to step 12.
12	Is the front's speed of movement 30 knots or greater?	If yes, forecast LLWS. If no, go to step 13.
13	Is the forecast area located in mountainous terrain?	If yes, go to step 14. If no, go to step 15.
14	Do the following conditions exist? Cloud bases greater than 8000 AGL Surface temperatures greater than 27° C (80° F) Surface temperature/dew point spread greater than 23° C (40° F) Virga/convective activity within 10 NM of runway approach	If yes, forecast LLWS. If no, go to step 15.
15	Do not forecast significant low-level wind shear	

Table 1.16. Vector difference directional charts.

(a) 0° to 12.5°

Speed A \ Speed B	5	10	15	20	25	30	35	40	45	50
5	0	5	10	15	20	25	30	35	40	45
10	5	1	5	10	15	20	25	30	35	40
15	10	5	1	5	10	15	20	25	30	35
20	15	10	5	2	5	10	15	20	25	30
25	20	15	10	5	2	5	10	15	20	25
30	25	20	15	10	5	3	6	10	15	20
35	30	25	20	15	10	6	3	6	10	15
40	35	30	25	20	15	10	6	4	6	11
45	40	35	30	25	20	15	10	6	4	7
50	45	40	35	30	25	20	15	11	7	5

(d) 77.6° to 102.5°

Speed A \ Speed B	5	10	15	20	25	30	35	40	45	50
5	7	11	15	20	25	30	35	40	45	50
10	11	14	18	22	26	31	36	41	46	50
15	15	18	21	25	29	33	38	42	47	52
20	20	22	25	28	32	36	40	44	49	53
25	25	26	29	32	35	39	43	47	51	55
30	30	31	33	36	39	42	46	50	54	58
35	35	36	38	40	43	46	49	53	57	61
40	40	41	42	44	47	50	53	56	60	64
45	45	46	47	49	51	54	57	60	63	67
50	50	50	52	53	55	58	61	64	67	70

(b) 12.6° to 45°

Speed A \ Speed B	5	10	15	20	25	30	35	40	45	50
5	2	6	10	15	20	25	30	35	40	45
10	6	4	7	12	16	21	26	31	36	41
15	10	7	7	9	13	18	23	27	32	37
20	15	12	9	9	12	15	19	24	29	33
25	20	16	13	12	12	14	17	21	26	30
30	25	21	18	15	14	14	16	19	23	27
35	30	26	23	19	17	16	17	19	22	25
40	35	31	27	24	21	19	19	19	21	24
45	40	36	32	29	26	23	22	21	22	24
50	45	41	37	33	30	27	25	24	24	24

(e) 102.6° to 135°

Speed A \ Speed B	5	10	15	20	25	30	35	40	45	50
5	8	13	17	22	27	32	37	42	47	52
10	13	17	21	26	31	35	40	45	50	55
15	17	21	25	30	34	39	44	49	53	58
20	22	26	30	34	38	43	47	52	57	62
25	27	31	34	38	43	47	51	56	61	65
30	32	35	39	43	47	51	56	60	65	69
35	37	40	44	47	51	56	60	64	69	73
40	42	45	49	52	56	60	64	68	73	77
45	47	50	53	57	61	65	69	73	77	81
50	52	55	58	62	65	69	73	77	81	86

(c) 45.1° to 77.5°

Speed A \ Speed B	5	10	15	20	25	30	35	40	45	50
5	5	8	13	18	23	27	32	37	42	47
10	8	10	13	17	22	26	31	36	41	46
15	13	13	15	18	22	26	30	35	40	44
20	18	17	18	20	23	26	30	35	39	44
25	23	22	22	23	25	28	31	35	39	43
30	27	26	26	26	28	30	33	36	40	44
35	32	31	30	30	31	33	35	38	41	45
40	37	36	35	35	35	36	38	40	43	46
45	42	41	40	39	39	40	41	43	45	48
50	47	46	44	44	43	44	45	46	48	50

(f) 135.1° to 167.5°

Speed A \ Speed B	5	10	15	20	25	30	35	40	45	50
5	9	14	19	24	29	34	39	44	49	51
10	14	19	24	29	34	39	44	49	53	58
15	19	24	29	33	38	43	48	53	58	63
20	24	29	33	38	43	48	53	58	63	68
25	29	34	38	43	48	53	58	63	67	72
30	34	39	43	48	53	58	62	67	72	77
35	39	44	48	53	58	62	67	72	77	82
40	44	49	53	58	63	67	72	77	82	87
45	49	53	58	63	67	72	77	82	87	92
50	54	58	63	68	72	77	82	87	92	96

(g) 167.6° to 180°

Speed A \ Speed B	5	10	15	20	25	30	35	40	45	50
5	9	14	19	24	29	34	39	44	49	51
10	14	19	24	29	34	39	44	49	54	59
15	19	24	29	34	39	44	49	54	59	64
20	24	29	34	39	44	49	54	59	64	69
25	29	34	39	44	49	54	59	63	69	74
30	34	39	44	49	54	59	64	69	74	79
35	39	44	49	54	59	64	69	74	79	84
40	44	49	54	59	64	69	74	79	84	89
45	49	54	59	64	69	74	79	84	89	94
50	54	59	64	69	74	79	84	89	94	99

1.3.5.1. Determine the absolute angular difference between the two winds on opposite sides of the front, approximately 50 NM apart (for example, if wind A is 03011 and wind B is 11019, the difference is 110 - 30 = 80°).

1.3.5.2. Select the graph in **Table 1.16** that corresponds to the angular difference (for this example, it is graph D, 77.6° to 102.5°).

1.3.5.3. From the proper graph, apply wind speed A and B (rounded to the nearest 5 knots). The vector difference is the intersection of Speed A and B (e.g., Speed A = 11 rounded to 10 knots. Speed B = 19 rounded to 20 knots. Vector difference is 22 knots). Use this vector difference in **Table 1.15**, step 10.

1.3.5.4. Rules of thumb for low-level wind shear associated with a variety of meteorological phenomena are given below:

1.3.5.4.1. LLWS with cold frontal boundaries. Low-level wind shear exists below 5000 feet for up to 2 hours behind a fast moving cold front. The potential persists until the depth of the cold air reaches the gradient level (2000 feet).

1.3.5.4.2. LLWS with warm frontal boundaries. Low-level wind shear exists below 5000 feet for up to 6 hours ahead of a surface warm front; it terminates with warm front passage. PIREPs are invaluable for forecasting wind shear in warm front situations. Strong vertical wind shears are usually accompanied by turbulence when the shear occurs in a (thermally) stable air mass.

1.3.5.4.3. LLWS with low level inversions. Shear occurs in these inversions with a light surface wind and a strong gradient level (2000 feet) wind. Always look for strong winds aloft when an inversion forms or is forecast to form. This frequently occurs under stable air mass conditions, typically at night, early morning, or evening, when the isobaric gradient supports strong winds.

1.3.5.4.4. LLWS with thunderstorm gust fronts. Wind speeds and directions associated with gust fronts are variable and hard to predict; the best way to forecast this feature is to identify it with radar. Low angle reflectivity products can often identify the gust front, and velocity products can identify the wind speeds and wind direction associated with the gust front. Crosscheck radar information with surface observations.

1.3.5.4.5. LLWS with a low-level jet. A typical low-level jet wind speed profile is calm to 8 knots at the surface, with a speed increase to 25 to 40 knots or more at 650 to 1,500 feet above ground level. Speed then decreases with height above 1,500 feet to approach the gradient level wind speed of 15 to 30 knots. They usually occur above very stable air; the core of the jet is just above the top of the inversion layer. Low-level jets are commonly found in the following areas:

1.3.5.4.5.1. Over desert coastal regions, especially in areas with cold upwelling currents.

1.3.5.4.5.2. Over equatorial upwelling currents.

1.3.5.4.5.3. Along the border of a thermal, or "heat", trough.

1.3.5.4.5.4. Along sharply-defined zones of heavy precipitation (such as the rear region of strong thunderstorms).

1.3.5.4.5.5. Intense low-level jets often occur over the western Indian Ocean, southern Iraq, and the Persian Gulf during the summertime Indian Monsoon season; they typically extend from east of Madagascar across eastern Somalia and into India. Speeds may exceed 60 knots at a core height of 5000 feet.

1.3.5.4.5.6. Low-level jets frequently occur along western coastal areas of South America, as well as Namibia and south of the equator. Core heights are normally between 800 and 5000 feet, but may rise to 5000-15000 feed in mountainous areas.

1.3.5.4.6. LLWS in mountain wave conditions. Mountain waves have high crests (amplitude) that cause strong turbulence aloft, and deep troughs that reach the ground and cause strong winds and wind shear far downstream from the mountain range. Under extreme mountain wave conditions, wind speeds at the surface can be as strong as the wind speed experienced at the mountaintop. The wave propagation distance downstream from the mountain range varies according to the distance between the crests in the waves (wavelength) in the mountain wave pattern. The nature of the mountain range, and many other factors, influence the shape, strength, and pattern of the waves. Mountain waves are challenging to predict, but consider the following criteria when forecasting for them:

1.3.5.4.6.1. Mountain waves are sometimes seen on satellite imagery as a series of cloud lines downwind and parallel to the mountain range. The cloud lines are perpendicular to the wind flow.

1.3.5.4.6.2. Mountains with steep leeward and gentle windward slopes create the largest amplitude mountain waves.

1.3.5.4.6.3. Winds flowing within 30 degrees of perpendicular to the ridgeline are more favorable for generating mountain waves. Also, a wind speed at the crest of about 25 knots, increasing with height, is most favorable for generating mountain waves.

1.3.5.4.6.4. Another important factor for mountain wave formation is upstream stability. Look for upstream temperature profiles that exhibit an inversion or a layer of strong stability near mountain top height, with weaker stability at higher levels.

1.3.6. Wind Forecasting Aids and Techniques – Wind gust calculator. After extensive empirical testing and statistical analysis, Air Force Weather personnel found that non-convective wind gusts (in knots) can be accurately estimated by multiplying the forecast sustained wind speed by 1.4. **Table 1.17** provides a quick-reference guide for wind speeds up to 50 miles per hour.

Table 1.17. Wind speed and wind gust calculator, using the 1.4 multiplier.

Wind speed (knots)	Wind gust (knots)	Wind gust (mph)	Wind speed (knots)	Wind gust (knots)	Wind gust (mph)
1	1.4	1.6	26	36.4	41.9
2	2.8	3.2	27	37.8	43.5
3	4.2	4.8	28	39.2	45.1
4	5.6	6.4	29	40.6	46.7
5	7	8.1	30	42	48.3
6	8.4	9.7	31	43.4	49.9
7	9.8	11.3	32	44.8	51.6
8	11.2	12.9	33	46.2	53.2
9	12.6	14.5	34	47.6	54.8
10	14	16.1	35	49	56.4
11	15.4	17.7	36	50.4	58.0
12	16.8	19.3	37	51.8	59.6
13	18.2	20.9	38	53.2	61.2
14	19.6	22.6	39	54.6	62.8
15	21	24.2	40	56	64.4
16	22.4	25.8	41	57.4	66.1
17	23.8	27.4	42	58.8	67.7
18	25.2	29.0	43	60.2	69.3
19	26.6	30.6	44	61.6	70.9
20	28	32.2	45	63	72.5
21	29.4	33.8	46	64.4	74.1
22	30.8	35.4	47	65.8	75.7
23	32.2	37.1	48	67.2	77.3
24	33.6	38.7	49	68.6	78.9
25	35	40.3	50	70	80.6

1.3.7. Wind Forecasting Aids and Techniques – Land and sea breezes. The following tips will be useful when forecasting sea and land breezes:

1.3.7.1. The most severe hazard associated with the sea breeze is the development of thunderstorms. In addition, visibility may be reduced in the cooler air behind a sea breeze front. Low-level clouds are associated with this air mass, but may not form until nocturnal cooling is large enough. Wind gusts are strongest and most noticeable near the sea breeze front, and wind shifts are associated with passage of a sea breeze front.

1.3.7.2. The amount of heating is crucial to the development of any sea breeze (or similar circulation); specifically, the development of a sufficiently large land-water temperature difference. Typically, this difference needs to be greater than 6°F, except under very weak synoptic conditions. The distribution of heating, both horizontally and vertically, determines the details of the sea breeze, and depends on environmental conditions including the type of land surface, the cloud cover, and low-level static stability. Sea breeze winds are forced perpendicular to the coast, but the actual wind can vary due to the synoptic scale flow within which the sea breeze develops. Offshore flow of less than 10 knots tends

to strengthen the sea breeze front and increase winds near the front, but not allow it to penetrate as far inland. Onshore flow tends to advect cooler air across the coast and often mask any sea breeze front, which will penetrate much further inland.

1.3.7.3. Forecast tools – surface data: Analyze land/water temperature trends; potential is high if the land temperature exceeds the adjacent water temperature by at least 6°F. Use the pattern of surface temperatures to assess the regions of strongest heating; the sea breeze will flow toward these regions. Check for a favorable low-level synoptic wind direction and speed (onshore, or less than 10 knots offshore); an increasing onshore component to coastal surface winds signals sea breeze initiation. Use temperature trends to estimate the time and magnitude of the maximum sea breeze; every 1°F increase in temperature over land relative to water increases the sea breeze about 1 knot. The time of maximum land-water temperature difference will coincide with the maximum breeze intensity and inland penetration.

1.3.7.4. Forecast tools – sounding and Skew-T: Use soundings to determine how deep a layer will be heated; this determines relative sea breeze strength; a deeper layer of similar temperature rise gives a stronger sea breeze. Assess the strength of tropospheric flow; relatively weak flow through a deep layer favors sea breeze formation. Assess stability parameters to determine the potential for deep convection along the sea breeze front.

1.3.7.5. Forecast tools – model output: Numerical model guidance can alert you to the probability of a sea breeze on a given day; compare mesoscale model forecasts from previous days to see how the model sea breeze compares to actual evolution. Knowing the typical evolution of the sea breeze for a given area can often provide the needed details about inland penetration, strength, and along-shore variations in the sea breeze. Combine model guidance for surface temperatures with trends in observations to time initial breeze formation and forecast time of maximum intensity and inland penetration. Use model output to check low-level flow and flow aloft.

1.3.7.6. Forecast tools – satellite data: Monitor the evolution of marine stratus that has penetrated inland for clearing or burn-off towards the coast. Use this to identify cloud edges along which a thermal gradient may exist that forces stronger or gusty winds. Check visible imagery loops to monitor cloud cover: morning-to-midday clear skies are usually required for sufficient differential heating of land versus adjacent water. Visible imagery loops will also reveal cumulus formation signaling early stages of breeze formation; monitor the cumulus for sea breeze front movement and intensification of convective cells along the sea breeze front. Visible imagery will also help to identify mesoscale features (fronts, convergence lines, outflow boundaries) and to anticipate interactions with a sea breeze front. Check infrared loops at night for clear skies and strong cooling over land -- favorable for land breeze formation. Use 10.7/3.9 micron channel difference product loops to monitor cumulus and stratus formation associated with a developing nighttime land breeze.
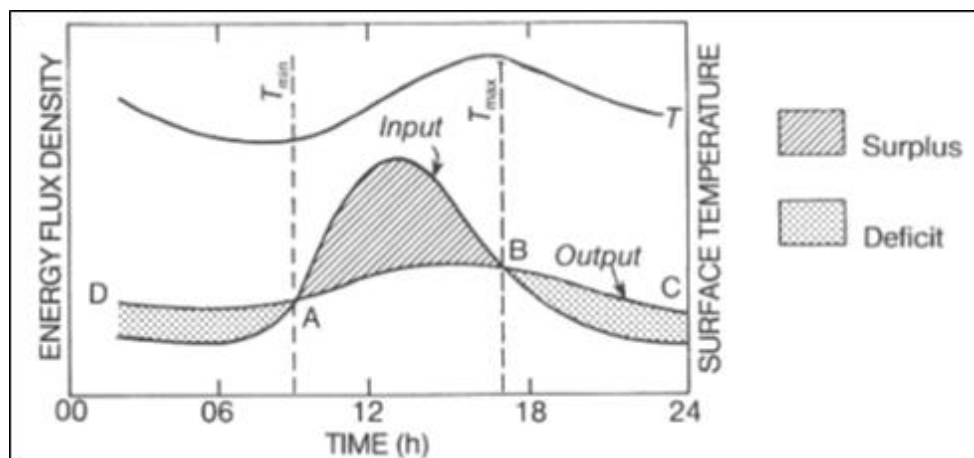
1.3.7.7. Forecast tools – radar: Sea breeze fronts show up as narrow zones of convergent winds or density differences; boundaries will be detected better in clear air mode than in precipitation mode. On reflectivity and spectrum width products, sea breeze fronts are seen as narrow lines of enhanced values. Monitor the base velocity to track movement of the sea breeze front. A change in wind direction across the sea breeze front will show up on Mean Radial Velocity products as radial convergence or azimuthal shear, depending on the orientation of winds with respect to the radar.

1.4. Temperature. Accurate temperature forecasts are important to the safety of Air Force personnel and the completion of critical missions. Extreme heat and cold are capable of causing injury or death in the absence of proper safety precautions. Additionally, only a few degrees can represent the difference between a routine rainfall event and a dangerous winter storm. As such, forecasters should possess a solid understanding of the environmental factors which influence temperatures, as well as the tools available to aid in the temperature forecast process. The kinetic energy of molecules in a substance determines the amount of heat within. The particular substance's specific heat determines how much additional heat energy must be stored before the temperature will rise by one degree. For example, the planet's oceans store vast amounts of heat energy. Still, the specific heat of water is very high, so its temperature will be lower than any other substance would be with the same amount of heat. A variety of instruments can be used to measure temperature, including thermocouple sensors (wires of different metals connected to a voltmeter), thermistors (thermal resistance devices), infrared measurement devices, bimetallic temperature devices, fluid-expansion temperature devices, and change-of-state measurements.

1.4.1. Factors influencing temperature. Several factors should be considered when making a temperature forecast.

1.4.1.1. *Incoming shortwave radiation.* Solar energy is the primary heat source in the atmosphere. As the surface is warmed, it emits higher amounts of longwave radiation. A balance is struck in the diurnal cycle between outgoing and incoming energy, as shown in **Figure 1.28**.

Figure 1.28. Standard surface model of daily atmospheric heating and cooling in relation to radiation gains and loses under clear skies.

1.4.1.2. *Wind.* Turbulent mixing tends to "average out" temperature over distances. Temperature and moisture advection also impact temperature; moist air has a higher specific heat and is less dense than dry air.

1.4.1.3. *Clouds and fog.* Clouds and fog block incoming solar radiation during the day and insulate the outgoing terrestrial radiation at night; the net effect is a decreased diurnal temperature variation.

1.4.1.4. *Surface cover.* Numerous possible combinations of concrete, steel, farmland, rooftops, water, ice, and snow have different albedos and emissivities. Snow reflects particularly well, decreasing absorbed radiation. Snow also insulates the ground and reduces outgoing radiation. Sand traps air and insulates the ground, and it also radiates intensely, allowing deserts to get cold at night.

1.4.2. General Temperature Forecast Tools.

1.4.2.1. *Climatology.* Most forecast locations across the world have decades' worth of archived weather data, providing a sound base for climatology. The 14th Weather Squadron (**https://climate.af.mil**) has a vast library of climatological temperature data; utilize their products (such as country climatologies, modeled diurnal curves (MODCURVES), operational climatic data summaries (OCDS-II), and surface climograms) for initial temperature guidance.

1.4.2.2. *Persistence.* Under the right conditions, persistence can work well for forecasting temperatures. Simply take the high and low temperatures from the previous day, and compare the yesterday's synoptic situation with today's conditions. If there have been no changes in either the air mass or the general weather (clouds, winds, etc.), this technique works accurately until changes occur.

1.4.3. Forecasting Maximum Temperatures.

1.4.3.1. *Within an air mass*. Use the following steps to forecast maximum temperatures within an air mass:
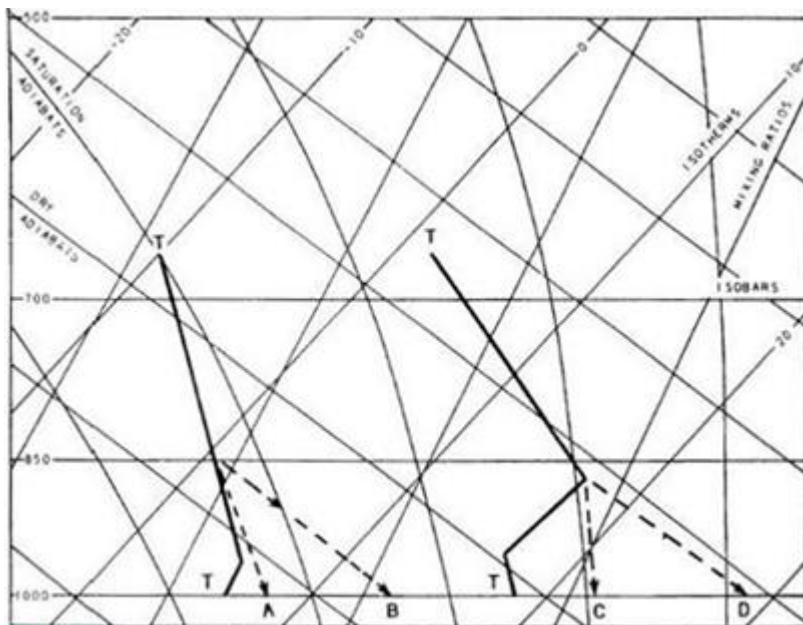
1.4.3.1.1. Examine current analysis and prognosis products to determine the source of the air mass expected over the station at verification time. Select a station 24 hours upstream and use its previous day's maximum temperature as a first estimate for the forecast.

1.4.3.1.2. Modify the first estimate for adiabatic effects by determining the elevation difference between the two stations (5.3°F/1000 feet).

1.4.3.1.3. Make a cloud cover forecast for the station, compare it to the cloud cover at the upstream station, and determine the difference in effects of insolation. Use diurnal temperature curves that consider cloud cover (such as MODCURVES) to make a final temperature forecast.

1.4.3.2. *Using the Skew-T diagram.* Calculations for the maximum temperature on the Skew-T should be done using a morning sounding. To calculate the maximum expected temperature for the day, first determine if the day will be cloudy, with little solar insolation received at the surface, or sunny, with a great deal of solar insolation received at the surface. If the day is expected to be mostly sunny, follow a dry adiabat from the 850 mb temperature to the surface pressure level and read the temperature at the intersection. For mountainous areas and high elevations, adjust to start at a pressure level approximately 5000 feet above the surface. If the day is expected to be mostly cloudy (broken-to-overcast cloud cover), follow a moist adiabat from the 850 mb level (or 5000-foot AGL pressure level) to the surface pressure level and read the temperature at the intersection. See **Figure 1.29** for examples of the maximum temperature computations for sunny and cloudy conditions. In summer air mass situations, strong radiation inversions routinely develop. If the plotted morning Skew-T shows a radiation inversion with a top between 4000 and 6000 feet, use the temperature at the top of the inversion (the warmest point in the inversion) as the starting point in the computation, instead of the 850 mb temperature.

Figure 1.29. Computation of maximum Skew-T temperature. With no inversion and (A) mostly cloudy skies, (B) mostly clear skies. With an inversion and (C) mostly cloudy skies, (D) mostly clear skies.

1.4.3.3. *Callen and Prescott method.* This method should be avoided near oceans, and is most accurate at high latitudes. It does not account for factors such as mixing, warm- and cold-air advection, and soil moisture, all of which can have a significant impact on maximum temperatures. These factors should be considered and the temperature forecast adjusted accordingly. The thickness of the 1000-850 mb layer (h) can be utilized to approximate the surface temperature maximum (TMAX) using the following equation: TMAX = -192.65 + 0.156h + K. Thickness should be in meters, and TMAX is output in °C. K is a correction term that depends on cloud cover and the current month of the year (refer to **Table 1.18** for the K values for different months and cloud classes). The cloud classes used in this method are defined as follows:

1.4.3.3.1. Class 0: Low and medium cloud generally less than half cover. High cloud not overcast. Fog only around dawn, if at all.

1.4.3.3.2. Class 1: Roughly 50% cloudiness. If fog occurs, it clears slowly during the morning.

1.4.3.3.3. Class 2: Mainly cloudy. If fog occurs, it clears by midday, but slowly.

1.4.3.3.4. Class 3: Overcast, possibly with rain or snow. Persistent fog.

Table 1.18. K-value correction factors for the Callen and Prescott method.

Month	Class			
	0	**1**	**2**	**3**
January	-4	-4	-5	-5
February	-3	-3	-4	-5
March	-1	-2	-3	-4
April	+1	0	-1	-2
May	+2	+1	0	-1
June	+4	+3	+1	0
July	+4	+3	+1	0
August	+3	+2	+1	0
September	+1	0	-1	-1
October	-1	-1	-2	-3
November	-2	-3	-4	-4
December	-4	-4	-5	-5

1.4.3.4. *Extrapolation.* This technique refers to the forecasting of a weather feature based solely on past motions of that feature. To use extrapolation techniques in short-range forecasting, it is necessary to be familiar with the positions of fronts and pressure systems, their direction and speed of movement, precipitation and cloud patterns that might affect the local terminal, and the upper-level flow that affects the movement of these weather patterns.

1.4.3.4.1. First, determine the air mass that is over the region during the forecast time of interest.

1.4.3.4.2. Check the high temperatures in the air mass for the preceding days.

1.4.3.4.3. Account for adiabatic changes; if the air is rising (upslope trajectory), subtract 1° to 3°C (1.8° to 5.4°F) (based on moist or dry adiabatic lapse rate) for every 1000 feet of ascent to allow for adiabatic cooling of the parcel as it rises. If the flow is downslope, add 1° to 3°C (1.8° to 5.4°F) for the corresponding ascent.

1.4.3.4.4. Adjust for modifications of the air mass, such as expected cloud cover, winds, and precipitation.

1.4.4. Forecasting Minimum Temperatures.

1.4.4.1. *Using the Skew-T diagram.* If the air mass is not expected to change from the sounding time to the forecast valid time, follow the moist adiabat passing through the 850 mb dew point temperature down to the surface – the temperature at the intersection is the expected minimum temperature. Use a forecast sounding if atmospheric changes are expected, and use the 700 mb level if the station elevation is above the 850 mb level.

1.4.4.2. *After cold frontal passage.* Forecast the coldest minimum temperature for the second morning after a cold front passes. By the second morning, the high is centered near or over the forecast location; with little wind and little or no temperature advection, the minimum temperature is colder than the morning before. During the second day, the high moves away and warm advection begins; the third morning's minimum temperature is generally warmer than the second.

1.4.4.3. *McKenzie method.* A minimum temperature forecast can be found by plugging the day's maximum temperature (TMAX) and the dew point (Td) at the time of TMAX into a simple equation: TMIN = 0.5(TMAX + Td) – K. K is a correction factor determined by the expected overnight weather conditions shown in **Table 1.19**. Subtract two additional degrees in the presence of a low-level temperature inversion.

Table 1.19. K-value correction factors for the McKenzie method.

Overnight Wx Conditions	K
Calm/clear skies throughout the night	8 or 9
Light wind/mostly clear	6 to 8
Light wind/broken clouds	4 to 7
Light wind/mostly cloudy or cloudy	2 to 3
Moderate wind/mostly clear	3 to 5
Moderate wind/broken clouds	2 to 4
Moderate wind/mostly cloudy or cloudy	1 or 2
Brisk winds (most cloud classes)	1 or 2

1.4.5. Additional Rules of Thumb. The following rules of thumb will be helpful if surface observations are forecaster's primary or only tool:

1.4.5.1. Plot hourly temperatures and dew points (time on the X-axis and temperature on the Y-axis) to establish station diurnal trend curves. It may take several days to establish a firm pattern, but this is an excellent limited-data temperature-forecasting tool.

1.4.5.2. Subtract the average diurnal variation for the month from the maximum temperature to estimate a minimum temperature when little change is expected in the cloud cover or air mass. Add the diurnal variation to the minimum temperature for estimating maximum temperature.

1.4.5.3. The moistness or dryness of the ground affects heating of the ground. Solar radiation evaporates moisture in or on the ground first, before heating the surface; this inhibits daytime maximum heating. Wet soil heats up and cools down much slower than dry soil.

1.4.5.4. Snow cover significantly affects daytime heating of the ground and air by reflecting solar radiation. Expect lower temperatures if there is snow cover. Minimum temperatures will also generally be colder if there is snow cover.

1.4.5.5. Air masses advected over an area with snow cover will cool if the air mass is warmer than the ground.

1.4.5.6. Moisture decreases the daily temperature range. For example, the spread between daily maximum and minimum temperatures ranges from only 3°C to 5°C (5°F to 10°F) in a wet-season tropical forest, to over 28°C (50°F) in dry, interior deserts.

1.4.5.7. High relative humidity (80% or greater) in the low-levels may inhibit cooling because moisture effectively traps long-wave heat transfer. A humid night may be 3°C (5°F) warmer than a drier night.

1.4.5.8. High winds temper nocturnal cooling due to turbulent mixing. At night, due to more rapid cooling of the air in the lowest levels, the air mixed down is warmer than air near the ground surface. One rule of thumb is to add 1°C (2°F) to the low temperature forecast if the winds are to be around 15 knots. Add up to 3°C (5°F) for winds of 35 knots. This technique does not consider warm- or cold-air advection.

1.4.5.9. Pressure trends help forecasters anticipate approaching fronts. Plotting hourly pressures allows diurnal pressure curves to be established. Large variations from the norm could indicate approaching frontal systems or pressure centers.

1.4.6. Temperature Indices. The military is cognizant of the risks associated with extreme temperatures, and several indices and guidelines are codified into policy for use under extreme temperature conditions. Refer to AFI 48-151, *Thermal Injury Prevention Program,* for details on the indices summarized below.

1.4.6.1. *Heat Index.* The heat index (also known as apparent temperature) considers the combined effects of air temperature and atmospheric moisture on human physiology. Refer to AFI 48-151 for current, Air Force-approved heat index values (and the associated risks) based on temperature and relative humidity levels.

1.4.6.2. *Wet-Bulb Globe Temperature (WBGT) Heat Stress Index.* The WBGT is a measure of the heat stress in direct sunlight. It takes into account temperature, humidity, wind speed, sun angle, and cloud cover. The computation of the WBGT involves 3 thermometers and is normally determined and disseminated by medical or disaster preparedness personnel. The WBGT is computed by adding 70 percent of the wet-bulb temperature, 20 percent of the black globe temperature, and 10 percent of the dry-bulb temperature. The wet-bulb temperature is the temperature to which air can be cooled solely via evaporation. The black globe temperature is measured using a special thermometer known as a black globe thermometer. Refer to AFI 48-151 for current, Air Force-approved WBGT heat stress index values and related information.

1.4.6.3. *Fighter Index of Thermal Stress (FITS).* The FITS was developed in 1979 to provide a measure of the thermal stress experienced by aircrew in fast aircraft with canopies and environmental control systems, engaged in combat sorties at low altitudes, direct sunlight or light overcast, and high outside temperatures. The FITS was derived from the WBGT using in-flight data on cockpit environments and assuming a fixed contribution from solar heating. The FITS table uses ground dry bulb and wet bulb temperatures to yield an estimate of cockpit thermal stress. FITS reference values and zones are not exact demarcations, but represent temperatures and humidities at which aircrews begin to experience heat-stress-related effects. These effects may vary with the individual, the particulars of the ground and flight aspects of the mission, the particular clothing worn, and other factors. FITS actions are therefore guidelines, rather than directives. Refer to AFI 48-151, Attachment 3, for details on FITS values and appropriate actions for the FITS zones.

1.4.6.4. *Wind chill.* Wind chill temperature combines the effects of low air temperatures with additional heat losses caused by the wind. To calculate the observed or forecast wind chill temperature, use **Table 1.20**.

Table 1.20. Wind chill temperature chart.

WIND SPEED (mph)	TEMPERATURE (°F)											
	10	5	0	-5	-10	-15	-20	-25	-30	-35	-40	-45
	EQUIVALENT CHILL TEMPERATURE											
5	1	-5	-11	-16	-22	-28	-34	-40	-46	-52	-57	-63
10	-4	-10	-16	-22	-28	-35	-41	-47	-53	-59	-66	-72
15	-7	-13	-19	-26	-32	-39	-45	-51	-58	-64	-71	-77
20	-9	-15	-22	-29	-35	-42	-48	-55	-61	-68	-74	-81
25	-11	-17	-24	-31	-37	-44	-51	-58	-64	-71	-78	-84
30	-12	-19	-26	-33	-39	-46	-53	-60	-67	-73	-80	-87
35	-14	-21	-27	-34	-41	-48	-55	-62	-69	-76	-82	-89
40	-15	-22	-29	-36	-43	-50	-57	-64	-71	-78	-84	-91
45	-16	-23	-30	-37	-44	-51	-58	-65	-72	-79	-86	-93
50	-17	-24	-31	-38	-45	-52	-60	-67	-74	-81	-88	-95

1.5. Pressure. Aircraft are affected by atmospheric pressure in many ways; takeoffs, landings, rate of climb, and true flight altitude are dependent on pressure values. This section begins with a general discussion of pressure, and then outlines several techniques to calculate and forecast sea-level pressure, altimeter settings, pressure altitude, density altitude, and D-values.

1.5.1. General Guidance. Atmospheric pressure is the force exerted on a surface by the weight of the air above it. Station pressure is simply the atmospheric pressure measured at the station, and is the base value from which sea-level pressure and altimeter settings are determined. Pressure changes most rapidly in the vertical, with the most rapid changes occurring near the surface, with more gradual changes with increasing height at higher altitudes. Horizontal variations in pressure are much smaller and are caused by synoptic-scale pressure centers.

1.5.1.1. *Air mass effects.* Air masses have different thermal properties; for example, a continental Polar (cP) air mass is colder, drier, and denser (higher pressure) than a maritime Tropical (mT) air mass. Pressure changes due to air-mass movements are best detected by extrapolating from upstream stations and determining pressure trends.

1.5.1.2. *Diurnal considerations.* Daily heating and cooling, as well as "atmospheric tides", cause diurnal pressure changes. On average, two maxima occur each day, at approximately 1000L and 2200L. Likewise, there are two average daily pressure minima, at approximately 0400L and 1600L. The difference between the maxima and minima is greatest near the Equator (about 2.5 mb), decreasing to virtually zero above 60° latitude.

1.5.1.3. *Standard atmosphere.* The standard atmosphere is a hypothetical vertical distribution of atmospheric temperature, pressure, and density representative of the "average" atmosphere; this ensures standardized altimeter calibrations and aircraft performance calculations. The standard atmosphere forms the basis of the Skew-T diagram, and is useful to compare current or expected conditions with the atmospheric standard. **Table 1.21** lists the pressures and temperatures associated with the standard atmosphere in 1000-feet increments, and **Table 1.22** lists the same data by pressure level.

1.5.2. Pressure and altitude definitions. It's important to be familiar with the following terms in this section; review the definitions below before proceeding to subsequent sections.

1.5.2.1. Station Pressure: The atmospheric pressure computed for the level of the station elevation.

1.5.2.2. Sea Level Pressure: The atmospheric pressure at mean sea level. In meteorology, mean sea level is used as the reference surface for all altitudes in upper-atmospheric work.

1.5.2.3. Indicated Altitude: The altitude read directly from a pressure altimeter when set to the prescribed altimeter setting.

1.5.2.4. True Altitude: The true vertical distance above mean sea level.

1.5.2.5. Absolute Altitude: The true vertical distance above ground level.

1.5.2.6. Pressure Altitude: The indicated altitude when the altimeter is set to 1013.2 mb (29.92 inches of mercury).

1.5.2.7. Density Altitude: The pressure altitude corrected for temperature variations from the standard atmosphere. Density altitude is used as a measure of aircraft performance.

Table 1.21. Standard atmospheric pressure and temperature – by altitude.

U.S. Standard Atmosphere by Altitude									
Altitude (ft)	Pressure		Temperature		Altitude (ft)	Pressure		Temperature	
	Millibars (mb)	Inches of Hg	°C	°F		Millibars (mb)	Inches of Hg	°C	°F
0	1013.2	29.92	15.0	59.0					
1,000	977.2	28.86	13.0	55.4	26,000	359.9	10.63	-36.5	-33.7
2,000	942.1	27.82	11.0	51.9	27,000	344.3	10.17	-38.5	-37.3
3,000	908.1	26.82	9.0	48.3	28,000	329.3	9.72	-40.5	-40.9
4,000	875.1	25.84	7.1	44.7	29,000	314.8	9.30	-42.5	-44.4
5,000	843.1	24.90	5.1	41.2	30,000	300.8	8.89	-44.4	-48.0
6,000	812.0	23.98	3.1	37.6	31,000	287.4	8.49	-46.4	-51.6
7,000	781.8	23.09	1.1	34.0	32,000	274.5	8.11	-48.4	-55.1
8,000	752.6	22.22	-0.8	30.5	33,000	262.0	7.74	-50.4	-58.7
9,000	724.3	21.39	-2.8	26.9	34,000	250.0	7.38	-52.4	-52.2
10,000	696.8	20.58	-4.8	23.3	35,000	238.4	7.04	-54.3	-65.8
11,000	670.2	19.79	-6.8	19.8	36,000	227.3	6.71	-56.3	-69.4
12,000	644.4	19.03	-8.8	16.2	37,000	216.6	6.40	-56.5	-69.7
13,000	619.4	18.29	-10.8	12.6	38,000	206.5	6.10	Constant to 65,000 ft	
14,000	595.2	17.58	-12.7	9.1	39,000	196.8	5.81		
15,000	571.8	16.89	-14.7	5.5	40,000	187.5	5.54		
16,000	549.2	16.22	-16.7	1.9	41,000	178.7	5.28		
17,000	527.2	15.57	-18.7	-1.6	42,000	170.4	5.04		
18,000	506.0	14.94	-19.7	-5.2	43,000	162.4	4.79		
19,000	485.5	14.34	-22.6	-8.8	44,000	154.7	4.57		
20,000	465.6	13.75	-24.6	-12.3	45,000	147.5	4.35		
21,000	446.4	13.18	-26.6	-15.9	46,000	140.6	4.15		
22,000	427.9	12.64	-28.6	-19.5	47,000	134.0	3.96		
23,000	410.0	12.11	-30.6	-23.9	48,000	127.7	3.77		
24,000	392.7	11.60	-32.5	-26.6	49,000	121.7	3.59		
25,000	376.0	11.10	-34.5	-30.2	50,000	116.0	3.42		

Table 1.22. Standard atmospheric pressure and temperature – by level.

U.S. Standard Atmosphere by Level							
Pressure Level	Height Above Mean Sea Level		Temperature	Pressure Level	Height Above Mean Sea Level		Temperature
(mb)	(m)	(ft)	(°C)	(mb)	(m)	(ft)	(°C)
1000	111	364	14.3	550	4,865	15,962	-16.6
950	540	1,773	11.5	500	5,574	18,289	-21.2
925	764	2,520	10.0	450	6,344	20,812	-26.2
900	988	3,243	8.6	400	7,185	23,574	-31.7
850	1,457	4,781	5.5	350	8,117	26,631	-37.7
800	1,949	6,394	2.3	300	9,164	30,065	-44.5
750	2,466	8,091	-1.0	250	10,363	33,999	-52.4
700	3,012	9,882	-4.6	200	11,784	38,662	-56.5
650	3,591	11,780	-8.3	150	13,608	44,647	-56.5
600	4,206	13,801	-12.3	100	16,180	53,083	-56.5

1.5.3. Pressure-Related Parameters.

1.5.3.1. *Sea level pressure (SLP).* SLP is simply the atmospheric pressure at mean sea level. It can be measured directly at sea level or determined from the observed station pressure at other locations. SLP is normally reported in millibars, and the standard is 1013.25 mb (29.92 inches of Mercury (Hg)). To obtain the sea level pressure, first find the height of the 1000 mb surface using the following formula (if the number is negative, the 1000 mb surface is below ground level): 1000 mb height = (500 mb height) – (1000-500 mb thickness). Then, divide the 1000 mb height by 7.5 mb/meters. Finally, add this value to 1000 mb. For an example, assume the 500 mb height is 5500 meters, and the 1000-500 mb thickness is 5300 meters. The difference between these is 200 meters, so this is the 1000 mb height. Dividing 200 by 7.5, we get 26.67 mb. Adding this to 1000 mb gives us a final value of 1026.67 mb.

1.5.3.2. *Altimeter setting.* The altimeter setting is the value of atmospheric pressure to which an aircraft altimeter scale is set so that it shows the altitude of an aircraft above a known reference surface. There are three different types of altimeter settings from the Q-code system: QNE, QNH, and QFE. This code system was developed when air-to-ground communications were by wireless telegraph and many routine phrases and questions were reduced to three-letter codes. **Table 1.23** describes each altimeter setting and how it affects the altimeter reading.

Table 1.23. Altimeter settings.

Altimeter Setting	Corresponding Pressure Altimeter reading on the ground	Corresponding Pressure Altimeter reading in the air
QNE (29.92 inches of Hg or 1013.25 mb)	Airfield pressure altitude	Altitude of aircraft in a standard atmosphere
QNH (Station pressure reduced to sea level)	Airfield elevation above sea level	Altitude of aircraft above sea level without consideration of temperature
QFE (Actual station pressure)	Zero elevation	Altitude of aircraft above sea level without consideration of temperature

1.5.3.2.1. QNH. QNH is the most common altimeter setting used by Air Force weather forecasters; find it by measuring the surface pressure and reducing it to sea level. When QNH is set, the altimeter indicates height above mean sea level. Follow the steps below to forecast the QNH.
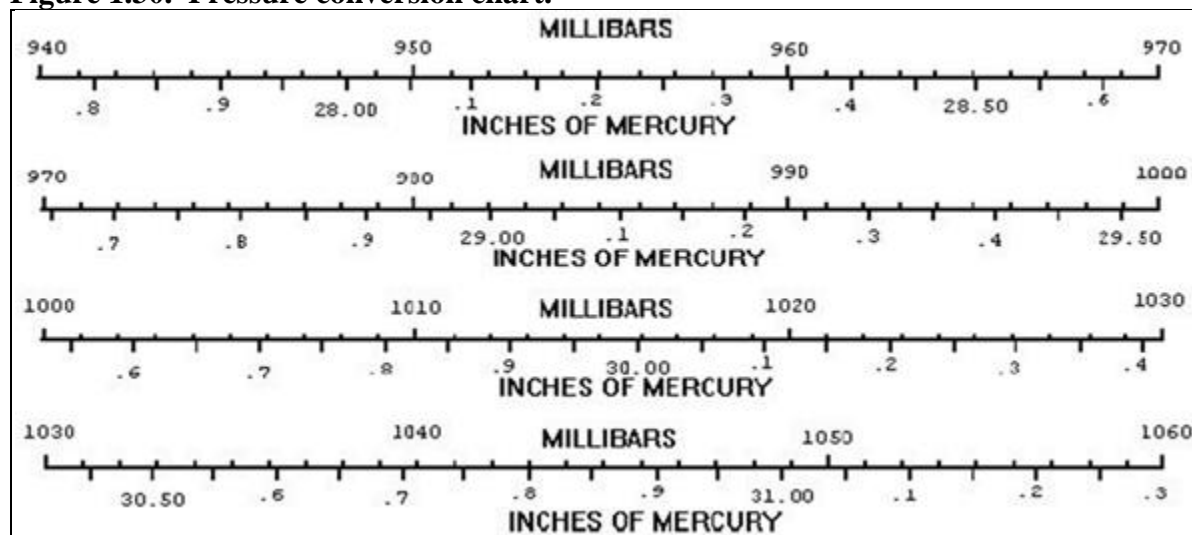
1.5.3.2.1.1. Find the current altimeter setting (for example, 29.98 inches).

1.5.3.2.1.2. Find the current sea level pressure (for example, 1015.5 mb).

1.5.3.2.1.3. Find the forecast sea level pressure (for example, 1020.5 mb).

1.5.3.2.1.4. Subtract the current and forecast sea level pressures (1020.5 - 1015.5 = 5.0).

1.5.3.2.1.5. Multiply the difference by .03 (5.0 X 0.03 = 0.15).

1.5.3.2.1.6. Add this value to the current altimeter setting to get the QNH (29.98 + 0.15 = 30.13).

1.5.3.2.1.7. After calculating QNH, make final adjustments for diurnal effects, upstream observations, and the synoptic situation. Subtract an additional 0.01 from the QNH value to compensate for the height of the aircraft altimeter above the ground.

1.5.3.2.2. Pressure conversion chart. **Figure 1.30** provides a simplified, graphical method for converting from millibars to inches of mercury and obtaining the altimeter setting. Refer to the chart, convert your value, and subtract 0.01 from this setting for the final value to compensate for the height of the aircraft altimeter above the ground.

Figure 1.30. Pressure conversion chart.

1.5.3.3. *Pressure altitude (PA).* According to the AMS Glossary of Meteorology, for aircraft flying above 18,000 feet mean sea level, PA is the indicated altitude of a pressure altimeter at an altimeter setting of 1013.2 mb (29.92 inches of mercury). In other words, it is the indicated altitude above the 1013.2 mb constant-pressure surface. Most aircrews require PA to calculate takeoff and landing data.

1.5.3.3.1. Simple PA formula. An approximate PA, using a given altimeter and field elevation (FE), in feet, is found by the following equation: PA = FE + [1000 (29.92 - QNH)]. In this formula, QNH can either be the observed or forecast altimeter setting; use the appropriate value for your situation. Use **Figure 1.30**, if necessary, to convert between millibars and inches of Hg. For a calculation example, if we have a field elevation of 590 feet and QNH of 29.72, plugging these values into the equation gives: PA = 590 + [1000 (29.92 – 29.72)]. Calculating the simple math results in a PA of 790 feet.

1.5.3.3.2. Scientific PA formula. The simple PA formula presented above is an approximation, and should be used only when other tools are unavailable. For official purposes, use the scientific formula in **Figure 1.31** below, where PA is pressure altitude in feet and Psta is station pressure in millibars:

Figure 1.31. Pressure Altitude formula.

$$PA = \left(1 - \left(\frac{P_{sta}}{1013.25}\right)^{0.190284}\right) * 145366.45$$

1.5.3.4. *Density altitude (DA).* DA is the pressure altitude corrected for temperature variations from the standard atmosphere. DA increases as air density decreases. Low air density adversely impacts aircraft performance, so pilots should expect degraded performance when the DA is high. Specifically, lift and thrust will be reduced, leading to longer takeoff rolls and reduced climb rates and payload capacity. Air density decreases as temperature, humidity, and altitude increase. Therefore, look for increasing DA as temperature, humidity, and altitude increase. This is critical for aircraft taking off or landing on short runways, especially those loaded down with weapons, cargo, or fuel. Also consider helicopters flying at high altitudes on rescue or other missions that increase weight with payloads and passengers during the mission.

1.5.3.4.1. DA computation method. To calculate DA, use the following formula: **DA = PA + (120 x DT).** Where PA is the pressure altitude, 120 represents a temperature constant, and DT is the air temperature minus the standard atmosphere temperature at the pressure altitude (in high temperatures or high humidities, this calculation may be up to 5% too high).

1.5.3.4.2. DA computation example. Given a station PA of 2010 feet, actual surface temperature of 30°C, and standard atmospheric temperature (for the given PA) of 11°C (see **Table 1.21** for standard atmospheric temperatures), the DA is calculated by the above equation. With these values, DT = 30°C – 11°C = 19°C, and the DA equation becomes DA = 2010 + (120 X 19). Calculating the simple math results in a DA of 4290 feet.

1.5.3.5. *D-Value.* The D-value is the difference between the true altitude of a pressure surface (obtained from sounding data) and the standard atmosphere altitude of this pressure surface. A simple calculation to obtain the D-value is given as: **D-value = True altitude – Standard altitude**. For example: given a mission altitude of 11,000 feet MSL, use the appropriate constant-pressure product for the flight level, in this case, the 700 mb chart. The standard height for the 700 mb level is 9882 feet MSL (from **Table 1.22**). Consulting a 700 mb analysis or sounding product gives a hypothetical 700 mb level of 9200 feet. The D-value would then be 9200 – 9882, or -682 feet.

Chapter 2

FLIGHT WEATHER ELEMENTS

2.1. Clouds.   Clouds form when water vapor changes to either liquid droplets (condensation) or ice crystals (deposition). This happens when air is cooled below its saturation point either directly (radiational cooling or advection) or by being raised higher in the atmosphere (adiabatic cooling).

2.1.1. Cloud development - adiabatic temperature change. Since air pressure decreases with altitude, adiabatic temperature change is the fundamental determinant of whether air will rise under its own energy. When air rises, it expands due to the lower ambient pressure. Similarly, when air sinks, it compresses. These pressure changes are associated with a change in temperature: rising air cools and sinking air warms. These are "adiabatic" temperature changes, resulting from processes that don't involve true heat transfer. The amount of temperature change with altitude is virtually static in non-saturated air; unsaturated air warms and cools at approximately 3°C for every 1000 feet, or around 9.8°C per kilometer (this is the dry adiabatic lapse rate). Saturated air cools less rapidly as it rises; water vapor condenses into liquid droplets when the air parcel is cooled further, and latent heat from this change of state keeps the air parcel warmer than a dry parcel would be at the corresponding height. In addition, warm air can hold much more water vapor than cold air.

2.1.2. Cloud development – stability and instability. Objects float in water due to the buoyant force caused by density differences. In the atmosphere, the density of an air parcel compared to its environment determines whether it will sink or rise. Generally, the temperature of an air parcel is what determines its density for a given pressure level. If a particular parcel is less dense (warmer) than the surrounding air, it will rise until it reaches the "equilibrium level," where it stops rising. The equilibrium level has the same temperature as the air parcel, and will no longer allow it to rise. If, however, the parcel is denser (colder) than the surrounding air, it will be forced to sink, creating a downdraft. Clouds are fundamentally formed by moist, rising air that cools beyond its dew point. The altitude where this occurs is the "lifted condensation level." Above this point, if the atmosphere is unstable, the cloud will continue to grow vertically and potentially produce precipitation. This does not always happen, however, and the structure of a cloud can give clues as to the atmospheric conditions that produced it. These clues are invaluable for aviators in determining where potentially dangerous updrafts and downdrafts are occurring.

2.1.3. Cloud Types and States of the Sky. Clouds are classified by their appearance and how they form: cumuliform clouds are produced by rising air in an unstable atmosphere, while stratiform clouds occur when a layer of air is cooled below its saturation point without extensive vertical motion. Although stratiform clouds produce less spectacular weather, they may often cause persistent low ceilings and poor visibilities, which may be critical to Air Force and Army operations. Clouds are further classified by the altitude at which their bases form: low, middle and high cloud layers. For details on the cloud types described in the sections below, refer to the International Cloud Atlas (**https://cloudatlas.wmo.int/coding-of-clouds.html**). Keeping these basics in mind will help in understanding the various techniques and rules available for forecasting clouds.

2.1.3.1. *Low Clouds.* Low clouds are classified as clouds forming from the surface to 6500 feet above ground level.

2.1.3.1.1. Cumulus (CU). Cumulus clouds are cottony in appearance, with an internal structure of updrafts and downdrafts. Cumulus clouds develop by atmospheric lifting, especially convection. The L1-variety cumulus cloud is defined by little vertical extent, and may appear flattened or ragged, and is indicative of good weather. The L2 towering cumulus cloud shows moderate-to-strong vertical development.

2.1.3.1.2. Stratocumulus (SC). Stratocumulus clouds are formed by the spreading out of cumuliform clouds, or the lifting and mixing of stratiform clouds. Precipitation from stratocumulus is usually light and intermittent. L4-type stratocumulus is formed by the spreading out of cumulus, while L5 are not formed by the spreading out of cumulus. The L8 variety are combined with cumulus, and have bases at different levels.

2.1.3.1.3. Stratus (ST). Stratus clouds are sheet-like in appearance, with diffuse or fibrous edges. They usually produce light continuous or intermittent precipitation, but not showery. The L6 type is a more-or-less continuous layer, ragged sheets, or a combination of both, but no stratus fractus. The L7 variety has the stratus fractus or cumulus fractus present, indicative of wet weather.

2.1.3.1.4. Cumulonimbus (CB). Massive in appearance with great vertical extent, cumulonimbus clouds are indicative of the most intense weather on Earth – heavy rain, hail, lightning, damaging winds, and tornadoes. The L3 variety are younger or weaker CB, where there is no anvil top or cirriform development, while the L9 type represents a mature CB with a cirriform anvil.

2.1.3.2. *Middle Clouds.* Middle clouds are classified as clouds forming between 6500 feet and 20,000 feet above ground level.

2.1.3.2.1. Altostratus (AS). Similar in appearance to stratus, but occurring at higher altitudes, altostratus clouds are dense enough to prevent objects from casting shadows, and do not create the "halo" phenomenon associated with lower clouds. Altostratus is mainly categorized by the M1 type, a grayish-bluish mid-level cloud layer.

2.1.3.2.2. Nimbostratus (NS). Thicker and darker than altostratus clouds, nimbostratus clouds usually produce light to moderate precipitation. Although classified as a middle cloud by definition, its base usually builds downward into the low cloud height range. Nimbostratus are categorized by the M2 designation.

2.1.3.2.3. Altocumulus (AC). The appearance of altocumulus is similar to stratocumulus, but consists of smaller elements. There are several different types of AC, covered by the classifications M3 through M9. Two important variations of AC are altocumulus standing lenticular (ACSL, M4), and altocumulus castellanus (ACC, M8). ACSL clouds are caused by the lifting action inherent in mountain waves, and indicate turbulence. ACC has greater vertical extent than regular AC, implying mid-level instability.

2.1.3.3. *High Clouds.* High clouds are classified as clouds forming above 20,000 feet above ground level.

2.1.3.3.1. Cirrus (CI). Cirrus clouds consist entirely of ice crystals. A partial halo around the sun or moon occasionally accompanies cirrus clouds; the presence of a complete halo indicates cirrostratus instead of cirrus. Cirrus are categorized as H1 through H4.
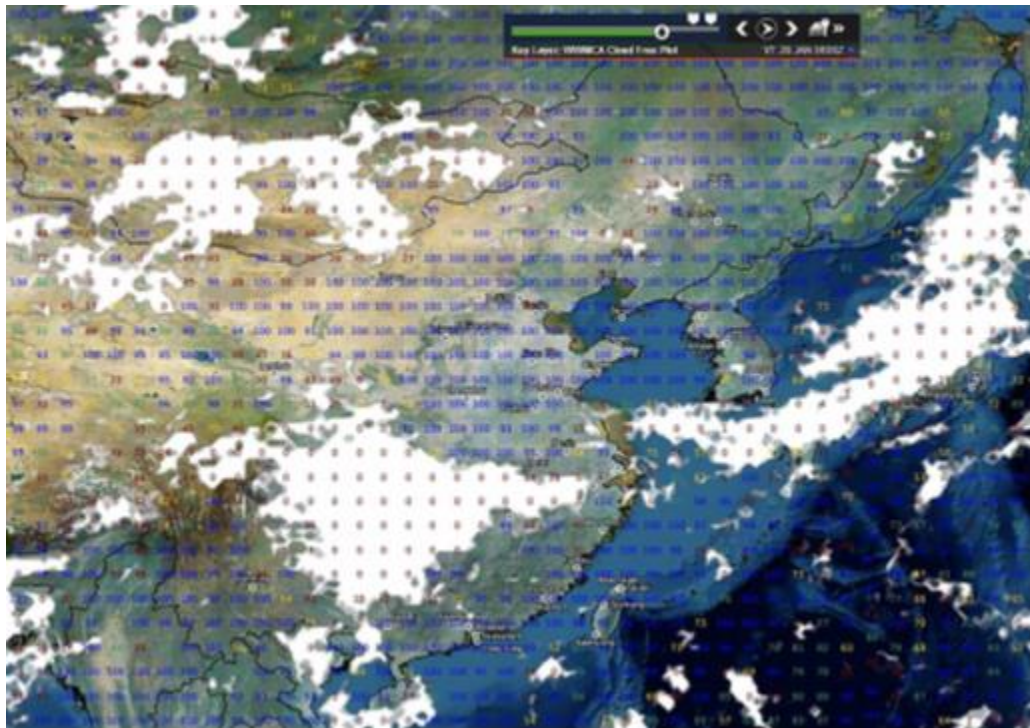
2.1.3.3.2. Cirrostratus (CS). Cirrostratus appear more "sheet-like" than cirrus clouds, and will produce complete halos if they are thin enough. CS is distinguishable from haze by its whiter and brighter appearance (haze is more yellowish-brown). CS is categorized as H5 through H8.

2.1.3.3.3. Cirrocumulus (CC). Cirrocumulus clouds appear similar to AC or ACC, but with smaller individual elements. Individual cloud elements of CC can be covered by your little finger when extended at arm's length; AC and ACC cannot. The elements can be so small that they are often difficult to see by the unaided eye. Some cirrocumulus clouds may resemble fish scales and are sometimes referred to as a "mackerel sky." CC are classified as H9.

2.1.4. General Cloud Forecasting Tools.

2.1.4.1. *Worldwide Merged Cloud Analysis (WWMCA).* The WWMCA provides an hourly analysis of cloud distribution based on information from five geostationary satellites and ten polar orbiting satellites; the satellite images are processed and merged into a single global cloud analysis. There are currently four WWMCA products available on AFW-WEBS: Cloud Mask, Total Cloud Cover, Cloud Top Height, and Cloud Free Plot. **Figure 2.1** is an example of the Cloud Free Plot over China and East Asia.

Figure 2.1. WWMCA Cloud Free Plot over China and East Asia.

2.1.4.2. *Climatology.* AFW-WEBS and the 14th Weather Squadron provide a detailed suite of cloud climatology products available – some of the most useful cloud products are detailed below.

2.1.4.2.1. Surface climograms. As a refresher, climograms are two-dimensional views of the likelihood of an event occurring at a given time of day and month of the year. Combined ceiling and visibility climograms are available for a variety of parameters, ranging from probability of ceilings less than 3000 feet and visibility less than three statute miles, down to probability of ceilings less than 100 feet and visibility less than one-quarter statute mile. Climograms can also produce red/yellow/green "stoplight" charts for ceiling thresholds from 100 to 25,000 feet, showing the annual probability of ceilings at those thresholds.
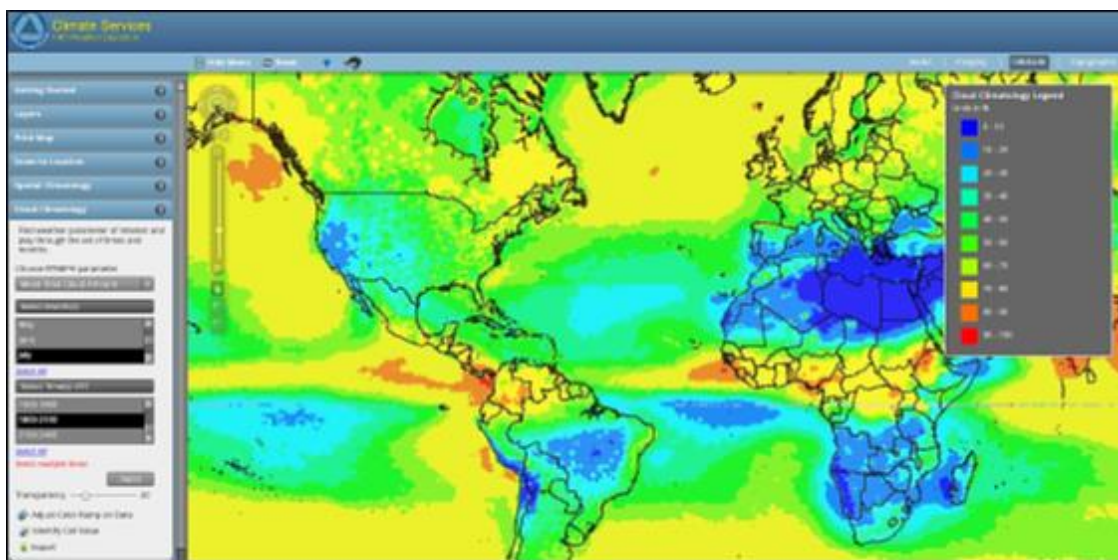
2.1.4.2.2. Operational Climatic Data Summaries (OCDS-II). The OCDS-II web application enables users to generate tables of the same ceiling and visibility probabilities as the surface climograms.

2.1.4.2.3. Wind Stratified Conditional Climatologies (WSCC). Given a set of initial conditions (month, time of days, wind direction, ceiling height, and visibility), the WSCCs indicate the likelihood that a particular ceiling category will be observed at a future time.

2.1.4.2.4. Surface Climatology maps. Geographical surface climatology maps can be produced for several combined ceiling and visibility categories (3000/3, 1500/3, and 1000/2); the maps are available for numerous regions around the world and can be stratified by month and time of day.

2.1.4.2.5. GIS Cloud Climatology. Multiple cloud-related parameters can be plotted using the GIS climate service tool; the maps can be stratified by month and time of day, and looped and zoomed to specific areas of interest. **Figure 2.2** shows an example product, displaying a global plot of mean cloud amount for the month of May, from 1800-2100 UTC.

Figure 2.2. Global plot of mean total cloud amount, May, 1800-2100 UTC.

2.1.4.2.6. WWMCA Climatology. The WWMCA climatology incorporates geostationary and polar orbiting satellite data as well as surface observed clouds. The latest 10 years of data are summarized to produce geographical maps, which can be generated for all regions around the world. Four parameters can be plotted: mean total cloud amount, standard deviation total cloud amount, mean cloud frequency by 20% band, and frequency of any ceiling.

2.1.4.3. Air Force NWP cloud forecasts. The Air Force produces two dedicated cloud forecast models, as well as several ensemble products; all of them are available on AFW-WEBS.

2.1.4.3.1. The Short Range Cloud Forecast (SRCF) model. The SRCF initializes with the most recent WWMCA and advects the analysis forward in time using several model variables (winds, temperatures, and relative humidity). The model produces a 12-hour forecast at 24 km resolution, with hourly updates. Total Cloud Cover and Cloud Free plots are available.

2.1.4.3.2. The Diagnostic Cloud Forecast (DCF) model. The DCF is calibrated using a 0-hour SRCF forecast (based on the WWMCA), and then run forward in time using predictor variables (e.g., pressure, relativity humidity, temperature, vertical velocity). Cloud Top, Cloud Base, and Total Cloud Cover products are available.

2.1.4.3.3. Ensemble products. Cloud forecasts are also available from the Air Force GEPS and MEPS ensembles; ceiling forecasts are calculated using an algorithm accounting for the impacts of precipitation, relative humidity, wind speed, precipitable water, and dust. The 20 km and 4 km MEPS also produce forecasts of the probability of cloud cover less than or equal to 20% and greater than or equal to 80%. Stamp charts of simulated cloud and cloud ceiling height are also available from the 20 km and 4 km MEPS; the stamp charts are unique in that they show nine ensemble members as small panels on the right-hand side of the image, with the control member as a large stamp on the left-hand side of the image. The user is therefore able to gauge forecast certainty, while still being able to see physically-relevant detail.

2.1.5. Determining cloud heights using a Skew-T.
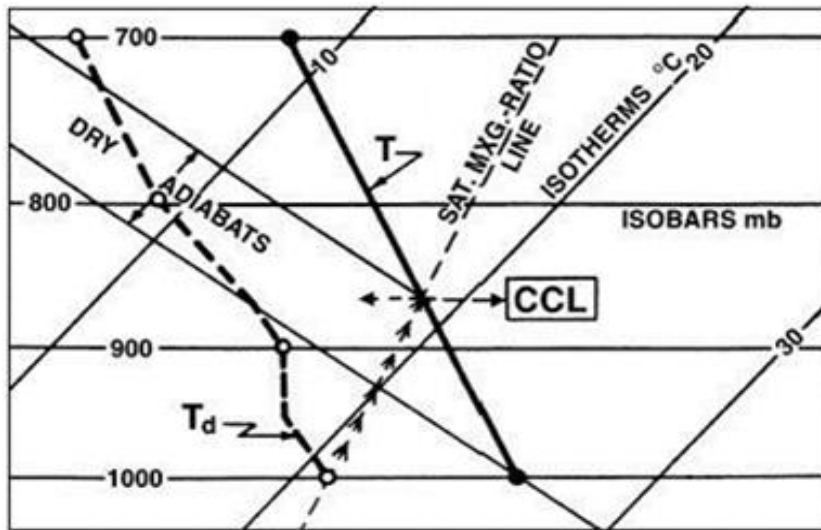
2.1.5.1. *Bases of stratus and stratocumulus – the Mixing Condensation Level (MCL).* The MCL is the lowest height at which saturation occurs after the complete mixing of the layer; use the MCL as base of stratus and cold-air stratocumulus decks. To find the MCL on a Skew-T, use the following procedures:

2.1.5.1.1. Determine the top of the layer height to be mixed (a subjective estimate based on winds, terrain roughness, original sounding, etc.). Stations in the cold air should have a pronounced low-level (but elevated) inversion. Use this as the top of the mixing layer.

2.1.5.1.2. Determine the average temperature and dew point within the layer.

2.1.5.1.3. Trace the average temperature up the dry adiabat and the average dew point up the mixing ratio line until they intersect; this is the MCL, and provides a good approximation of stratus or stratocumulus base heights, if they form. **Figure 2.3** illustrates this process.

Figure 2.3. Calculation of the MCL.

2.1.5.2. *Bases of non-precipitating cumuliform clouds – the Convective Condensation Level (CCL).* The CCL is the height to which a parcel of air, if heated sufficiently from below, will rise adiabatically until it is saturated and condensation begins. In most cases, the bases of cumuliform clouds will form about 25 millibars above the CCL; the CCL serves as the generation height of cumuliform clouds produced solely from convection. There are two methods of finding the CCL – the simplest technique (the "parcel method") uses only the surface dew point. In cases of high variations in surface layer moisture content, an average moisture value of the lowest layer is more representative (the "moist layer method").

2.1.5.2.1. CCL Parcel Method (**Figure 2.4**). From the surface dew point, proceed up the Skew-T parallel to the saturation mixing ratio line until it intersects the temperature curve. The intersection point is the CCL.
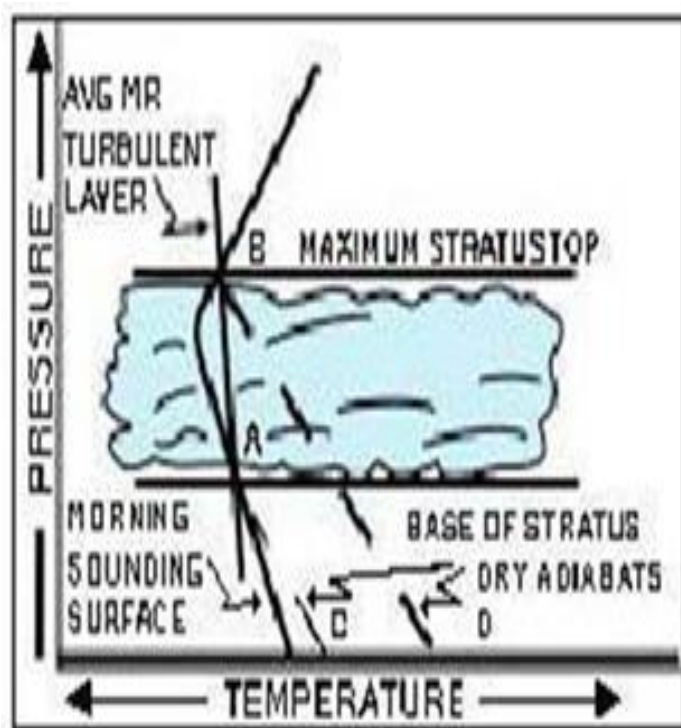
Figure 2.4. CCL Parcel Method.

Base of Convective Clouds using Surface Dewpoint Depressions			
Dewpoint Depression (°C)	Estimated Cumulus Height (ft)	Dewpoint Depression (°C)	Estimated Cumulus Height (ft)
0.5	200	1.0	400
1.5	600	2.0	800
2.5	1,000	3.0	1,200
3.5	1,400	4.0	1,600
4.5	1,800	5.0	2,000
5.5	2,200	6.0	2,400
6.5	2,600	7.0	2,800
7.5	3,000	8.0	3,200
8.5	3,400	9.0	3,600
9.5	3,800	10.0	4,000
10.5	4,200	11.0	4,400
11.5	4,600	12.0	4,800
12.5	5,000		

2.1.5.2.2. CCL Moist Layer Method. A layer is defined as "moist" if it has an RH of 65% or greater at all levels. In practice, the moist layer does not extend past the lowest 150 mb of the sounding. After finding the depth of the moist layer (or lowest 150 mb of the sounding, whichever is smaller), find the mean mixing ratio of this layer. Follow the mean mixing ratio line of the moist layer to the point where it crosses the temperature curve of the sounding. The intersection point is the CCL.

2.1.5.3. *Bases of convective clouds using dew point depressions.* **Table 2.1** provides a quick reference of expected cumulus cloud bases based on current or forecast surface dew point depression; the table is not suitable for use at locations in mountainous or hilly terrain, and should be used only when clouds are formed by active surface convection in the vicinity. Use with caution when the surface temperature is below freezing, due to the difficulties in accurately determining dew points at low temperatures.

Table 2.1. Expected bases of convective clouds from surface dew point depression.

2.1.6. Cloud Forecasting Using 700 mb Features. The location and coverage of mid-level clouds can be estimated by using the following guidelines on the 700 mb chart.

2.1.6.1. If 700 mb height contours and isotherms are parallel to the front, expect an extensive cloud band. If the height contours and isotherms are perpendicular to the front, expect a narrow cloud band.

2.1.6.2. If 700 mb streamlines are cyclonic, extensive cloud cover will occur. If the streamlines are anticyclonic, cloud cover will be sparse.

2.1.6.3. A 700 mb ridge passing ahead of a cold front generally coincides with low and middle cloud formation.

2.1.6.4. A 700 mb trough passing after a cold front generally coincides with low and middle cloud clearing.

2.1.7. Formation, advection and dissipation of low stratus. Air cooled by contact with a colder surface may be transferred upwards by turbulent mixing caused by the wind. The height to which the cooling is diffused upwards depends on the stability of the atmosphere, the wind speed, and the roughness of the surface. One study found the mean depth of the turbulent layer to be 60 meters (200 feet) for each knot of wind at ground level up to a surface wind speed of 16 knots. With stronger winds, the depth was independent of wind speed, averaging 1066 meters (3500 feet) in the early morning, rising during the day to 1200 meters (4000 feet). When the air is cloud-free but initially stable in the lower layers, the layer of turbulent mixing is very shallow. Cooling is confined to very low levels, resulting in the formation of very low stratus or fog.

2.1.7.1. *Stratus Forecasting and Wind Speed.* Wind speed is usually the dominant factor in determining fog or stratus formation (local topography is also an important consideration). While there's no single critical wind speed threshold for fog/stratus formation, stratus will typically form due to nocturnal cooling with surface wind speeds exceeding 5-10 knots at a coastal location, 10-15 knots at an inland site, and over 25 knots in a valley location.

2.1.7.2. *Empirical Rules.* The level at which stratus forms over land is related to wind speed and the influence of local orographic features, but the dependence of cloud height on temperature and humidity prevents any simple relationship between cloud height and wind speed. The height of stratus in meters above level ground is 20 to 25 times the surface wind speed in knots (70 to 80 times for height in feet). If advected stratus clears during the morning, the dissipation temperature gives the best estimate of the temperature at which the cloud will re-form during the evening.

2.1.7.3. *Dissipation of Stratus Using Mixing Ratio and Temperature.* Manual analysis of the morning Skew-T is an excellent tool to determine the dissipation time of stratus. Use the following steps to determine the surface temperatures needed to begin dissipating and to completely dissipate stratus (see **Figure 2.5**).
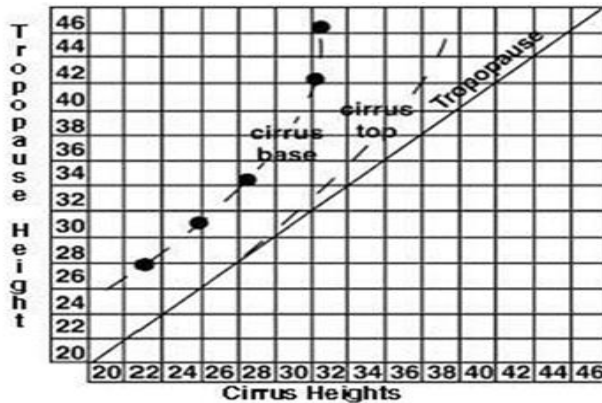
2.1.7.3.1. Find the average mixing ratio between the surface and the base of the inversion.

2.1.7.3.2. Find the intersections of the average mixing ratio line and the temperature curve (the approximate height of the base is at point A, and the top of the stratus deck is at point B).

2.1.7.3.3. Follow the dry adiabat from point A to the surface, and label the surface intersection point as C. This point is the surface temperature required to start dissipation.

2.1.7.3.4. Follow the dry adiabat from point B to the surface, and label the surface intersection point as D. This point is the surface temperature required for complete dissipation.

Figure 2.5. Stratus dissipation technique, using mixing ratio and temperature.
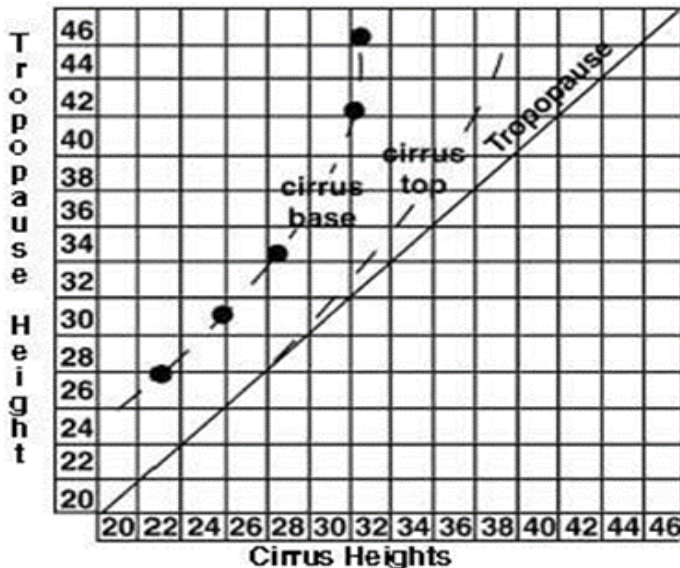
2.1.8. Forecasting Convective Cirrus Clouds. For purely convective cirrus (frontal or thunderstorm), the following rules of thumb apply.

2.1.8.1. When there is straight-line or anticyclonic flow at 200-300-mb downstream from a thunderstorm area, cirrus may appear the next day and advance ahead of the ridgeline.

2.1.8.2. When there is cyclonic flow at 200-300-mb downstream from a thunderstorm area, cirrus is not likely to appear (it may appear, however, if the cyclonic flow is weak.)

2.1.9. Forecasting Cirrus Clouds – Tropopause Method. **Figure 2.6** provides a quick reference to forecast cirrus bases and tops based on the tropopause height; the figure resulted from a multi-year study of the relationship between the tropopause and cirrus bases/tops. To use this method, find the current tropopause height (in thousands of feet) and read across the figure to determine the average cirrus bases and tops (also in thousands of feet.)

Figure 2.6. Tropopause method of forecasting cirrus bases and tops.

2.1.10. Forecasting Snow-Induced Clouds. When snow falls through an atmospheric layer with temperatures greater than 0°C, the snowflakes start to melt. If the dry- and wet- bulb temperatures at ground level are initially greater than 0°C, the snow ultimately reaches the ground without melting. This is due to an isothermal layer, with a temperature near 0°C, establishing itself near the ground. The air is also cooled below its wet-bulb temperature, supersaturation occurs, and stratus clouds form with bases at or very near ground level.

2.1.11. Forecasting Rain-Induced Clouds. Evaporation from falling rain may cause supersaturation and the formation of clouds. The base of the cloud layer will be at a height where the temperature lapse rate decreases significantly or becomes negative (a positive lapse rate exists when temperature decreases with height).

2.1.12. General Cloud Forecasting Rules of Thumb. The following rules are empirical in nature, and may need adjustment for location and current weather regime.

2.1.12.1. The cloud base of a layer warmer than 0°C is usually located where the dew point depression decreases to less than 2°C.

2.1.12.2. The cloud base of a layer between 0°C and –10°C is usually located at a level where the dew point depression decreases to less than 3°C.

2.1.12.3. The cloud base of a layer between –10°C and –20°C is usually located where the dew point depression decreases to less than 4°C.

2.1.12.4. The cloud base of a layer less than –25°C is usually located where the dew point depression decreases to less than 6°C, but can occur with depressions as high as 15°C.

2.1.12.5. For two adjacent layers in which the dew point depression decreases with height more sharply in the lower layer than in the upper layer, the cloud base should be identified with the base of the layer showing the sharpest decrease with height.

2.1.12.6. The top of the cloud layer is usually indicated by an increase in dew-point depression. Once a cloud base has been determined, the cloud is assumed to extend up to the level where a significant increase in dew- point depression starts. The gradual increase in dew-point depression that usually occurs with height is not considered significant.

2.1.12.7. 500-mb dew-point depressions of 4°C or less coincide with overcast mid-level cloudiness.

2.2. Turbulence. Turbulence poses a significant threat to Air Force personnel and operations. Encounters with severe and extreme turbulence can lead to structural damage to aircraft, and injury to passengers and crew. Accurate forecasts of turbulence are therefore essential to the success of Air Force operations.

2.2.1. Levels of Intensity. Turbulence is defined as the "Random and continuously changing air motions that are superimposed on the mean motion of the air" Turbulence intensity is based on the impact to aircraft flying through an area of concern:

2.2.1.1. *Light Turbulence.* The aircraft experiences slight, erratic changes in attitude and/or altitude, caused by a slight variation in airspeed of 5 to 14 knots with a vertical gust velocity of 5 to 19 feet per second. Light turbulence is typically found in the following areas:

2.2.1.1.1. Mountainous regions, even with light winds.

2.2.1.1.2. In and near cumulus clouds.

2.2.1.1.3. Near the tropopause.

2.2.1.1.4. At low altitudes in rough terrain, when winds exceed 15 knots.

2.2.1.1.5. At low altitudes flying over varying terrain with different surface heating coefficients (such as a grassy field next to a concrete surface, or a shoreline where water meets land.)

2.2.1.2. *Moderate Turbulence.* The aircraft experiences moderate changes in attitude and/or altitude, but the pilot remains in positive control at all times. There are usually small variations in airspeed of 15 to 24 knots; vertical gust velocity is 20 to 35 feet per second. Moderate turbulence is found in the following areas:

2.2.1.2.1. In towering cumuliform clouds and thunderstorms.

2.2.1.2.2. Within 100 NM of the jet stream on the cold-air side.

2.2.1.2.3. At low altitudes in rough terrain when the surface winds exceed 25 knots.

2.2.1.2.4. In mountain waves (up to 300 miles leeward of a ridge), with winds perpendicular to the ridge exceeding 50 knots.

2.2.1.2.5. In mountain waves as far as 150 miles leeward of the ridge and within 2000 to 3000 feet of the tropopause when winds are perpendicular to the ridge is 25 to 50 knots.

2.2.1.3. *Severe Turbulence.* The aircraft experiences abrupt changes in attitude and/or altitude, and may be out of the pilot's control for short periods. There are usually large variations in airspeed greater than or equal to 25 knots and the vertical gust velocity is 36 to 49 feet per second. Severe turbulence occurs:

2.2.1.3.1. In and near mature thunderstorms.

2.2.1.3.2. Near jet stream altitude and about 50 to 100 miles on the cold-air side of the jet core.

2.2.1.3.3. Up to 50 miles leeward of a ridge, if a mountain wave exists and winds perpendicular to the ridge are 25 to 50 knots.

2.2.1.3.4. In mountain waves as far as 150 NM leeward of the ridge, and within 2000 to 3000 feet of the tropopause when winds perpendicular to the ridge exceed 50 knots.

2.2.1.4. *Extreme Turbulence.* The aircraft is violently tossed about and is nearly impossible to control. Structural damage may occur. Expect rapid fluctuations in airspeed of 25 knots or greater and a vertical gust velocity of 50 feet per second or greater. Extreme turbulence is rare, but is most likely to occur:

2.2.1.4.1. In mountain waves in or near a rotor cloud.

2.2.1.4.2. In severe thunderstorms.

2.2.2. Aircraft Turbulence Sensitivities. Different types of aircraft have different sensitivities to turbulence; **Table 2.2** lists the categories for a variety of military and civilian aircraft in their default flight configurations. An aircraft's sensitivity to turbulence varies considerably with its weight (amount of fuel, cargo, munitions, etc.), air density, wing surface area, wing sweep angle, airspeed, and attitude. Turbulence information in Terminal Aerodrome Forecasts (TAFs) is specified for Category II aircraft; use caution when applying TAF turbulence data to a specific aircraft type, configuration, and mission profile. **Table 2.3** is a turbulence conversion guide between different aircraft categories; modify the forecast for the aircraft type, as required.

2.2.2.1. *Fixed Wing Aircraft Effects.* Generally, the effects of turbulence on fixed wing aircraft are increased with:

2.2.2.1.1. Non-level flight.

2.2.2.1.2. Increased airspeed.

2.2.2.1.3. Decreased aircraft weight.

2.2.2.1.4. Increased wing surface area.

2.2.2.1.5. Decreased air density / increased altitude.

2.2.2.1.6. Decreased wing sweep angle (wings more perpendicular to the fuselage).

2.2.2.2. *Rotary Wing Aircraft Effects.* Generally, the effects of turbulence on rotary wing aircraft are increased with:

2.2.2.2.1. Increased airspeed.

2.2.2.2.2. Decreased aircraft weight.

2.2.2.2.3. Decreased lift velocity (the faster the liftoff, the less the turbulence).

2.2.2.2.4. Increased rotor blade arc (the longer the blade, the greater the turbulence).

Table 2.2. Aircraft Turbulence Category Type.

Aircraft Type (see Note 2)		Common Name	Turbulence Category (see Note 1)
Military Aircraft Turbulence Categories			
Military Identifier	**FAA Identifier**		
AH-1 (see Note 3)	HUCO	Cobra/Huey Cobra	I
OH-58 (see Note 3)	B06	Kiowa	
RQ-7B (see Note 6)		Shadow	
UH-1 (see Note 3)	B212	Iroquois (Huey)	
T-41D	C172	Mescalero	
T-51A	C150	Cessna 150	
TG-15A/B	TG15	Duo Discus/Discus Glider	
AH-64 (see Note 3)	H64	Apache	II
B-2A (see Note 5)	B2	Spirit	
B-52H	B52	Stratofortress	
C-5M	C5	Super Galaxy	
C-9A/C	DC93	Nightingale/Skytrain	
C-20B (see Note 5)	GLF3	Gulfstream III	
C-20H (see Note 5)	GLF4	Gulfstream IV	
C-21A	LJ35	Learjet 35	
C-130 (see Note 7)	C130	Hercules, Spectre, Commando II, etc.	
C-145A	M28	Skytruck	
C-146A	DO328	Dornier 328 Wolfhound	
C-37A/B	GLF5	Gulfstream V	
C-40B/C (see Note 5)	B737	BBJ, Clipper	
CC-18-180	PA18	Cubcrafters Top Cub	
CH-47 (see Note 3)	H47	Chinook	
CV-22 (see Note 4)	V22	Osprey	
DO-328	DO328	Dornier 328	
E-8	E8	JSTARS	
H-3 (see Note 3)	S61	Sea King	
H-53 (see Note 3)	H53	Sea Stallion/Sea Dragon	

H-60 (see Note 3)	H60	BlackHawk/SeaHawk/PaveHawk	
KC-135R/T	K35R	Stratotanker	
OC-135B		Open Skies	
PC-12	PC-12	Pilatus PC-12	
RC-135		Rivet Joint	
T-38A	T38	Talon	
T-53A	SR20	Cirrus/Kaydett	
TG-16A	TG16	DG-1000 Club Glider	
U-21	BE10	King Air	
U-28	PC12	N/A	
UH-72 (see Note 3)	UH72	Lakota	
VC-25	B742	Air Force One	
A-29		EMB 314 Super Tucano	
C-12 J	B190	Airliner	
C-12 C/D/F	BE-20	King Air/Super King Air	
C-17A	C17	Globemaster III	
C27J	C27	Spartan	
C-32A (see Note 5)	B752	Boeing 757, Air Force Two	
EA-6B	A6	Prowler	
EC-130H	C130	Compass Call	
EO-5C		DHC-7-102/103	
E-9A	E9	Bombardier Dash 8, Widget	
E-4B	B742	NAOC	
E-11A	E11	Bombardier Global Express/XRS	
F-15C/D	F15	Eagle	
F-18 (A-D)	F18	Hornet	
F-18 (E/F/G)	F18	Super Hornet (E/F)/Growler (G)	III
F-22	F22	Raptor	
KC-10A	DC10	Extender	
KC-46A		Pegasus	
MC-12	MC12	Huron	
MQ-1B/C	MQ1	Predator/Gray Eagle	
MQ-9	MQ9	Reaper	
QF-4		Phantom (Drone)	
RC-26B	SW4	Metroliner	
RO-6A		DHC-8-311/315	
RQ-4	RQ4	Global Hawk	
T-1A	BE40	Jayhawk	
T-38C	T38	Talon (for UPT)	
T-6A	TEX2	Texan 2	
U-2S	U2	Dragon Lady	
UV-18B	DHC6	Twin Otter	

UV-20	PC6T	Pilatus Turbo Porter	
A10C	A10	Thunderbolt II	
B-1B	B1	Lancer	
E-3B/C/G	E3TF/E	Sentry	IV
F-15E	F15	Strike Eagle	
F-16C	F16	Fighting Falcon	
F-35A	F35	Lightning II	

Civilian Aircraft Turbulence Categories

Civilian Identifier	FAA Identifier		
C-152	C152	Cessna Aerobat	
C-172	C172	Cessna Skyhawk	
C-175	C175	Cessna Skylark	
C-182	C182	Cessna Skylane	
C-185	C185	Slywagon	I
DA-20	DA20	Diamond Katana	
PA-38	PA38	Piper Tomahawk	
PAY-3	PAY3	Piper Cheyenne	
A-300	A306, A30B	Airbus A300	
A-319	A319	Airbus A319	
A-320	A320	Airbus A320	
A-340-200	A342	Airbus A340	
A-340-300	A343	Airbus A340	
A-340-500	A345	Airbus A340	
A-340-600	A346	Airbus A340	
B-200	BE20	Beechcraft Super King Air	
B-350	BE30	Beechcraft Super King Air	
B-727	B721,B722,B72Q,R721,R722	Boeing 727	
B-737-600	B736	Boeing 737-600	
B-737-700	B737, C-40	Boeing 737-700, BBJ	
B-737-800	B738	Boeing 737-800	
B-737-900	B739	Boeing 737-900	II
B-747	B741, B742,B743,B74D,B744	Boeing 747	
B-777	B772, B773	Boeing 777	
BE-20	BE20	Beechcraft Super King Air	
C-208	C208	Cessna Caravan, U-27	
C-310	C310	Cessna 310, L-27	
C-402	C402	Cessna 402 Businessliner	
C-414A	C414	Cessna Chancellor	
C-421	C421	Cessna Golden Eagle	
CL-600	CL60	Canadair Challenger 600	
CRJ	CRJ1, CRJ2, CRJ7, CRJ9	Canadair Regional Jet	
DC-8	DC8	Douglas DC 8, Super 62	
G-520	EGRT	Egret	

Gulfstream IV & V	GLF4, GLF5	Gulfstream IV, V	
L-13	L13	Blanik Glider	
L-23	L23	Super Blanik Glider	
LJ-25/35/55/60	LJ25/35/55/60	Learjet 25/35/55/60	
MD-80	MD81, MD82, MD83, MD87, MD88	McDonnell Douglas MD-80	
PA-18	PA18	Piper Super Cub	
SR-20	SR20	Cirrus	
B-737/200	B732	Boeing 737-200	
B-757	B752	Boeing 757-200	
B-767	B762, B763	Boeing 767-200, 767-300	
DC -8 (Super 63)	DC86	Douglas DC 8-60 Series	
DC-10	DC10	McDonnell Douglas DC-10, MD-10	**III**
DHC-6	DHC6	DeHavilland Twin Otter	
E-145	E145	Embraer Regional Jet 145	
JS-41	JS41	BAe Jetstream 41	
MD-11	MD11	McDonnell Douglas MD-11	

Note 1: The Turbulence Categories in this table were derived using such aircraft considerations as wing span, wing area, aspect ratio, taper ratio, wing sweep, and others. The table therefore should be considered authoritative; however, an aircraft's weight, airspeed, and/or altitude may change its turbulence category from its default value found in this table. Original source document is AFWAL-TR-81 3058. For updates and aircraft additions, contact AFLCMC/XZMG, DSN 785-2299/2310.

Note 2: If an aircraft is not listed, the following conservative Turbulence Categories can be made: Jets and multi-engine prop/turbo-prop aircraft that fly at/above FL180 can be considered Category II. All other aircraft should be considered Category I (not related to AIRMETs/SIGMETs).

Note 3: Turbulence Categories for helicopters is primarily determined from aircrew feedback. The methodology used for fixed-winged aircraft is not applied to helicopters due to their added complexity.

Note 4: The CV-22 displays aspects of flight that include rotor-wing operations and therefore objective gust load calculations and turbulence categorization are not possible for rotor phase of flight (e.g. takeoff/landing).

Note 5: Turbulence categories for aircraft with gust alleviations systems (passive or active) are likely less susceptible to turbulence than their computed category.

Note 6: Turbulence categories for Small UAVs (Mean Aerodynamic Chord less than 2 ft), cannot be determined using the Gust Loads Formula and therefore should be considered Category I.

Note 7: This turbulence category applies to all Modified/Basic Mission Designators and Model Series (except for the EC-130H/J models which are CAT III)

Table 2.3. Turbulence Conversion Chart.

Turbulence intensities for different categories of aircraft			
Cat. I	Cat. II	Cat. III	Cat. IV
N	N	N	N
(L)	N	N	N
L	(L)	N	N
L - (M)	L	(L)	N
M	L - (M)	L	(L)
M - (S)	M	L - (M)	L
S	M - (S)	M	L - (M)
S - (X)	S	M - (S)	M
X	S - (X)	S	M - (S)
X	X	S - (X)	S
X	X	X	S - (X)
X	X	X	X

Key: N = None, ( ) = Occasional (less than 1/3 of the time), L = Light, M = Moderate, S = Severe, X = Extreme

2.2.3. Causes of Turbulence. Turbulence is caused by abrupt, irregular movements of air that create sharp, quick updrafts/downdrafts. These updrafts and downdrafts combine, and create conditions that move aircraft unexpectedly. There are two basic atmospheric conditions that cause turbulence to occur: thermal conditions and mechanical mixing.

2.2.3.1. *Thermal Turbulence.* Surface heating can generate turbulent conditions; as solar radiation heats the surface, the air above it is warmed by contact. Warmer air is less dense than cooler air, so "bubbles" of warm air rise upward as updrafts. Uneven surface heating and cooling of elevated air parcels causes areas of downdrafts as well. These vertical motions may be restricted to the low levels, or may generate cumulus clouds that grow into thunderstorms. Thermally-induced turbulence has the following characteristics:

2.2.3.1.1. Normally confined to the lower troposphere (surface to 10,000 feet).

2.2.3.1.2. Maximum occurrence between late morning and late afternoon.

2.2.3.1.3. The main impact to flight operations is during terminal approach and departure and during low-level flights.

2.2.3.1.4. Moderate turbulence may occur in hot, arid regions, as the result of irregular convective currents from intense surface heating.

2.2.3.1.5. The strongest thermal turbulence is found in and around thunderstorms. Moderate or severe turbulence can be found anywhere within the storm, including the clear air along its outer edges. The highest probability of turbulence is found in the storm core, between 10,000 and 15,000 feet.

2.2.3.2. *Mechanical Turbulence.* Mechanical turbulence is caused by horizontal and vertical wind shear, and is the result of pressure gradient differences, terrain obstructions, or frontal zone shear. General characteristics of mechanical turbulence include:

2.2.3.2.1. Turbulence results from a combination of horizontal and vertical wind shears.

2.2.3.2.2. Turbulence layers are usually 2000 feet thick, 10 to 40 miles wide, and several times longer than wide.

2.2.3.2.3. Wind shear turbulence may result from strong horizontal pressure gradients alone. It occurs when the pressure gradient causes a horizontal shear in wind direction or speed.

2.2.3.2.4. Local terrain can magnify gradient winds to cause strong winds and turbulence near the surface. This creates eddy currents that can make low-level flight operations hazardous.

2.2.3.2.5. Most turbulence resulting from upper frontal zone shear occurs between 10,000 feet and 30,000 feet.

2.2.3.2.6. The jet stream causes most turbulence in the upper troposphere and lower stratosphere, usually occurring in patches and layers, with strongest turbulence on the low-pressure (cold air side) of the jet stream.

2.2.3.2.7. Strong turbulence is often associated with irregular and mountainous terrain. The greater the irregularity of the terrain and the sharper the slope of mountains, the greater the intensity and vertical extent of the turbulence.

2.2.3.2.8. Fronts may produce moderate or greater turbulence; the intensity depends on the strength and speed of the front (strong fronts may create updrafts of 1000 feet per minute in a narrow zone just ahead of the front). Over rough terrain, fronts typically produce moderate or greater low-level turbulence. Over flat terrain, fronts moving faster than 30 knots typically produce moderate or greater low-level turbulence.

2.2.4. Turbulence Environments. Several atmospheric and environmental factors are considered particularly favorable for turbulence production, as detailed below.
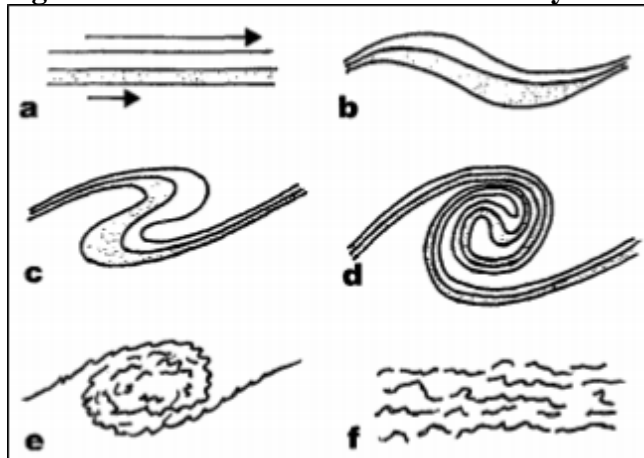
2.2.4.1. Strong vertical and/or horizontal wind shear. Both vertical and horizontal wind shear are key ingredients for the development of CAT. Horizontal and vertical shear create eddies that can produce turbulence in the presence or absence of static instability (i.e., convective processes). These eddies are capable of propagating great distances before dissipating into laminar (smooth) flow. Vertical wind shear of at least 6 knots/1,000 feet, or horizontal wind shear of at least 40 knots/150 miles, is generally needed to produce CAT. Shear of this magnitude can often be found near the jet stream, where wind speed changes significantly over relatively small vertical and horizontal distances.

2.2.4.2. Decreasing potential temperature with height in the planetary boundary layer (PBL). At least some static instability is necessary for the development of turbulence, unless wind shear is very strong. In a dry PBL, the environment is statically unstable if the potential temperature decreases with height. This allows for the development of positively buoyant thermals that can contribute to turbulence production. Turbulence that develops in a statically unstable environment acts to reduce the instability and return the air to a laminar (non-turbulent) state. However, in some cases, such as in the PBL on a sunny day, the warm ground acts to continuously heat and destabilize the air, allowing turbulence to continue throughout the day. Note that if the environment is conducive to deep, moist convection, the lapse rate of the equivalent potential temperature should be used instead of potential temperature, because it accounts for the presence of water vapor.

2.2.4.3. Dynamic instability.

2.2.4.3.1. Dynamic instability can be evaluated by a Richardson Number of less than 1 and optimally less than 0.25 (see **Table 2.4**). If vertical wind shear is strong enough, turbulence can develop in a statically stable environment. When this occurs, the environment is considered to be dynamically unstable. Turbulence is produced dynamically when dense air initially resides beneath less-dense air, with a velocity shear between the layers. The flow in this initial state is laminar (see **Figure 2.7** panel a). If the shear increases to a critical value, the flow becomes dynamically unstable and waves form on the surface (see **Figure 2.7** panel b). These waves grow in amplitude until they break (see **Figure 2.7** panels c-e). The breaking waves are known as Kelvin-Helmholtz waves. In the case of each wave, some lighter air rolls underneath denser air, leading to areas of static instability. The static instability and dynamic instability lead to turbulence production; eventually, the turbulence causes mixing and momentum transfer, reducing the shear and instability. The shear falls back below the critical value, the turbulence decays (see **Figure 2.7** panel f), and the flow returns to a laminar state. This process is thought to occur during the onset of CAT, often near jet streams such as the nocturnal jet or the planetary-scale jet stream. In these cases, turbulence can persist for days. This entire process is illustrated in **Figure 2.7**.

Figure 2.7. Kelvin-Helmholtz wave lifecycle.

2.2.4.3.2. Richardson number. Dynamic instability can be evaluated using the Richardson number (Ri) as indicated in **Table 2.4** The Ri is the ratio of static stability to vertical wind shear. In general, turbulence will not develop when the Ri is greater than 1, because the static stability term is greater than the shear term, and static stability tends to drain off turbulent kinetic energy. When the wind shear increases to the point that it overpowers static stability, turbulence becomes more likely. As a general rule, turbulence is possible when the Ri is less than 1, and probable when the Ri is less than 0.25, which is the critical Richardson number. It is at this point that the shear is strong enough for the flow to become dynamically unstable and for Kelvin-Helmholtz waves to develop. Note that statically unstable air results in a negative Ri, and therefore implies dynamic instability.

Table 2.4. Richardson Number calculation and interpretation.

Richardson Number formula:	
$$Ri = \dfrac{\dfrac{g}{\theta}\left(\dfrac{\delta\theta}{\delta Z}\right)}{\left(\dfrac{\delta V}{\delta Z}\right)^2}$$	
g = acceleration due to gravity $\delta\theta/\delta Z$ = change in potential temperature over a vertical layer	
θ = potential temperature $\delta V/\delta Z$ = vector wind shear occurring over the vertical layer	

Ri Value	Turbulence Likelihood
Greater than 1	Unlikely
Less than 1	Possible
Less than 0.25	Probable

2.2.4.4. Deep, moist convection (thunderstorms). Deep, moist convection always produces turbulence, because it is associated with both static instability and dynamic instability. Additionally, strong updrafts, downdrafts, and vertical and horizontal wind shear exist within and around thunderstorms. Thunderstorms also produce gravity waves, which are vertically propagating waves, driven by the temperature profile of the environment. These can cause severe turbulence as far as 20 miles from the nearest storm. Avoidance of in-cloud convective turbulence can be achieved through the use of radar and satellite imagery, or through visual identification. Near-cloud turbulence, however, presents a special challenge because it is not detectable with standard on-board and ground-based radar. In order to avoid near-cloud turbulence, FAA guidelines stipulate that aircraft should avoid by at least 20 miles (laterally) any thunderstorm identified as severe or giving an intense radar echo (especially under the anvil of a large cumulonimbus.) They also recommend that aircraft clear the top of a known or suspected severe thunderstorm by at least 1000-ft altitude for each 10 knots of wind speed at the cloud top (a guideline that likely exceeds the altitude capability of most aircraft.)

2.2.4.5. Strong convergence at jet stream or tropopause level. Convergence is the compaction of a fluid caused by confluence of flow or deceleration of air parcels; convergence aloft at jet stream level or at the tropopause results in sinking motions, which in some cases can cause turbulence. Convergence aloft can also produce propagating gravity waves by disturbing a tropopause inversion above an area of frontogenesis, which may lead to turbulence.

2.2.4.6. Acceleration of air parcels at jet stream level to super-geostrophic speeds. Just as convergence aloft caused by confluence of streamlines or deceleration of air parcels can cause turbulence, diffluence and divergence aloft may also result in turbulent conditions. The geostrophic wind is usually an excellent approximation of the actual wind in the free atmosphere, especially at jet stream level. Turbulence can be created when geostrophic winds accelerate into or out of a jet streak and become super-geostrophic for a short time.

2.2.4.7. An "S-shaped" temperature profile above the tropopause. Stratospheric turbulence can be a major detriment to aircraft operating at ultra-high altitudes, such as the U-2 and Global Hawk. The most common stratospheric turbulence diagnostic is the presence or lack of an "S" shape in the Skew-T temperature profile above the tropopause, such as in **Figure 2.8**. The high risk area for turbulence is the middle of the "S", where the temperature decrease (lapse rate) is adiabatic or super-adiabatic ($\geq 9.8°C/km$). This layer is characterized by strong static instability due to the steep lapse rates. Additionally, wind speeds above the tropopause are often in excess of 100 knots, so strong vertical and horizontal wind shear can be present as well. The U-2 community developed the following procedure for stratospheric turbulence forecasting utilizing the "S" layer:
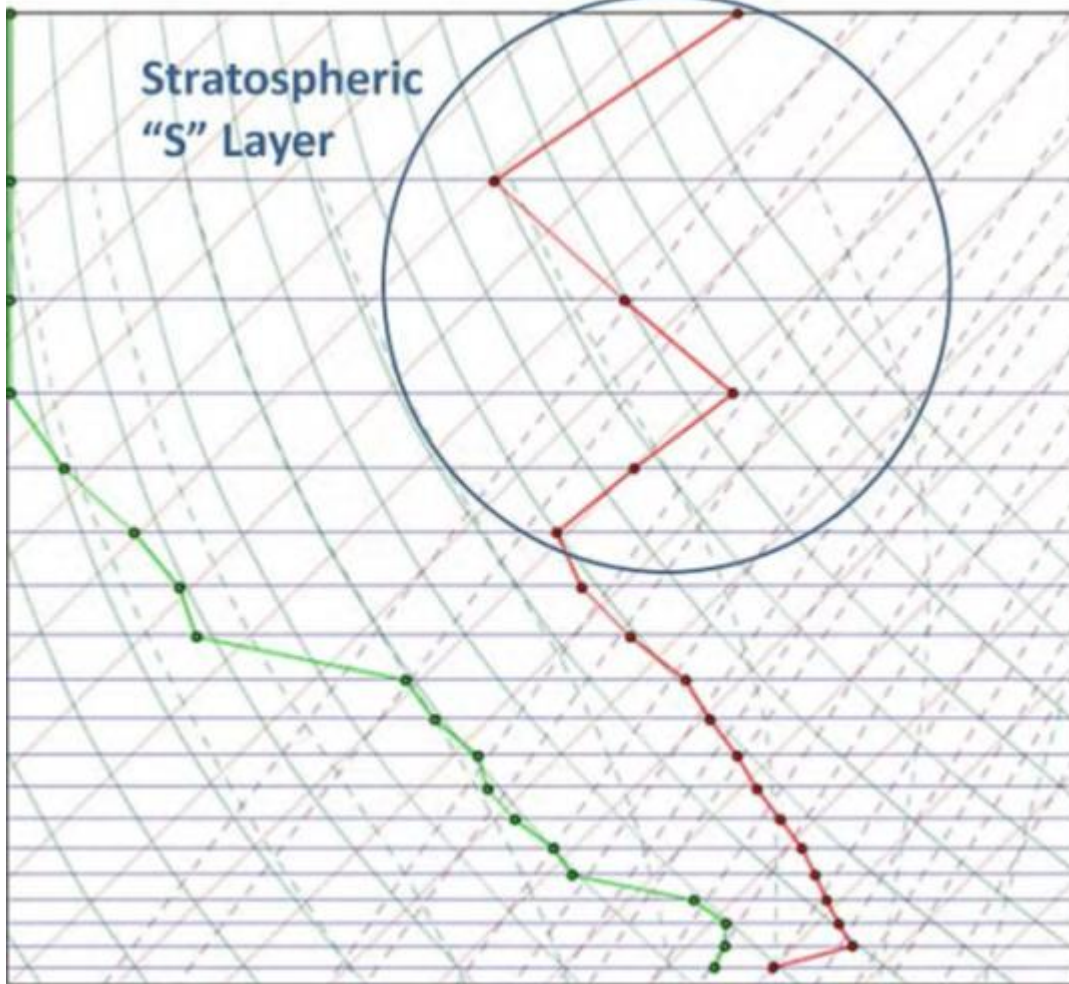
2.2.4.7.1. Use the most recent Skew-T to locate the tropopause, which is characterized by a temperature increase of at least 2°C/km for several km. The tropopause height varies with latitude and season, but is often found between 300 mb and 100 mb.

2.2.4.7.2. Less than 3°C of warming per 1,000 feet above the tropopause indicates that turbulence is unlikely.

2.2.4.7.3. 3°C to 5°C of warming per 1,000 feet above the tropopause indicates that light to moderate turbulence is possible.

2.2.4.7.4. More than 5°C of warming per 1,000 feet above the tropopause indicates that severe turbulence is possible.

Figure 2.8. "S-shaped" tropospheric temperature profile, indicating potential turbulence.
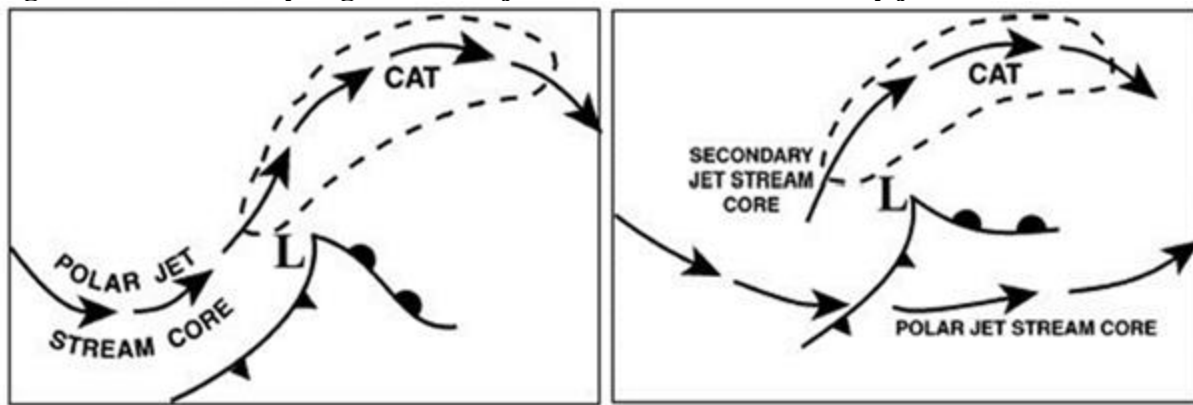
2.2.5. Clear Air Turbulence (CAT). CAT is a form of mechanical turbulence, and includes all turbulence not associated with visible convective activity (such as high-level frontal and jet stream turbulence, or turbulence occurring in high-level, non-convective clouds). The typical meteorological conditions under which CAT forms are described below.

2.2.5.1. CAT surface and upper-level patterns.
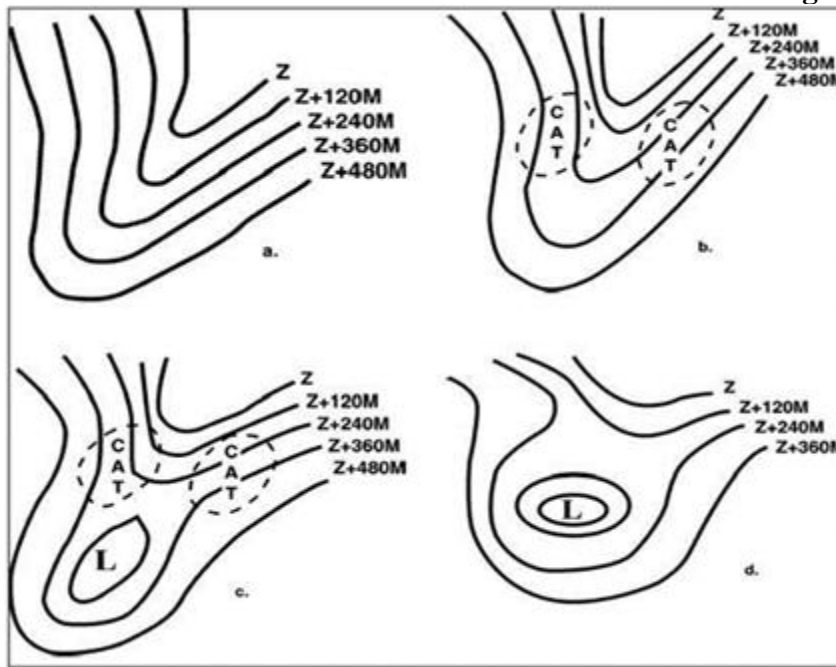
2.2.5.1.1. Surface cyclogenesis. When cyclogenesis occurs, CAT is expected near the jet stream core, north-northeast of the surface low development (see left image in **Figure 2.9**). In some cases, the surface low redevelops north of the main jet, with a formation of a secondary jet (see right image in **Figure 2.9**); CAT typically occurs in a similar location along the secondary jet stream core. CAT intensity is dependent on several factors; the strength of cyclogenesis, the proximity to mountains, the intensity of the jet core, and the amplification and curvature of the downstream ridge. For cyclogenesis less than 1 mb/hour, expect moderate CAT. For cyclogenesis greater than or equal to 1 mb/hour, anticipate moderate to severe CAT.

Figure 2.9. Surface cyclogenesis and jet-core CAT and secondary jet-core CAT.

2.2.5.1.2. Upper level lows. The potential for moderate CAT exists during the development of cut-off upper-level lows; the sequence shown in **Figure 2.10** shows the areas of expected CAT during the various stages of cut-off low development. CAT usually first appears in the areas of confluent and diffluent flow; once the low is fully cut off, CAT diminishes to light in the vicinity of the low.

Figure 2.10. CAT during the development of an upper-level low. Patterns b and c show the areas of moderate CAT as the low breaks off from the trough.

2.2.5.1.3. CAT criteria at 500 mb. The following patterns at 500 mb may be indicative of CAT:

2.2.5.1.3.1. Shortwave troughs near one another (double troughs).

2.2.5.1.3.2. A well-defined thermal trough.

2.2.5.1.3.3. A narrow band of strong winds with strong horizontal wind shears.
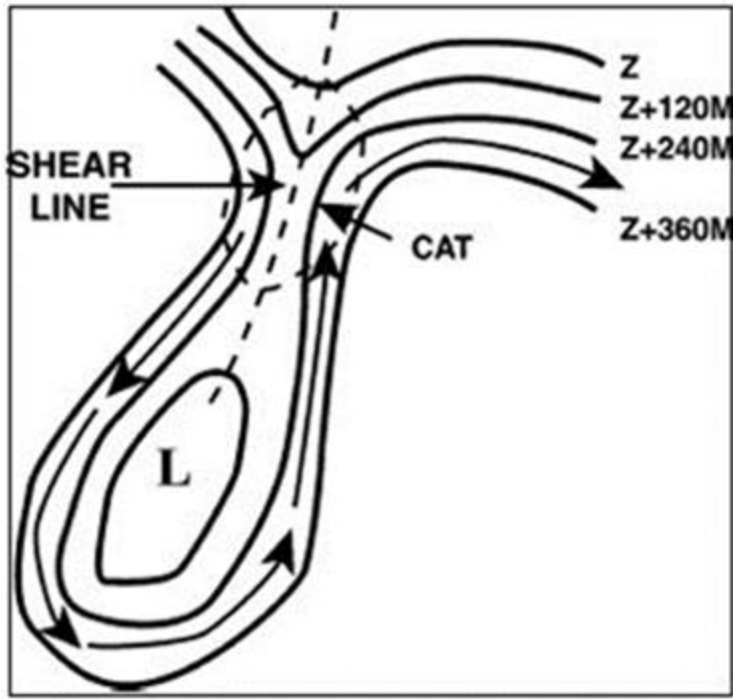
2.2.5.1.3.4. A closed isotherm cold pocket moving through an open flow pattern (i.e., height field with no closed contours).

2.2.5.1.3.5. 500-mb winds greater than 75 knots in areas with wind shifts greater than or equal to 20°, and tight thermal gradients.

2.2.5.1.3.6. Troughs associated with a surface frontal wave (often indicated by sharply curved isotherms around the northern edge of a warm tongue).

2.2.5.1.4. Shear lines in upper-level lows. In this scenario, the potential for CAT is greatest between the two curved portions of the jet near the narrow neck of the cut-off low (see **Figure 2.11**); this is the area near the shear line. Forecast moderate CAT when the jet stream is greater than or equal to 50 knots around the closed upper-level low; forecast severe CAT if the jet reaches 115 knots.
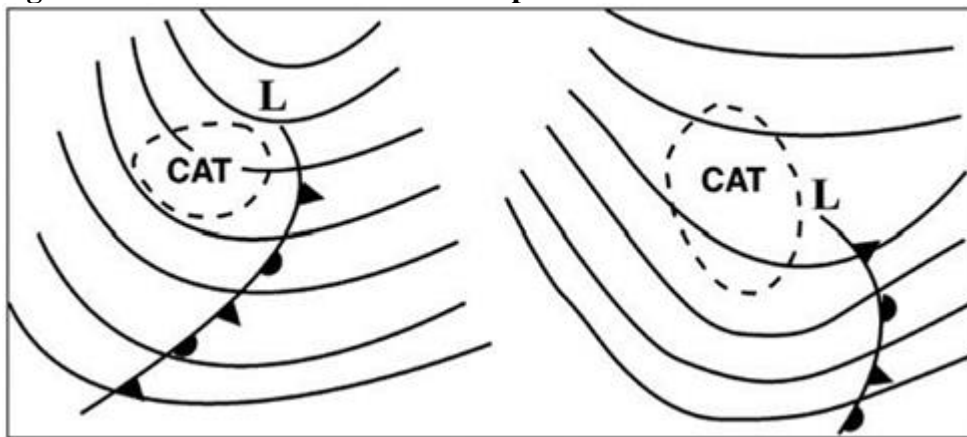
Figure 2.11. CAT area along a shear line associated with an upper level low.

2.2.5.2. CAT Wind Patterns.

2.2.5.2.1. Diffluent winds. Most CAT occurs during formation of diffluent upper-level wind patterns; once the diffluent pattern becomes established, CAT may weaken in the diffluent zone. However, when a surface front is present (or forming), the potential for CAT increases in the areas of upper-level diffluent flow near the surface system (see **Figure 2.12**)

Figure 2.12. CAT in a diffluent wind pattern.

2.2.5.2.2. Strong winds. CAT forms in areas of strong winds when isotherms and height contours are nearly parallel, and only minor variations exist in wind direction (about 20° per 4 degrees of latitude) with exceptionally tight thermal gradients. CAT can also occur along and above a narrow band of strong 500 mb winds when horizontal wind shears are strong on either side of the band, especially if the winds are highly ageostrophic.

2.2.5.2.3. Confluent jet streams. When two jet stream cores converge to within 250 NM, the potential for CAT increases. Since the poleward jet is usually associated with colder temperatures and is lower than the second jet, the poleward jet will often undercut the other, producing strong vertical wind shears. The potential CAT area ends where the jets diverge to a distance of greater than 5° latitude.

2.2.5.3. CAT Thermal Patterns.

2.2.5.3.1. Temperature gradients at and above 300 mb. Temperature gradients at the 300, 250, and 200 mb pressure levels provide key indicators for CAT potential; expect CAT when a temperature gradient greater than or equal to 5°C/120 NM is observed or forecast, and at least one of the following is observed:

2.2.5.3.1.1. Trough movement greater than or equal to 20 knots.

2.2.5.3.1.2. Wind shift greater than or equal to 75° in the region of cold advection.

2.2.5.3.1.3. Horizontal wind shear greater than or equal to 35 knots/110 NM (~200 km).

2.2.5.3.1.4. Wind component normal to the cold advection is greater than or equal to 55 knots.
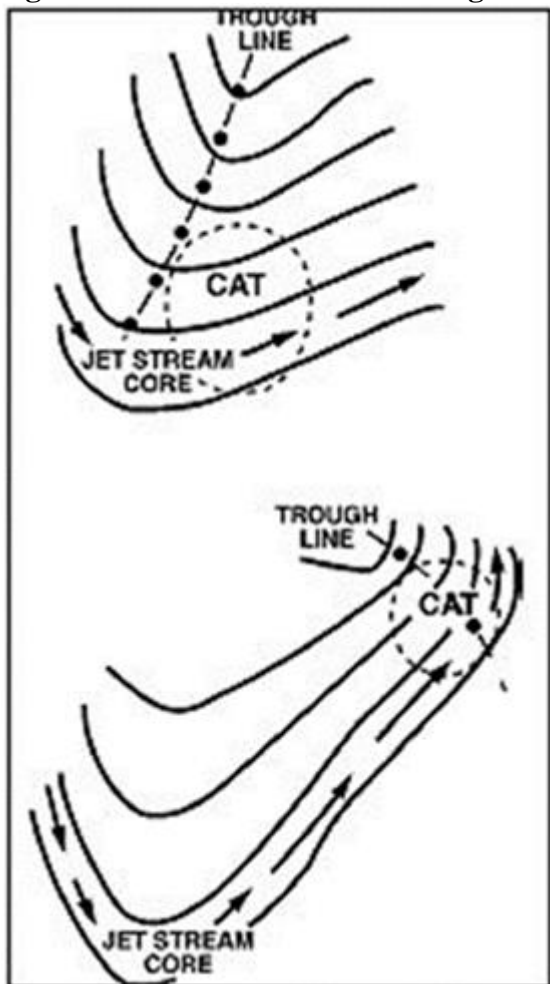
2.2.5.3.2. Open-isotherm patterns. Noticeable "bulging" of a cold-air tongue in a relatively tight thermal gradient may occur at or near the base of the trough; in these cases, the isotherms curve more sharply than the height contours and moderate turbulence is possible between 25,000 and 35,000 feet.

2.2.5.3.3. Closed-isotherm patterns. CAT is often found in the development of a moving, closed cold-air isotherm at 500 mb when the height contours are not closed (see **Figure 2.17**.) In this situation, multiple reports of moderate or greater CAT were received; in these scenarios, CAT is likely between 24,000 and 37,000 feet.

2.2.5.4. CAT Trough and Ridge Patterns.
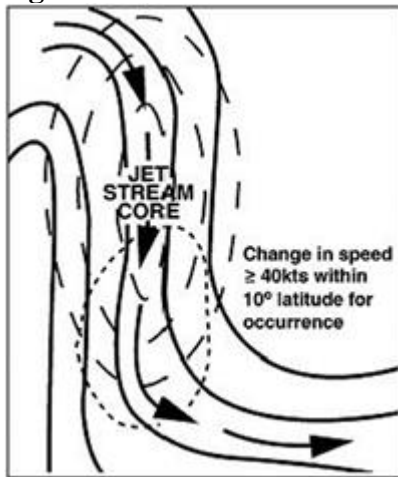
2.2.5.4.1. Shearing troughs. Rapidly moving troughs north of a jet may produce CAT in the confluent flow at the base of the trough (see **Figure 2.13**); the turbulent area is typically concentrated north of the jet stream core.

Figure 2.13. CAT areas in shearing troughs.

2.2.5.4.2. Strong wind maximum to the rear of the upper trough. CAT potential is high when a strong north-south jet is located along the backside of an upper trough; it usually occurs in the area of decreasing winds between the base of the trough and the max wind upstream. Minimum wind speed changes required for CAT occurrence are greater than or equal to 40 knots within 10° of latitude. If the difference between the jet core and the minimum wind speed is greater than or equal to 60 knots, CAT is most likely to occur between the jet core and the base of the trough, centered on the warm-air side of the jet (see **Figure 2.14**.)

Figure 2.14. CAT with wind maximum to the rear of the upper trough.
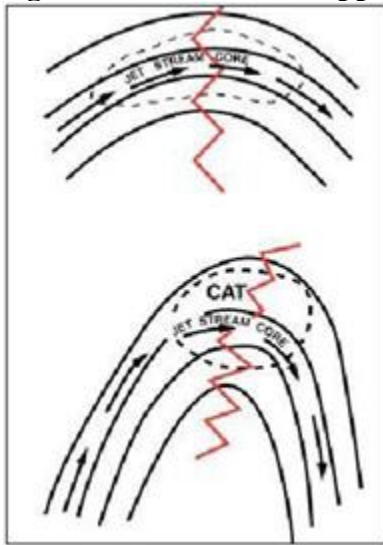
2.2.5.4.3. Deep pressure trough at 500 mb. With a deep pressure trough at 500 mb, CAT typically forms in a sharply anticyclonic, persistent isotherm pattern downwind of the trough.

2.2.5.4.4. Double trough configuration. Strong CAT is often associated with two troughs when they are close enough together that the trailing trough influences the airflow into the leading trough. This pattern is often associated with a flat or flattening ridge between the troughs, which advects warm air into the base of the lead trough. Although the double trough can be detected at a number of levels, the 500-mb product is the best to use.

2.2.5.4.5. Upper level ridges. Expect CAT on both sides of the jet near the area where the jet undergoes maximum latitudinal displacement in an amplifying ridge (see **Figure 2.15**.) Maximum CAT is located in the area of greatest anticyclonic curvature (usually within 250 NM of the ridge axis and elongated in the direction of the flow). Expect moderate or greater CAT when the vertical wind shear is greater than or equal to 10 knots/1000 feet, or when the winds are greater than 135 knots in the area of broad anticyclonic curvature.

Figure 2.15. CAT with upper level ridges.

2.2.5.5. Forecasting CAT using upper air data.

2.2.5.5.1. 700 mb and 850 mb height and temperature fields. At 700 mb and 850 mb, use the heights and temperatures to identify regions of thermal advection, wind components perpendicular to mountain ridges, mid or low level turbulence, and frontal boundaries.

2.2.5.5.2. 500 mb height, temperature, and vorticity fields. Focus on areas of thermal advection, short-wave troughs, and wind components perpendicular to mountain ridges. The 500 mb level can also be used to approximate jet stream positions and upper-air synoptic patterns; for example, place the subtropical jet near the –11°C isotherm, the polar front jet near the –17°C isotherm, and the northern branch jet near the –30°C isotherm.

2.2.5.5.3. 250 mb jet stream. Analyze the 250 mb winds closely to determine the current and future jet stream core position.

2.2.5.5.4. 200 mb height and temperature fields. Look for regions of strong isotherm packing in association with strong wind flow; the 200 mb isotherms align closely with the 500 mb vorticity pattern, and can indicate short waves and developing weather systems.

2.2.6. Mountain Wave (MW) Turbulence. The most severe type of terrain-induced turbulence is mountain wave turbulence. It most often occurs in clear air and in a stationary wave downwind of a prominent mountain range. It is caused by the mechanical disturbance of the wind by the mountain range. Mountain wave intensity depends on several factors:

2.2.6.1. Wind speed and direction. Winds flowing within 30 degrees of perpendicular to the ridgeline, with little change in direction with height, are most favorable for generating mountain wave turbulence. Mountaintop wind speeds of about 25 knots, increasing with height, are also favorable for generating mountain waves. Mountain waves can extend as far as 300 NM leeward of the mountain range when the wind component perpendicular to mountain range exceeds 50 knots. A wave can extend as far as 150 NM when the perpendicular component exceeds 25 knots.
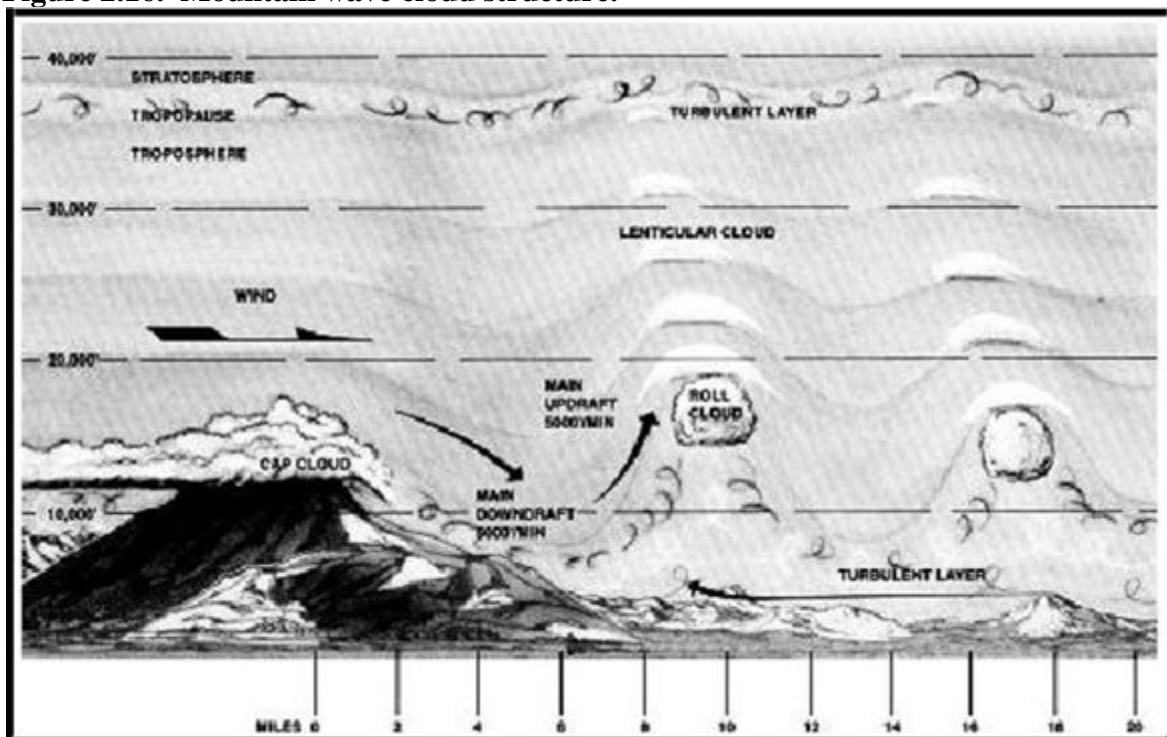
2.2.6.2. Height and slope of the mountain. High mountains with steep leeward and gentle windward slopes produce the most intense turbulence.

2.2.6.3. Upstream stability. Look for upstream temperature profiles that exhibit an inversion or a layer of strong stability near mountain top height, with weaker stability at higher levels; this can enhance mountain wave turbulence downstream.

2.2.6.4. Inversions. An inversion capping the tropopause induces a stronger downward wave and can cause wave amplification (and enhanced mountain wave turbulence).

2.2.6.5. There are several different types of clouds associated with MW turbulence; **Figure 2.16** illustrates the structure of a strong mountain wave and the associated cloud patterns.

Figure 2.16. Mountain wave cloud structure.

2.2.6.5.1. Cap clouds. Cap clouds "hug" the mountaintop and flow down the leeward side with the appearance of a waterfall. Cap clouds are potentially hazardous, since they can obscure the top of the mountain and are associated with strong downdrafts (5000-8000 feet per minute).

2.2.6.5.2. Roll clouds. Roll clouds, also called a rotor clouds, appear as a line of cumulus parallel to the ridgeline. They form on the leeside and have bases near the height of the mountain peak and tops near twice the height of the peak. Roll clouds are extremely turbulent, with strong updrafts (5000 feet per minute) on the windward side and intense downdrafts (5000 feet per minute) on its leeward edge. Roll clouds may form immediately on the lee of the mountain, or up to 10 miles downstream.

2.2.6.5.3. Lenticular clouds. Lenticular clouds are relatively thin, lens-shaped clouds with bases above roll clouds and tops extending to the tropopause. They have a tiered or stacked look due to atmospheric stability above the mountain ridge. All lenticular clouds are associated with turbulence. In polar regions, lenticular clouds can appear as high in the stratosphere as 80,000 feet; these are called "mother-of-pearl" (nacreous) clouds.

2.2.6.6. Favorable conditions for MW turbulence development:

2.2.6.6.1. Temperature of -60ºC or colder at the tropopause.

2.2.6.6.2. Jet stream over or just north of the ridge line.

2.2.6.6.3. A cold front approaching or stationary to the north of the mountain range.

2.2.6.6.4. Cold air advection across or along the mountain range.
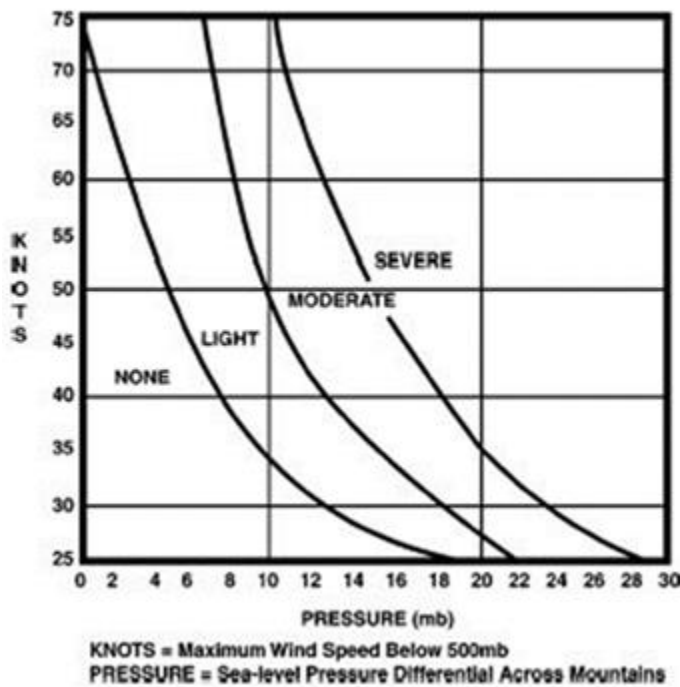
2.2.6.7. MW turbulence occurrence indicators:

2.2.6.7.1. Rapidly falling pressure to the lee side of mountains with significant differences on the windward side.

2.2.6.7.2. Lee-side gusty surface winds at nearly right angles to the mountains.

2.2.6.7.3. Observations of ACSL, rotor clouds or cap clouds.

2.2.6.7.4. A lee-side cirrus trench (the Foehn gap).

2.2.6.7.5. A well-defined lee-side trough.

2.2.6.7.6. PIREPS indicating mountain wave turbulence.

2.2.6.7.7. Blowing dust picked up and carried aloft to 20,000 feet MSL or higher.

2.2.6.8. MW turbulence forecasting guidance. Used in conjunction, the parameters in **Table 2.4** and nomogram in **Figure 2.17** can provide guidance in forecasting mountain wave turbulence.

Table 2.5. Low level mountain wave turbulence guidance chart.

Low-level Mountain Wave Turbulence (Surface to 5000 feet above the ridge line)			
Wind component normal to the mountain range at mountaintop is greater than 24 knots, **and:**	Turbulence Intensity		
	Light	Moderate	Severe
Surface pressure change across mountain is:	See Figure 2.17	See Figure 2.17	See Figure 2.17
850 mb temperature difference across mountain is:	Less than 6° C	6° C – 9° C	Greater than 9° C
850 mb temperature gradient across mountain is:	Less than 4°C/60 NM	4° C – 6° C/60 NM	Greater than 6° C/60 NM
Lee side surface gusts are:	Less than 25 kt	25 – 50 kt	Greater than 50 kt
Winds below 500 mb greater than 50 knots:	Increase turbulence by one degree of intensity (i.e., moderate to severe)		

Figure 2.17. Mountain Wave Turbulence nomogram.

KNOTS = Maximum Wind Speed Below 500mb
PRESSURE = Sea-level Pressure Differential Across Mountains

2.2.7. Wake Turbulence. Every aircraft generates two counter-rotating vortices off each wingtip; wake turbulence results when an aircraft encounters vortices from another aircraft. Vortex generation begins when the nose wheel lifts off the ground and ends when the nose touches back down again during landings. A vortex forms at a wingtip as air circulates outward, upward, and around the wingtip. The diameter of the vortex core varies with the size and weight of the aircraft; the largest vortices can be up to 50 feet in diameter, with a much larger area of turbulence.

2.2.7.1. Wake turbulence dissipation. Wake vortices usually stay fairly close together (about 3/4 of the wing span) until dissipation; they sink at a rate of 400 to 500 feet per minute and stabilize about 900 feet below the flight path, where they begin to dissipate. Atmospheric turbulence increases the dissipation rate of wake turbulence, while ground effects and surface winds can alter the low-level vortex characteristics. As a vortex sinks into the boundary layer, it begins to move laterally at about 5 knots; a crosswind will decrease the lateral movement of a vortex moving toward the wind and increase the movement of a vortex moving with the wind. This could hold one of the vortices over the runway for an extended period or allow one to drift onto a parallel runway. Vortices persist longer during inversions.

2.2.7.2. Wake turbulence avoidance. The Federal Aviation Administration has published the following rules for avoiding wake turbulence (from their Aeronautical Information Manual):
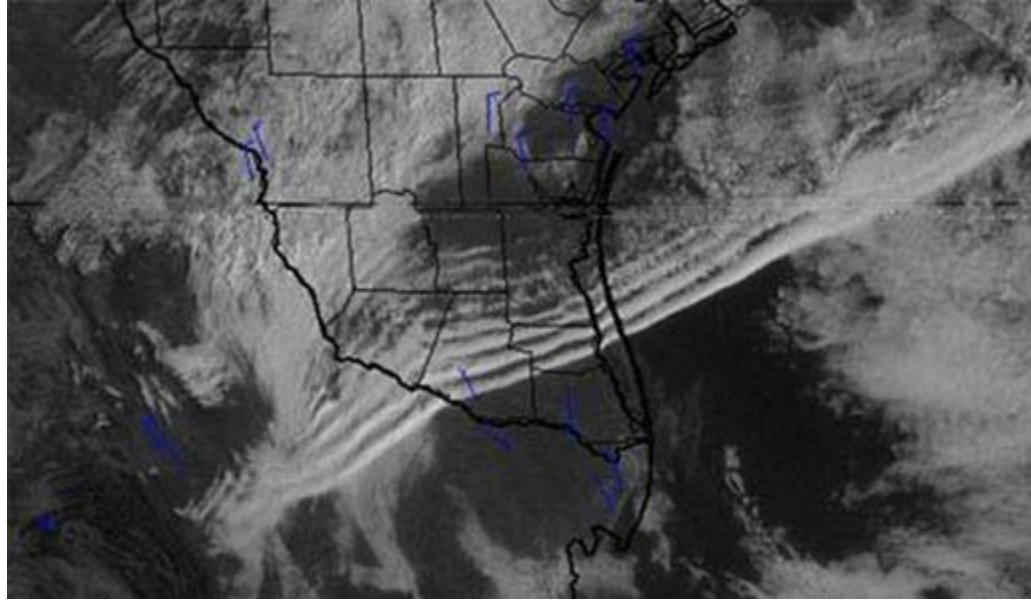
2.2.7.2.1. If two aircraft fly in the same direction within 15 minutes of each other, the second should maintain an altitude equal to or higher than the first. If required to fly slightly below the first, the second aircraft should fly upwind of the first.

2.2.7.2.2. Vortex generation begins with liftoff and lasts until touchdown. Therefore, aircraft should avoid flying below the flight path of a recent arrival or departure.

2.2.7.2.3. Stable conditions combined with a crosswind of about 5 knots may keep the upwind vortex over the runway for periods of up to 15 minutes.

2.2.8. Gravity Waves and Stratospheric Turbulence. Stratospheric turbulence is fundamentally different from tropospheric turbulence – while tropospheric CAT is primarily caused by horizontal and vertical wind shears, stratospheric CAT is primarily caused by the breaking of gravity waves. A gravity wave is generated when an air parcel at equilibrium with its environment is rapidly vertically displaced (see **Figure 2.18**) – this can happen due to orographic forcing (mountains), or when an air parcel is trapped under an inversion (thunderstorm downburst near a cold front). As the air parcel is forced upwards, it expands, cools, and becomes heavier than its surrounding environment. The air parcel begins to sink, accelerating through the equilibrium point, where it compresses, warms, and becomes lighter than its surrounding environment, accelerating back upwards, where the process repeats. This up-and-down motion as the parcel travels downstream is a gravity wave. Gravity waves that propagate into the stratosphere increase in amplitude with height, due to decreasing air densities. Typical wavelengths range from 5 to 5000 km horizontally, and .1 to 5 km vertically; gravity waves on the order of 10-100 km wavelength typically generate turbulence felt by aircraft. Depending on atmospheric stability, they can last from about 5 minutes to over a day.

Figure 2.18. Gravity waves on visible satellite imagery.
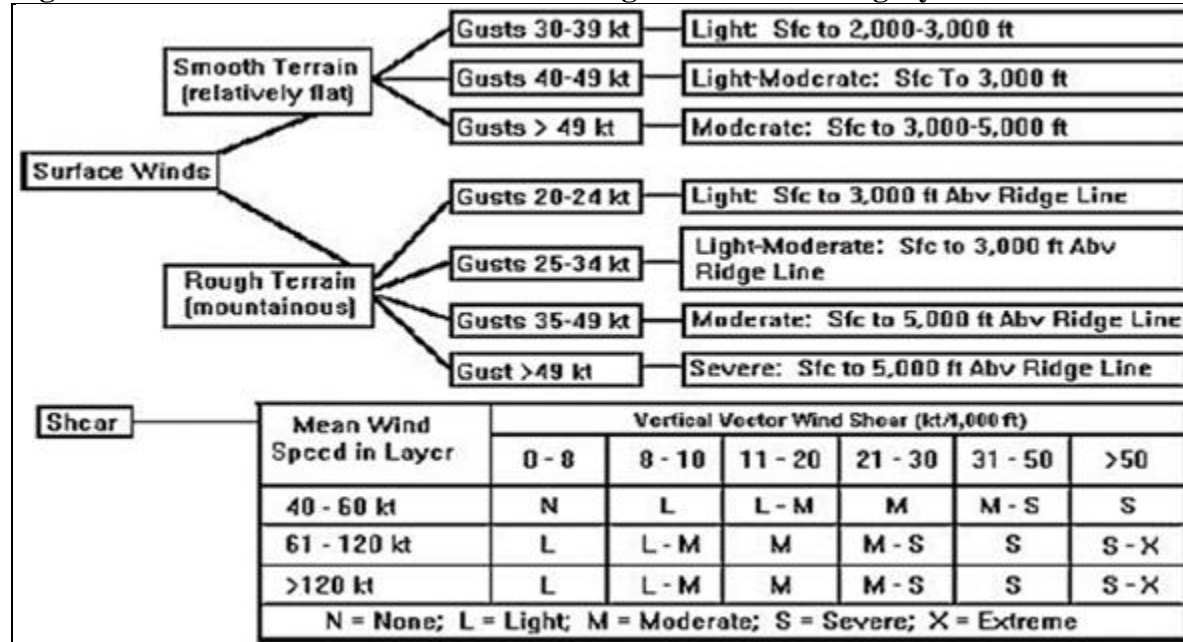
2.2.9. Forecasting Aids. The tools in this section are provided to aid in accurate turbulence forecasting; use them as applicable to assist in predicting turbulence conditions.

2.2.9.1. General turbulence locations. Refer to **Table 2.5** for a summary of areas where turbulence is expected.

Table 2.6. Expected turbulence locations.
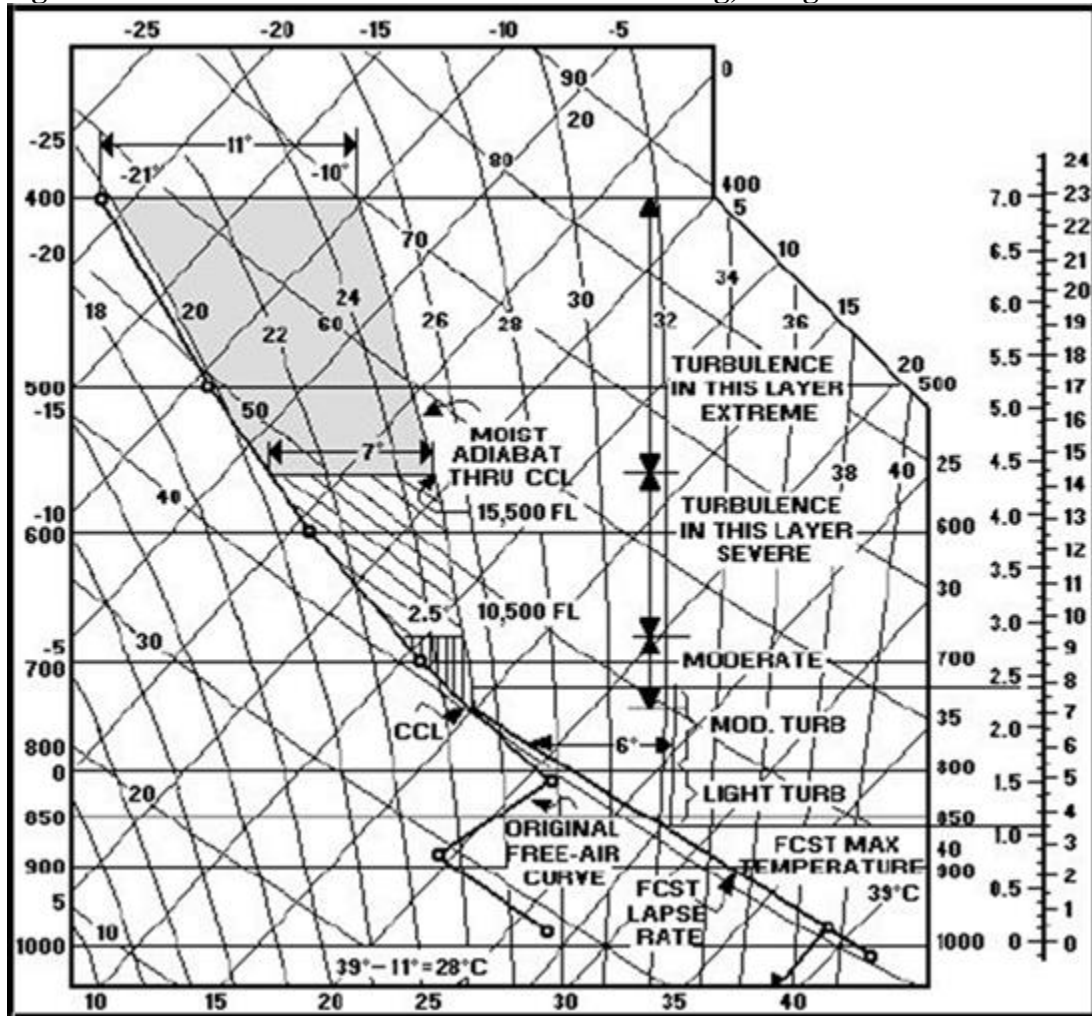
Always anticipate light-or-greater turbulence in the following areas:	
Thunderstorms	
Areas of strong thermal advection, such as:	Cold air advection
	Warm air advection
	Strong upper-level fronts
	Rapid surface cyclogenesis
	Outflow areas of cold-region jet streams
Areas of larger vertical shear, particularly below strong stable layers near:	Tilted ridges
	Sharp ridges
	Tilted troughs
	Confluent jet streams
Areas of significant horizontal directional and/or speed shear, such as:	Mountainous regions
	Diffluent upper-level flow
	Developing cut-off lows
	Sharp anticyclonic curvature

2.2.9.2. Low-level turbulence (surface to 10,000 feet) forecasting flowchart. Use **Figure 2.19** as a quick-reference guide for forecasting low-level turbulence for Category II aircraft; refer back to **Table 2.3** to adjust to other aircraft types as necessary.

Figure 2.19. Low-level turbulence forecasting flowchart – Category II aircraft.

2.2.9.3. Forecasting convective cloud turbulence. This method forecasts turbulence in convective clouds by analyzing two atmospheric layers (surface-9000 feet and above 9000 feet) on the Skew-T diagram (see **Figure 2.20**) The forecast method is designed for Category II aircraft; adjust with **Table 2.3** as necessary for other types of aircraft.

Figure 2.20. Convective cloud turbulence forecasting, using the Skew-T.

2.2.9.3.1. Surface-9000 foot layer. Analyzing this layer estimates the buoyant potential in the lower atmosphere, and estimates turbulence in thunderstorms. First, use the convective temperature to forecast the maximum surface temperature, then project a dry adiabat from the convective condensation level (CCL) to the surface – this gives the convective temperature. Adjust this temperature using temperature curves for local effects. Next, subtract 11°C from the final forecast maximum temperature, and follow this isotherm to its intersection with the dry adiabat projected upward from the forecast maximum temperature. If the intersection is above 9000 feet, no turbulence is expected below 9000 feet MSL. If the intersection is below 9000 feet, follow the moist adiabat from the intersection of the isotherm and the dry adiabat upward to the 9000-foot level; the temperature difference between this moist adiabat and the free-air temperature curve determines the severity of the turbulence, as well as the limits of the layers of each degree of turbulence (refer to **Table 2.6**.)

Table 2.7. Surface-9000 foot temperature difference vs. turbulence intensity.
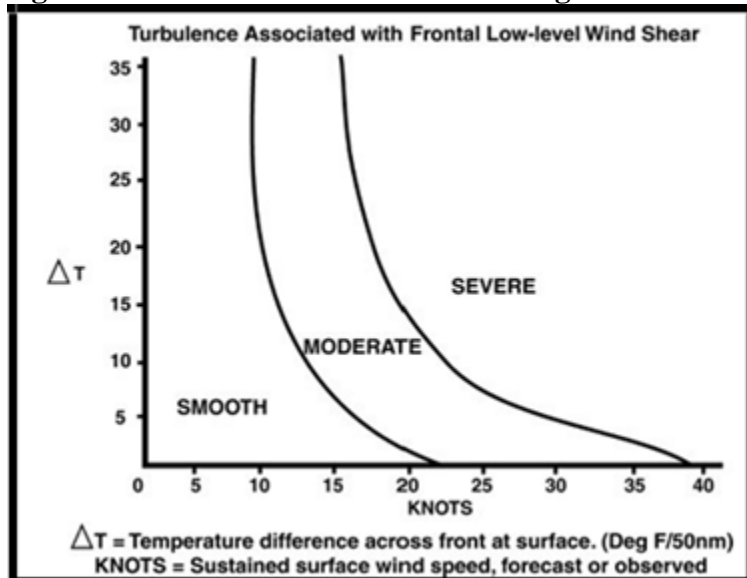
Layers where temperature difference is:	Turbulence is forecast as:
0° to 6°C	Light
6° to 11°C	Moderate
11°C or more	Severe

2.2.9.3.2. Layer above 9000 feet. Follow the moist adiabat that passes through the CCL upward to the 400 mb level; the maximum temperature difference between this moist adiabat and the forecast free-air temperature curve is the central portion of the most turbulent area. The expected intensity of the turbulence based on upper-level temperature differential is shown in **Table 2.7**.

Table 2.8. Layer above 9000 feet temperature difference vs. turbulence intensity.

Layers where temperature difference is:	Turbulence is forecast as:
0° to 2.5°C	Moderate
2.5° to 7°C	Severe
7°C or more	Extreme

2.2.9.4. Low-level turbulence nomogram. **Figure 2.21** is a quick-reference nomogram, predicting turbulence using winds and temperature differences across a surface front.

Figure 2.21. Low-level turbulence nomogram.

2.2.9.5. Satellite signatures and turbulence forecasting.

2.2.9.5.1. Deformation zone. Deformation zones are regions where the atmosphere is undergoing contraction in one direction and elongation or stretching in the perpendicular direction, relative to the motion of the air stream (**Figure 2.22**); a visible cloud border is often located near and parallel to the stretching axis. Moderate to severe turbulence is likely when:
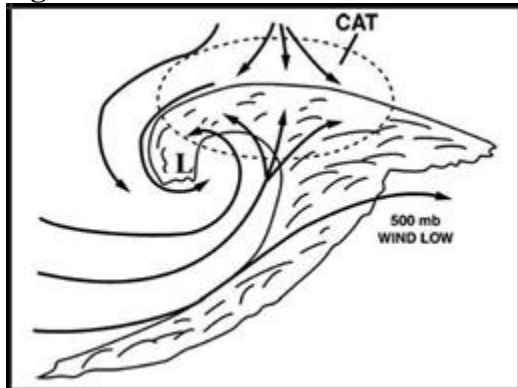
2.2.9.5.1.1. Cyclogenesis is in progress, accompanied by a building or rapidly moving upper ridge to the east of the storm.

2.2.9.5.1.2. The cloud system is encountering confluent (opposing) flow caused by a blocking upper-level system (a closed low or anticyclone) downstream.

2.2.9.5.1.3. The low and associated comma cloud system are dissipating.

2.2.9.5.1.4. A flattening of the cloud border is occurring on the upstream side of the comma.

Figure 2.22. Turbulence in a deformation zone.

2.2.9.5.2. Wave cloud signatures.

2.2.9.5.2.1. Transverse bands. Transverse bands are irregular, wave-like cirrus cloud patterns that form nearly perpendicular to the upper level flow (**Figure 2.23**); they are usually associated with the low-latitude subtropical jet stream and indicate large vertical and possibly horizontal wind shear. Wider and thicker transverse bands are more likely to contain severe turbulence, due to the added presence of thermal instability.

Figure 2.23. Transverse bands.

2.2.9.5.2.2. Billow clouds. Billow clouds (**Figure 2.24**) are cirrus or middle-level clouds which are regularly spaced, narrow, and oriented parallel to the upper flow. They are most often seen when a strong jet intersects either a frontal cloud system or a line of cumulonimbus clouds at a large crossing angle. The anvil debris of convective clouds in these situations extends well downstream from its source. Although individual waves dissipate quickly (less than 30 minutes), new waves can form nearby under favorable conditions. The longer the wavelength of the billows, the better the chance for significant turbulence.

Figure 2.24. Billow clouds.

2.2.9.5.2.3. Water vapor imagery darkening. On water vapor imagery, elongated bands or large oval-shaped darkening regions are indicative of moderate or greater turbulence. This darkening is usually accompanied by cold air advection and convergence in the mid- and upper-levels of the troposphere, as stratospheric air descends into the upper troposphere. Moderate or stronger turbulence is likely when image darkening occurs (occurs over 80% of the time in one study), especially when the darkening persists for at least 3 hours.

2.2.9.5.2.4. Mountain waves. Mountain waves (**Figure 2.25**) are stationary waves situated downwind of a prominent mountain range, caused by the orographic disturbance of the wind. The waves exhibit a stationary, narrow clearing zone parallel to steep mountain ranges. They may also occur in Chinook wind synoptic situations, near or just east of the upper ridge and south of the jet stream.

Figure 2.25. Mountain waves.

2.2.9.6. Vertical cross sections. Analyzing atmospheric vertical cross sections can provide tremendous insight into the atmospheric structures that contribute to turbulence development. Analyzing wind speeds (10 knot intervals) and temperature (at 5°C intervals) will reveal jet cores and strong vertical temperature gradients associated with atmospheric turbulence; frontal boundaries and areas of wind shear will also become evident.

2.2.9.7. Doppler weather radar. Weather radar provides multiple unique capabilities to detect and display turbulence indicators, such as frontal boundaries, low-level jets, gust fronts, and upper-level wind shear.
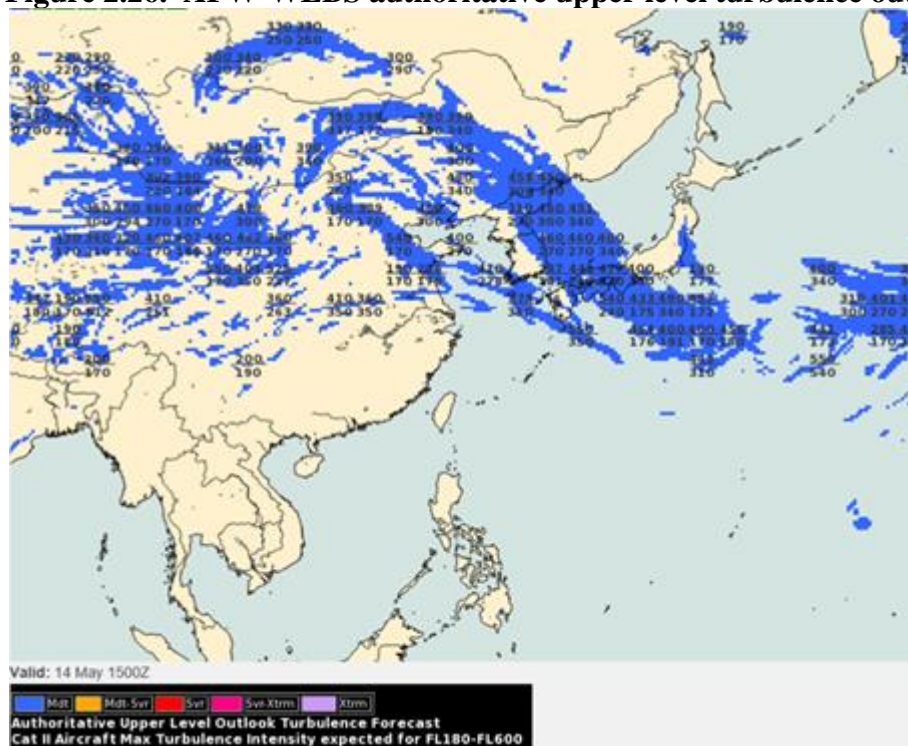
2.2.9.7.1. Spectrum Width. Though not conclusive, spectrum width values of 8-11 knots have been associated with moderate turbulence for Category II aircraft, and values 12 knots and higher may be indicative of severe turbulence. Use the spectrum width product to corroborate suspected turbulence areas found using other forecast products.

2.2.9.7.2. VAD Wind Profile. Use the radar's wind profiler to examine the current and past vertical wind structure to identify turbulent features evolving over time (e.g., inversions, wind shifts, and development of jet streams). Look for areas of sharp turning in the winds with high wind speeds to identify strong local vertical wind shear.

2.2.9.7.3. Base velocity. Areas of sudden speed or directional shifts are associated with wind shear and atmospheric turbulence. Intense shear regions, such as the tops of thunderstorms associated with storm top divergence, can also be located using base velocity.

2.2.9.7.4. Vertically Integrated Liquid (VIL). High VIL values indicate a strong potential for severe convective weather, and associated wind shear and atmospheric turbulence.

2.2.9.8. AFW-WEBS Low-level and Upper-level turbulence guidance. AFW-WEBS provides global forecaster-in-the-loop turbulence outlooks for low-level (surface-18,000 feet) and upper-level (18,000-60,000 feet) forecasts (**Figure 2.26**); areas of expected turbulence are color-coded with bases and tops indicated in numerical format.

Figure 2.26. AFW-WEBS authoritative upper level turbulence outlook.

Valid: 14 May 1500Z

Authoritative Upper Level Outlook Turbulence Forecast
Cat II Aircraft Max Turbulence Intensity expected for FL180-FL600

2.2.9.9. The Stratospheric Layer Advanced Turbulence (SLAT) Index (see **Table 2.8**). The SLAT index is based on the "S-shaped" stratospheric temperature profile. SLAT values typically range from 0 to 15, with higher values indicative of moderate or greater stratospheric turbulence potential. High values are obtained from a large difference (but less than 10) between the temperatures at the top and bottom of the "S" layer, indicative of a steep lapse rate in the mixed layer; they also result from shallow inversion lapse rates and/or a thin mixing layer (small DZ) In the mountains, SLAT values can exceed 100, possibly indicative of vertically-propagating mountain waves.

Table 2.9. Stratospheric Layer Advanced Turbulence Index.

Stratospheric Layer Advanced Turbulence Index formula:

$$ SLAT = \frac{\{gamma_{ml} - (gamma_t + gamma_b)\} * (20,000 - DZ)}{10 - (T_{max} - T_{min})} $$

$gamma_{ml}$ is the lapse rate in the mixing layer
$gamma_t$ is the lapse rate of the inversion above the mixing layer
$gamma_b$ is the lapse rate of the inversion below the mixing layer
DZ is the thickness (in feet) of the mixing layer
T_{max} is the temperature at the top of the lower inversion
T_{min} is the temperature at the bottom of the upper inversion

2.2.9.10. Turbulence climatology. The 14th Weather Squadron provides global climatologies of monthly and annual turbulence frequency for several atmospheric layers (FL210-270, 300-350, and 350-400), these products are available on their website.

2.3. Icing. Structural icing interferes with aircraft control by increasing drag and weight while decreasing lift, while engine-system icing reduces the effective power of aircraft engines. The accuracy of icing forecasts begins with accurate predictions of precipitation, clouds, and temperature. Aircraft icing generally occurs between the freezing level and -40ºC (icing can occur at -42ºC in the upper parts of cumulonimbus clouds). The frequency of icing decreases rapidly with decreasing temperatures, becoming rare at temperatures below -30ºC. The normal atmospheric vertical temperature profile usually restricts icing to the lower 30,000 feet of the atmosphere. In the middle latitudes (such as in most of the United States, Northern Europe, and the Far East), icing is most frequent in winter; frontal activity is frequent, and the resulting cloud systems are extensive, creating favorable icing conditions. Polar regions are normally too cold in the wintertime to contain the concentration of moisture necessary for icing; locations at higher latitudes (such as Canada and Alaska) usually experience optimal icing conditions in the spring and fall.

2.3.1. Icing Formation Processes. Clouds are not water vapor, but instead consist of water droplets and/or ice crystals that form when the atmosphere becomes saturated. Once saturated, the atmosphere produces and maintains clouds through multiple processes, including the addition of water vapor, cooling and lifting by convective or mechanical/orographic processes, and convergence.

2.3.1.1. *Terrain.* Air lifted mechanically by terrain can spur development of a broad range of cloud types, from small cap clouds over mountain peaks to widespread cloud decks covering hundreds of kilometers. An example of a terrain effect is upslope easterly winds over the western high plains, which create widespread cloudiness as the air is forced westward over the gently rising terrain – this pattern generally occurs after passage of an arctic or polar front. These clouds often result in broad areas of icing conditions, which can last for days at a time. Icing hazards can also develop in orographic clouds, which tend to develop along mountaintops and ridges and can persist for days if the winds and moisture are consistent. Winds blowing perpendicular to ridgelines provide the most favorable conditions for orographic cloud development.

2.3.1.2. *Fronts.* Fronts act like "moving terrain", forcing one air mass up and over another. Fronts can be areas of enhanced icing due to the presence of convection and ample moisture. Although the lifting over a moving cold air mass can have a broad extent, the most intense lifting tends to be limited to narrow bands of clouds near the surface frontal location. The icing threat posed by a cold front varies based on the strength and extent of the associated lift and ultimately, the aircraft's flight altitude and trajectory through the frontal cloud. A flight path perpendicular to the cloud band can reduce the icing threat, while a path parallel to the cloud band can be particularly hazardous due to the prolonged time within the cloud.

2.3.1.3. *Cyclones.* Cyclonic circulations generate convergence of air at the center of low-pressure systems, resulting in large scale rising motion and cloud formation. Large scale dynamic processes, such as warm air advection and differential vorticity advection, also lead to broad regions of uplift and cloudiness. The area ahead of an active and stationary warm front, and behind the surface low center, is the primary region where icing occurs; this area provides optimal conditions for the formation of supercooled droplets and freezing precipitation. The extensive horizontal and vertical extent of a synoptic-scale cyclone can result in long exposures of aircraft to icing conditions, depending on the flight path and altitude.

2.3.2. Phase Transitions. Water is a unique substance; at typical tropospheric pressures and temperatures, it can exist in three phases – liquid, solid, and vapor. The transitions between these phases determine the likelihood and amount of liquid water available for icing. There are six main categories of phase change processes, described below.

2.3.2.1. *Condensation.* Condensation is the transition of water vapor to liquid water; this phase transition forms liquid water clouds. Clouds are formed when rising air cools to its dew point temperature; as an air parcel rises, it expands and cools adiabatically, and vapor condenses onto small airborne particles called cloud condensation nuclei (CCN). As the air continues to rise and cool, additional condensation takes place on these activated droplets and the droplets continue to grow.

2.3.2.2. *Evaporation.* Evaporation is the transition of liquid water to vapor; when clouds mix with the surrounding dry environment, droplets evaporate due to their exposure to sub-saturated conditions. If enough dry air is mixed in, clouds will completely dissipate. This entrainment and mixing process is a common occurrence in both convective and stratiform clouds; stratus can change to stratocumulus and eventually dissipate as dry air is entrained.

2.3.2.3. *Freezing*. Freezing is the transition of liquid water to ice. Liquid water droplets do not necessarily freeze at 0° C; droplets may become supercooled, persisting at temperatures well below 0° C. In order for a supercooled droplet to freeze, it must come into contact with a small particle called an ice nucleus. The ability of these ice nuclei to catalyze droplet freezing is temperature dependent; at temperatures warmer than -12° C to -15° C, few active nuclei exist and clouds are likely to be composed primarily of liquid droplets rather than ice crystals. If a cloud lacks a sufficient concentration of ice nuclei, widespread areas of supercooled water can exist, and icing is likely. When temperatures approach -40° C, an ice nucleus is no longer needed and droplets freeze spontaneously.

2.3.2.4. *Melting*. Melting is the transition of ice to liquid water. Melting can remove accumulated ice from the airframe if the pilot is able to safely descend (or in more rare cases ascend) to temperatures warmer than 0° C. Knowledge of the freezing level altitude and depth of the above-freezing air is a critical part of icing forecasts; if the freezing layer extends down to the surface, there may be no escape from icing conditions other than flight above or around the cloud or horizontally toward warmer air. These actions are often impossible for smaller aircraft that have limited range, altitude, and ability to handle icing.

2.3.2.5. *Deposition*. Deposition is the transition of water vapor to ice. At a given temperature, the vapor pressure over a water surface is greater than that over an ice surface. If water droplets and ice crystals exist in the same environment (called mixed phase conditions), vapor molecules in the air will deposit on an ice crystal rather than condense onto a water droplet; the ice crystals grow at the droplets' expense. Deposition creates sub-saturation conditions, and the droplets evaporate to maintain water saturation, leaving additional water vapor available for ice crystal growth. In mixed-phase clouds, glaciation (the transition of the cloud from supercooled liquid to ice) takes place rapidly; it begins in the highest part of the cloud and moves downward, as ice crystals become larger and heavier and fall through the cloud. In stratiform clouds with tops colder than -15° C, significant icing conditions are not expected because at these colder temperatures, ice nuclei generally are active, forming ice and leading to glaciation of the cloud. The exception is in cumuliform (including stratocumulus) clouds with strong enough updrafts to supply both the liquid droplets and ice crystals with enough condensate for coexistence.

2.3.2.6. *Sublimation*. Sublimation is the transition of ice to water vapor; this process occurs in a sub-saturated, below-freezing environment where ice particles transition directly to water vapor without melting.

2.3.3. Icing factors. Icing severity and type depends on the properties of the aircraft as well as the atmospheric conditions; forecasters must focus on diagnosing the icing environment. The meteorological quantities most closely related to icing severity and type are detailed below.

2.3.3.1. *Liquid water content*. Cloud liquid water content (LWC) is extremely important for determining icing potential, but is difficult to quantify. LWC is the density of liquid water in a cloud, expressed either as grams of water per cubic meter (g/m3) or grams per kilogram (g/kg) of air. If the temperature is below freezing, the liquid water content is a measure of how much supercooled liquid water (SLW) is available to accrete on the aircraft.

2.3.3.2. *Temperature*. Temperature affects both the severity and type of icing. For icing to occur, the outside air and airframe temperatures must be below 0° C. Since supercooled droplets (SLD) need an ice nucleus to freeze, and ice nuclei are strongly temperature dependent, most icing takes place at temperatures between 0° and -20° C. The physical limit to icing is at -40° C, where liquid droplets freeze without the presence of ice nuclei.

2.3.3.3. *Droplet size*. Droplet size has a significant influence on icing conditions when they are larger than 40 microns; these larger drops persisting in subfreezing temperatures are called supercooled large drops (SLD) and can present a significant icing hazard. SLD includes freezing drizzle (diameters 40 to 200 microns) and freezing rain (diameters greater than 200 microns). Droplet size influences the collection efficiency of drops on the airframe; small droplets have little mass and momentum, so they tend to be swept around the airframe as the airplane passes. As droplet size increases, they will begin to accumulate near the leading edge of the wing, where the air diverges to go around the airfoil.

2.3.3.4. *Altitude*. Theoretically, there is no altitude limit for icing; icing conditions may be present from the surface to the stratosphere. In practical terms, however, optimal icing conditions are only found in a narrow band of the atmosphere. Studies have shown that 50% of all icing cases occur between 5000 and 13,000 feet, with a peak occurrence near 10,000 feet.

2.3.4. Icing types and amounts.

2.3.4.1. *Rime Icing.* Rime ice is a milky, opaque, and granular deposit with a rough surface (**Figure 2.27**); it forms by the instantaneous freezing of small, supercooled water droplets as they strike the aircraft. This instantaneous freezing traps a large amount of air, giving the ice its opaqueness and making it very brittle. It is most frequently encountered in stratiform clouds, but can also occur in cumulus clouds. Rime ice is lightweight, brittle, and fairly easily removed.
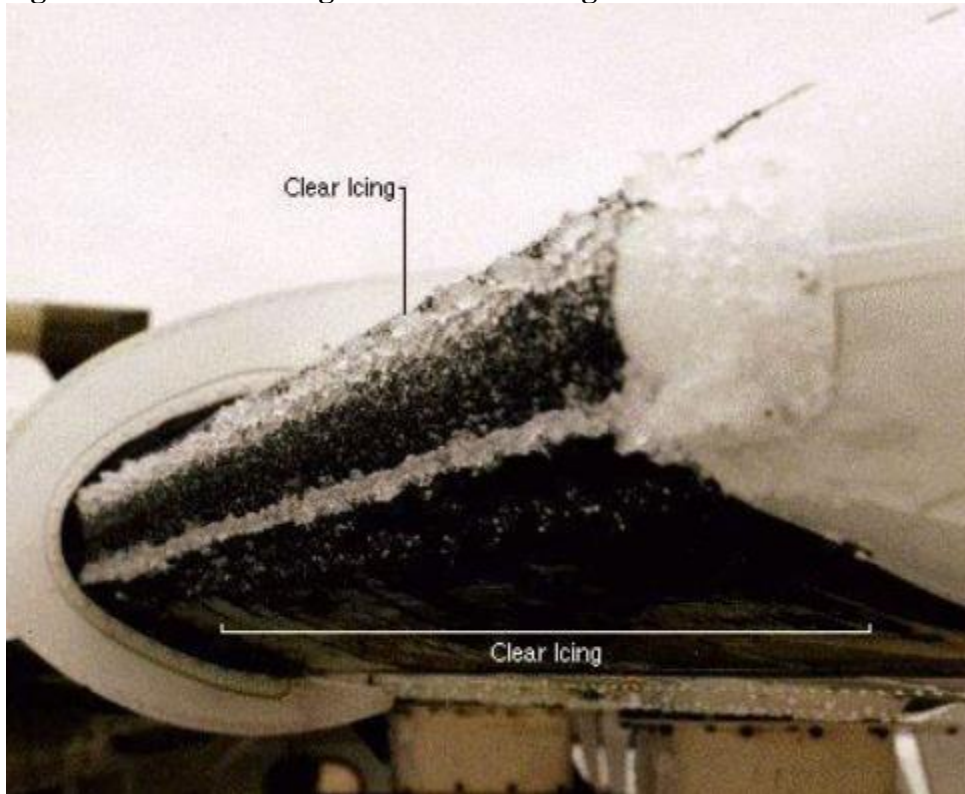
2.3.4.2. *Clear Icing.* Clear ice is a glossy ice, identical to the glaze forming on trees and other objects as freezing rain strikes the Earth; it's the most serious type of icing because it adheres so firmly to the aircraft. Conditions most favorable for clear ice formation are high water content, large droplet size, and temperatures slightly below freezing. Clear icing is most frequently encountered in cumuliform clouds and during freezing precipitation, and can be smooth or rough (**Figure 2.28**) It's smooth when deposited from large, supercooled cloud droplets or raindrops that spread, adhere to the surface of the aircraft and slowly freeze. If mixed with snow, ice pellets or small hail, it is rough, irregular, and whitish; the deposit then becomes very blunt-nosed with rough bulges building out against the airflow. Clear ice is hard, heavy, and tenacious; its removal is difficult.

2.3.4.3. *Mixed Icing.* Due to small-scale variations in liquid water content, temperature, and droplet sizes, an airplane can encounter both rime and clear icing along its flight path – this results in mixed icing. Ice particles become embedded in clear ice, building a very rough accumulation, sometimes in a mushroom shape on leading wing edges.

Figure 2.27. Rime Icing.

Rime Ice

Figure 2.28. Clear Icing – smooth and rough varieties.

2.3.4.4. *Icing Type and Temperature.* The type of icing is dependent on multiple variables (liquid water content, airframe characteristics, etc.), but temperature can be a good indicator of expected icing type. The general relationship between temperature and icing type is outlined in **Table 2.9**

Table 2.10. Icing type based on temperature.

Temperature of atmospheric layer	Expected icing type
0º to -10ºC	Clear
-10º to -15ºC	Mixed
-15ºC to -40ºC	Rime

2.3.4.5. *Icing Amounts.* Icing potential is dependent upon aircraft type and design, flight altitude, and airspeed as well as the atmospheric conditions. General classifications for icing amounts are defined in the Federal Aviation Administration's Flight Information Handbook, and are listed in **Table 2.10**

Table 2.11. Icing amount definitions.

Icing amount	Definition
Trace	Ice becomes perceptible. The rate of accumulation is slightly greater than the rate of sublimation. It is not hazardous unless encountered for an extended period of time (over one hour, even though de-icing/anti-icing equipment is not used.
Light	The rate of accumulation may create a problem if flight is prolonged in this environment (over one hour). Occasional use of de-icing/anti-icing equipment removes/prevents accumulation. It does not present a problem if the de-icing/anti-icing equipment is used.
Moderate	The rate of accumulation is such that even short encounters become potentially hazardous, and use of de-icing/anti-icing equipment or diversion is necessary.
Severe	The rate of accumulation is such that de-icing/anti-icing equipment fails to reduce or control the hazard. Immediate diversion is necessary.

2.3.5. Icing in Precipitation. Clear icing caused by droplets larger than cloud-size (greater than 40 microns) poses an especially hazardous icing problem; this type is often referred to as supercooled large droplet (SLD) ice. Large droplets tend to form a very lumpy texture, which significantly disrupts airflow and aerodynamics. These drops can flow large distances along the airfoil, impacting the aircraft farther aft than smaller cloud-sized droplets and accreting on surfaces beyond the reach of de-icing equipment.

2.3.5.1. Physical mechanisms for icing development. SLD are formed in two ways: through melting of ice and subsequent supercooling of the drops (warm layer process), or through droplet growth processes within a supercooled environment (collision-coalescence). In the first case, the presence of the ice phase is needed; in the second case, it is not. In either case, the presence of freezing precipitation at the surface is a good initial indicator of SLD aloft.

2.3.5.1.1. Warm layer process. During a precipitation event, warm intrusions aloft often result in favorable conditions for SLD formation, and the possibility of SLD clear ice accretion increases The precipitation types most often associated with a warm layer process during the cold season are either freezing rain (ZR) or freezing drizzle (ZL). Freezing rain and freezing drizzle can result from snowflakes falling through and melting in a layer of warm air aloft (usually at least 2° to 3° C), then continuing to fall into a layer of subfreezing air below. The warm layer must be deep enough to melt frozen precipitation; if the low-level cold layer is too cold or too deep, the supercooled drops (ZL or ZR) can refreeze to ice pellets.
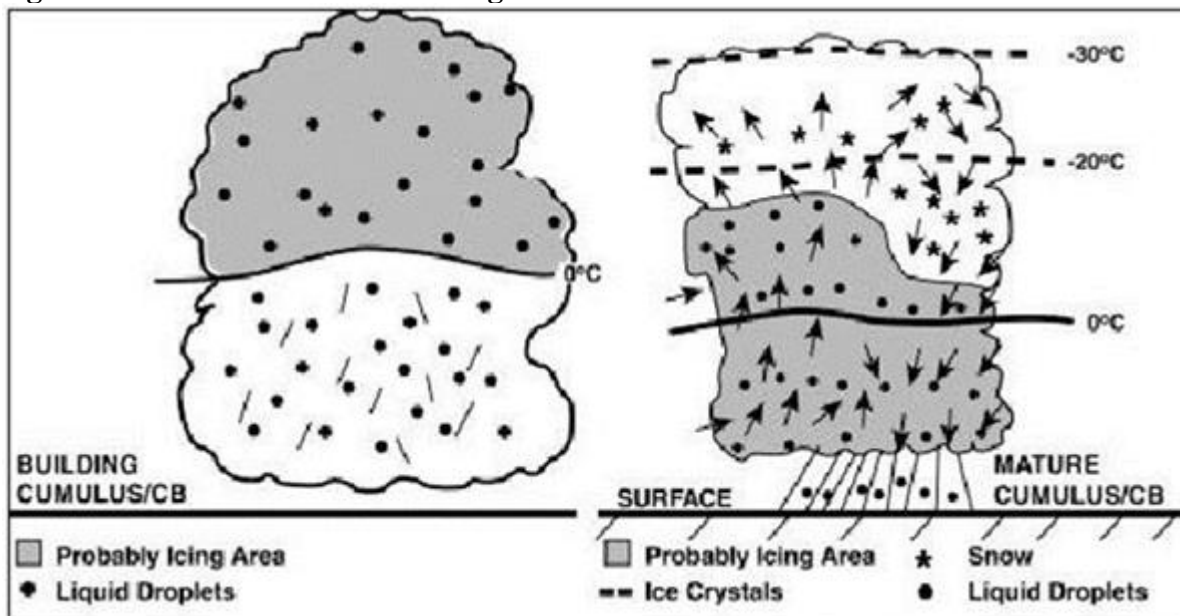
2.3.5.1.2. Collision-coalescence. ZR and ZL can also form by collision and coalescence of droplets. This process doesn't require a preliminary ice phase (as the warm layer process does), and no warm layer is required. Clouds typically have a wide distribution of drop sizes, resulting in a distribution of fall speeds. If the distribution is large enough, some drops will collide with one another and coalesce into larger drops. When the largest drops reach approximately 20 microns in size, the collision-coalescence process begins; it can rapidly transform cloud-sized droplets into larger drizzle drops (between 200 and 500 microns) or even raindrops (greater than 500 microns).

2.3.5.2. Meteorological considerations for icing.

2.3.5.2.1. *Stratiform clouds.* Stable air masses often produce stratiform clouds with extensive areas of relatively continuous potential icing conditions; icing intensities in stratiform clouds generally range from light to moderate, with maximum intensity in the cloud's upper portions. Both rime and mixed icing are observed in stratiform clouds. High-level stratiform clouds (such as cirrostratus contain mostly ice crystals and produce little icing. Stratiform cloud icing typically occurs in mid- and low- level clouds, in a layer between 3000 and 4000 feet thick, and rarely occurs more than 5000 feet above the freezing level. Multiple layers of stratus clouds may be so close together that flying between layers is impossible. In these cases, maximum depth of continuous icing conditions rarely exceeds 6000 feet.

2.3.5.2.2. *Cumuliform clouds.* Unstable air masses produce cumuliform clouds with a limited horizontal extent of potential icing conditions. Icing generally occurs in the updraft regions in mature cumulonimbus, but is confined to a shallow layer near the freezing level in a dissipating thunderstorm (see **Figure 2.29**) Icing intensities range from light in small cumulus to moderate or severe in towering cumulus and cumulonimbus. The most severe icing occurs in cumulus clouds just prior to entering the cumulonimbus stage. Although icing occurs at all levels above the freezing level in building cumulus, it is most intense in the upper half of the cloud. The zone of icing in cumuliform clouds is smaller horizontally but greater vertically than in stratiform clouds. Icing (usually clear or mixed) is more variable in cumuliform clouds, because many of the factors conducive to icing depend largely on the particular stage of the cloud's development.

Figure 2.29. Cumuliform cloud icing locations.
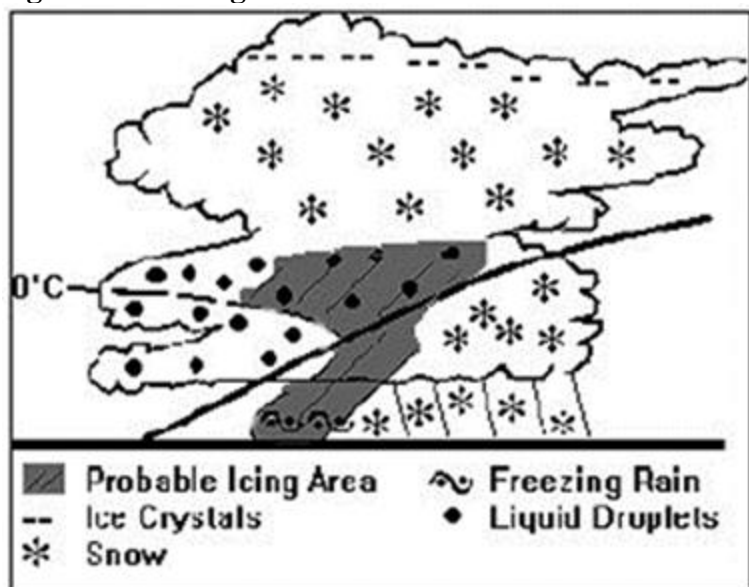
2.3.5.2.3. *Cirriform clouds.* Icing rarely occurs in cirrus clouds, even though some non-convective cirriform clouds do contain a small proportion of water droplets. Moderate icing can occur in the dense cirrus and anvil tops of cumulonimbus, however, where updrafts may contain considerable amounts of supercooled water.

2.3.5.2.4. *Frontal systems.* For significant icing to occur above a frontal surface, lifted air must cool to temperatures below freezing, and be at or near saturation. If the warm air is unstable, icing may be sporadic; if it is stable, icing may be continuous over an extended area. While precipitation forms in the relatively warm air above the frontal surface at temperatures above freezing, icing generally occurs in regions where cloud temperatures are colder than 0°. Generally, this layer is less than 3,000 feet thick. Icing below a frontal surface most often occurs in freezing rain or drizzle; as precipitation falls into the cold air below the front, it may become supercooled and freeze on impact with aircraft. Freezing drizzle and rain occur with both warm fronts and shallow cold fronts.
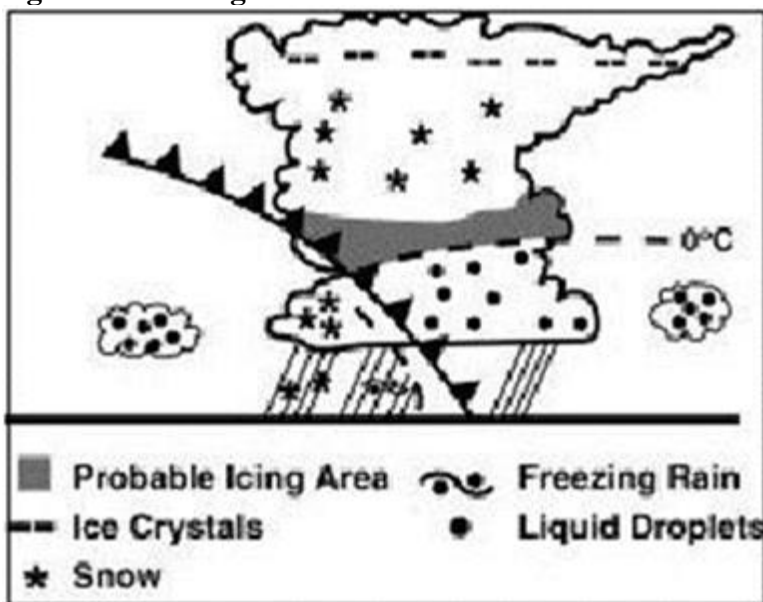
2.3.5.2.4.1. Warm frontal icing characteristics (**Figure 2.30**) Warm frontal icing is usually widespread, and can extend well ahead of the front. Light rime icing occurs in altostratus up to 300 miles ahead of the warm frontal surface position; mixed/clear icing can occur 100-200 miles ahead of the surface position.

Figure 2.30. Icing with a warm front.

2.3.5.2.4.2. Cold frontal icing characteristics (**Figure 2.31**) Icing associated with cold fronts is typically not as widespread as it is with warm fronts, since cold fronts generally move faster and have less cloudiness. Clear icing is more prevalent than rime icing in the cumuliform clouds associated with the cold front; light icing usually occurs in the extensive layers of supercooled stratocumulus clouds behind the front, while moderate icing occurs in the supercooled cumuliform clouds up to 100 miles behind the cold front surface position (most likely directly above the frontal zone). Icing conditions in the stratiform clouds of a widespread, slow-moving cold frontal cloud shield are similar to warm frontal icing.

Figure 2.31. Icing with a cold front.

2.3.5.2.4.3. Stationary/occluded frontal characteristics. Icing associated with occluded and stationary fronts is similar to that of warm or cold frontal icing. Moderate icing also frequently occurs also with deep, cold, low-pressure areas where frontal systems are indistinct; icingcan be severe in freezing precipitation.
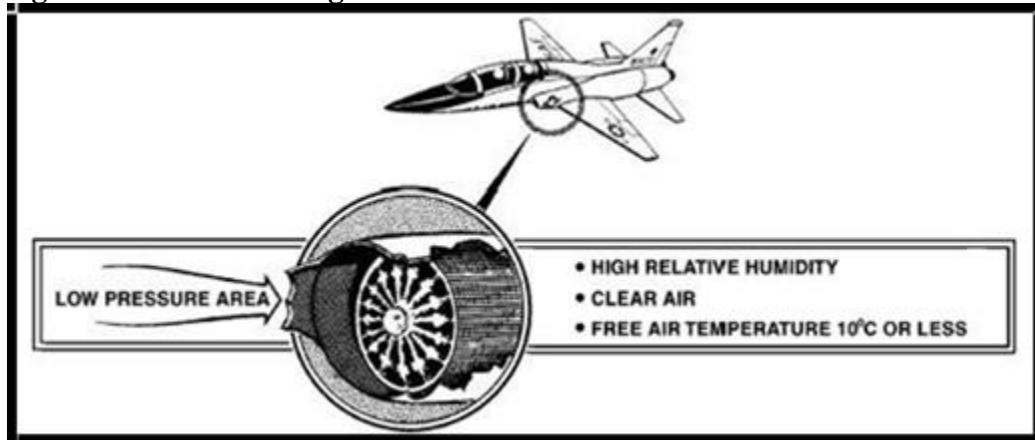
2.3.5.3. Other Icing Conditions.

2.3.5.3.1. Terrain. Icing is more likely (and more severe) in clouds over mountainous regions than over other terrain; mountain ranges cause upward vertical motion on their windward side. Strong upslope flow can lift large water droplets as much as 5,000 feet into sub-freezing layers above a peak, resulting in supercooled water droplets. In addition, when a frontal system moves across a mountain range, the normal frontal lift combines with the mountain's upslope effect to create extremely hazardous icing zones.

2.3.5.3.2. Induction icing. In addition to the hazards created by structural icing, an aircraft can also be affected by icing of its power generation structures (i.e., the engine). Ice can develop on air intakes under the same conditions favorable for structural icing; when it occurs, icing is most common in the air induction system, but may also be found in the fuel system. The main effect of induction icing is power loss due to blocking of the air before it enters the engine. On rotary-wing aircraft, a loss of manifold pressure combined with air intake screen icing may force the immediate landing of the aircraft.

2.3.5.3.2.1. Air intake ducts. In flights through clouds containing supercooled water droplets, air intake duct icing is similar to wing icing. The ducts can be susceptible to icing in other conditions, however, even when skies are clear and temperatures are above freezing. During taxiing, takeoff, and climb, reduced pressure forms in the intake system (**Figure 2.32**), which can lower temperatures to the condensation and/or sublimation point. If condensation/sublimation occurs, ice may form on the intake, which decreases the radius of the duct opening and limits the air intake. Ice formed on these surfaces can later break free, causing potential foreign object damage (FOD) to internal engine components.

Figure 2.32. Intake icing.

2.3.5.3.2.2. Carburetor icing. Carburetor icing can be treacherous, and may lead to complete engine failure (**Figure 2.33**); it can form under seemingly benign conditions even when structural icing doesn't occur. Ice in the carburetor may partially or totally block the flow of the air/fuel mixture into the engine, leading to reduced engine performance or even total engine failure in the most severe icing cases. Carburetor icing forms when moist air, drawn into the carburetor, is cooled to a dew point temperature less than 0°C (frost point). Carburetor icing can occur in a wide range of atmospheric conditions, but it's most likely when relative humidity is high (above 80%) and temperatures are between 21°C (70°F) and -7°C (20°F) (**Figure 2.34**)

Figure 2.33. Carburetor icing.
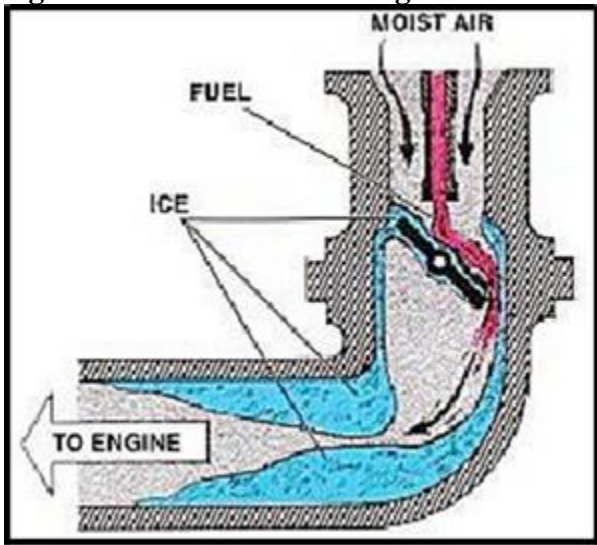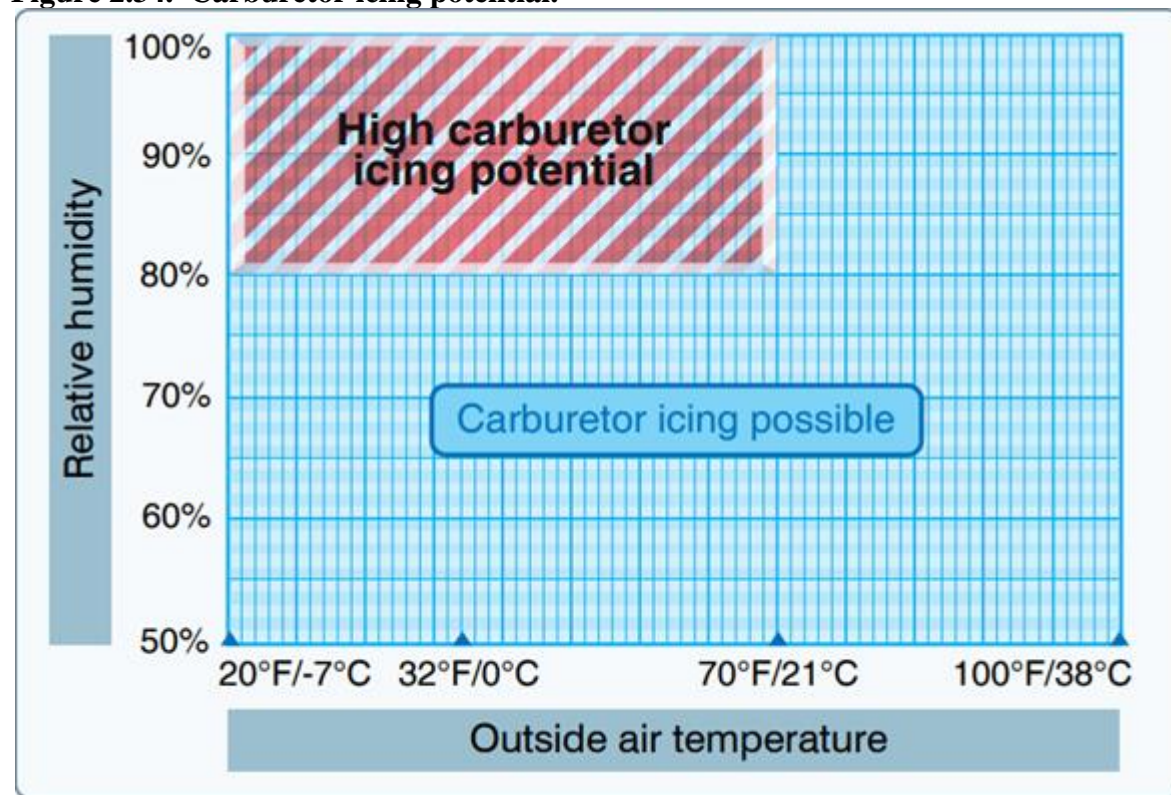
Figure 2.34. Carburetor icing potential.

2.3.6. Icing Products and Procedures. The products and procedures listed in this section can assist in determining the potential for icing.

2.3.6.1. *AIRMETS, SIGMETS, PIREPS, and AIREPS*. Use these products to verify icing forecasts, to locate icing areas that impact the forecast area, and to identify synoptic icing conditions. PIREPS and AIREPS are critical data sources, since they originate from aircrews and act as in-situ observations; solicit aircrews aggressively for reports, so other aircrews may benefit from their reporting.

2.3.6.2. *Upper air temperature and dew point.* Consult upper-air soundings along the flight route for temperatures and dew point spreads at flight level, and refer to **Table 2.11** to determine icing potential. In addition, pay close attention to the upper-level flow to identify upstream icing, which may advect into the route of flight by the time the aircraft reaches the area.

Table 2.12. Icing potential based on temperature and dew point depression.

Unfavorable atmospheric conditions for icing			
Temperature	Dew point depression		Forecast
0°C to -7°C	Greater than 2°C		none
-8°C to -15°C	Greater than 3°C		none
-16°C to -22°C	Greater than 4°C		none
lower than -22°C	any spread		none
Favorable atmospheric conditions for icing			
Temperature	Dew point depressio	Advection	Forecast	Probability
0°C to -7°C	2°C or less	Neutral/weak CAA	Trace	75%
		Strong CAA	Light	80%
-8°C to -15°C	3°C or less	Neutral/weak CAA	Trace	75%
		Strong CAA	Light	80%
0°C to -7°C	2°C or less	None – associated areas with vigorous cumulus buildups due to surface heating	Light	90%
-8°C to -15°C	3°C or less			

2.3.6.3. *Upper air composite data.* Upward vertical motion in the vicinity of a jet stream maximum, combined with adequate moisture and CAA, produce a high probability of icing; when these features are located in close proximity, icing is likely. Use additional information in this section to determine icing type and intensity.

2.3.6.3.1. Vorticity. Use a 500 mb chart to show areas of positive and negative vorticity advection (PVA/NVA). Overlay the vertical velocity product (OVV) to show vertical motion.

2.3.6.3.2. Wind speed (jet stream). Use 300 and 200 mb charts to highlight locations of jet streams, with emphasis on wind speed maxima and minima.

2.3.6.3.3. Moisture. Analyze the 850, 700, and 500 mb charts for moisture. Sufficient moisture, combined with cold-air advection, indicates icing potential in those regions.

2.3.6.3.4. Thermal advection patterns. Evaluate the 1000-500 mb, 1000-700 mb, or 1000-850 mb thickness products for thermal advection patterns; CAA increases the possibility of icing.

2.3.6.4. *Icing from freezing precipitation.* Analyze surface isotherms in one color, and overlay 850 mb isotherms in another color. In a third color, overlay 850 mb moisture data (dew point depressions of 2°, 3°, and 4° C). Look for areas on the composite chart with high moisture, surface temperatures below freezing, and 850 mb temperatures above freezing; precipitation in these areas is likely to be freezing rain or freezing drizzle, with icing likely.

2.3.6.5. *Vertical cross sections.* Vertical cross sections can show the amount of moisture in the atmosphere and the associated temperatures and dew-point depressions at the levels of interest; evaluate cross sections to see where the following rules of thumb might apply:

2.3.6.5.1. Relative humidity. Values greater than 65% indicate broad areas of icing potential.

2.3.6.5.2. Temperature and dew point depression. Refer back to **Table 2.12** for icing type based on temperature, and to **Table 2.14** for icing potential based on combined temperatures and dew point depressions. In addition, use the rules of thumb below:
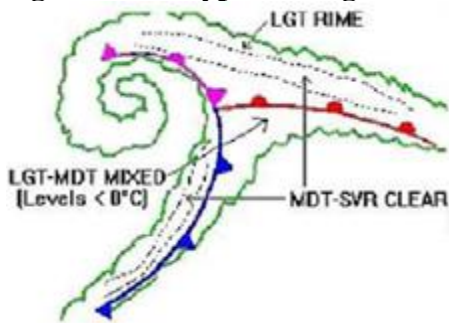
2.3.6.5.2.1. Forecast rime icing when temperatures at flight level are colder than -15°C, or when temperatures are between -1°C and -15°C in stable, stratiform clouds.

2.3.6.5.2.2. Forecast clear icing when temperatures at flight level are between 0°C and -8°C in cumuliform clouds, or when freezing precipitation is occurring.
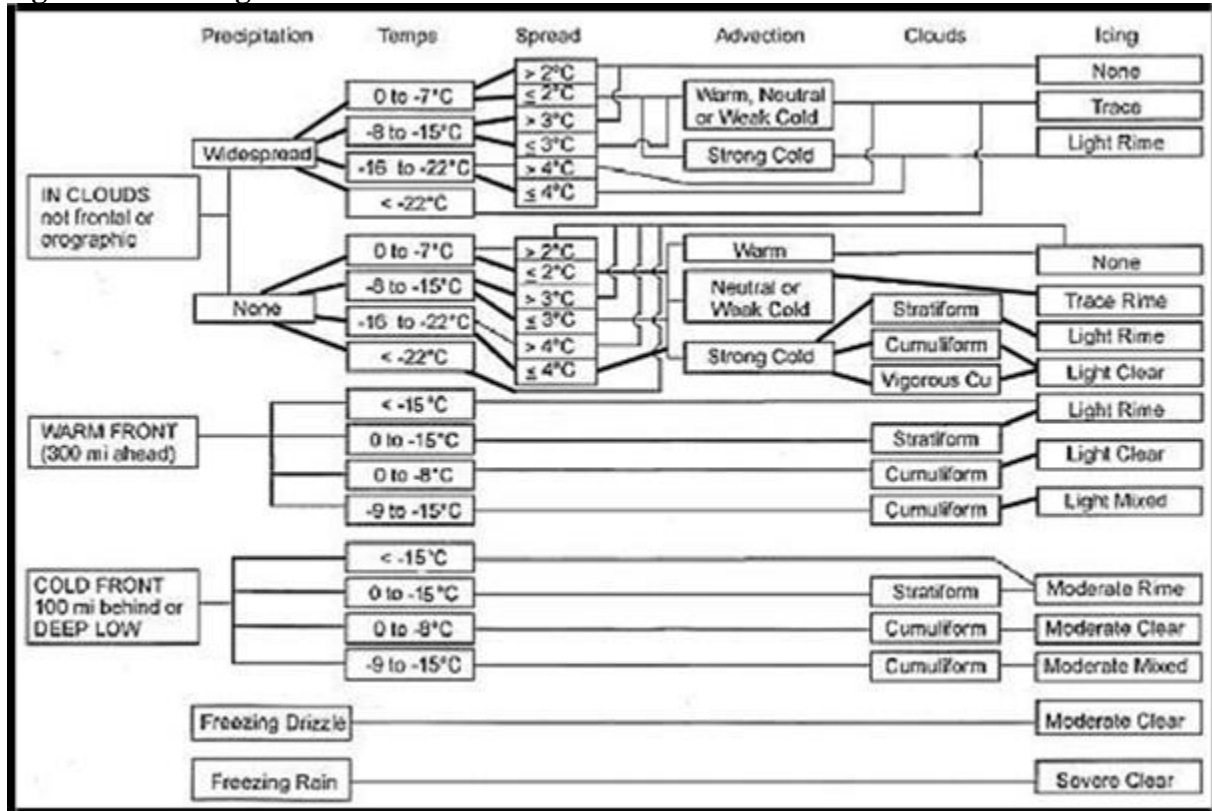
2.3.6.5.2.3. Forecast mixed icing when temperatures at flight level are between -8°C and -15°C in unstable clouds.

2.3.6.6. *Surface products.* If no other data is available, surface products can be used as a guide for potential icing conditions; icing potential exists along frontal cloud shields, low-pressure centers, and precipitation areas along the route of flight (see **Figure 2.35**) Icing conditions can exist up to 300 miles ahead of a warm front, up to 100 miles behind a cold front, and over a deep, almost vertical low pressure center.

Figure 2.35. Typical icing areas in a mature cyclone.

2.3.6.7. *Combined icing flowchart.* **Figure 2.36** combines multiple atmospheric phenomena into a quick-reference icing flowchart; use it for a quick-reference guide for potential icing conditions.

Figure 2.36. Icing flowchart.

2.3.7. Determining Icing Potential Using Radar. Although there is no NEXRAD product specifically designed to forecast icing, reflectivity and velocity products can assist in determination of potential icing areas.

2.3.7.1. *Identifying CAA.* Base velocity and the VAD Wind Profile (VWP) are key products for determining CAA. – Base velocity will indicate CAA via the backward S-shaped pattern in the zero isotach, and the VWP will reveal CAA by showing winds backing with height (the same pattern you see on the Skew-T). The VWP is also a valuable tool to monitor real-time changes in the vertical profile between the morning and afternoon soundings, and should be used to augment Skew-T observations.

2.3.7.2. *Bright band identification.* The Base reflectivity product will show the freezing level as a ring of enhanced reflectivity (30 to 45 dBZ) around the Radar Data Acquisition Unit (RDA). This enhanced area is called the bright band, formed when frozen precipitation melts as it falls through the freezing level. The height of the outer edge of the bright band is the height of the freezing level (0ºC); it's found by placing the cursor on the area of interest and reading the elevation to the right of the reflectivity panel. After determining the height of the freezing level, the next step is to determine the height of the -22° C isotherm, the minimum temperature threshold for icing conditions (find it by using Skew-T data or PIREPs within the local area). Use the radar cursor to locate the -22° C elevation on the reflectivity product; any reflectivities between the freezing level and -22° C height present an icing threat.

2.3.7.3. *Dual-polarization melting layer detection.* Dual-polarization base data variables can also be used to detect the melting layer. The melting layer will be depicted as a ring of noisy differential reflectivity (ZDR) values and low correlation coefficient (CC) values. A weak signature may also be found in the specific differential phase (KDP) product. Aircraft icing is most likely for planes located between the freezing level and the height of the -22°C isotherm. Icing is also possible within the melting layer if freezing rain is occurring. Icing is not expected below the melting layer, where rain is the primary precipitation type.

2.3.8. Determining Icing Potential Using Satellite. Compare visible, near-infrared, and infrared imagery along the guidelines below to find supercooled clouds during daytime hours. Embedded lighter gray shades sometimes occur with heavier icing due to large cloud droplet sizes (higher liquid water content) or slightly thicker clouds.
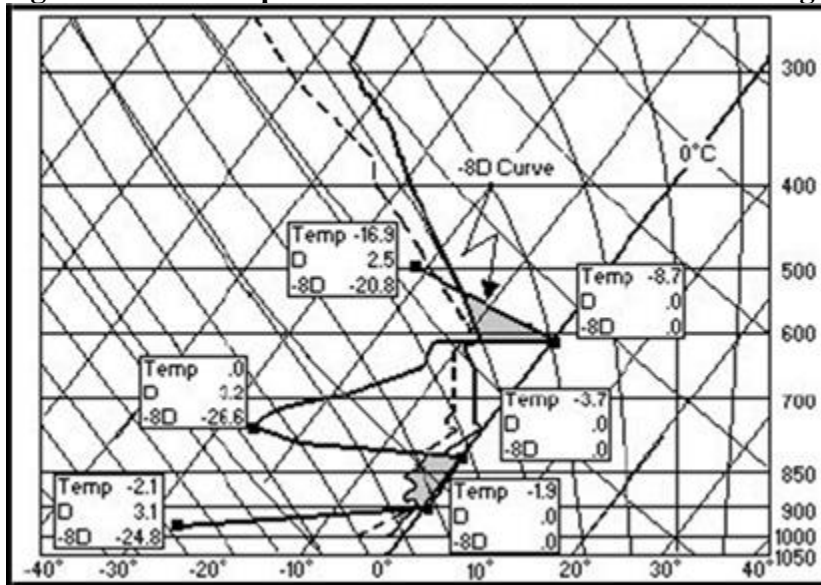
2.3.8.1. *Visible Imagery.* Brighter clouds on visible imagery imply greater thickness and high water content. Visible data can also assist in the identification of embedded convection.

2.3.8.2. *Near-Infrared Imagery.* Small water droplets are more reflective than larger ones, water clouds are more reflective than ice clouds, and warm backgrounds radiate more than cold backgrounds. Therefore, during the daytime, ice clouds (relatively large ice particles, poorly reflective, and cold) will be darker than small droplet water clouds (smaller droplets, higher reflectivity, and warmer). Supercooled clouds, composed of small water droplets, may be very cold (as low as -20°C), but will appear brighter during the daytime due to reflected radiation.

2.3.8.3. *Infrared Imagery.* If cloud-top temperatures are between 0°C and -20°C, and are not covered by higher clouds, icing may be present. However, if cloud tops are close to 0°C, the in-cloud temperature may be above freezing and no icing will occur.

2.3.9. Determining Icing Potential Using a Skew-T Diagram. A common method of icing potential determination on a Skew-T is the "-8D Method" (**Figure 2.37**), which uses the dew point depression multiplied by -8 to identify layers of the atmosphere where icing is likely.

Figure 2.37. Example of the "-8D Method" for determining icing potential.

2.3.9.1. *-8D Method Procedures.*

2.3.9.1.1. From the sounding, find the dew point depression at 0°C; this is "D".

2.3.9.1.2. Multiply D by -8, and plot this number (as a temperature) at the 0°C level on the Skew-T.

2.3.9.1.3. Repeat the two steps above for each temperature level from 0°C to –22°C, to find the -8D value at each temperature level.

2.3.9.1.4. Connect the -8D points with a line to determine the vertical profile; icing layers are likely where the -8D curve is to the right of the temperature curve. In the example in **Figure 2.37**, the likely icing areas are highlighted in gray (900-800 mb and 600-525 mb).

2.3.9.1.5. Use the cloud type, observed precipitation, temperature, and dew point to forecast the type and intensity of icing.

2.3.9.2. *-8D Method Rules of Thumb.*

2.3.9.2.1. When the temperature curve lies to the right of the –8D curve in a subfreezing layer, icing is not likely; the layer is subsaturated.

2.3.9.2.2. When the dew-point depression is 0°C, the –8D curve is on the 0°C isotherm. Light rime icing will likely occur in a region of altostratus or nimbostratus, with moderate rime icing occurring in cumulonimbus, cumulus, and stratus cloud types.

2.3.9.2.3. When the dew-point depression is greater than 0°C and the temperature curve lies to the left of the –8D curve in the subfreezing layer, the layer is supersaturated with respect to ice and probably subsaturated with respect to cloud droplets. If altostratus, altocumulus, or stratocumulus is expected in this layer, light rime icing is likely. If the layer contains cirrus, cirrocumulus, or cirrostratus, light frost is likely to sublimate on aircraft. In cloudless regions, light frost may also form through direct sublimation of water vapor.

2.3.10. Icing Summary. Icing forecasting begins with a solid understanding of the physical processes responsible for icing and a thorough knowledge of the atmospheric conditions over your area of responsibility. If icing is suspected, begin with the general rules in this section (tailored with local rules of thumb and techniques) and analyze the atmosphere for location, type, and severity of icing. When icing is probable, use the techniques and tools provided here to further refine the icing forecast.

2.4. Miscellaneous Weather Elements.

2.4.1. Flight Level Winds. Accurate flight level wind forecasts allow aircrews to plan appropriate fuel requirements, resulting in safer and more efficient missions. The following tools and products can assist in flight level wind forecasting; use them in conjunction with other atmospheric information, if available, and adjust as necessary.

2.4.1.1. *Constant pressure products.* Flight level winds can be estimated from upper-level constant pressure charts; use the product nearest to the desired level and extrapolate as necessary. The relationship between the isotherms and height contours will indicate the wind speed trend; if there's a tightening thermal gradient and CAA (**Figure 2.38**), flight level winds are increasing. In the opposite scenario of a loosening thermal gradient and WAA (**Figure 2.39**), expect decreasing flight level winds. When isotherms and height contours are parallel, wind speeds will remain constant.

Figure 2.38. Increasing flight level winds with CAA.
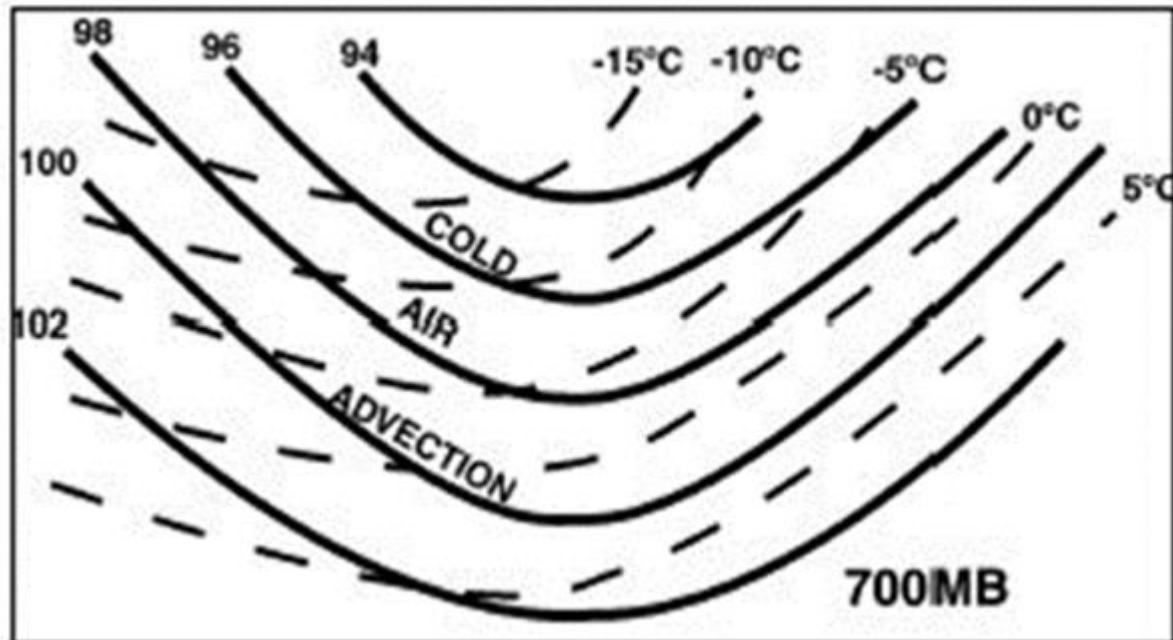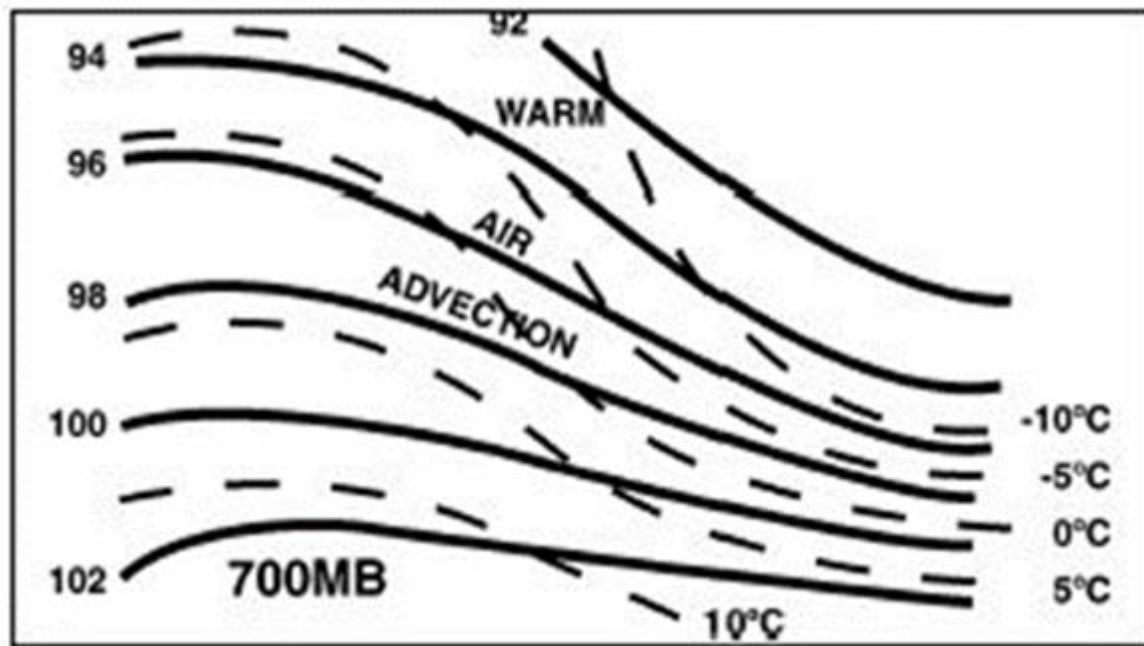
Figure 2.39. Decreasing flight level winds with WAA.

2.4.1.2. *Satellite imagery*. Interpret wind directions and speeds using cloud shape, size, and orientation.

2.4.1.3. *Vertical cross sections*. Cross sections are best used to locate synoptic features such as jet streams, jet cores, and wind patterns; use them to take a quick look at conditions along the flight route. Keep in mind that wind speeds are interpolated between data points or model grid points.

2.4.2. Climb Winds. Forecast climb winds using upper-level wind products or rawinsonde data; see below for specific examples of resources available to forecast climb winds.

2.4.2.1. *Upper air products*. Locate the area of interest, and read the winds directly from the appropriate upper level charts, interpolating winds between the standard levels.

2.4.2.2. *Cross sections*. Cross section plots and associated contours can provide insight into short-term atmospheric changes; use this product to review wind trends at or near your station or to investigate wind behavior during a specific weather event. Extrapolate the information on these plots to produce a short-range wind forecast.

2.4.2.3. *VAD Wind Profile (VWP)*. The VWP on Doppler radar provides a time versus height profile of wind direction and speed above the radar. Several previous profiles (one per volume scan) can be displayed simultaneously. The product is useful for observing local changes in vertical wind shear, including backing of low-level winds and development of nearby jet streams (including the low-level jet). Precipitation creates a high concentration of scatterers; therefore, VWPs usually give good wind estimates when precipitation is occurring. The amount of scatterers available in the radar beam affects the radar's ability to make good wind estimates; scatterers are often scarce in clear, cold air, so the VWP may not be reliable in those conditions. In some cases, the radar may produce no wind information at all.

2.4.2.4. *Radiosondes and Skew-T data.* Locate sounding data nearest to the area of interest and derive climb winds directly from the standard and supplemental levels. These soundings are used to plot the Skew-T, so they give representative winds within about an hour of the time of the sounding run. Remember that sounding data doesn't present an instantaneous profile of the winds directly above the radiosonde site; balloons ascend at a rate of about 1000 feet per minute, and in a one-hour ascent time, the balloon is carried downwind from 20 to 100 NM and to an altitude as high as 60,000 feet by the prevailing upper-level winds.

2.4.3. Temperature. Use centrally-produced forecast products to forecast temperatures aloft. If the temperature is in a layer between standard levels, interpolate between the base and the top of the layer. If you know only one boundary temperature, then extrapolate using an assumed lapse rate of 2°C (5.5°F) per 1,000 feet in the troposphere, and isothermal in the stratosphere.

2.4.4. Thunderstorms. Thunderstorm forecasts for high-level flights are similar to forecasts for low-level operations, with one main caveat; do not underestimate thunderstorm tops. Pilots can usually detect individual thunderstorms at high altitudes better than at low altitudes, but they may not be able to fly over them due to aircraft ceiling limitations. To find thunderstorm tops, begin with satellite imagery to get temperatures and heights of the coldest convective cloud tops. Use the radar to get the heights of thunderstorms in the local area, using Echo Tops and height values from base reflectivity. Check SIGMET bulletins and PIREPS for additional information and airborne observations.

2.4.5. Condensation Trails (Contrails). Contrails are elongated, tubular-shaped clouds composed of water droplets or ice crystals that form behind an aircraft when the wake becomes supersaturated with respect to water or ice. They can present a military concern if an aircraft wishes to avoid detection, as contrails allow for easy spotting and tracking of a vessel in flight. Contrails can also spur development of a cloud deck where none previously existed, creating potential hazards for aerial refueling or other operations that require clear skies with unrestricted visibility.

2.4.5.1. *Engine exhaust contrails.* The most common (and most visible) type of contrails result from engine exhaust; they form when water vapor within exhaust gases mix with and saturate the air in the wake of a jet aircraft. Whether or not the wake reaches saturation depends on the ratio of water vapor to heat in the exhaust gas as well as on the pressure, temperature, and relative humidity of the air in the environment.
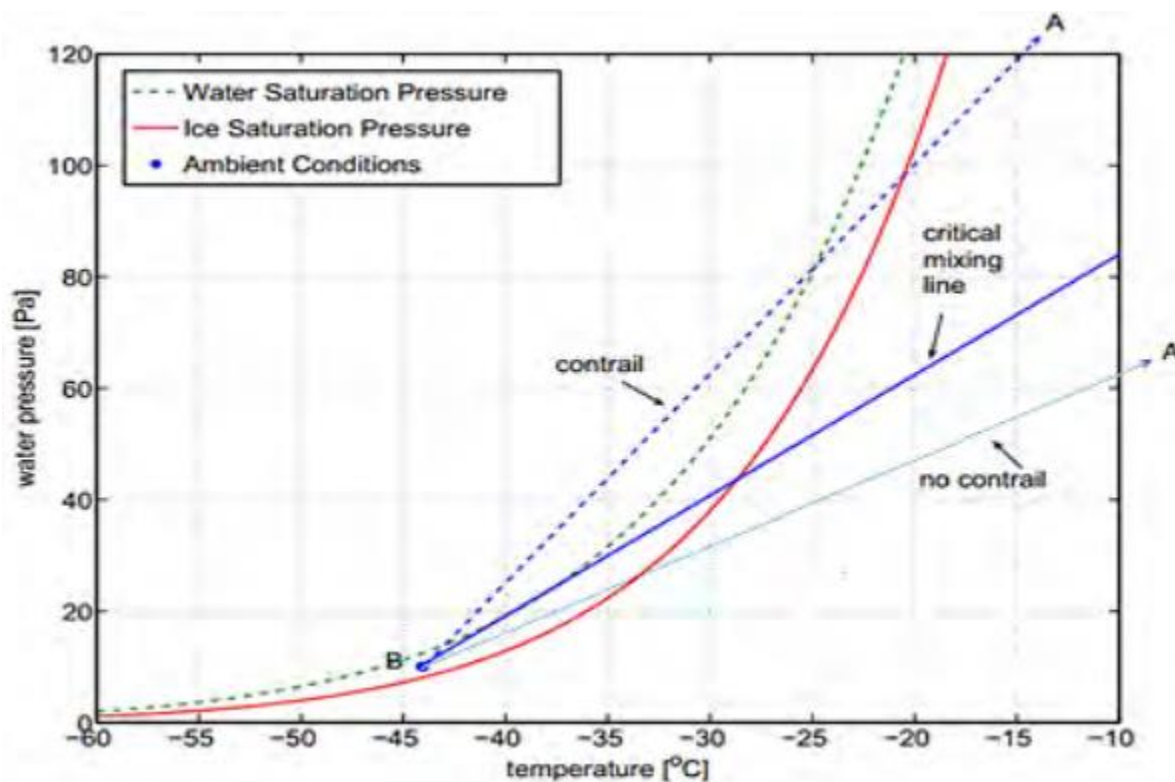
2.4.5.2. *Aerodynamic contrails.* Aerodynamic contrails form from the momentary reduction of air pressure as air flows at high speeds past an airfoil; these contrails usually form at the tips of the wings and propellers. They are relatively rare, and occur only for short periods in a nearly-saturated atmosphere. Aerodynamic contrails occur during extreme flight maneuvers and are virtually impossible to forecast; a small change in altitude or reduction in airspeed is usually enough to stop their formation.

2.4.5.3. *Instability contrails*. Flying through undisturbed, moist, unstable air can initiate instability contrails. Unstable air requires an initial disturbance to begin rising under the power of its own buoyancy. The slight, sudden influx of warm engine exhaust, or the disturbance produced by the airplane itself, sometimes induces unstable air parcels to rise and condense.

2.4.5.4. Contrails are also divided into groups based on their duration. Short-lived contrails appear as a short tail behind an aircraft and last for only a few minutes, indicating that moisture is sufficient, but marginal, for cloud formation. Persistent (non-spreading) contrails appear as long, narrow white lines and remain visible long after the airplane has disappeared. These contrails form when moisture is more abundant. Finally, persistent (spreading) contrails are long, broad, fuzzy lines. These contrails are long-lasting and may spread out until they resemble natural cirrus clouds.

2.4.5.5. Contrail formation. As noted above, most contrails form when an exhaust plume of heated and moistened air, carbon dioxide, and unburned hydrocarbons mixes with the ambient air at high altitudes. The mixture is assumed to possess temperature and moisture values between those of the jet exhaust and ambient air. If this intermediate temperature and moisture combination condenses, a contrail forms; this process is illustrated in **Figure 2.40**. Point A in the figure represents the exhaust plume's characteristics (which will vary in terms of vapor pressure (moisture) and temperature), while point B represents the ambient air characteristics. The Clausius-Clapeyron curves for water and ice are also shown. The blue line between points A and B is the "mixing line," which gives the condition of the mixed air as time passes. If the "mixing line" crosses only the ice saturation curve (as in the case of the pale blue line), it's not enough to create a contrail; the mixing line must cross both the ice and water curves (as in the case of the dark blue dashed line), enabling the formation of water droplets. Thus, the determining factor is essentially the slope of the mixing line. If the slope exceeds that of the "critical mixing line," then contrails will form. For a given vapor pressure in the plume, lower exhaust temperatures are actually more conducive to creating contrails because the slope of the mixing line is greater. Still, in any case, higher moisture content will increase the odds of contrail formation. Contrails forming at the "critical mixing line" will not last as long as those at lines with higher slopes. Contrails forming at higher slopes, with greater supersaturation, will be persistent.

Figure 2.40. Graphical representation of contrail formation.

2.4.5.6. The Appleman contrail forecasting method. The Appleman method derives from a 1953 study of contrail formation, and assumes mixing of hot jet exhaust and ambient environmental air. At a given flight altitude, only the flight altitude temperature and relative humidity are required to make a "yes" or "no" contrail forecast. This method tends to more accurately predict the non-occurrence of contrails than the occurrence of contrails. An Appleman chart is shown in **Figure 2.41**; the following rules apply to its use:
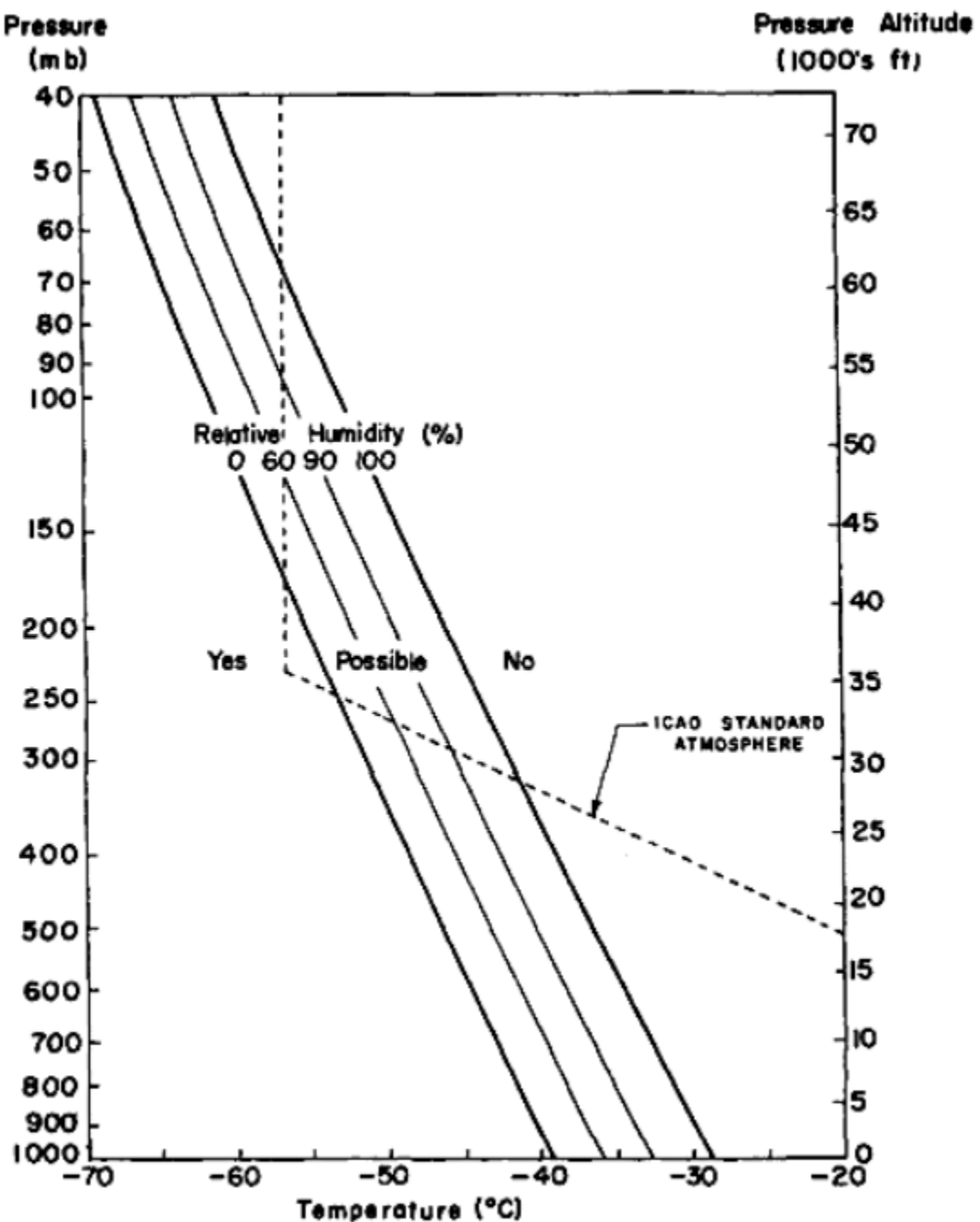
2.4.5.6.1. If the flight altitude temperature is to the right of the 100% curve, forecast no contrails regardless of the relative humidity. Here, contrails should never form, even in saturated air.

2.4.5.6.2. If the flight altitude temperature is to the left of the 0% curve, always forecast contrails, no matter the relative humidity. In this area, contrails should always form, even when the relative humidity is 0 percent.

2.4.5.6.3. If the flight altitude temperature is between the 0% and 100% curves, contrails will form if (and only if) the actual relative humidity is equal to or greater than the value indicated at that point on the graph. This is the uncertain or "possible" area.

2.4.5.6.4. If the humidity along the route is unknown, assume a 40% relative humidity if there are no clouds and a 70% relative humidity if there are clouds.

Figure 2.41. Appleman chart, for contrail forecasting.

2.4.5.7. Engine type. The conditions for contrail formation vary slightly according to engine type. Specifically, contrails may develop at somewhat warmer temperatures behind high-bypass engines than low- and non-bypass engines. The term "bypass" refers to how a turbine engine operates. During normal operation, the intake air is split into two parcels, which move through the engine at different speeds. One parcel is compressed and heated (and slowed in the process), then sent out the exhaust nozzle; this is the portion that turns the fan blades. The other parcel "bypasses" both the compressor and the combustion chamber; this is the portion that increases momentum. A high-bypass engine will have a large fraction of the intake air bypass the compressor and combustion chamber. Conversely, a low-bypass engine will have a small fraction of the intake air bypass the compressor and combustion chamber. Appleman diagrams tailored to non-, low-, and high-bypass engines are provided in **Figure 2.42**, and **Table 2.12** shows the engine type for a variety of military aircraft.

Figure 2.42. Appleman charts for non-bypass, low-bypass, and high-bypass engines.
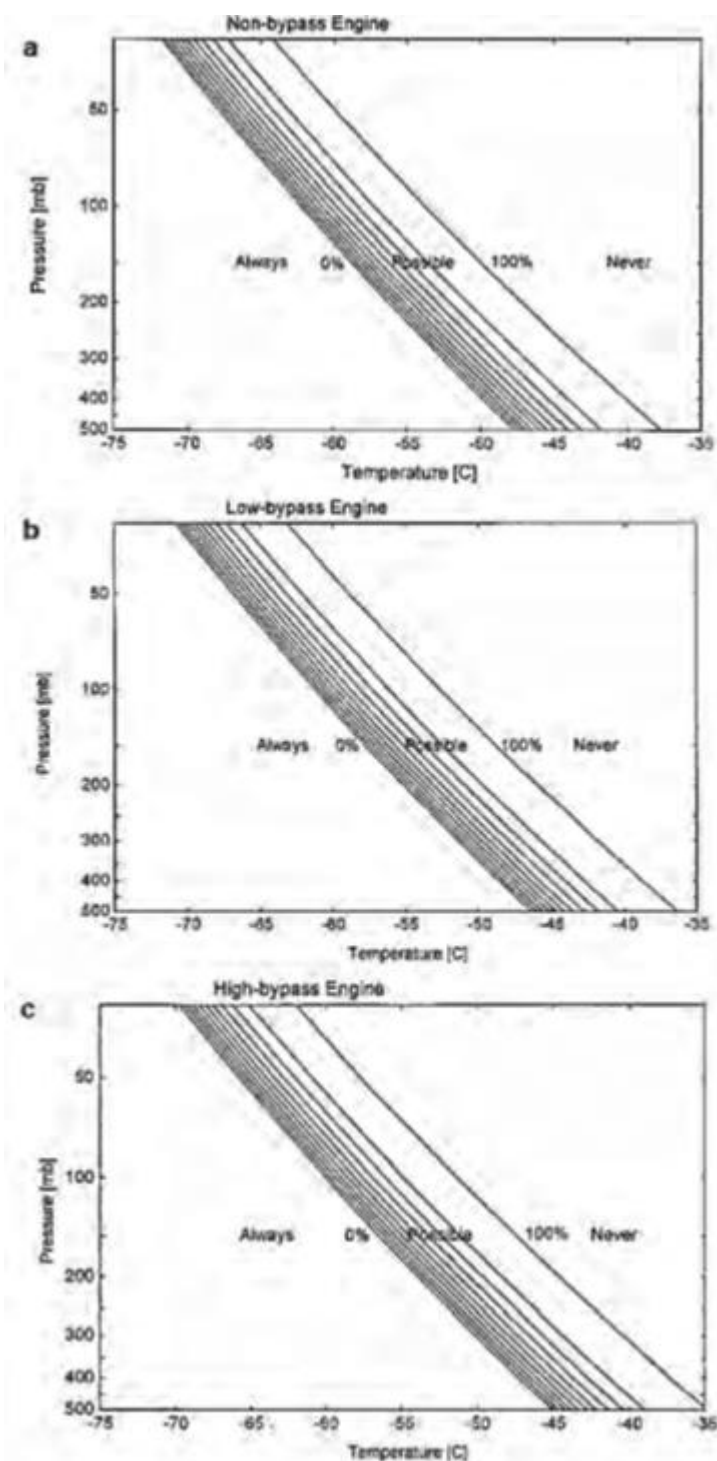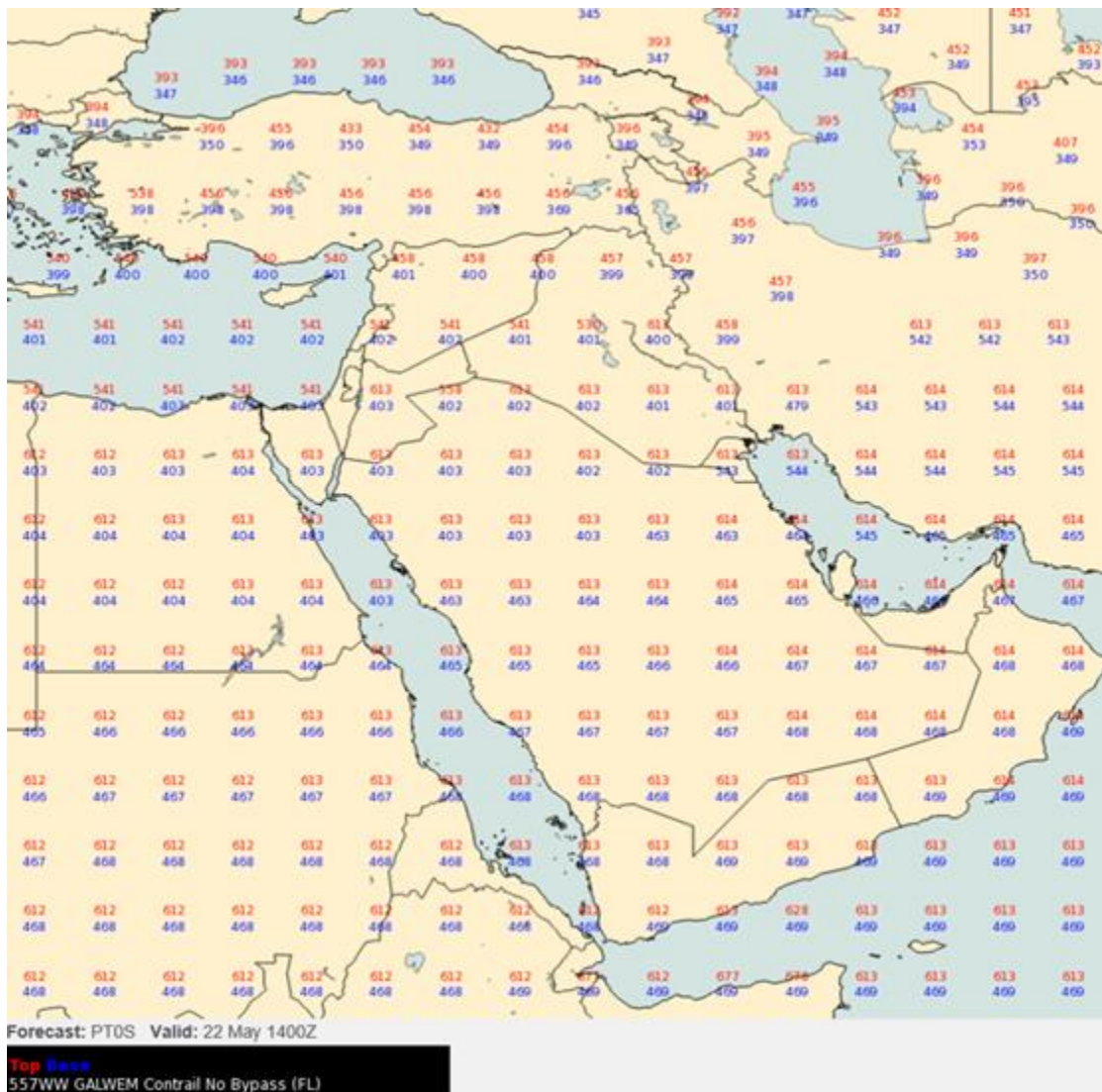
Table 2.13. Engine bypass type for military aircraft.

Aircraft	Engine MFR	Engine	Engine Type
T-38	General Electric	J85-GE-5	Turbojet (no bypass)
U-2	General Electric	F-118-101	Turbojet (no bypass)
KC-135 A	Pratt & Whitney	J57-P-59W	No bypass
B-1B	General Electric	F-101-GE-102	Low-bypass Turbofan
B-52 H	Pratt & Whitney	TF33-P-3/103	Low-bypass Turbofan
C-9 A/C	Pratt & Whitney	JT8D-9	Low-bypass Turbofan
C-141 A/B	Pratt & Whitney	TF33-P-7	Low-bypass Turbofan
F-15 A/B/E	Pratt & Whitney	F-100-PW-220/229	Low-bypass Turbofan
F-15 C/D	Pratt & Whitney	F-100-PW-220/229	Low-bypass Turbofan
C-21 A	Garrett	TFE-731-2-2B	Low-bypass Turbofan
F-16 C/D	Pratt & Whitney	F-100-PW-200/220/229	Low-bypass Turbofan
C-17 A	Pratt & Whitney	F-117-PW-100	Low-bypass Turbofan
F-16 C/D	General Electric	F-110-GE-100/129	Low-bypass Turbofan
KC-135 E	Pratt & Whitney	TF-33-PW-102	Low-bypass Turbofan
B-2	General Electric	F-118-GE-100	Low-bypass Turbofan
F-117 A	General Electric	F-404-F1D1	Low-bypass Turbofan
E-3 A	Pratt & Whitney	TF33-PW-100A	Low-bypass Turbofan
C-5 M	General Electric	CF6-80C2-L1F	High-bypass Turbofan
E-4 B	General Electric	CF-6-50E2	High-bypass Turbofan
KC-10 A	General Electric	CF-6-50C2	High-bypass Turbofan
KC-46	Pratt & Whitney	PW-4062	High-bypass Turbofan
KC-135 R/T	CFM International	CFM-56	High-bypass Turbofan
A-10	General Electric	TF34-GE-100	High-bypass Turbofan
VC-25 A	General Electric	CF6-80C2B1	High-bypass Turbofan

2.4.5.8. *GALWEM contrail forecast products.* The contrail forecast products available on AFW-WEBS are based on the Appleman method; model forecasts are created for high bypass, low bypass engines, and no bypass engines. If contrails are expected, GALWEM charts will show the lower and upper altitudes at each gridpoint, in hundreds of feet, between which contrails are likely to form – the lower level in blue, and the upper level in red (**Figure 2.43**) Remember to select the appropriate forecast product (high, low, or no bypass) for the supported aircraft.

Figure 2.43. GALWEM no bypass forecast product. High bypass and low bypass versions are also available.

2.4.5.9. *Temperature/Pressure method for forecasting contrail probability.* Accuracy of contrail forecasts can be degraded by uncertainty in relative humidity measurements at high altitudes; if the relative humidity values aren't available, use **Table 2.13** for a guide to estimate contrail probabilities based on temperatures at a given pressure level.

Table 2.14. Probabilities of contrail formation based on temperature and pressure level.

Pressure (mb)	Contrail Probability

Pressure (mb)	95%	90%	75%	50%	25%	10%	5%
150	-60.5°C	-59.3°C	-57.1°C	-55.5°C	-53.6°C	-51.5°C	-50.7°C
175	-58.8°C	-57.4°C	-55.3°C	-53.6°C	-51.4°C	-49.6°C	-48.5°C
200	-58.5°C	-56.6°C	-54.8°C	-53.1°C	-51.0°C	-48.5°C	-47.0°C
250	-58.1°C	-56.3°C	-53.8°C	-52.2°C	-50.1°C	-47.1°C	-45.3°C
300	-55.5°C	-54.0°C	-52.0°C	-50.7°C	-49.1°C	-46.3°C	-44.3°C
350	N/A	-49.9°C	-49.4°C	-49.0°C	-48.0°C	-45.9°C	-43.6°C

2.4.6. Forecasting In-Flight Visibility for Air Refueling MEFs. The most critical period of an air refueling mission is just prior to "hookup", when pilots and boom operators need acceptable visual conditions to dock the fueling arm with the aircraft being serviced. Aircrews base their GO/NO GO decisions for air refueling on in-flight visibility of less than one nautical mile. Air refueling operations are usually conducted at altitudes above 23,000 feet, with 29,000 feet considered the optimal flight level. Aircraft involved in air refueling operations will often descend or ascend within the 5,000-foot air-refueling route window to seek better in-flight visibility. In-flight visibility is optimal (7+ nautical miles) when the refueling track is cloud free, but many routes tend to cover several hundred miles, so clouds can be a risk along at least a portion of the track. The following rules of thumb, from multiple legacy sources, can assist with air refueling forecasts.

2.4.6.1. *Air refueling cloud cover.* If cloud decks are greater than 2000 feet thick, in-cloud flight visibility can be estimated by total cloud cover. Clear conditions equate to 7+ nautical mile visibility, while 3/8 or less cloud cover indicates visibility between 3 and 7 nautical miles. 3/8 to 5/8 cloud cover means 1-3 nautical mile visibility conditions, and 6/8 to 8/8 cloud coverage indicates visibility of less than 1 nautical mile.

2.4.6.2. *Temperature and dew point depressions.* Temperatures below -30°C mean in-flight visibility of 1/2 nautical mile for each degree of dew-point depression. Example: A dew-point depression of 4°C (SCT to BKN) would yield an in-flight visibility of 2 nautical miles, and 1°C (OVC) would yield 1/2 nautical mile.

2.4.6.3. *Cirriform cloud thickness.* In thin cirrus clouds, vertical visibility is usually better than horizontal visibility; even if a ground observer can see through a cirrus deck, or a pilot can see the ground through it, the horizontal visibility will most likely be limited. If a cirrus deck is thin-broken to thin-overcast, forecast 1-2 nautical mile in-cloud visibility. If the cirrus deck is thicker (opaque, broken, or overcast), forecast 1/2 nautical mile in-cloud visibility.

2.4.6.4. *Thunderstorm cirrus.* Thunderstorm cirrus are often layered and patchy, and varying in-flight visibility is common. If there is 3/8 or less cloud cover at flight level, forecast greater than 3 nautical miles in-flight visibility. If there is significant cloud cover (5/8 or more) but at least 2,000 feet vertical airspace with 3/8 or less clouds between layers, forecast 1 to 3 nautical miles. If there is significant cloud cover (5/8 or more) and less than 2,000 feet vertical airspace with 3/8 or less clouds between layers, forecast less than 1 nautical mile.

2.4.7. Cirrus Forecasting.

2.4.7.1. In general, cirrus occurrence is often associated with the following phenomena:

  2.4.7.1.1. Confluent airflow.

  2.4.7.1.2. Over a ridge extending upstream toward the trough

  2.4.7.1.3. An area to the south and within 300 miles of the jet stream

  2.4.7.1.4. Convective activity through a deep layer.

  2.4.7.1.5. The area ahead of a surface warm front or occlusion.

  2.4.7.1.6. Anticyclonic curvature of the 1000-500 mb thickness lines.

  2.4.7.1.7. Positive vorticity advection.

  2.4.7.1.8. Dew point depressions of 10°C or less at 400, 450 and 500 mb.

  2.4.7.1.9. Closed jet isotachs of over 100 knots.

2.4.7.2. Most cirrus layers are thin and less than 1000 feet thick. For opaque cirrus, when the tropopause is low (around 35,000 feet), the average thickness is about 4000 feet. When the tropopause is high (around 45,000 feet), the average thickness is about 8000 feet.

2.4.7.3. Cirrus bases tend to lower, and vertical thickness tends to increase, with increasing degrees of cloudiness. The average thickness of scattered cirrus over the mid-latitudes is about 3700 feet with bases around 32,000 feet. The cirrus increased to 6900 feet thick with bases lowering to 27,000 feet with overcast cirrus.

2.4.7.4. Most cirrus tops are less than 2000 feet below the tropopause when it's near 35,000 feet. If the tropopause is near 45,000 feet, cirrus tops will normally be about 5000 feet below.

2.4.7.5. There is more cirrus in summer than in winter due mainly to thunderstorm activity, which supplies additional upper-level moisture for cirrus formation.

2.4.7.6. There is no significant diurnal variation in cirrus, although surface observations tend to show more cirrus in the daytime. Observing nighttime cirrus is difficult; the hours around sunrise and sunset show the largest amounts of cirrus being reported. Thunderstorm cirrus shows a marked increase over land during afternoon hours, while it increases over water during the overnight hours.

2.4.7.7. Thin overcast cirrus usually occurs in a layer 4000 to 6000 feet thick. There is usually enough visibility through the layer to allow visual air refueling hookup.

2.4.7.8. Contrail-produced cirrus can present risks to military operations; morning air refueling routes that are relatively cloud-free may produce contrail cirrus that may render a track unusable in the afternoon. Determine the probability of contrails at AR altitudes and forecast accordingly. Visible satellite data can indicate increasing cirrus from contrails.

2.4.7.9. Cirrus tops associated with the polar jet stream generally occur within 1000 feet of the maximum wind (either above or below). In a well-developed pattern, the tops of cirrus often slope upward from the polar to the subtropical jet stream (especially in the area east of the upper trough and up to the ridgeline).

2.4.7.10. Cirrus tops generally occur below the height of the maximum wind in the subtropical jet stream, at an average distance of 4000 feet below. Thin cirrus can attain greater heights, extending up to the altitude of the jet core.

2.4.7.11. Established cirrus decks usually lower 650 feet per 12 hours.

2.4.7.12. Cirrus bases occur near areas of strong vertical shear of the horizontal wind, and tend to be more opaque in areas of strongest shear or maximum wind speed.

2.4.7.13. Advective cirrus is most frequently observed during daytime hours; bases usually form between 33,000 and 39,000 feet, while tops are usually found between 37,000 and 43,000 feet.

2.4.7.14. Thunderstorm cirrus usually dissipates within six hours of the dissipation of the lower part of the initial cloud system, but the cirrus frequently recurs downstream early the next day.

2.4.8. Ditch Headings and Wave Heights. Aircrews require ditch heading and wave height information for operations conducted over water; winds and waves pose a significant hazard to pilots facing the possibility of ditching in the ocean or in a large lake. High winds and the associated high waves are the most significant concern. If surface winds are relatively light (typically 15 knots or less), aircrews plan their approach parallel to any swells. With winds greater than 15 knots, pilots will attempt to descend into the wind and then land as parallel as possible to the main swells. Buoy observations can be used to determine current wind speed and direction, and ship observations contain wind direction and wind speed as well as wave height information. The Navy also provides a suite of oceanographic forecast products, accessible at **https://www.metoc.navy.mil/fnmoc/oceanography.html**.

2.4.9. Sea Surface Temperatures. Sea surface temperatures are an additional concern for over-water operations; the water temperature affects an aircrew's survival ability if forced to bail out or ditch. The colder the water temperature, the more protective equipment required; the heavier cold-weather survival suits can reduce crew agility due to the bulkiness of the suit, as well as increase discomfort on long flights, so it's critical for the crew to only utilize these measures when necessary. Buoy observations can be used to determine current sea surface temperatures, and the Navy's model forecasts are accessible from the link above.
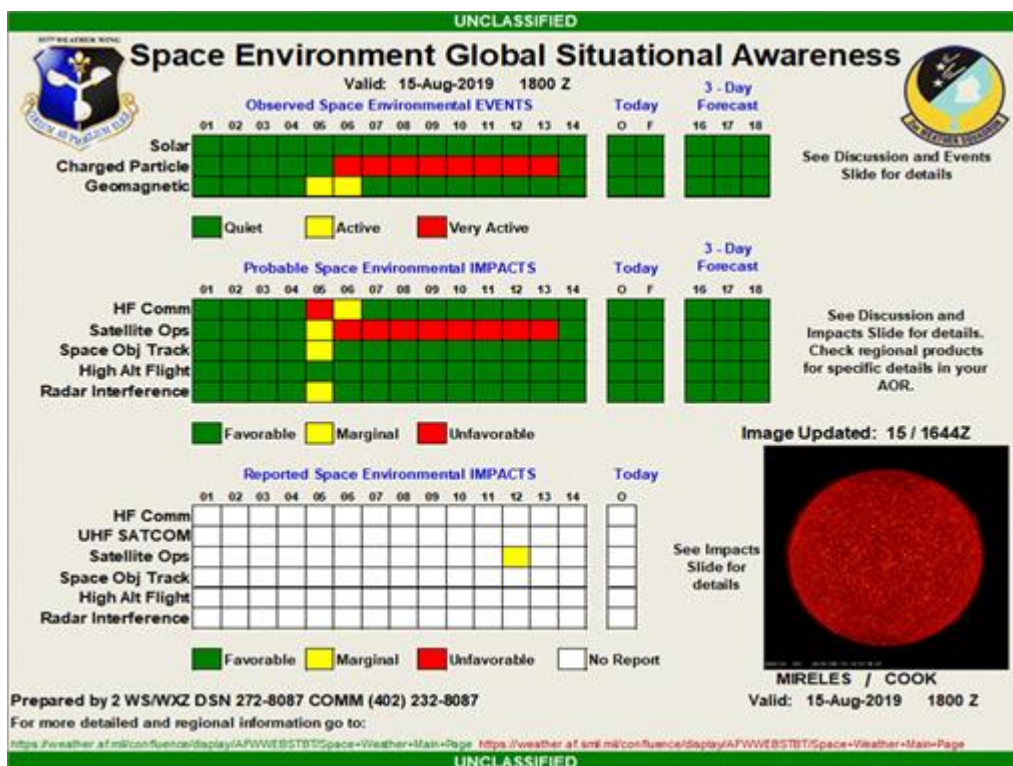
2.4.10. Space Weather and the Space Environment. Space weather results from solar activity interacting with the near-earth space environment, which produces effects that can impact military operations. The sun continuously emits electrically charged particles and electromagnetic radiation; these particles and radiation interact with the Earth's magnetic field and atmosphere in a variety of ways. The sun emits radiation over the entire electromagnetic spectrum; the most intense emissions occur in the visible part of the spectrum, with significant emissions also occurring in the near-ultraviolet and infrared portions. Particles emitted from the sun (primarily protons, but occasionally cosmic rays) can reach the Earth in as little as 15 minutes to as much as a few hours after the occurrence of a strong solar flare. The major impact of these protons is felt over the polar caps, where the particles are able to penetrate to low altitudes through funnel-like cusps in the Earth's magnetosphere. The impact of a proton event can last for a few hours to several days after a flare ends. The sources of solar charged particles include solar flares, disappearing filaments, eruptive prominences, and solar sector boundaries (SSBs) or high-speed streams (HSSs) in the solar wind. Except for the most energetic particle

events, these charged particles tend to be guided by the interplanetary magnetic field (IMF) that lies between the sun and the Earth's magnetosphere. The intensity of a particle-induced event generally depends on the size of the solar flare, filament, or prominence, its position on the sun, and the structure of the intervening IMF.

2.4.10.1. *Space weather impacts to operations.* Space weather events can impact military operations in many ways; effects are typically felt in the realms of communication and navigation (high frequency comm, GPS, and satellite communications), radar operations, satellite operations (command and control, low-earth orbit object tracking, and spacecraft health and behavior), and aircrew radiation exposure. The forecast products summarized below provide forecasts of space weather phenomena, as well as a guide for the expected operational impacts from those phenomena.

2.4.10.1.1. The Space Environment Global Situational Awareness "Stoplight Chart". Available on AFW-WEBS, and updated every six hours, the space stoplight chart is a useful quick-look guide indicating space weather events and their impact on operations (**Figure 2.44**) The stoplight chart is accompanied by three other products giving greater detail on the current space environmental situation; a discussion slide provides a narrative summary of the events and impacts shown on the Space Environment slide, an events slide describes significant events for the past 7 days that directly drive changes in the Space Environment slide, and an impacts slide lists reported impacts on DoD operations for the past 7 days. The observed environmental events and probable operational impacts listed on the stoplight chart consist of the following topics:

Figure 2.44. Space weather stoplight chart.

2.4.10.1.1.1. Solar activity. The first row on the top of the Events section shows the overall activity level of the sun, based on the occurrence of moderate or greater X-ray flares and significant solar radio bursts.

2.4.10.1.1.2. Charged particle environment. The second Events category shows the observed and forecast potential for charged particles significantly above normal background levels; these occur due to solar events or enhanced geomagnetic activity.

2.4.10.1.1.3. Geomagnetic activity. The third row of the Events section shows the overall geomagnetic activity level of the Earth's magnetic field. Increases in geomagnetic activity are caused by streams of solar particles interacting with the planet's magnetic field; these particles originate from solar flares, coronal mass ejections, disappearing filaments, and coronal holes.

2.4.10.1.1.4. HF Communications. Shown on the first line of the Impacts section, HF communications can be degraded due to changes in the ionosphere. Moderate-to-strong solar flares emit x-rays, which enhance lower levels of the ionosphere and absorb HF signals. Strong solar flares may disrupt the entire HF spectrum, if sufficiently energetic. Strong geomagnetic activity can also result in degraded HF comm by decreasing the ionosphere's ability to reflect HF signals. Strong geomagnetic activity also leads to enhanced aurora in the northern and southern high latitudes which can significantly degrade HF communications.

2.4.10.1.1.5. Satellite operations. The second Impacts line shows the observed and forecast potential for degradation or damage to satellites on orbit; these impacts usually result from particle interactions with the spacecraft. Particles can deposit electrical charge on or within satellite bodies, causing damage via a discharge, or can damage the satellite through collision or by overwhelming or disorienting the satellite's sensors. These impacts are determined by observing or forecasting the number and energy of particles in the space environment (e.g. increased by flares or coronal mass ejections), geomagnetic activity which can enhance and accelerate particles in the space environment, and corroborating space environmental conditions with observed satellite anomalies.
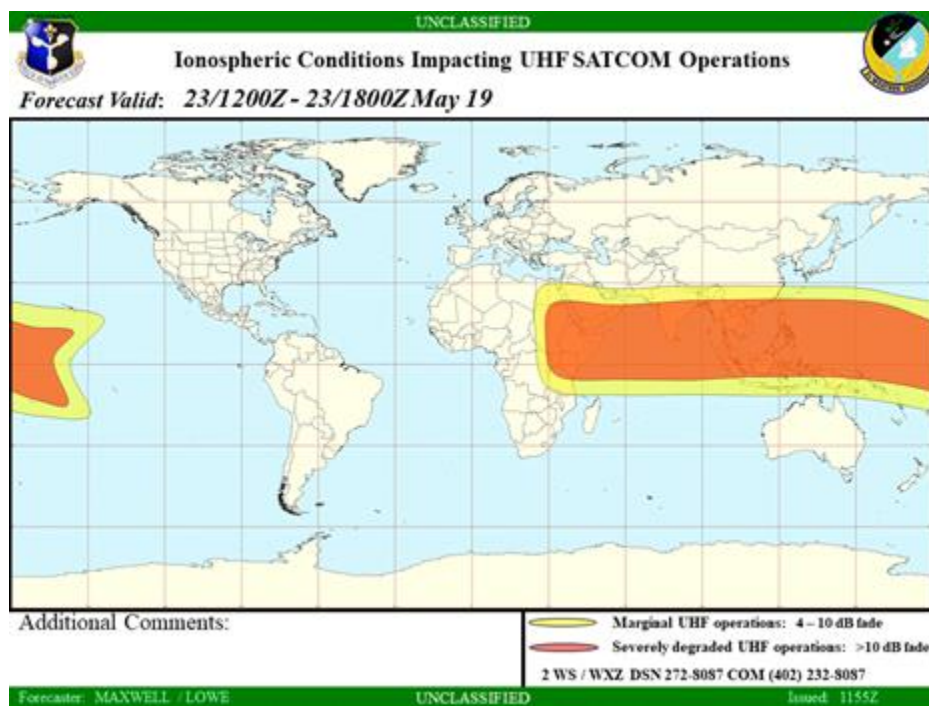
2.4.10.1.1.6. Space object tracking. The third Impacts category examines the observed and forecast potential for unexpected changes in satellite orbits; these changes result from an increase or decrease in the drag normally experienced by an object orbiting the Earth. Changes in drag may result from geomagnetic activity, as well as the heating or cooling of the upper atmosphere due to changes in the sun's radiation output (energy from x-rays and other charged particles can heat and expand the upper atmosphere).

2.4.10.1.1.7. High altitude flight. The high altitude flight Impact line considers the effects of cosmic rays and high-energy protons on aircrews operating at extremely high altitudes, such as the U-2, where atmospheric protection is at a minimum. The observations and forecasts for this criteria consider the maximum level of radiation exposure at an altitude of 67,000 ft; the parameter is YELLOW for dose rates greater than 10 millirems/hr and RED for dose rates exceeding 100 millirems/hr.

2.4.10.1.1.8. Radar interference. The final Impacts category shows observed and forecast degradations to operations for space tracking radars. Radio frequency bursts from the sun can cause interference to radars when the sun is in their field of view. Additionally, anomalous returns can occur when geomagnetic activity disturbs the ionosphere.

2.4.10.1.2. Ionospheric UHF SATCOM impacts map (**Figure 2.45**) This product is a global, graphical bulletin issued four times per day, valid for the following six hours. It shows forecast regions of expected marginal (4-10 db fade) and severe (greater than 10 db fade) UHF propagation degradation. Potential impact areas represent the worst-case scenario for long-haul UHF communications attempted in the affected region.

Figure 2.45. UHF SATCOM impacts chart.
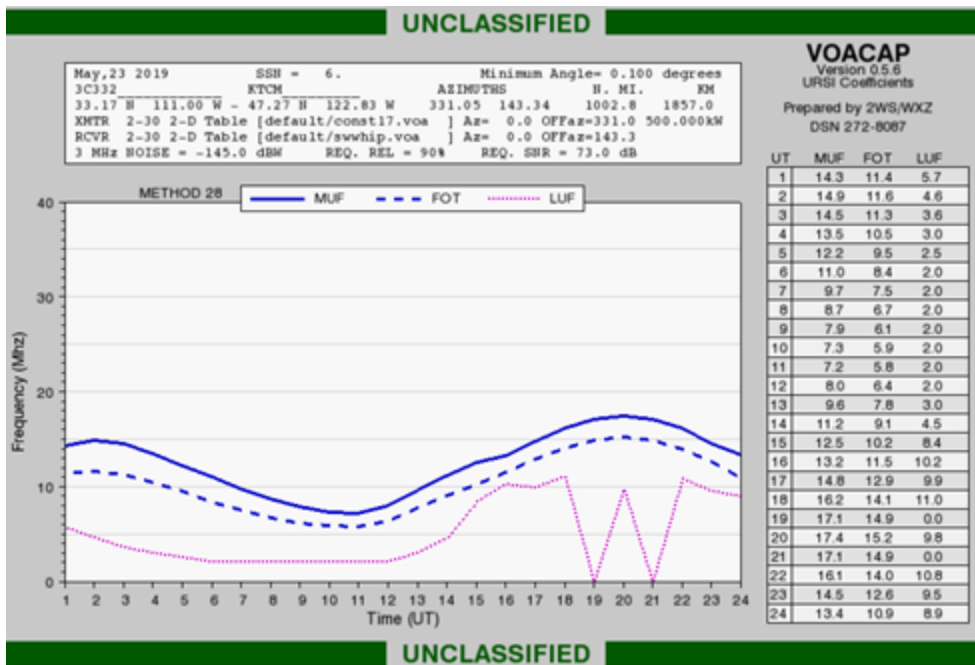
2.4.10.1.3. Ionospheric HF propagation impacts map. Similar to the UHF SATCOM impacts map, the HF propagation impacts map is a global, graphical bulletin issued four times a day, valid for the following six hours, showing areas of expected marginal and severe degradations to HF communications. Impact areas represent the worst-case scenario for operations in the affected region.

2.4.10.1.4. Point-to-point HF radio usable frequency forecast (**Figure 2.46**) These forecasts provide predictions of HF radio propagation conditions, including Maximum Usable Frequency, Frequency of Optimum Transmission, and Lowest Usable Frequency. This product can be tailored for specific equipment and signal path, allowing for a precise, user-specific look at HF comm conditions.

2.4.10.1.5. Other graphical products. There are several other space weather impacts products available on AFW-WEBS, such as GPS error maps, SATCOM scintillation forecasts, and HF illumination maps – use as required to support your customer's space weather needs.

Figure 2.46. Point-to-point HF radio usable frequency forecast chart.

UNCLASSIFIED

VOACAP
Version 0.5.6
URSI Coefficients

Prepared by 2WS/WXZ
DSN 272-8087

May,23 2019   SSN =   6.   Minimum Angle= 0.100 degrees
3C332   KTCM   AZIMUTHS   N. MI.   KM
33.17 N 111.00 W - 47.27 N 122.83 W   331.05 143.34   1002.8   1857.0
XMTR 2-30 2-D Table [default/const17.voa] Az= 0.0 OFFaz=331.0 500.000kW
RCVR 2-30 2-D Table [default/swwhip.voa] Az= 0.0 OFFaz=143.3
3 MHz NOISE = -145.0 dBW   REQ. REL = 90%   REQ. SNR = 73.0 dB

METHOD 28   —— MUF   - - - FOT   ·········· LUF

UT	MUF	FOT	LUF
1	14.3	11.4	5.7
2	14.9	11.6	4.6
3	14.5	11.3	3.6
4	13.5	10.5	3.0
5	12.2	9.5	2.5
6	11.0	8.4	2.0
7	9.7	7.5	2.0
8	8.7	6.7	2.0
9	7.9	6.1	2.0
10	7.3	5.9	2.0
11	7.2	5.8	2.0
12	8.0	6.4	2.0
13	9.6	7.8	3.0
14	11.2	9.1	4.5
15	12.5	10.2	8.4
16	13.2	11.5	10.2
17	14.8	12.9	9.9
18	16.2	14.1	11.0
19	17.1	14.9	0.0
20	17.4	15.2	9.8
21	17.1	14.9	0.0
22	16.1	14.0	10.8
23	14.5	12.6	9.5
24	13.4	10.9	8.9

Frequency (Mhz) — Time (UT)

UNCLASSIFIED

2.4.10.1.6. Space Weather Bulletins. The 2nd Weather Squadron produces a wide range of warning and routine space weather bulletins; they can be found on AFW-WEBS or subscribed to on an as-needed basis. These bulletins provide summary information on significant space weather events; the warning bulletins are issued as needed when significant events occur, while the routine bulletins are issued on a regularly scheduled basis. Warning bulletins are issued for geomagnetic events, x-ray events, short-wave fade events, satellite charging and radiation dosage events, solar flares, and energetic particle events. Details on several of the more complex warning bulletins are provided below.

2.4.10.1.6.1. Major solar flare event warning (WOXX51 KGWC). These bulletins are issued when a strong solar flare is observed; these events result in enhanced x-ray and radio frequency emissions. If enhanced x-ray emissions are expected, high frequency systems may experience short-wave fades up to 30 MHz persisting for several hours, while low and very low-frequency systems may experience sudden phase advances during the event. For enhanced radio frequency emissions, high frequency systems will likely experience radio frequency interference during the event, especially those that are oriented towards the sun.

2.4.10.1.6.2. Geomagnetic event warning (WOXX54 KGWC). This bulletin is issued with a forecast or observed geomagnetic disturbance; potential operational impacts are widespread.

2.4.10.1.6.2.1. HF systems operating in middle and auroral zones will experience Maximum Usable Frequency depressions during the disturbance. Long east-west paths (over 3000 km) extending poleward of 55° latitude may experience non-great circle propagation, multipathing, and auroral zone absorption.

2.4.10.1.6.2.2. Poleward-pointing HF/VHF/UHF radars equatorward of the auroral zone may observe enhanced clutter, interference, and false targeting.

2.4.10.1.6.2.3. VHF and UHF space track radars operating through the auroral zone may experience unusual signal degradation and refraction, causing ranging and pointing errors.

2.4.10.1.6.2.4. VHF, UHF and SHF satellite communication systems operating through the auroral zone may experience enhanced phase/amplitude scintillation.

2.4.10.1.6.2.5. LF and VLF systems operating across the auroral and polar regions may experience phase advances during the event.

2.4.10.1.6.2.6. Geosynchronous and other high altitude satellites may experience spacecraft charging, especially when in the midnight to sunrise sector. Subsequent discharges may cause electrical upsets. Similar charging problems may occur on low altitude satellites with inclinations transiting auroral latitudes.

2.4.10.1.6.2.7. Low altitude polar orbiting satellites may experience increased atmospheric drag due to enhanced atmospheric density. This effect will begin approximately 6 hours after the storm starts, and last until approximately 12 hours after the storm ends.

2.4.10.1.6.3. Energetic particle event warning (WOXX53 KGWC). These bulletins notify users of forecast or observed enhancements of energetic particles in the near-earth environment. Potential operational impacts associated with these events are:

2.4.10.1.6.3.1. Satellite-borne sensors may be contaminated, damaged or destroyed by direct collision with high-energy particles.

2.4.10.1.6.3.2. Geosynchronous and other high altitude satellites (or satellites in lower orbits, but with paths through the auroral zones) may experience problems associated with internal charging and discharging associated with the energetic particle environment, as well as single event upsets (SEU) associated with the cosmic ray environment.

2.4.10.1.6.3.3. High altitude aircraft traversing polar latitudes may be exposed to enhanced radiation levels.

2.4.10.1.6.3.4. High latitude HF communication (generally poleward of 55° latitude) will experience degraded operations or a complete blackout due to the increased ionization from the charged particles entering the auroral zone (a polar cap absorption event.)
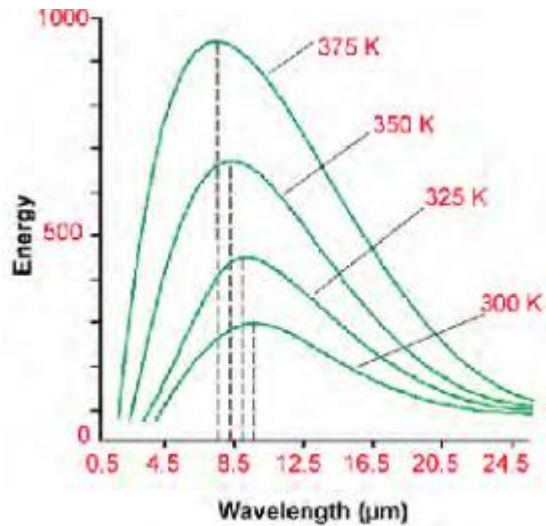
2.4.10.1.6.3.5. Spacecraft personnel, especially those engaged in extra-vehicular activity (EVA) in polar orbit, may be exposed to enhanced radiation levels.

2.4.11. Electro-Optics. Electro-optical (EO) systems, such as precision guided munitions and target acquisition systems, detect electromagnetic (EM) energy or electromagnetic radiation (EMR). EMR may be thought of as coupled electric and magnetic waves, both propagating in the same direction and oriented at right angles to each other. A wave is characterized by its wavelength (λ) and where this wavelength falls in the electromagnetic spectrum. Wavelengths are measured in micrometers (μm); one μm is one-millionth of a meter. The wavelengths of visible light range from 0.4 μm (violet) to 0.74 μm (red). Wavelengths shorter than those of violet include ultraviolet, X-ray, and gamma ray. EO systems do not use any wavelengths shorter than visible, but they do take advantage of longer wavelengths. These may include infrared (IR) wavelengths from 0.75 to 1000 μm (1 mm) and microwaves from 1 mm to 1 m. All EMR moves at the same constant speed, the speed of light (c). If EMR of all different wavelengths moves at the same speed, then the frequency (n) of these waves must be inversely proportional to the wavelength ($n = c/\lambda$). EMR with a long wavelength has a low frequency and vice versa. For example, ultraviolet radiation (short wave) has a higher frequency than infrared (long wave) radiation. Generally, visible, IR, and ultraviolet radiation are characterized by their wavelengths, while radar and radio waves may be discussed either in terms of frequency or wavelength.

2.4.11.1. Black body radiation. Any object that has a temperature above absolute zero (0 K or -273°C) emits or radiates EMR. Electro-optical systems use this emitted energy to form an image. Infrared systems use the emitted energies of the targets and backgrounds themselves. Visual systems use radiation emitted from another source, usually the sun, which is reflected off the target and background. There are three laws or principles that describe the emission of EM radiation by an object: 1) Planck's law, 2) The Stefan-Boltzmann law, and 3) Wien's law. These laws describe the properties of black body, a theoretical object that absorbs all the energy that falls upon it, regardless of its angle of incidence or wavelength. No perfect black body exists, but it serves as a useful approximation. A black body has a constant temperature, so it must be in thermal equilibrium with its environment. This requires a black body to emit as much energy as it absorbs, otherwise its temperature would change. EO sensors detect the emitted energy. The amount of energy emitted at each wavelength depends only on the temperature and not on the wavelengths of absorbed energy.

2.4.11.1.1. Planck's Law. Planck's law describes the amount of energy emitted by a blackbody at a specific temperature for each wavelength of the EM spectrum. When energy versus wavelength is plotted on a graph, a characteristic Planck curve, or energy spectrum, is developed for each temperature. **Figure 2.47** shows the Planck curves for several black bodies at different temperatures. With increasing temperature, the energy increases and the peak shifts left to a shorter wavelength. There is always a certain amount of energy given off at every wavelength for each object, though it may be infinitesimally small at some wavelengths.

Figure 2.47. Planck curves for black bodies at a range of temperatures.

2.4.11.1.2. Stefan-Boltzmann Law. The Stefan-Boltzmann law relates the total amount of energy emitted at all wavelengths of the EM spectrum to the temperature of the blackbody. This is equal to the area under each curve, which is greater for hotter objects. It is expressed mathematically by: $E = \sigma T^4$ where E is the power per unit area leaving the object (also known as the exitance), with units of Watts per square meter; σ is 5.67 X 10-8 (the Stefan-Boltzmann constant); and T is the absolute temperature of the object, in Kelvins. The key result of the Stefan-Boltzmann law is that small differences in temperature result in large differences in the amount of emitted energy. For example, as **Table 2.14** shows, a temperature rise from 300 to 350 K nearly doubles the emitted energy. This is due to the fourth-power relationship between temperature and radiated energy.

Table 2.15. Comparison of temperature of an object and its emitted energy.

Stefan-Boltzmann Law	
Temperature (K)	**Emitted Energy (Watts/m2)**
300	459
325	633
350	851
375	1121

2.4.11.1.3. Wien's Law. As described above, the Planck curve has a distinct single peak; Wien's law relates the wavelength of this peak to the temperature of the object by the following equation: $\lambda_{max} = 2898 / T_{Kelvin}$ where λ_{max} is the wavelength of maximum emitted energy in microns. The wavelength of the peak decreases as temperature increases. Climatological temperatures and the temperatures of man-made objects range from approximately 250 to 350 K. These correspond (roughly) to energy peaks ranging from 12 to 8 μm, respectively, which fall in the far infrared portion of the spectrum. Electro-optical sensors are designed to detect energy around the peaks of Planck curves for two reasons. First, the maximum energy for activation of the sensor is the peak energy. The second reason is a bit subtler. If two objects have slightly

different temperatures and their peaks are in the same region of the spectrum, then the maximum contrast between the objects is found near the peaks rather than out on the "wings" of the curve. If the sensor is designed to form an image of the target scene, then it should be tuned to wavelengths close to the peaks of most objects. For example, visible systems use primarily reflected sunlight. The sun's temperature is approximately 6,000 K, so λmax is approximately 0.5 μm. This is in the green portion of the visible spectrum. Visible systems are generally used in the daytime, but night vision goggles and low-light level TV sensors use sunlight reflected off the moon or scattered by the nighttime sky.
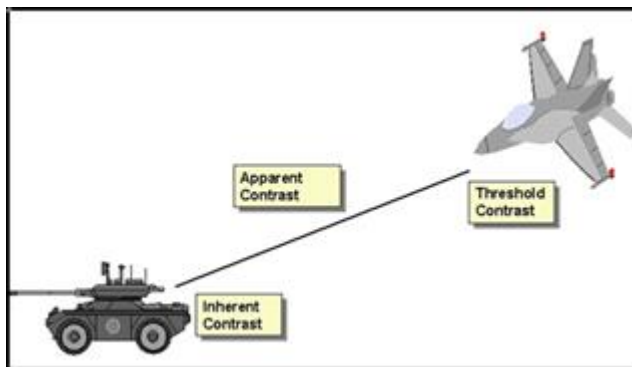
2.4.11.2. Contrast. In order to see an image other than a black screen, there needs to be some sort of contrast. For visual wavelengths, contrast is a difference in color and/or brightness. For IR wavelengths, it is a difference in temperature. There are three types of contrast (**Figure 2.48**):

2.4.11.2.1. Inherent contrast. The actual contrast between two objects based solely on their physical properties (i.e., color, illumination, and emitted IR radiation); this is the "true" difference between the target's EM emissions and the emissions of its background. The greater the inherent contrast, the easier it will be to detect and identify the target. For example, a hot tank against a cold, snow-covered background will have a strong inherent contrast, while the same tank on a concrete highway during a summer afternoon will have a weak inherent contrast.

2.4.11.2.2. Apparent contrast. The contrast a person or an EO sensor detects at a given distance from the target scene; this is the difference between EM energy received from the target and the EM energy received from the target's surrounding background at long distances. Because of the distance and effects of atmospheric scattering and absorption, there is very little difference between EM energy received from the target and background. At long distances, the target won't be detectable against its background.

2.4.11.2.3. Threshold contrast. The smallest contrast that can be detected by a sensor or by the human eye. For an EO sensor, threshold contrast depends on the sensor design. For the human eye, threshold contrast is the contrast where 50 percent of observers can detect a target against its background. In simplest terms, this is the point where a target becomes detectable by an EO system.

Figure 2.48. Inherent, apparent, and threshold contrast.

2.4.11.2.4. Visual contrast. For visual systems, contrast is defined as the difference in reflectance or albedo between target and background; reflectance is the ratio of the amount of energy at a specific wavelength reflected by an object to the amount incident upon it, and albedo is the ratio of the amount of energy over a band of wavelengths reflected by an object to the amount that is incident upon it. There are two ways to define inherent visual contrast; the first is: **Contrast = (Target reflectance – Background reflectance) / (Greater of the two reflectances).** In this definition, contrast for a black (R = 0) target on a white (R = 1) background is equal to -1. For a white target on a black background, contrast is equal to +1. The absolute value of the contrast for either situation is 1; the sign just tells if the target is black and the background is white, or vice versa. When contrast is defined this way, it doesn't matter whether the reflected light comes from the target or the background; this method works well when the target and background are about the same size. If the target is much smaller than the background, however, a better way of defining contrast is: **Contrast = (Target reflectance – Background reflectance) / (Background reflectance).** When contrast is defined this way, values range from -1 (black target on white background) to +∞ (white target on a black background). Nothing is perfectly black or perfectly white, so contrast can never be +∞, but this formula suggests that white targets on black backgrounds should be easier to see. This formula takes into account the difference between light coming from the target and light coming from the background. It may be more useful to consider the signal-to-noise ratio of the target scene rather than merely the contrast. Light coming from the target provides useful information (signal) while light coming from the background provides useless information (noise). If all of the light coming from the target scene comes from the background, it gives no information about the target; it's all noise (but not as much noise as would come from a pure white background). But if all the light comes from the target (signal), then any energy detected by the sensor is from the target. It is therefore much easier to find a white target on a black background (high signal-to-noise) than a black target on a white background (low signal-to-noise).

2.4.11.2.5. Infrared contrast. Infrared contrast is defined simply as a radiometric temperature difference between target and background: **Contrast = Target radiative temperature – Background radiative temperature.** In this expression, contrast is calculated by using the radiative (or radiometric) temperature, rather than the physical temperature, of the object. The radiative temperature represents the energy lost by radiation, and is the temperature an object would appear to have if it were a true black body. The radiative temperature of an object depends on a property of its material called emissivity (ε). Since, by definition, a blackbody emits all of the energy it receives, there are no true blackbodies; most objects are considered "gray bodies". All energy received by an object is absorbed, reflected, or transmitted; gray bodies only absorb a percentage of all incident energy. For example, brick and concrete emit over 90% of the energy they receive. On the other hand, a polished steel object may emit less than 10% of the energy it receives. A blackbody has an emissivity of 1.0, but a gray body's emissivity is less than 1.0. To understand the difference between physical and radiative temperature, consider the examples in **Table 2.15**; objects A and B are both black bodies, so each object's physical temperature is also its radiative temperature. Objects A and C have the same physical temperature, but the radiative temperatures of B and

C are the same because B is a blackbody and C is a gray body. Object A is a blackbody ($\varepsilon = 1$) with a temperature of 300 K. From a distance, it appears to have a temperature of 300 K (its radiative temperature). Object B is a blackbody ($\varepsilon = 1$) with a temperature of 280 K. Likewise, it has a radiative temperature of 280 K. Now consider object C; its physical temperature is 300 K, but it is a gray body with an emissivity of only 0.67. Because it's not efficient at emitting energy, the object only emits the energy of a 280 K black body -- it has a radiative temperature of 280 K even though its physical temperature is 300 K! The conclusion here is that the radiative temperature of an object is always less than or equal to its actual temperature; emissivities of most materials are close to 1, but materials such as polished metals, sand, and calm water may have low emissivities and appear colder than they actually are.

Table 2.16. Three hypothetical objects, showing the relationship between emissivity and physical/radiative temperatures.

Object	Physical Temp	Emissivity	Radiative Temp
A	300 K	1	300 K
B	280 K	1	280 K
C	300 K	0.67	280 K

2.4.11.2.5.1. Reflectivity of IR. There is another reason materials with low emissivities may appear cold; all energy incident upon an object must either be absorbed, pass through the object (transmitted), or be reflected by the object. Mathematically, this is represented as: **Absorptivity + Reflectivity + Transmissivity = 1.**

2.4.11.2.5.1.1. Targets and backgrounds are usually opaque, so transmissivity is normally zero. Kirchoff's law tells us that absorptivity equals emissivity, so, if absorptivity (emissivity) is small, then reflectivity must be high, or: **Emissivity + Reflectivity = 1.**

2.4.11.2.5.1.2. Objects with low emissivities and high reflectivities will appear very cold; this holds even if their physical temperatures are high. It's not uncommon for corrugated sheet metal buildings or certain types of sand showing up cold in IR sensors even on the hottest summer days; the low emissivity of the sheet metal or sand means the reflectivity is high, and little energy is absorbed.

2.4.11.3. Thermal response. An object's temperature varies over the course of a day; objects heat up and cool off at different rates, so contrasts between objects and backgrounds may vary dramatically over a 240-hour period. A material's heating or cooling rates depend on four factors: absorptivity, thermal conductivity, thermal capacity, and surface-to-mass ratio.

2.4.11.3.1. Absorptivity. As previously discussed, absorptivity is a measure of how much energy is absorbed by the skin of an object. IR sensors detect skin temperatures; objects with high absorptivities heat up faster than objects with low absorptivities, so daytime temperatures are higher for objects with high absorptivities. At night, objects with high absorptivities also radiate heat more rapidly than objects with low absorptivities, so nighttime temperatures are lower for objects with high absorptivities.

2.4.11.3.2. Thermal conductivity. This is a measure of how rapidly heat is transferred within a material, and determines how rapidly heat is transferred from the surface of an object into its interior. If an object's conductivity is low, more heat remains at its surface, and the object will have higher daytime skin temperatures. At night, radiative cooling reduces surface temperatures, and any heat stored by the object conducts to the surface slowly. However, the surface cools rapidly. In general, the lower the conductivity, the faster an object heats up or cools off.

2.4.11.3.3. Thermal capacity. Thermal capacity is a measure of how much heat an object can store; it depends on the object's specific heat (energy required to raise the temperature of a unit of mass by 1°C) and the total mass of the object. Thermal capacity moderates diurnal heating and cooling processes by acting as an internal heat source or reservoir. At night, stored heat conducts to the surface and offsets heat lost to radiative cooling. The lower the thermal capacity, the faster an object heats up or cools off.
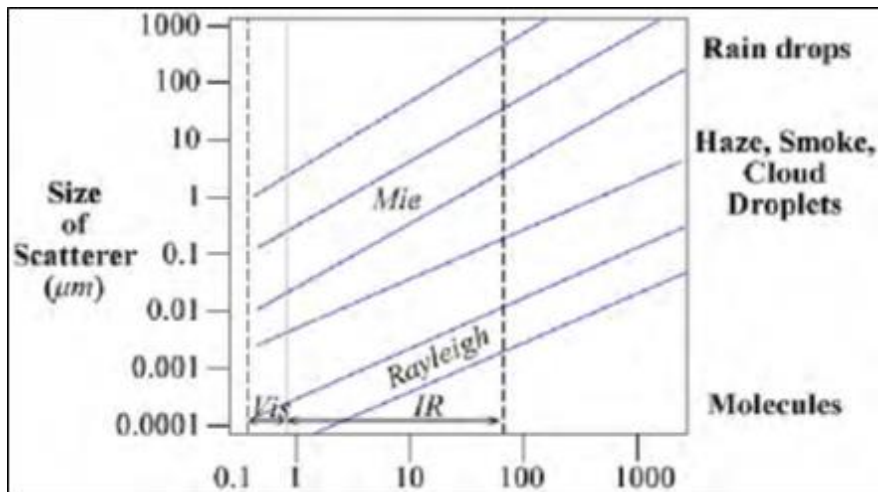
2.4.11.3.4. Surface-to-mass ratio. Objects gain or lose heat through their surfaces, but store it throughout their mass. Therefore, the surface area-to-mass ratio will profoundly influence the rate of thermal transfer for an object. To understand how the surface-to-mass ratio of objects changes with size, consider two cubes. The first one is a 1-kg mass that measures 1 meter on a side. The other is an 8-kg mass that measures 2 meters on a side. The volume of the first cube is 1 cubic meter and its surface area is 6 square meters, for a surface-to-mass ratio of 6:1. Since the two cubes are made of the same material, the volume of the second cube is 8 cubic meters, while its surface area is 24 square meters, for a surface-to-mass ratio of 3:1. The larger cube will not heat up or cool off as fast as the smaller cube because its surface-to-mass ratio is only half as large. Smaller objects have a greater thermal response only when everything else is equal. The shape of an object also affects its ratio. For example, one kilogram of material in the shape of a cube would have less surface area if the same mass of material were shaped like a sphere. Another example would be to take the hypothetical 1-kg sphere and flatten it out like a pizza; notice that a pizza cooks much faster than a loaf of bread.

2.4.11.3.5. The properties of absorptivity, thermal conductivity, and thermal capacity work in concert with the shape and size of an object to determine its thermal response. For example, if two objects are made of the same material, their absorptivities, conductivities, and specific heat will be the same. However, an object's size and shape will also significantly affect the rate at which it heats and cools because of the surface area-to-mass ratio.

2.4.11.4. Extinction. Apparent contrast is always less than inherent contrast. As EMR travels from the target scene to the sensor, some of the photons coming from the target (target light) are scattered and the constituents in the air absorb others. Both of these processes remove target image photons (signal) from their path to the sensor and degrade the image the sensor sees. Both processes apply to all wavelengths; however, in visible wavelengths, scattering is the predominant cause of extinction, while in IR wavelengths, absorption predominates.
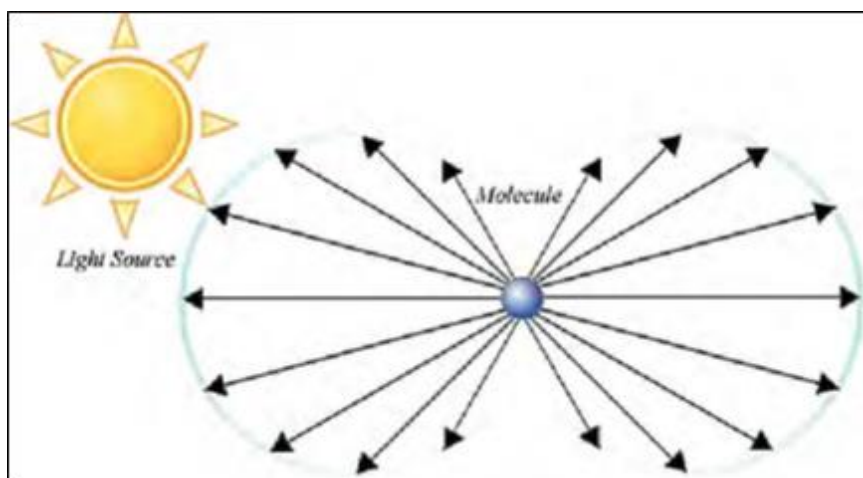
2.4.11.5. Scattering of visible wavelengths. Scattering is defined as the redirection of photons by molecules, aerosols, or other particles in the air. The type of scattering is determined by the size parameter $X = 2\pi r/\lambda$, where r is the radius of the scattering particle, and λ is the wavelength of the EMR being scattered. **Figure 2.49** shows a graphical relationship of scatterer size, wavelength, and scattering type.

Figure 2.49. Type of scattering, based on wavelength and scatterer size.
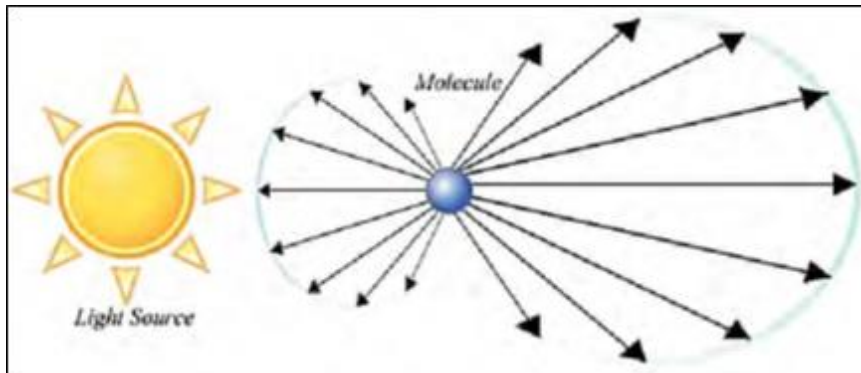
2.4.11.5.1. Rayleigh scattering. For Rayleigh (or molecular) scattering to occur, the wavelength of scattered EMR is much greater than the particle doing the scattering, so X less than 1. Rayleigh scattering is primarily caused by oxygen, nitrogen, and water vapor molecules in the atmosphere. Rayleigh scattering is isotropic, meaning the light is scattered equally in all directions (**Figure 2.50**). Rayleigh scattering also depends on wavelength; shorter wavelengths (blues) are scattered more than longer wavelengths (reds). This is one reason the sky appears blue; blue photons coming from the sun are scattered many more times than red photons and are more widely distributed across the sky. There is always Rayleigh scattering occurring in the atmosphere, but this type of scattering is generally not a problem for EO sensors.

Figure 2.50. Rayleigh scattering.

2.4.11.5.2. Mie scattering. Mie scattering is caused by aerosols, particulates, haze droplets, cloud droplets, and water droplets in the atmosphere; the size of the scatterers are approximately the same as the wavelength of light. Unlike Rayleigh scattering, which is omnidirectional, Mie scattering is predominantly forward-scattered (anisotropic); refer to **Figure 2.51**. Mie scattering is independent of wavelength; all wavelengths are scattered equally. Mie scattering is evident on hazy days; visibility is reduced, and the air has a whitish or grayish appearance. When the relative humidity is greater than 75%, aerosols grow into the size range for Mie scattering to occur. As a general rule of thumb, Mie scattering reduces visibility below the criterion for unrestricted visibility (less than 7 miles).

Figure 2.51. Mie scattering.

2.4.11.5.3. Geometric scattering. The worst contrast degradation is caused by geometric scattering, where the size of the scatterer is much greater than the wavelength of light. Geometric scattering is primarily caused by cloud or fog droplets and precipitation; as the size and number of droplets increase, more light gets scattered in a backward direction. A familiar example of geometric scattering is the effect of turning on your high beams on a foggy night. Like Mie scattering, geometric scattering is also independent of wavelength. Because geometric scattering is so detrimental, most EO sensor systems require a cloud-free line of sight.
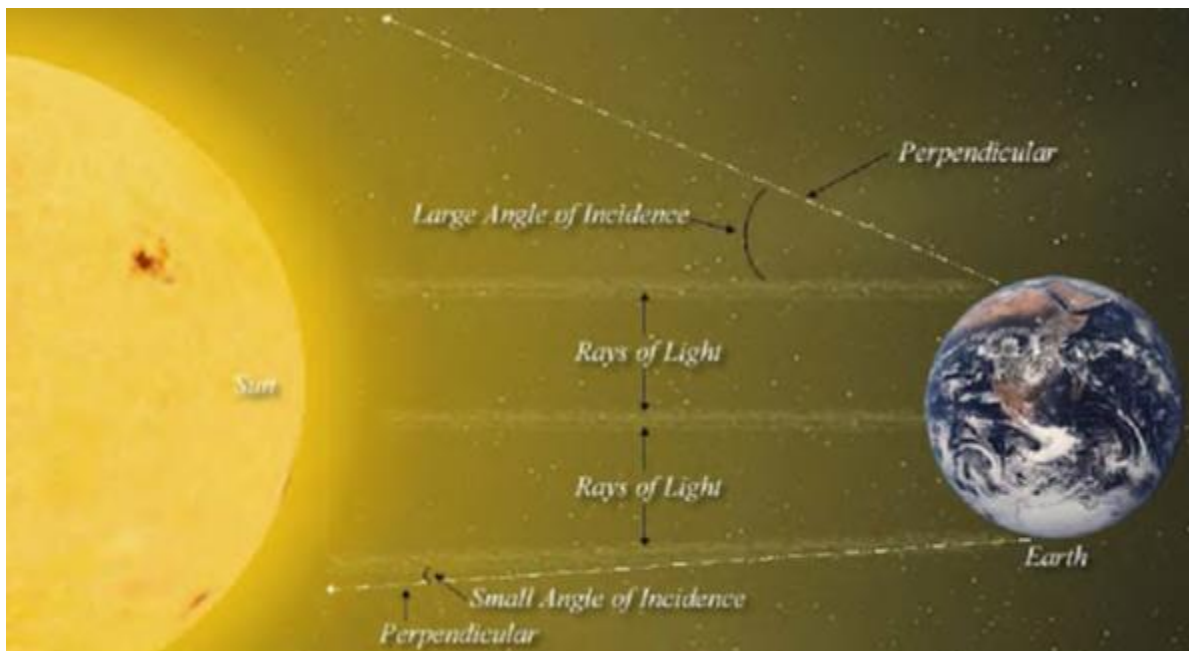
2.4.11.6. Absorption of IR wavelengths. Although scattering of IR wavelengths does occur, the most significant cause of infrared contrast degradation is absorption. Water vapor is the primary absorber of infrared energy; looking across the EM spectrum, there are two "windows" in the infrared where water vapor absorption is minimal; these windows occur from 3.5 to 4.2 μm and 8.5 to 13.0 μm. Most IR EO sensors operate between these wavelength ranges.

2.4.11.7. Environmental effects on EO systems.

2.4.11.7.1. Inherent visible contrast. The environment affects inherent visible contrast chiefly by influencing the amount of illumination a target receives. Illumination can be affected by a number of factors, including cloud cover, sun angle, and precipitation. Overcast clouds reduce the illumination of the target scene. Partly or mostly cloudy conditions can cause the illumination of the target scene to vary rapidly, depending on the amount of cloud.

2.4.11.7.1.1. Sun angle. Sun angle has the most direct effect on illumination; it varies with the time of day, the day of the year, and the location (latitude and longitude) of the target. The angle of incidence (**Figure 2.52**) is measured between the sun ray and a perpendicular line at the point of incidence; the greater the angle of incidence, the less energy is received per square unit of area. A second factor in sun angle effects is the depth of the atmosphere through which the sun's energy travels; this is primarily a function of latitude. The atmosphere is thicker near the equator, and thins toward polar regions. As the angle of incidence increases, the slant range path of the energy through the atmosphere also increases. Solar elevation angles are therefore much higher in the summertime than in the wintertime, and are also greater closer to the tropics. Sun angle determines not only the amount of illumination received by a target, but also impacts shadow length.

Figure 2.52. Sun angle and angle of incidence.

2.4.11.7.1.2. Precipitation. Precipitation may also affect inherent visible contrast by changing a target's reflectivity; rain may create differences in the reflectivities of painted surfaces, particularly by making dull or flat paints on combat vehicles appear duller. Rain may also cause the reflectivities of camouflage, sands, and soils to decrease, making them darker. Snow, if deep enough, can severely reduce contrast by covering the target and background or make dark objects stand out conspicuously if the ground is covered and the targets are not. Smaller scatterers such as dust may settle on the target and affect the inherent visible contrast, changing the reflectivity. Camouflage and smoke are deliberately used to reduce contrast as well.

2.4.11.7.2. Apparent visible contrast. Weather conditions affect contrast transmission more than they influence inherent contrast. If clouds are present in any amount between the target and sensor, they block the view entirely. Visual systems, therefore, require a Cloud-Free Line-of-Sight (CFLOS). As indicated in **Table 2.16**, natural visibility restrictions, such as fog, haze, precipitation, and dust degrade target acquisition and lock-on by reducing visibility. The single most important parameter in determining lock-on and acquisition ranges for visible systems is visibility. In the battlefield environment, there are restrictions to visibility besides those that occur naturally. Obscurants such as smoke may be used to deliberately shield moving targets from sight. Battlefield Induced Contaminants (BIC) such as smoke from burning targets and dust raised by bomb impacts also obscure the target scene. These conditions may change rapidly and be difficult to forecast accurately, even with the most current intelligence information.

Table 2.17. General effects of weather and other obscurations on EO sensors.

Obscuration	Vis/Near IR	Short-Wave IR	Mid-Wave IR	Long-Wave IR	Millimeter Microwave
Low visibility	Severe	Moderate	Low	Low	None
Rain / Snow	Moderate	Moderate	Moderate	Moderate	Moderate / Low
High Humidity	Low	Low	Moderate	Moderate	Low / None
Fog / Clouds	Severe	Severe	Moderate / Severe	Moderate / Severe	Moderate / Low
Oil / Smoke	Severe	Moderate	Low	Low	None
Phosphorous / Dust	Severe	Severe / Moderate	Moderate	Moderate	Low / None

2.4.11.7.3. Inherent thermal contrast. There are many more environmental effects on inherent thermal contrast than there are on inherent visible contrast. Vehicular IR targets have self-heated engines; they supply their own EMR. The operating condition of the target (i.e., whether it is off, idling, or exercising/running) has a great effect on the amount of energy it emits, and therefore, the contrast. If only the sun (passively heated) heats the target, its contrast with the background is dependent upon differences in the absorptivity, thermal conductivity, and thermal capacity of the target and background. Self-heated targets also receive passive heating, and both must be taken into account to determine their temperatures.

2.4.11.7.3.1. Precipitation. Rain and snow equalize the temperatures of passively heated objects and their backgrounds and reduce thermal contrast. As precipitation covers the targets and backgrounds, conduction between target and background materials and the precipitation causes all temperatures to become more or less the same. Self-heated targets, however, stand out against homogeneous backgrounds (like recently fallen rain on a concrete background). However, conductive heat transfer is not the only effect precipitation will have. The uneven evaporation (and evaporative cooling) of rain and the melting of snow can cause an increase in thermal complexity (number of objects that may be mistaken for a target). When a target scene is more complex, an aircraft must get closer to sort out targets and backgrounds. Recent precipitation is also important in determining thermal contrast. It can obliterate the thermal contrast of passively heated targets and backgrounds and enhance the contrast for self-heated targets. The thermal responses of objects determine how quickly thermal contrast is restored once precipitation has ended. For this reason, be sure to consider the recent weather in the target area when preparing an EO forecast, rather than just the forecast conditions for the time-on-target.
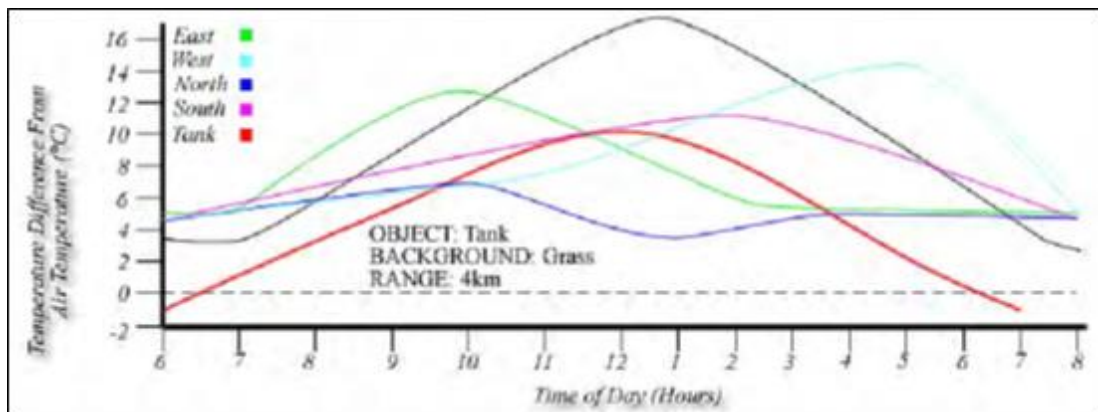
2.4.11.7.3.2. Clouds. Clouds reduce insolation to passively heated objects, and therefore reduce the thermal contrast between passively heated targets and backgrounds. Backgrounds appear more homogeneous (less complex), but passively heated targets blend in with them. As with precipitation, self-heated targets appear warm against a homogeneous background. Clouds also reduce the net amount of radiative cooling of targets and backgrounds at night, thereby reducing thermal contrast of passively heated objects. The temperatures of exercised self-heated targets are fairly uniform throughout the day, so these appear warm against cooler backgrounds at night. Thicker low and mid-clouds reduce thermal contrast more than thinner high clouds. Scattered clouds have very little effect, while the effect of broken or overcast clouds may be quite significant.

2.4.11.7.3.3. Wind. Wind increases the amount of heat lost from all objects, and reduces contrast for all target scenes. In other words, the greater the wind speed, the less the thermal differences between targets and backgrounds. The degree to which wind cools a target varies the most for low wind speeds, generally less than 10 knots. It is therefore critical to forecast wind speeds with the highest possible degree of accuracy when wind speeds are low. An eight-knot wind cools a target much more than a one-knot wind, but a 50-knot wind speed will not have more effect than a 20-knot wind.

2.4.11.7.3.4. Thermal crossover. Passively heated objects heat up and cool off at different rates and by different amounts over the course of the day. An object with a rapid thermal response will be warmer than an object with slow thermal response in the late morning and afternoon; it will also be cooler than an object with slow thermal response in the pre-dawn hours. If a target is warmer than its background during the day and cooler than the background at night, there are two times each 24-hour period when their temperatures are the same – these are the crossover times, and they vary depending on the target, background, and viewing direction. Thermal crossover times are the worst times of the day for using IR systems. For

exercised self-heated targets, crossover occurs only on very hot days on certain backgrounds such as desert sands and asphalt roads. On very hot days, these backgrounds may heat up to the same temperature as the self-heated target and make IR systems difficult to use. In this situation, crossover may occur only in the afternoon when target and background temperatures are the same. Targets and backgrounds may stay "crossed-over" for the entire afternoon. All sensors have different thresholds for contrast, so temperature ranges that cause a crossover for one sensor may not for a different senor. Thermal crossover is a function of viewing direction; for example, consider a tank that has not been exercised for several days. The graph in **Figure 2.53** shows the daytime temperature curve for each side of the tank with a grass background. As you can see, whether or not a target is hotter or colder than the background depends on both the time of day and the viewing angle.

Figure 2.53. Thermal crossover of a tank against a grassy background.

2.4.11.7.4. Apparent thermal contrast. Thermal contrast transmission is affected mostly by the presence of water in the air, either in vapor or droplet form. The most severe restrictions on contrast transmission are due to precipitation. Rain, snow, and other forms of precipitation cause severe attenuation of target/background contrast transmission due to absorption by droplets. Similarly, clouds severely attenuate contrast transmission. High absolute humidities (high dew points) restrict thermal contrast transmission by water vapor absorption. The higher the amount of moisture in the atmosphere, the worse the IR sensors perform. Dew point and absolute humidity are a much better indication of actual moisture in the lower atmosphere, since relative humidity is directly related to temperature. Lithometeors, such as dust and haze, have little effect in dry air. However, when the relative humidity increases to about 90% or higher, large haze droplets can form that impair apparent contrast to the same extent as fog and rain droplets.

2.4.12. Chemical downwind messages (CDMs). CDMs are model-produced, alphanumeric forecasts designed for predicting dispersion of chemical or biological agents; they are available for single or multiple stations under the alphanumeric model output menu on the point-based products section of AFW-WEBS. They provide wind, stability, temperature, relative humidity, significant weather, and cloud cover predictions to assist in determining chemical dispersion patterns. With their small file size and alphanumeric content, they are ideal for low bandwidth or limited data scenarios in austere conditions.

2.4.13. Effective downwind messages. These bulletins provide information on dispersion of radioactive fallout from a nuclear detonation; the GALWEM-produced messages provide wind speed and direction forecasts for multiple sizes of warhead detonation. They are available for single or multiple stations under the alphanumeric model output menu on the point-based products section of AFW-WEBS.

2.4.14. Volcanoes. Volcanoes and associated ash are a clear and present danger to any and all air operations. The source, properties, and dangers of ash are explored below.

2.4.14.1. Volcanic eruptions. Any vent in the Earth's crust that emits molten rock or gas can be called a volcano. Building pressure in the magma chamber beneath the surface can lift the earth above it, producing the commonly known conical mountain. The quantity and gaseous content of subterranean magma are the two main factors in determining a volcanoes explosive power when it erupts.

2.4.14.2. Types of lava. A hallmark of a volcano is the lava expelled at high pressure and temperature. This lava is comprised of molten rock and various gases, compressed into a glowing, glutinous liquid. Lava eventually cools and hardens, forming pumice and other rocks, even creating islands or archipelagos (Hawaii is a good example) The Earth generates enormous amounts of energy in the core, which dissipates as heat throughout the planet's interior. When tectonic plates interact and move against one another, water may infuse into the boundary. The presence of water in the mantle lowers the necessary temperature for the sliding rock to melt, and magma forms more easily. Magma that rises to the surface is called lava. There are three main types of magma: Basaltic, Andesitic, and Rhyolitic. There are chemical variations between these types, but the biggest difference among them is the amount of silica dissolved in the magma. Magma is a thick, viscous substance when melted, and the higher the silica content, the more viscous magma will become. More viscous magma traps more gas, and builds up to higher pressure, leading to more explosive eruptions.

2.4.14.2.1. Basaltic magma has the lowest silica, potassium, and sodium content, with high levels of iron, magnesium, and calcium. It has very low viscosity, partially due to the very high temperature at which it forms. As such, Basaltic magma traps very little gas and does not produce explosive eruptions or expel significant ash.

2.4.14.2.2. Andesitic magma has somewhat higher silica levels, and intermediate levels of iron, magnesium, calcium, sodium, and potassium. It is cooler than Basaltic magma, and thus is more viscous and traps more gas, creating eruptions of intermediate intensity.

2.4.14.2.3. Rhyolitic magma has the highest silica, potassium, and sodium content, with low levels of iron, magnesium, and calcium. It is the coolest and most viscous of magma types, trapping considerable amounts of gas and producing the most explosive eruptions.

2.4.14.3. Types of eruptions. A volcanic event can generally be characterized as one of four types of eruption (Hawaiian, Strombolian, Vulcanian, Plinian), each with its own specific characteristics.

2.4.14.3.1. Hawaiian eruptions tend to expel a very fluid and non-gaseous Basaltic magma. Thus, Hawaiian eruptions create flowing lava at high temperature. With the highest lava fountain reaching about a meter, very little ash is produced. Hawaiian eruptions are comparatively weak, but may occur with considerable frequency, up to every few months; active volcanoes all over the Earth are continuously oozing magma in slow Hawaiian eruptions.

2.4.14.3.2. Strombolian eruptions are more explosive due to having slightly higher silicate Andesitic magma. Its higher viscosity holds more gas, and results in slightly more explosive events. Some ash may be produced, reaching no more than 10 km in altitude. Cinder cones may build up around the vent over time, as ejected magma typically falls near the source. Strombolian eruptions tend to consist of short blasts, but in rare cases may continuously erupt for an extended period.

2.4.14.3.3. Vulcanian eruptions have even more explosive power due to their Andesite or Rhyolite magma. Lava blocks or bombs can be expected, with an ash plume reaching 20 km high, well over 65,000 feet. It is important to note that more destructive volcanic eruptions do occur, but with increasing rarity according to their strength. Vulcanian eruptions may occur on the order of every few years.

2.4.14.3.4. Plinian eruptions are the largest and most violent variety. Plume heights from the resulting ash can reach 55 km. Widespread ash deposits will result from a Plinian eruption, as well as fast-moving hot ash flows along the ground known as pyroclastic clouds. An individual volcano may experience a Plinian eruption only once every few hundred thousand years, but typically there are a handful of worldwide Plinian eruptions per century. The devastation from a major Plinian eruption may lead to mass extinctions, but such explosive eruptions occur far less often than the weaker types.

2.4.14.4. Volcanic ash. Volcanic ash begins its life as pulverized, molten rock at high temperature and pressure under Earth's the crust. When explosively ejected into the atmosphere, flecks of lava may reach many kilometers in altitude. Starting at temperatures greater than 1000˚C, these fragments cool and solidify as jagged microscopic particles that disperse as fine powder – this powder is volcanic ash. It's comprised of various crystallized minerals, rock, and glass. Volcanic ash is extraordinarily abrasive; if inhaled, it can rapidly cause lung damage. The chemical components of ash can quickly transform a lake into sulfur dioxide, a highly acidic and dangerous substance. Volcanic ash also poses a serious threat to aviation, as its abrasiveness can have catastrophic impacts to engine components if the particles are ingested through jet engines and carburetors. The severity of ash cloud interaction is measured on a scale from zero to five.

2.4.14.4.1. Class 0 encounters, with no damage to the airplane, occur when flying through finely dispersed clouds of ash, likely a considerable distance from the volcano. Particles may find their way into the cabin, resulting in the odor of sulfur or creating a strange haze. St. Elmo's Fire is a harmless discharge of static from ash striking aircraft surfaces. Less harmless is the erosion seen on an aircraft's leading edges, windows, lights, fuselage, and engine components.

2.4.14.4.2. Class 1 encounters result in noticeable interactions with ash in the cabin, engine, and on the aircraft's exterior. If ingested into jet engines, volcanic ash can cause havoc; ash melts at around 1100˚C, while jet engines operate at temperatures near 1400˚C. Flying through ash clouds effectively introduces lava into the combustion chamber of a jet engine, which can quickly lead to degraded performance and compromised engine components. Ash may liquefy and adhere to turbojet engine fan blades, slowing or even stopping the engines.

2.4.14.4.3. Class 2 encounters result in significant amounts of dust entering the cabin, requiring oxygen use, deposits of ash within the engines, and damage to the aircraft's exterior. Encountering a stationary cloud of dust at high speed is dangerous enough, and volcanic ash is far more dangerous due to its sharp, glassy structure. Moving engine components, leading edges of wings, the nose, and cockpit glass can be pitted or corroded, decreasing visibility. Flight instruments may be compromised if their sensors are partially or totally obstructed.

2.4.14.4.4. Class 3 encounters are even more dangerous, with damage to the engines and/or electrical systems, plugging of instrument systems, and even contamination of the hydraulic fluids occurring. Effects from lower-class encounters may also occur.

2.4.14.4.5. Class 4 encounters exhibit most or all of the above problems, and in addition require an in-flight restart of one or more engines after exiting the ash cloud.

2.4.14.4.6. Class 5 encounters are hypothetical; they've never occurred in real life. A class 5 encounter would be marked by engine failure or other damages being so severe that the aircraft crashes as a result.

2.4.14.5. Ash visualization and communication. Because of the high altitude that ash typically reaches in the troposphere and stratosphere, it may travel at velocities well over 100 knots with the jet stream. As such, it is difficult to accurately and completely observe an ash plume without utilizing satellite imagery. While not strictly a meteorological target, there are frequencies of radiation at which ash can be observed. Visible imagery is one of the best tools, but is limited to daytime observation. Additionally, the grayish-brown cloud of ash may be obscured or infused with cloud, reducing its visibility. Infrared radiation is another excellent tool, given that it can be used at night as well. Also, ash tends to exhibit a unique thermal signature near its source; the enormous heat of an eruption is followed by a cooling period as the ash ascends. The energy of convection considerably cools the rising plume, however, and a clearly visible cold region is quickly established. The corresponding IR and Visible channels will show a distinguishable temperature difference, despite the fact that the visible ash is less obvious against the cloud background. This cold temperature is from ash rising far above the level of any cloud development, and as such reaching a much lower temperature. After 24 hours, however, the ash signature may be difficult to distinguish from normal clouds. Another limitation of observing ash with satellites is parallax error - the displacement of high-altitude targets at polar latitudes. Because the ash is observed so far above the ground, it gives the appearance of occurring further poleward than in reality. Communication is key when danger is present from volcanic eruptions; Pilot reports (PIREPs) and Significant Meteorological Reports (SIGMETs) are essential sources of information. Local news reports can also provide relevant information, especially if an eruption occurs near major city centers.

2.4.14.6. Volcanic forecasting. Volcanic Ash Advisory Centers (VAACs) cover a specific region of the world, and are comprised of experts that coordinate efforts to keep the public aware of eruptions and resultant ash clouds. VAACs produce advisories and graphics on potential activity as well as ongoing eruption events. Within the Air Force, the 2nd Weather Squadron utilizes VAAC products to produce worldwide advisories and model forecasts; these products are available from the AFW-WEBS Environmental Events section.
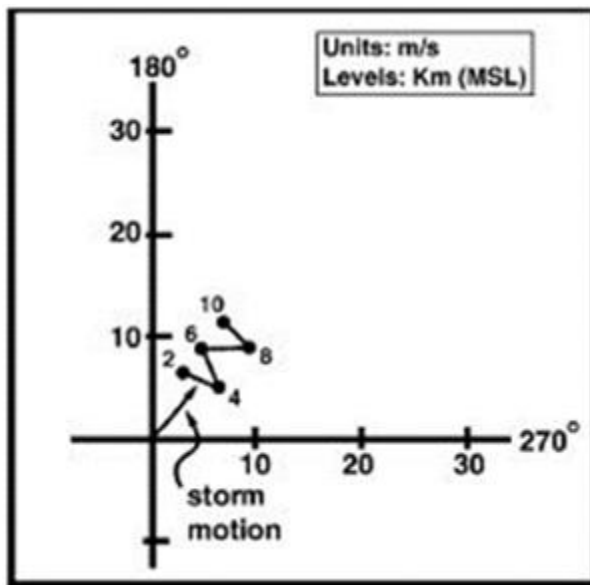
Chapter 3

CONVECTIVE WEATHER

3.1. Thunderstorms. Thunderstorm-produced severe weather consists of a combination of tornadoes, hail, strong winds, lightning, and heavy rainfall. There are three basic types of thunderstorms: single cell, multi-cell, and supercell. While upward vertical motions and instability of an air mass determine whether thunderstorms will occur, wind shear strongly influences the type of thunderstorms to expect. In general, the greater the shear, the more likely the convection will be sustained. Each type of storm can be identified by a distinctive hodograph pattern, which is a visual depiction of the wind shear.

3.1.1. Single cell thunderstorms. Single cell storms are short-lived (30 to 60 minutes) cells with one updraft that rises rapidly through the troposphere. Precipitation begins at the mature stage, in   a single downdraft. When the downdraft reaches the surface, it cuts off the updraft and the storm dissipates. **Figure 3.1** shows a typical hodograph for a single-cell storm. Single cell storm characteristics include weak vertical and horizontal wind shears, a random shear profile on the hodograph, and storm motion with the mean wind pattern in the lowest 5-7 km of the atmosphere. Severe weather does not normally occur with single cell storms, but may be possible in stronger and longer-duration cells. High winds and hail are possible, but short-lived, and tornadoes are rare.
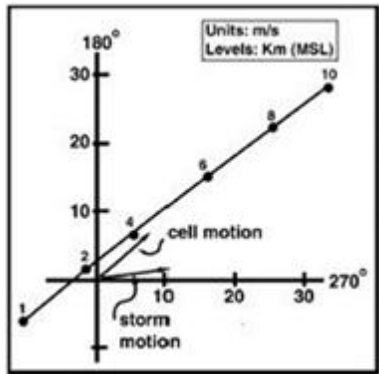
Figure 3.1. Single cell thunderstorm hodograph.

3.1.2. Multi-cell thunderstorms. Multicellular storms are clusters of short-lived single-cell storms; each cell generates a cold outflow that can form a gust front. Convergence along these boundaries causes new cells to develop every 5-15 minutes in the convergent zone. These storms are longer in duration than single cell storms, since they typically regenerate along the gust front. **Figure 3.2** shows a typical hodograph for a multicellular storm. Multi-cell storms have a straight-line or unidirectional shear profile, and show strong directional shear in the lower levels with strong speed shear aloft. Individual cell motions coincide with the mean
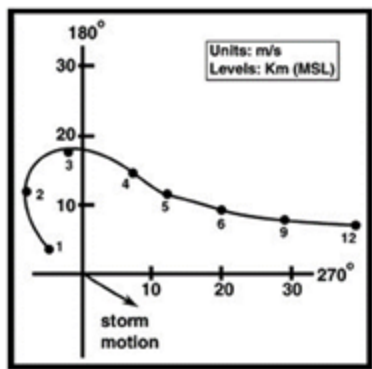
wind, and storm clusters will move in the direction of the gust front and to the right of the mean wind. Severe weather is possible with multi-cell storms, including flash flooding from slow-moving cells, large hail near downdraft centers, and weak, short-duration tornadoes along gust fronts near updraft centers.

Figure 3.2. Multi-cell thunderstorm hodograph.
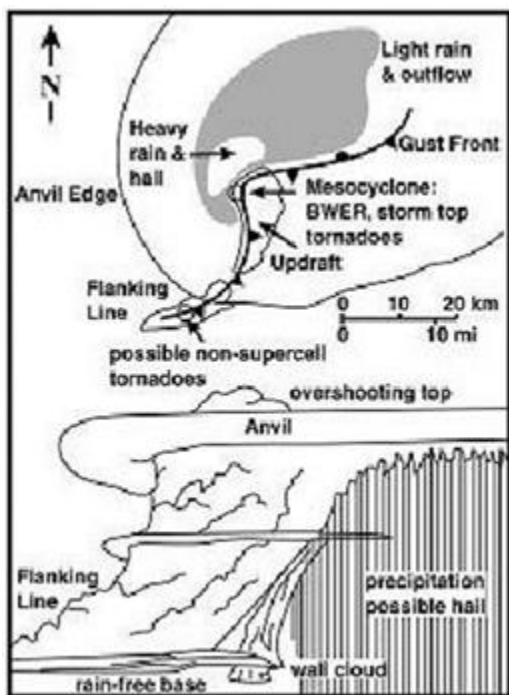
3.1.3. Supercell thunderstorms. Supercell thunderstorms consist of a rotating updraft, a forward- flanking downdraft that forms the gust front, and a rear-flanking downdraft. Supercells may exist for several hours, and are a frequent producer of severe weather. They are characterized by wind speeds increasing with height, and a curved shear profile in lower levels, becoming straight-line above 3 km (**Figure 3.3** shows a typical hodograph for a supercell.) They will have at least 70° of directional shear in the first 3 km of the atmosphere, and the shear vector veers with height in the low levels, which produces rotation of the storm updraft. A cyclonically-curved hodograph is associated with cyclonically rotating cells that will move to the right of the mean low-level wind; anticyclonically-curved hodographs indicate storms moving to the left of the mean wind – these types of storms are notorious hail producers. There are three types of supercells: classic, high precipitation (HP), and low precipitation (LP).

Figure 3.3. Supercell thunderstorm hodograph.
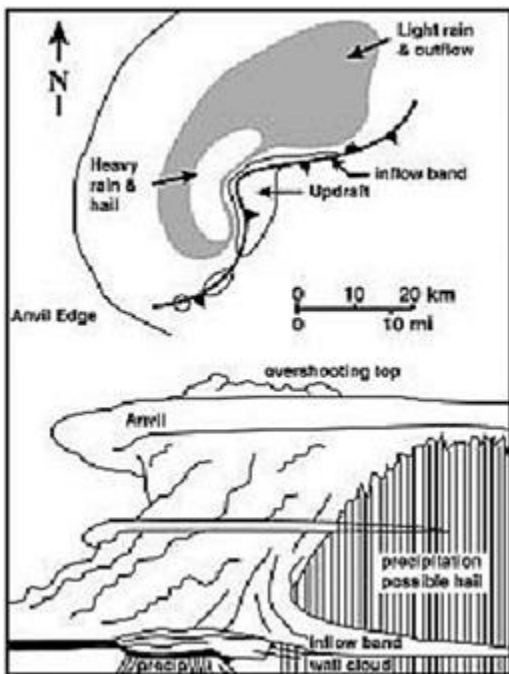
3.1.3.1. Classic supercell (**Figure 3.4**). Classic supercells are usually isolated from the main thunderstorm outbreak, and are identified by the classic "hook echo" in the low-level reflectivity pattern and bounded weak-echo region (BWER) aloft. Supercells are capable of producing several types of severe weather: golf ball size hail, wind gusts in excess of 50 knots (along the gust front and from microbursts in the rear-flanking downdraft), and tornadoes.

Figure 3.4. Classic supercell.
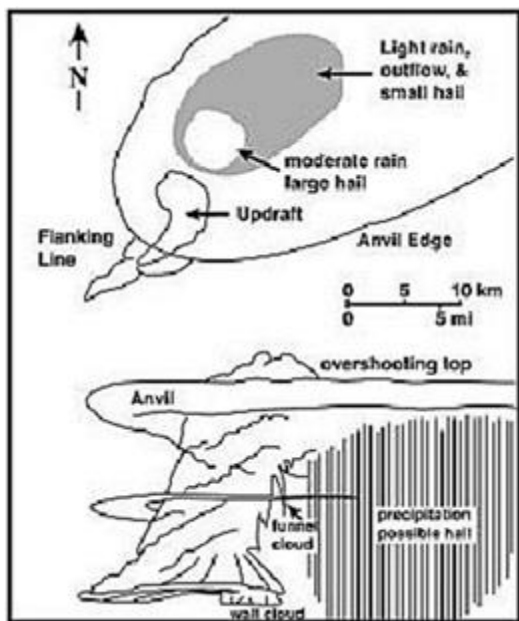
3.1.3.2. High-precipitation (HP) supercells (**Figure 3.5**). HP supercells develop in deep, moist layers with high moisture values; they produce heavier rain than classic supercells and are not as isolated. Radar patterns associated with HP cells are more varied than the classical "hook", and have the potential to evolve into bow echo configurations. HP supercells are capable of producing extremely heavy rain, high winds, hail, and tornadoes.

Figure 3.5. High-precipitation supercell.
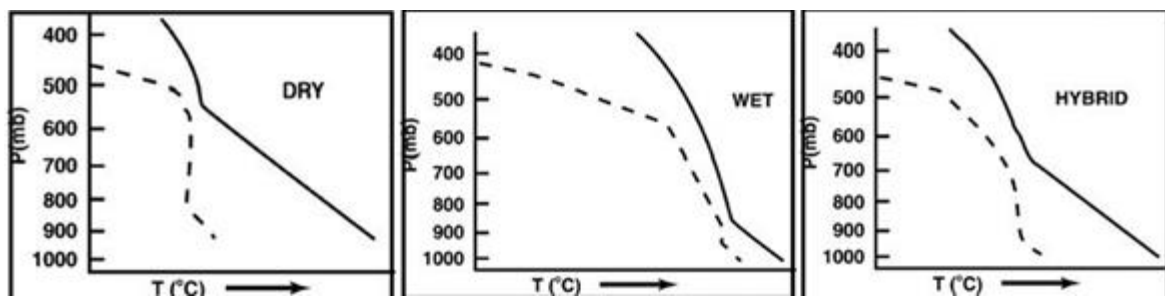
3.1.3.3. Low-precipitation (LP) supercells (**Figure 3.6**). These types of supercells produce smaller amounts of precipitation than other supercell types, and have a rather benign appearance on radar. Although smaller in diameter than classic supercell storms, they are still capable of producing severe weather such as large hail and tornadoes.

Figure 3.6. Low-precipitation supercell.

3.1.4. Dry, wet, and hybrid microbursts. Microbursts are dynamically enhanced, concentrated downdrafts from thunderstorms that result in damaging surface winds with gusts of 50 knots or greater at the surface. They usually occur in the rear-flanking downdraft region of supercell storms, and may also be found behind the gust front. These events are not restricted to large supercell storms, however; they can come from innocuous-looking, high-based rain clouds (dry microbursts), from single and multicellular pulse storms (wet microbursts), or from hybrid microbursts that combine dry and wet characteristics. The microburst type depends on the type of environment in which the storm forms; **Figure 3.7** portrays typical atmospheric profiles for dry, wet, and hybrid microbursts.

Figure 3.7. Microburst atmospheric profiles (Dry, Wet & Hybrid).

3.1.5. Derechos. Derechos are straight-line wind events that originate from severe convective storms; there are two main variants of this event. The first type of derecho is a rapidly-propagating segment of an extensive squall line, usually associated with a strong, migratory low-pressure system occurring in the late winter or early spring. The second type develops in association with a relatively weak frontal system in a moisture-rich environment, showing characteristics of both squall lines and non-linear types of mesoscale convective systems (MCS) – these are usually late spring or summertime events.

3.1.6. Thunderstorm hazards – severe convective winds. The following are key components that must be examined when characterizing an environment conducive to convective winds:

3.1.6.1. Downdraft Convective Available Potential Energy (DCAPE). High downdraft instability is one of the key ingredients for severe convective winds. The amount of downdraft instability is diagnosed using a parameter called DCAPE; it's a measure of the amount of energy available for air parcel descent through the atmosphere. As DCAPE increases past 800 J kg^{-1}, the probability of strong downdrafts and severe convective winds increases. Values of DCAPE are increased by low-level warm air advection, low-level moisture advection, mid-level cold air advection, ans mid-level dry air advection (evaporative cooling increases negative buoyancy, increasing downdraft strength). Therefore, environments with steep low- and mid-level lapse rates (decreasing temperature) and dry mid-level air will have high values of DCAPE. If thunderstorms develop in such environments, strong downdrafts and severe convective winds are likely. The magnitude of DCAPE can also be diagnosed by examining the difference between the equivalent potential temperature (theta-e) in the low-levels and in the mid-levels. Theta-e is the temperature an air parcel would have if it was expanded (lifted) dry adiabatically to its LCL and then lifted moist adiabatically to the top of the atmosphere where all moisture condenses out of it. The parcel is then compressed (lowered) dry adiabatically to 1000 mb. High theta-e in the low-levels and low theta-e aloft (usually between 400 mb and 600 mb) is indicative of high downdraft instability.

3.1.6.2. Low and mid-level moisture profile. Convective winds may occur if the low-levels are moist and the mid-levels are dry, or if the low-levels are dry and the mid-levels are moist. They will not occur if both the low- and mid-levels are dry, because thunderstorms are unlikely to develop at all. They may occur if both the mid- and low-levels are moist due to precipitation loading, but are rare in this type of environment. Dry air aloft, characterized by relative humidity less than 50% allows much of the moisture that is lifted into the dry layer to evaporate. Evaporation is a thermodynamic process that cools the ambient air, increasing its density and decreasing the buoyancy. Dry air aloft is best characterized by examining values of equivalent or wet-bulb potential temperature between 600 mb and 400 mb. Both of these values account for the moisture and temperature characteristics of an air parcel, and the colder they are, the more negatively buoyant the air. In fact, downdrafts are believed to originate at the level of minimal wet-bulb or equivalent potential temperature aloft. If the mid-levels are moist (RH greater than 75%) and the low-levels are dry (RH less than 75%), high-based thunderstorms may develop that also pose a convective wind threat. High-based precipitation may develop in the mid-levels. As it falls into the dry air below 700 mb, most of it will evaporate, resulting in additional cooling of the downdraft. In most cases like this, the downdraft is also sustained by steep low- and mid-level lapse rates during descent, which promote negative buoyancy.

3.1.6.3. Low-level vertical wind shear (VWS) profile. A strong VWS profile enhances the potential that strong winds aloft will be able to come to the surface, as long as the strongest wind in the surface to 6 km above ground level (AGL) layer is at least 20 knots. This additional mass increases negative buoyancy-driven downdraft magnitude. Steep low- and mid-level lapse rates allow winds from aloft to come to the surface, and this probability increases if the VWS profile (especially in the low-levels) is relative unidirectional, or in-phase. The low-level VWS profile will also control the direction of thunderstorm propagation and influence the speed of the associated thunderstorm gust front. Stronger gusts are likely with fast-moving thunderstorms because of the propagation component and associated gust front speed. Most convective wind events are caused by organized thunderstorm structures in environments of sufficient VWS that also have favorable thermodynamic profiles.

3.1.6.4. Low-level lapse rates. Steep low-level lapse rates are not critical for convective winds, especially wet microbursts, but they do increase the negative buoyancy necessary for momentum transfer from aloft to the surface and for associated downbursts. Steep lapse rates are an indication of cold air aloft and warm air at the surface. Cold air on tap of warm air creates instability for both upward vertical motions and downward vertical motions. Lapse rates exceeding $8°C$ km^{-1}, and especially approaching dry adiabatic, are optimal for convective wind development. Convective winds can also occur with lapse rates as shallow as $5°C$ km^{-1} if the low-levels are very moist and conducive to wet microbursts or generic downbursts due to precipitation loading, evaporation, and melting. Dry microbursts require very steep low-level lapse rates (usually dry adiabatic) for downdraft maintenance during descent, because the precipitation loading component is lacking throughout the downdraft's evolution, except at the onset. In addition, downdrafts in a dry adiabatic environment tend to warm rapidly via compression.

3.1.6.5. Height of minimum wet bulb potential temperature aloft. Downdrafts are theorized to originate at the level of minimum wet bulb potential temperature (or equivalent potential temperature) aloft; the altitude of this level plays a role in the speed of descending air as it reaches the surface. In general, downdrafts that originate above 18,000 feet will have too much time to warm via compression during their descent, especially if the downdrafts are unsaturated, and resultant surface wind gusts will be weaker. Similarly, if downdrafts originate below 12,000 feet, the downdraft may not have enough time to accelerate before reaching the surface, rendering it weaker. The optimal layer for downdraft origination is between approximately 12,000 feet and 18,000 feet AGL (plus or minus 2,000 feet), or between 700 mb and 500 mb. Downdrafts originating in this layer experience an optimal balance of compressional warming vs. mass acceleration.

3.1.7. Thunderstorm hazards – hail. The following key parameters must be examined when characterizing an environment conducive to hail formation:

3.1.7.1. Mid-level lapse rates. For locations at mean sea level (MSL), lapse rates between 700 mb and 500 mb should be at least $6°C$ km^{-1}, and optimally steeper than that. Locations at higher elevations should use the 600 mb and 400 mb lapse rate. Steep mid-level lapse rates lead to increased instability in the hail growth zone, which is usually between $-10°C$ and $-30°C$. In this region, ice crystals and supercooled water droplets coexist in great supply. Instability in this layer promotes the vertical motions (via positive buoyancy) necessary for ice crystal formation and growth into hailstones. In addition, the steeper the

mid-level lapse rates, the colder it is aloft and the easier it will be for hailstones to grow via riming of supercooled water droplets. Steep mid-level lapse rates also increase the depth of the hail growth zone, providing a greater area where hail growth is favored.

3.1.7.2. Wet bulb zero (WBZ) height. The WBZ zero height is the height at which the wet bulb temperature is 0°C. The WBZ height is a good proxy for the lowest level at which hail growth is possible; below the WBZ level, melting will inhibit hail growth. Most hail reaches the surface when the WBZ height is between 5000 and 11,000 feet AGL. The lower the WBZ level, the deeper the cloud depth where hail growth is possible. In addition, a low WBZ level means a shallower melting layer exists, so hailstones will have less time to melt before reaching the surface in such an environment. If the WBZ level is below 5000 feet AGL, the environment is likely too cold and stable for hail development.

3.1.7.3. Mid-level moisture profile. Dry air aloft, usually characterized by relative humidity less than 50% above 700 mb (or 600 mb for higher elevations), is favorable for severe hail. Dry air aloft aids in hail growth primarily by causing evaporative cooling that makes the upper-atmosphere more conducive to hail growth, and it also lowers the WBZ height. Dry air aloft is also an indicator of convective instability when the lower atmosphere is sufficiently moist. This will result in strong updrafts capable of supporting large hailstones. Convective instability is diagnosed by examining the profile of equivalent potential temperature, or theta-e. A layer where theta-e decreases with height is convectively unstable and will be more prone to hail production. Dry air aloft will usually be characterized by steep lapse rates as well, which further enhances instability and hail potential.

3.1.7.4. Convective instability. High instability, generally characterized by Convective Available Potential Energy (CAPE) greater than 500 J kg^{-1}, favors the production of severe hail. Strong updrafts are needed for hailstone production and to allow hailstones to remain suspended so they can grow via riming, accretion, and aggregation. An environment of high instability (high CAPE) can support such strong updrafts. The magnitude of maximum upward vertical motion is directly proportional to the amount of CAPE; the larger the CAPE, the stronger the UVM and resultant thunderstorm updrafts. In general, for ½" hailstones to reach the surface, at least 500 J kg^{-1} of CAPE is necessary. At least 700 J kg^{-1} is necessary for ¾" hailstones, and at least 2,000 J kg^{-1} is needed for 2" hailstones.

3.1.7.5. Surface to six km VWS profile. Strong VWS, generally characterized by surface to six km wind shear exceeding 15 knots, supports hail formation. Strong VWS enhances hail potential by increasing updraft strength via mesoscale pressure perturbations that result in a strong vertical pressure gradient force. It also ventilates thunderstorm updrafts by tilting storms downshear, so the downdrafts that develop don't fall into the updrafts. In other words, strong VWS keeps downdrafts away from updrafts, which allows hailstones to be suspended for a longer period and allows updrafts to maintain their strength. Large hail is possible in environments with CAPE as low as 500 J kg^{-1} that have strong VWS. In fact, hail is more likely in low CAPE/high VWS environments than in those characterized by high CAPE and low VWS. For maximum severe hail potential, both high CAPE and strong VWS are necessary. This is most commonly the case during the spring months in the mid-latitudes, especially late April and May.

3.1.7.6. Low-level moisture. Low-level moisture is critical for hail production; moisture must be present to be transported to the LCL, where hailstones originate as water droplets, and then into the -10°C to -30°C hail growth zone, where graupel and eventually hailstones form. The best variable for identification of deep low-level moisture is Precipitable Water (PW); this is the depth of water that would accumulate if all the water in the atmosphere fell out as precipitation. For severe hail formation, PW should be less than 1.5" but greater than 0.5". While not a critical problem for severe hail development, higher amounts of PW (greater than 1.5") increase the likelihood that any updrafts that are able to develop will become loaded with liquid water, therefore decreasing their strength and also the likelihood that they can support severe hail. The largest hailstones are observed in environments that have high CAPE, strong VWS, and low PW. However, if the environment is too dry as indicated by PW values less than 0.5", the positive buoyancy needed for updraft development and maintenance will not be achieved, reducing hail potential.

3.1.7.7. Surface elevation. High elevation locations, especially those where the surface is above 900 mb (approximately 4000 feet), are most favored for large hail. Because temperature generally decreases with increasing height in the troposphere, locations with higher elevations will have easier access to cold air aloft. This means that, on average, the WBZ level is closer to the surface. Consequently, the melting layer below the WBZ level is shallower, giving hailstones that develop above the WBZ level a shorter depth in which to melt. In addition, because wind speeds generally increase with height in the troposphere, higher elevations are able to tap into stronger winds aloft, which enhance the surface to six km VWS profile.

3.1.8. Thunderstorm hazards – heavy rainfall. The following key parameters must be examined when determining if an environment is favorable for heavy rain:

3.1.8.1. Precipitable Water (PW). The higher the PW, the more water vapor that is available to condense and eventually turn into precipitation. Generally, precipitable water of at least 1 inch (or greater than 100% of normal) is necessary for heavy rain. Values of 1.5 inches (or greater than 150% of normal) characterize a very favorable heavy rain environment.

3.1.8.2. Relative humidity in the lowest 200 mb of the atmosphere. The lifting of a deep layer of moist air results in more efficient precipitation production than the lifting of a shallow layer of moist air. Therefore, RH of at least 70% in the lowest 200 mb of the atmosphere is generally necessary for heavy rain. An even deeper layer of high RH (up to 500 mb) further increases precipitation efficiency by reducing entrainment of dry midlevel air.

3.1.8.3. Surface dew points. The dew point is the temperature to which air must be cooled at constant pressure for water vapor to condense into liquid. Because most water vapor is confined to the lowest 200 mb of the atmosphere, near moisture sources (oceans, lakes, rivers), the surface dew point is an important proxy for the amount of water vapor available for precipitation development. As the surface dew point exceeds 55°F and approaches 60°F and higher, the amount of low-level water vapor available for precipitation production increases substantially, and so does the chance of heavy rainfall. Surface dew points are regularly in excess of 65°F during the late spring and summer months in the lower and mid-latitudes, which is when many heavy rain events occur.

3.1.8.4. Moisture convergence. Moisture convergence is the advection of water vapor (moisture) against a convergent boundary such as a front, coastline, or complex terrain. Moisture speed convergence can also occur as stronger winds meet up with slower winds, causing a local increase in dew points and relative humidity. Moisture convergence acts as a source of low-level lift for precipitation production, and also increases dew points and relative humidity as more water vapor is brought into an area and "pools" along a boundary. Greater horizontal and vertical depth of moisture inflow and convergence increases heavy rainfall potential. Of particular importance is persistent southerly inflow and convergence within the left exit region of a low-level jet along a quasi-stationary low-level frontal boundary. This can signify the potential for several inches of rainfall. Once convection has developed, continued moisture inflow and convergence can maintain the convection, even in the absence of other forcing mechanisms.

3.1.8.5. K index. The K index accounts for both stability and the presence or lack of deep moisture available for precipitation and thunderstorm development; it's given by: **KI = (T850 – T500) + (Td850 – DD700).** Where T850 is the temperature at 850 mb (°C), T500 is the 500 mb temperature (°C), Td850 is the 850 mb dew point (°C), and DD700 is the dew point depression at 700 mb in °C. High instability and deep moisture result in large K index numbers; values of at least 25, and especially over 30, are indicative of heavy rainfall potential.

3.1.8.6. Surface to six km wind shear. Thunderstorms that develop in a low vertical wind shear environment move slowly and may dump heavy rain over the same locations for several hours. Heavy rainfall is most favored when surface to 6 km wind shear is less than 15 knots.

3.1.8.7. Winds directed from a moisture source in the lowest 200 mb above the surface. Low-level winds (surface to 850 mb) directed from a moisture source are another key ingredient for heavy rainfall. Winds directed from a moisture source continuously advect moisture into a region, and if thunderstorms are ongoing, they serve as moist inflow for thunderstorm maintenance as other moisture precipitates out. This is why much more precipitation can fall during a strong thunderstorm than indicated by the PW value. Moist inflow continuously replenishes the lower atmosphere and maintains or increases the current value of PW.

3.1.8.8. Equivalent potential temperature (theta-e) advection. Theta-e is the temperature air would have if it was lifted dry adiabatically to its LCL, and then lifted moist adiabatically from the LCL to the top of the atmosphere, allowing all water vapor to condense out, then lowered dry adiabatically to 1000 mb. Theta-e is an excellent diagnostic of both the temperature and moisture content of air. Warm, moist air will have higher theta-e values than cold, dry air. Therefore, strong positive theta-e advection into an area of responsibility signifies an increased potential for heavy rain. Heavy rain potential is further enhanced if the low-level, high theta-e air impinges on a boundary such as a front or complex terrain, leading to moisture convergence.

3.1.8.9. Thickness diffluence. Organized convection, accompanied by heavy rainfall, can occur in or near a region where 1000-500 mb thickness isopleths are diffluent. Thickness diffluence implies low-level convergence, upper-level divergence, or both, and is therefore favorable for convective development. Thickness diffluence is usually located along or near the southern edge of the mid-tropospheric westerlies.

3.1.8.10. Jet streams. There are four regions of jet-enhanced divergence that are favorable for convective development and associated heavy rainfall: the right entrance region of a jet streak, the left exit region of a jet streak, the exit region of a jet streak approaching the top of a ridge axis, and the anticyclonic shear axis to the right of a jet core. Of particular importance is a coupled jet streak, which causes enhanced lift and thunderstorm potential. Additionally, coupling between an upper-level jet streak and the low-level jet can enhance thunderstorm potential by increasing low-level convergence and lift toward an area of upper-level divergence. Heavy rainfall is also likely near the nose and/or the left side of the low-level jet axis, where speed convergence, confluent flow, frontogenesis, and lift are maximized.

3.1.9. Thunderstorm hazards – lightning. The following key parameters must be analyzed when determining if the environment is favorable for lightning production:

3.1.9.1. K index. As discussed in the previous section, the K index accounts for both stability and the presence or lack of deep moisture available for precipitation and thunderstorm development; high instability and deep moisture result in large values, indicative of lightning potential. Deep low-level moisture is required for the eventual creation of ice crystals, graupel, and supercooled water droplets aloft. Supercooled water droplets collide with ice crystals to form graupel. When graupel and ice crystals collide, a charge transfer occurs. Strong vertical motions, potentially indicated by a high K index value, drive the lighter ice crystals toward the top of the cumulonimbus cloud, while the heavier graupel particles fall to the middle or lower portions, and a charge separation is created. Instability (and a source of lift) is needed for the aforementioned moisture to be transported to higher heights, condense/coalesce, and turn into supercooled water droplets, ice crystals, and graupel. K index values greater than 30 indicate a strong likelihood of efficient lightning production.

3.1.9.2. Lifted index (LI). The LI is an indicator of stability, particularly at mid-levels (i.e., the 700-500 mb layer). The equation for the LI is: **LI = Te500 – Tp500.** Where Te500 is the temperature of the environment at 500 mb and Tp500 is the temperature of an air parcel lifted to 500 mb from near the surface. LI values less than or equal to -1°C (less than or equal to +1°C for locations above 1,000 meters) indicate the presence of mid-level instability, which supports upward vertical motion within the layer where lightning production is favored, generally between -10°C (lower to middle portion of a cumulonimbus cloud) and -25°C (upper portion of a cumulonimbus cloud). Further, lift in the 0°C to -20°C layer favors the creation of supercooled water droplets, ice crystals, and graupel.

3.1.9.3. Showalter Stability Index (SSI). The SSI is calculated by lifting a parcel of air dry adiabatically from 850 mb to its lifting condensation level, then moist adiabatically to 500 mb. The 500 mb parcel temperature is then subtracted from the 500 mb environmental temperature; if the SSI is greater than zero, the environment is stable. Increasingly negative values indicate greater instability and thunderstorm potential. Note, however, that low-level moisture must extend to at least 850 mb for the SSI to be representative. Several thunderstorm studies showed that 81% of days without lightning had SSI values greater than 0, while 90% of lightning days had SSI values less than 0. Using the predictor of greater than/less than 0, the SSI accurately predicted whether lightning would occur 96% of the time.

3.1.9.4. Convective Available Potential Energy (CAPE) between 0° and -20°C. Another key parameter for lightning production is at least 200 J kg^{-1} of CAPE in the 0°C to -20°C layer. Lightning production becomes especially likely when CAPE exceeds 600 J kg^{-1}. CAPE is a measure of the energy available for air parcel ascent from the level of free convection to the equilibrium level. However, large CAPE in the 0°C to -20°C layer is especially important for lightning formation because this is the layer where ample upward vertical motion is needed to allow the microphysical processes to take place which create supercooled water droplets, ice crystals, and graupel. The larger the CAPE in this layer, the stronger the ascent, and the more efficient the microphysical processes become.

3.1.9.5. Convergence in the planetary boundary layer (PBL). Mechanical or moisture convergence in the PBL (the lowest 2 km of the troposphere, on average) favors lightning production. Convergence in this layer lifts water vapor upward where it can eventually form into supercooled water droplets, ice crystals, and graupel.

3.1.9.6. Capping in the PBL. A weak cap to upward vertical motion, represented by a Lid Strength Index (LSI) less than 6°C and/or Convective Inhibition (CIN) greater than -100 J kg^{-1}, is favorable for lightning. Weak capping does not overly suppress upward vertical motion, which allows moisture to be carried aloft for the development of supercooled water droplets, ice crystals, and graupel.

3.1.9.7. Relative humidity about the lifting condensation level (LCL). RH should generally be greater than or equal to 90% in the 75 mb layer above the LCL if thunderstorm development is to occur. (Note: For areas above 1000 meters, RH should be greater than or equal to 70% in the 50 mb layer above the LCL.) Air parcels that are saturated at the LCL become diluted by dry air as they ascend above the LCL when the relative humidity is too low; dry air decreases the buoyancy of the ascending parcels, and often causes their ascent to cease.

3.1.9.8. Precipitable Water. When precipitable water steadily increases over time (at least 0.1" in 6 hours) and/or exceeds 150% of normal, lightning becomes increasingly likely. Steadily increasing and/or high PW is indicative of increasing/substantial water vapor available for the eventual creation of supercooled water droplets, ice crystals, and graupel, all of which contribute to the thunderstorm electrification process.

3.1.10. Thunderstorm hazards – tornadoes. The following key parameters must be analyzed when determining if the environment is favorable for tornadoes:

3.1.10.1. Zero to three km wind profile. An environment conducive to tornadogenesis will be characterized by a veering (clockwise turning) wind profile in the lowest 3 km of the troposphere. Tornadoes can develop with veering or backing winds in the lower troposphere, and even with straight winds that have strong speed shear. However, in the Northern Hemisphere, the majority of tornadoes occur in environments where the low-level winds veer with height. A particularly favorable environment will feature surface winds from the southeast at greater than 15 knots. The veering winds create positive horizontal vorticity (spin) that can be tilted into the vertical by an updraft.

3.1.10.2. Zero to six km wind shear. A strong, deep layer of vertical wind shear is favorable for the development of tornadoes; a favorable shear profile is generally characterized by wind shear from the surface to six km of at least 30 knots, with values greater than 40 knots being optimal. This magnitude of deep layer vertical wind shear ventilates thunderstorm updrafts, separating them from negatively buoyant downdrafts. In this manner, the updraft of a supercell can be maintained for several hours. Additionally, substantial 0-6 km wind shear creates a strong vertical pressure gradient, which enhances updrafts already produced by mechanical lift (fronts, low-convergence, etc.) and positive buoyancy (sufficiently large CAPE).

3.1.10.3. Inflow layer wind speeds. If warm, moist winds exceeding 15 knots are ingested into a thunderstorm's inflow layer, updraft strength will be enhanced and updrafts will be maintained. Further, strong inflow layer winds can enhance the low-level vertical wind shear profile, increasing tornado potential. Once inflow is cut off or becomes too weak, thunderstorm outflow from negatively buoyant and precipitation-loaded downdrafts tends to overwhelm ongoing thunderstorms, thereby eliminating the potential that they will spawn tornadoes.

3.1.10.4. Storm Relative Helicity (SRH). SRH estimates a thunderstorm's potential to acquire a rotating updraft given an environmental vertical wind shear profile. Larger SRH values are indicative of a higher probability that rotating updrafts will develop in ongoing thunderstorms. SRH is not a "tornado predictor" by itself; it's conditional upon thunderstorm development, and not useful unless thunderstorms are ongoing, since it's calculated in a storm relative framework. Traditionally, 0-3 km SRH is used to evaluate storm type and rotation potential; values greater than $250 \text{ m}^2 \text{ s}^{-2}$ suggest an increased threat of tornadoes with supercells, and 0-3 km SRH values exceeding $300 \text{ m}^2 \text{ s}^{-2}$ are usually found in environments that produce violent tornadoes. 0-1 km SRH is an indicator of the potential for low-level rotation, and has been found to be useful for distinguishing between non-tornadic and tornadic supercells. At least $100 \text{ m}^2 \text{ s}^{-2}$ of 0-1 km SRH is needed for tornadogenesis on most occasions. Frontal and outflow boundaries often focus and enhance SRH, leading to an increased probability of tornadogenesis.

3.1.10.5. CAPE. Tornadoes can occur within a very wide range of CAPE values, but most tornadoes occur when CAPE is between $1,500 \text{ J kg}^{-1}$ and $4,000 \text{ J kg}^{-1}$. Maximum updraft strength is directly proportional to the amount of CAPE, so the larger the CAPE, the stronger the resultant updraft that can develop to tilt horizontal vorticity into the vertical.

3.1.10.6. Convective Inhibition (CIN). A weak cap to upward vertical motion, indicated by CIN greater than -100 J kg^{-1}, is favorable for severe thunderstorm development because excess energy builds up below the cap. This energy is released if the cap breaks, leading to explosive thunderstorm development. However, if the cap is too strong, thunderstorms will have a difficult time developing in the first place and tornado potential will be greatly reduced.

3.1.10.7. Bulk Richardson Number (BRN). The BRN is a non-dimensional ratio of CAPE to vertical wind shear, and is used to characterize connective-storm types for various environments. Small CAPE and large shear values result in small BRN values (commonly found during the late autumn and winter months); thunderstorms may develop in this environment, but they are likely to be sheared apart. Conversely, large CAPE and small shear values result in large values of the BRN (commonly found during the summer months); thunderstorms developing in this environment are likely to be pulse storms that do not develop into supercells. Values of BRN between 10 and 45 are indicative of an optimal balance of CAPE and vertical wind shear for supercell and possible tornado development.

3.1.10.8. The lifting condensation level (LCL). The LCL is the level at which an unsaturated ascending air parcel becomes saturated; it's an excellent proxy of cumuliform cloud bases. An LCL near the surface indicates the presence of substantial boundary layer moisture, and thunderstorm updrafts are therefore less likely to entrain dry air. This increases positive buoyancy and the potential for tornadogenesis. Additionally, when the LCL is low, cold outflow is less likely to undercut the updraft and interfere with developing tornadic circulations. Most tornadoes occur when the LCL is below 1,500 meters, and significant (EF2+) tornadoes almost always occur when the LCL is 1,000 meters or lower.

3.2. Synoptic Patterns. There are several basic synoptic weather patterns that can produce severe weather in the mid-latitudes; areas for likely thunderstorm development often experience some combination of mid-level jets or wind shear, dry-air intrusions between 850 mb and 700 mb, and low-level moisture gradients. These parameters are proven severe thunderstorm triggering mechanisms, and can help identify where severe thunderstorm outbreaks will occur in each of the synoptic patterns. Mid-level jets (wind speed and shear maxima between 700-500 mb) can indicate areas of thunderstorm and tornado development. Dry-air intrusions at 700 mb are a major triggering mechanism for tornadoes, and can be used to pinpoint areas of potential severe thunderstorm development. Dry-air intrusions are difficult to identify by a particular temperature/dew-point spread or relative humidity, since the values vary widely from case to case. They can often be identified by looking at the intensity with which drier air is being forced into the moist air. Most severe thunderstorm outbreaks are associated with strong low-level (below 700 mb) moisture gradients; the gradient axes are generally located on the windward side of the outbreak area. The intensity of the storm is proportional to the tightness of the moisture gradient along the wind component from dry to moist air. When the 850 mb or 925 mb product is not representative of moisture below 700 mb, the moisture gradient can often be determined from satellite imagery and model-generated vertical cross sections. **Table 3.1** shows an empirical relationship between various values of these parameters and the potential for severe thunderstorm development.

Table 3.1. Severe thunderstorm development potential.

Parameters	Weak	Moderate	Strong
Mid-level jet speed	35 knots	35-50 knots	Greater than 50 knots
Horizontal shear	15 knots/90 NM	15-30 knots/90 NM	Greater than 30 knots/90 NM
Wind crossing the axis of 700 mb dry intrusions and moisture boundaries	Less than 20°	20°-40°	Greater than 40°
Surface dew point	Less than 13°C	13°C-18°C	Greater than 18°C
850 mb dew point	Less than 8°C	8°-12°C	Greater than 12°C
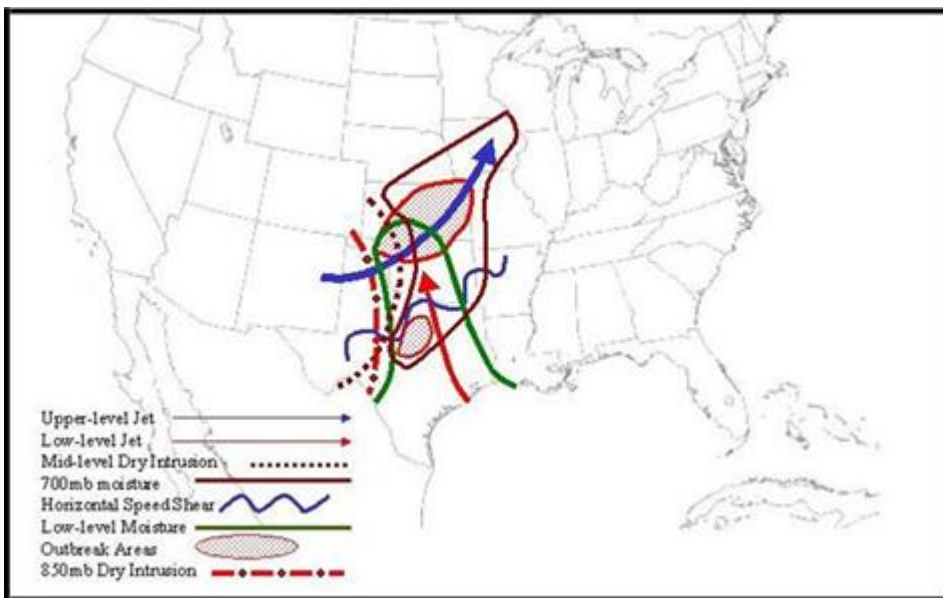
3.2.1. Classic Synoptic Convective Weather Patterns. Identifying severe synoptic patterns is essential to identifying areas of potentially severe thunderstorms; successful severe weather forecasting is dependent on the ability to analyze, coordinate, and assess the relative values of a multitude of meteorological variables and mentally integrate and project these variables three-dimensionally in space and time. Identification of severe synoptic patterns saves time and allows a focused effort on the threat area. In the severe weather patterns outlined below, the parameters are morning depictions (12Z for CONUS), while the outbreak areas are depicted at the time of occurrence, which may later in the day; advection of severe weather parameters must be taken into account.

3.2.1.1. Type A synoptic pattern (dryline). With this type of synoptic pattern (**Figure 3.8**), thunderstorms initially form on the edge of a sharp moisture gradient. Storms tend to form rapidly in widespread, isolated clusters.

3.2.1.1.1. Characteristics. The type A pattern is defined by a well-established southwesterly 500 mb jet, a distinct surface-to-700 mb warm dry-air intrusion from the southwest, low-level confluence along the dry line, and low-level moisture advection from the south, ahead of the dry air. Convective development with this pattern is characterized by extremely rapid growth (15-30 minutes) from inception to maturity, with almost immediate production of large hail, damaging winds, and tornadoes.

3.2.1.1.2. Initial outbreak area. Severe storm formation is usually confined to the edge of the dry air at 850 mb and 700 mb, and the convergence area between the moist and dry air (the area of maximum moisture gradient). These storms will form rapidly, in isolated clusters, along the leading edge of the dry intrusion. Sharp, well-defined squall lines aren't common with this pattern.

Figure 3.8. Type A severe weather synoptic pattern - dryline.
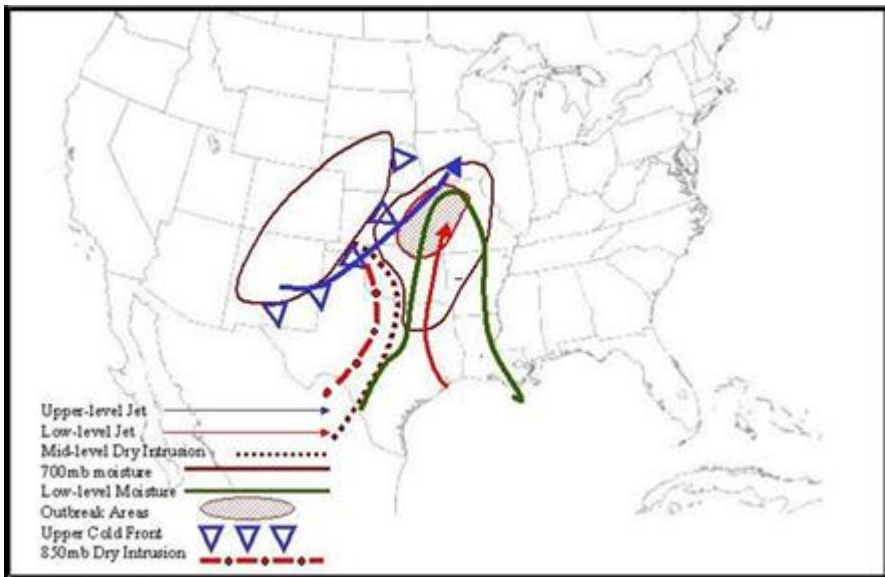
3.2.1.1.3. Severe weather area. In a type A pattern, severe weather typically extends up to 200 miles to the right of the 500 mb jet, and from the area of maximum low-level convergence to the area of rapidly decreasing moisture along the moisture gradient. The most violent storms usually form where the jet meets the moist/dry air convergence area. A secondary outbreak area can occur along and 150 miles to the right of the 500 mb horizontal speed shear zone; it extends from the maximum low-level convergence area to the point where low level moisture decreases on the dry side of the moisture gradient.

3.2.1.1.4. Trigger mechanisms. Type A storm development can be triggered by several factors, such as diurnal heating, passage of an upper-level jet max, low level intrusions of warm, moist air east of the dryline, or mid-level dry air moving into a moist region.

3.2.1.1.5. Timing. In type A situations, look for thunderstorms to develop at the time of maximum heating, or up to 6 hours afterwards. Under normal circumstances, convection is usually capped by an inversion until the convective temperature is reached. Once convective activity has started, expect it continue for at least 6-8 hours, and possibly longer. The convective activity may last until the moist and dry air are completely mixed, changing the airmass's stability.

3.2.1.2. Type B synoptic pattern (frontal). The Type B pattern (**Figure 3.9**) is defined by prefrontal squall lines with one or more mesoscale lows. These squall lines form at the intersection of the low-level jet and the upper-level jet. The lows often form in the area of the intersection of the low-level jet and the warm front and are frequently accompanied by tornadic outbreaks.

Figure 3.9. Type B severe weather synoptic pattern - frontal.

3.2.1.2.1. Characteristics. Type B systems are characterized by a well-defined 500 mb jet stream, a well-defined dry air intrusion between the surface and 700 mb, a strong unstable wave with associated warm and cold fronts, and a low-level jet, which is instrumental in transporting warm, moist air from the south. Most type B systems have frontal and/or pre-frontal squall lines, with strong cold-air advection behind the front. There will also be cool, moist air present along the 500 mb and 700 mb trough axes – the axes will lie to the immediate west of the threat area. Low and mid-level confluence between low-level warm air and mid-level cooler air will also be present.

3.2.1.2.2. Severe weather. The severe weather occurring with the type B pattern is associated with strong cold air advection and strong cold fronts. This type of system can occur at any time of the year, but it's most frequent in the spring. As cold air moves into the threat area, it collides with warm, moist air advecting from the south. This collision of contrasting air masses leads to strong thunderstorms.

3.2.1.2.3. Severe weather areas. Several events occur in the initial severe weather area, beginning with the development of mesoscale lows at the intersection of the low-level jet and the warm front; as the meso-low develops, upward vertical motion in the area is increased. The location of severe weather depends on the speed of the cold front, coupled with the speed of the dry intrusion area. The best potential for severe weather is along and 150 miles to the right of the horizontal speed zone of the upper-level jet, but the area of concern can extend down to the leading edge of the dry air intrusion. The threat area does not extend into the dry air, as the absence of moisture decreases the chance of thunderstorm development.

3.2.1.2.4. Trigger mechanisms. The main trigger for type B systems is an approaching cold front, coupled with the dry air intrusion; the cold front provides lift, and the dry air decreases stability. Intersecting lines of discontinuity can also spur initial development; watch for intersecting squall lines or upper and lower-level jet streams, and the intersection of a low-level jet with a warm front.

3.2.1.2.5. Timing. In this pattern, thunderstorms can occur anytime, and may last all day and night. Type B thunderstorms do not require diurnal heating, and as long as the airmass stays unstable, thunderstorms in a squall line can persist.
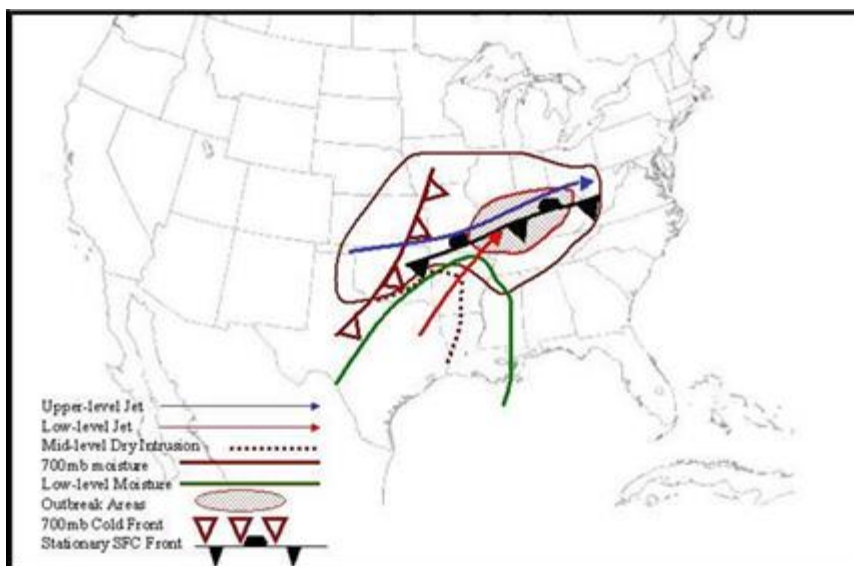
3.2.1.3. Type C synoptic pattern (overrunning). Type C patterns (**Figure 3.10**) generate severe weather conditions by overrunning – warm, moist air overrunning cold, dense air. If the warm air is sufficiently unstable, the lift over the cold air enhances upward motion and enhances the development of thunderstorms.

3.2.1.3.1. Characteristics. Type C patterns have an east-to-west oriented stationary front, with warm, moist overrunning tropical air. In addition, a west-southwest to west-northwest upper-level jet or a strong 500 mb westerly horizontal wind speed shear zone will be present. There will also be a 700 mb dry intrusion advecting in from the southwest.

3.2.1.3.2. Severe weather. Damaging winds and large hail are possible in a type C pattern; tornadoes may occur when surface dew points are 50°F or higher; latent heat release at dew points that high may provide sufficient energy for tornado formation.

3.2.1.3.3. Severe weather areas. Scattered thunderstorms will develop on and north of the stationary front due to the overrunning; in the overrunning region, a squall line may form along the leading edge of the dry air intrusion and thunderstorms may reach severe levels. The severe threat area extends from approximately 50 miles west of the axis of maximum overrunning to the eastern edge of the overrunning.

Figure 3.10. Type C severe weather synoptic pattern – overrunning.

3.2.1.3.4. Trigger mechanisms. The overrunning is the chief trigger for type C scenarios; maximum diurnal heating and a dry-air intrusion where thunderstorms are already occurring are several other triggers under this pattern.
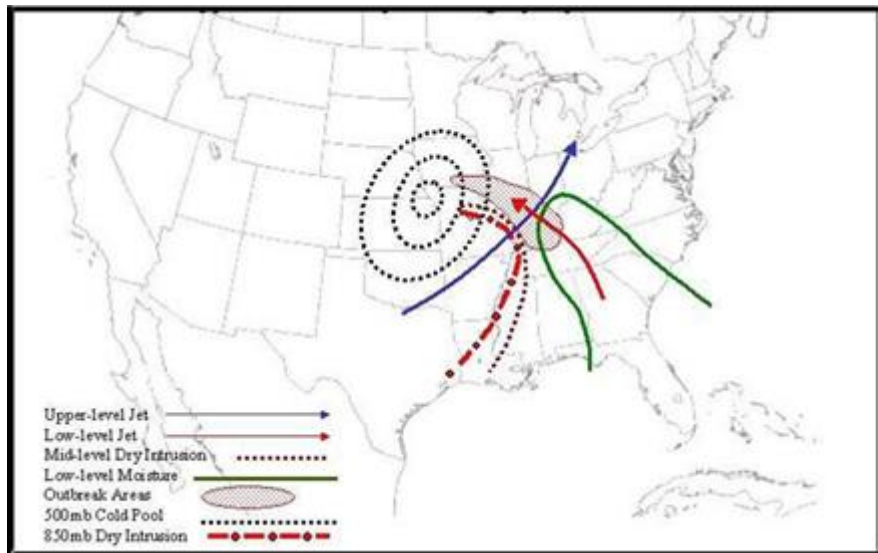
3.2.1.3.5. Timing. Severe thunderstorm occurrence and duration depends on the onset time of dry air intrusion and maximum heating; severe weather continues until the dry air intrusion decreases or moves out. Severe activity can last up to 6 hours after maximum heating.

3.2.1.4. Type D synoptic pattern (cold core). Type D patterns (**Figure 3.11**) are noted for funnel clouds and large hail. Tornadoes are rare, but can occur with strong systems. The defining feature of a type D system is the cold core.

3.2.1.4.1. Characteristics. Type D systems have a deep, southerly upper-level jet, along with a deepening surface low, a 500 mb cold-core low, and cool dry air advection at all levels. There will also be a low-level jet advecting warm, moist air from the south-southeast, under the cold air aloft.

3.2.1.4.2. Severe weather. Hail and funnel clouds may occur with these types of scenarios. Funnel clouds in the Type D Pattern are often referred to as "cold air" funnels, as their formation is caused by warm air moving under cold air aloft, which is associated with a cold core low at 500 mb.

Figure 3.11. Type D severe weather synoptic pattern – cold core.

3.2.1.4.3. Severe weather areas. Thunderstorms will form in the area between the upper-level jet and the closed isotherm center at 500 mb. Severe weather may occur in the region bounded by the cold core low, the front edge of the dry air intrusion, the east-northeast limit of the underrunning warm air, and the area approximately 150 miles right of the upper-level jet.
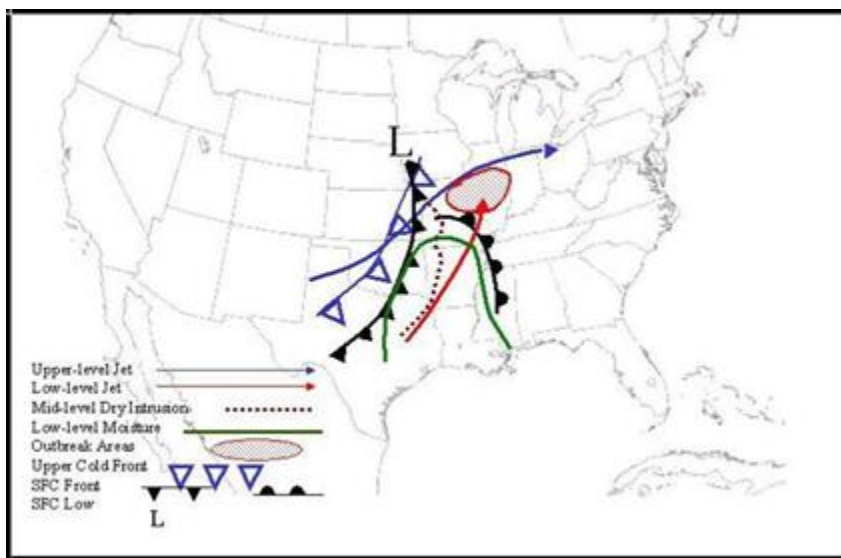
3.2.1.4.4. Trigger mechanisms. There are two main triggers for type D systems; intense low-level confluence and decreasing stability due to the upper-level cold air moving over warm, moist air.

3.2.1.4.5. Timing. Severe weather typically occurs during or shortly after max heating, with a rapid decrease in intensity after sunset.

3.2.1.5. Type E synoptic pattern (squall line). With type E systems (**Figure 3.12**), frontal or prefrontal squall lines are usually well defined; the squall lines may be fast or slow moving. In either case, severe storms develop rapidly.

3.2.1.5.1. Characteristics. Type E systems have a well-defined upper-level westerly jet, along with a well-defined dry air region bounded by a 700 mb warm sector. Low level convergence will be present, along with moderate-to-strong southerly low-level flow advecting warm, moist air over cooler, drier air. In addition to developing ahead of cold fronts, squall lines associated with the type E pattern also develop ahead of warm and occluded fronts. Squall lines may form as a line, or may organize into a line from a cluster of cells; the component of low-level winds shear perpendicular to the line orientation is the most critical factor for squall line structure and evolution. A typical squall line life cycle is to evolve from a narrow band of intense convective cells to a broader, weaker system. The timing of this evolution is strongly dependent on the magnitude of the low-level vertical wind shear; stronger shear leads to longer-lived squall line systems.

Figure 3.12. Type E severe weather synoptic pattern – squall line.

3.2.1.5.2. Severe weather areas. Severe weather may develop along and south of the upper-level jet but north of the 850 mb warm front. The west-east boundary is from the 700 mb cold front to the area of increasing stability. Thunderstorms form in the overrunning warm air between the 850 mb warm front and the upper-level jet axis, where the 700 mb dry air intrusion meets the frontal lifting of the warm, moist air in the low-levels, and the strong 500 mb cold air advection. A secondary threat area exists where the 700 mb dry air intrusion extends south of the 850 mb warm front. Thunderstorms can develop along the 500 mb horizontal speed shear zone and along transitory, active squall lines.

3.2.1.5.3. Trigger mechanisms. The main drivers for severe development in type E systems are frontal lifting of warm, moist and unstable air, a 700 mb dry air intrusion, diurnal heating, and cold air advection at 500 mb.

3.2.1.5.4. Timing. Thunderstorms develop with the onset of 500 mb cold air advection into the severe outbreak area; maximum severe activity occurs from the time of maximum heating to a few hours after sunset. Severe storms may continue until midnight, or until the airmass becomes more stable.

3.3. Convective Weather Tools. The thermal instability of an air parcel can be expressed as a numerical value using a wide variety of stability indices; these tools are aids for determining severe weather potential, and should not be used as the sole basis for making a thunderstorm forecast.

3.3.1. Stability Indices. **Table 3.2** lists various general thunderstorm indices and threshold values, and **Table 3.3** shows indices and threshold values for severe weather potential. **Table 3.4** and **Table 3.5** show various tornado indicators. Thresholds vary from location to location, so closely monitor these indices to discover the best value for local use and adjust accordingly; the best way to evaluate a threshold is to keep a continuous record of their effectiveness. Regional values are provided where available. Each index is described in further detail below.

3.3.1.1. *Convective Available Potential Energy (CAPE).* CAPE is a measure of the convective instability of the atmosphere and thus, the potential for thunderstorms. CAPE values are not a direct indicator of severe weather; they should be used in conjunction with helicity (a measure of the rotation potential of a column of air). Depending on helicity, severe thunderstorms and tornadoes can occur under a wide range of CAPE values.

Table 3.2. General thunderstorm (instability) indicators.

General Thunderstorm (Instability) Indicators				
Index	Region	Weak (Low)	Moderate	Strong (High)
CAPE		300 to 1000	1000 to 2500	2500 to 5300
Cross Totals (CT)	East of Rockies	<18 No TSTMS	18 to 19	=> 20
	Gulf Coast	<16 No TSTMS	20 to 21	
Dynamic Index	Airmass TSTMS	Positive numbers		Negative numbers
Fawbush-Miller Index		0 to -2	-2 to -6	<-6 Svr Possible
GSI Index	Mediterranean	>8		<8
K Index (KI)	East of Rockies	20 to 26	26 to 35	>35
	(mT air masses),			
	and the Tropics			
	West of Rockies	15 to 21	21 to 30	>30
	(mT)			
KO Index (KO)	Cool, moist			
	climates: Europe,	>6	2 to 6	<2
	Pacific NW			
Lifted Index (LI)		0 to -2	-3 to -5	-5 and lower
S-Index	Europe, April-	< 39	≥ 40 and < 46	≥ 46
	September only	No thunderstorms	Thunderstorms possible	Thunderstorms likely
Showalter Stability Index (SSI)	US	> +3	+2 to -2	< -3 Svr Psbl
	Europe	> 2	< 2	
		No thunderstorms	Thunderstorms	
Total Totals (TT)	West of Rockies	48 to 51	52 to 54	> 54
	East of Rockies	44 to 45	46 to 48	> 48
	Europe	> 42	> 48	> 50
Vertical Totals (VT)	US: general			> 26
	Gulf Coast			> 23
	West of Rockies	< 28	28 to 32	> 32
		No thunderstorms		
	UK			> 22
	W. Europe			> 28

3.3.1.2. *Bulk Richardson Number (BRN)*. Discussed in detail earlier in the chapter, the BRN is a better indicator of storm type than of storm severity or storm rotation; it's useful in differentiating between weak, multi-cellular storms (non-severe) and supercell-storm (severe) types. This index is a measure of turbulent energy (a ratio of buoyancy to vertical wind shear) in a column of air to enhance or hinder convective activity. The BRN is most accurate when the CAPE index is between 1500 and 3500 J/kg; when CAPE is less than 1000 J/kg and accompanied by moderate wind shear, the BRN may indicate supercells, but the lack of buoyancy is likely to inhibit severe weather occurrence. If CAPE is greater than 3500 J/kg with a moderate wind shear environment, BRN values may suggest multi-cell storms (non-severe storms), but the buoyant energy will be sufficient to produce tornadoes and large hail. BRN values between 10 and 45 are indicative of supercell and possible tornado development.

Table 3.3. Severe thunderstorm indicators.

Severe Thunderstorm Indicators				
Index	**Region**	**Weak (Low)**	**Moderate**	**Strong (High)**
Bulk Richardson Number (BRN)		> 50		10 to 50
		Multi-cellular storms		Supercells
Cross Totals (CT)	East of Rockies	22 to 23	24 to 25	> 25
	Gulf Coast	16 to 21	22 to 25	> 25
	West of Rockies	< 22	22 to 25	> 25
Modified Lifted Index (MLI)	Europe	0 to -2	-3 to -5	-5 and lower
Surface Cross Totals (SCTI)	East of 100°W			=> 27
	High Plains			=> 25
	Foothills of Rockies			=> 22
SWEAT Index	Midwest and Plains	< 275	275 - 300	=> 300
	(unreliable at higher elevations)			
Thompson Index (TI)	Over the Rockies	20 to 29	30 to 34	=> 35
	East of Rockies	25 to 34	35 to 39	=> 40
Total-Totals (TT)	West of Rockies	55 to 57	58 to 60	=> 61
	East of Rockies	48 to 49	50 to 55	=> 56
Wet-Bulb Zero (WBZ) Height	Not for use with deep mT air masses	< 5,000 ft	5,000 to 12,000 ft	7,000 to 9,000 ft
			Large Hail	Tornado

Table 3.4. Tornado indicators.

Tornado Indicators		
Index	**Value**	**Interpretation**
Energy/Helicity Index (EHI)	0.8 to 1	Weak tornadoes.
	1 to 4	Strong tornadoes.
	> 4	**Violent tornadoes.**
Lifted Index (LI)	< -6	Tornadoes possible.
Mean Storm Inflow (MSI)	> 20	Mesocyclone development possible.
Showalter Index (SSI)	< -6	Tornadoes possible.
Storm Relative Directional Shear (SRDS)	> 70	Mesocyclone development possible
Storm Relative Helicity (SRH)	> 400	Tornadoes possible.
SWEAT Index	≥ 400	Tornadoes possible.
Wet-Bulb Zero (WBZ) Height	7,000 to 9,000 ft (mP)	Families of tornadoes.
	≥ 11,000 ft (mT)	Single tornadoes.

Table 3.5. Tornado forecasting tools.

Tool	Parameter(s) Measured	Indicator for:
Bulk Richardson Number (BRN).	Buoyancy and wind shear.	Storm type: multicell, supercell.
Convective Available Potential Energy (CAPE).	Buoyancy.	Potential updraft strength, which relates to storm intensity.
Energy/Helicity Index (EHI).	Combines CAPE and SRH.	Tornadoes.
Mean Storm Inflow (MSI).	Storm relative winds.	Mesocyclone development.
Storm Relative Directional Shear (SRDS).	Low-level vorticity (i.e., strong low-level cyclonic circulation).	Mesocyclone development.
Storm Relative Helicity (SRH).	Potential for a rotating updraft, horizontal vorticity due to wind shear.	Supercells and tornadoes.
Hodographs.	Vertical and horizontal directional and speed shear, mean wind, storm motion, storm inflow, helicity.	Storm type: single cell, multicell, and supercell.

3.3.1.3. *Cross Totals (CT).* The CT index compares low-level moisture and upper-level temperature; it's optimized for thunderstorm coverage and severity east of the Rockies and along the Gulf Coast. The CT value is contingent on the low-level moisture band being at 850 mb and the cold air pocket at 500 mb; if the moisture and cold air are centered slightly above or below these levels, CT values will not be a reliable indicator of thunderstorm coverage or severity.

3.3.1.4. *Dynamic Index.* This index is designed for airmass thunderstorms; positive values indicate stability, and negative numbers indicate a conditionally unstable air mass. A triggering mechanism is needed for thunderstorms to occur when conditionally unstable; diurnal heating is usually enough to trigger the convection.

3.3.1.5. *Energy/Helicity Index (EHI).* The EHI should only be used if strong thunderstorms are forecast. EHI is a combination of CAPE and Storm Relative Helicity (S-RH), which measures the contribution of convective instability of the atmosphere and shear vorticity to the potential for tornado formation. Strong-to-violent tornadoes are associated with a wide range of CAPE values: large CAPE values combined with low wind shear and low CAPE values combined with high wind shear are both capable of producing conditions favorable for the development of tornadoes.

3.3.1.6. *Fawbush-Miller Stability Index (FMI).* This index is similar to the Showalter Stability Index, except it emphasizes the low-level (surface) moisture rather than the 850 mb moisture. Only use the FMI when the Showalter appears to be misrepresenting the low-level moisture.

3.3.1.7. *GSI Index.* This index was developed for use in the central Mediterranean, using the following procedure:

3.3.1.7.1. Obtain the minimum temperature/dew point spread (°C) between 650 mb and 750 mb.

3.3.1.7.2. Obtain the average wet-bulb temperature in the lowest 100 mb by the equal area method. From this point, follow the saturation adiabat to the 500 mb level. Subtract the temperature where the saturation adiabat crosses the 500 mb level from the observed 500 mb temperature (°C).

3.3.1.7.3. Add the values from Step 1 and Step 2 above to calculate GSI.

3.3.1.8. *K index.* As illustrated earlier in this chapter, the K index is primarily used for forecasting heavy rain and lightning potential; it is not an indicator of severe weather. It works best in the summer east of the Rockies in maritime-tropical (mT) air masses and in any tropical region. It has limited use in overrunning situations and in mountainous regions.

3.3.1.9. *KO Index.* The KO index, created by the German Weather Bureau, is sensitive to moisture and works best for cool moist climates (i.e., Europe, Pacific Northwest). The KO Index's drawback is its complexity. The KO equation is: **KO = (Qe500 + Qe700)/2 – (Qe850 + Qe1000)/2.** Where Qe is the equivalent potential temperature at a given level. To find Qe, first find the lifting condensation level (LCL) for the given pressure level. Continue up the moist adiabat until all moisture is removed from the parcel. This occurs at the level where the moist and dry adiabats become parallel. From there, continue up the dry adiabat to the top edge of the chart. There, read Qe directly. Do this for each of the four pressure levels in the equation and plug into the equation. The result is the KO index.

3.3.1.10. *Lifted Index (LI).* As discussed earlier in this chapter, the LI is useful for lightning potential determination; it can be used successfully at most locations, since it contains a good representation of the low-level moisture. This index counters deficiencies in the Showalter Index when low-level moisture and/or inversions are present. However, it fails to consider cold air above 500 mb. Threshold values are generally lower than the Showalter Index.

3.3.1.11. *Modified Lifted Index (MLI).* The MLI considers the destabilizing effects of cold air aloft, which the LI fails to take into account. It works well as a severe thunderstorm indicator in Europe, and has also been used with success in the CONUS. It gives poor results when the -20°C level is above 500 mb (too warm) or below the LCL (too cold).

3.3.1.12. *S Index.* The German Military Geophysical Office developed the S index as a variation of the Total Totals (TT) index. The S Index adds moisture available at 700 mb to a variable parameter based on the Vertical Totals Index (VT). The addition of 700 mb moisture tailors this index for sections of Europe since low-level heating is usually less intense in parts of Europe than it is in the States, and 700-mb moisture is a good predictor of thunderstorm development there. The S Index is useful from April to September. It can be computed from the equation shown in **Table 3.6**.

Table 3.6. S-Index calculation.

S = TT – (700T – 700Td) – A where A is defined as follows:	
VT	**A**
Greater than 25	0
Greater than 22 but less than 25	2
Less than 22	6

3.3.1.13. *Severe Weather Threat Index (SWEAT).* The SWEAT index is designed to predict severe storms and tornadoes, rather than ordinary thunderstorms. High SWEAT values do not necessarily mean that severe weather will occur, since it doesn't consider triggering mechanisms. High SWEAT values based on the morning sounding do not

necessarily imply severe weather will occur, but if SWEAT values remain high for the forecast sounding, then severe weather potential is high.

3.3.1.14. *Showalter Stability Index (SSI).* As discussed earlier in this chapter, the SSI is useful for determining lightning potential; this index works best in the Central United States, with well- developed systems. This index should only be used as a first indication of instability. It doesn't work well if a frontal surface or inversion is present between 850 mb and 500 mb. It also is not a good predictor of severe weather when low-level moisture is present below 850 mb.

3.3.1.15. *Storm-Relative Directional Shear (SRDS).* SRDS is used to measure the amount of directional shear in the lowest 3 km of the atmosphere; strong directional shear contributes significantly to storm rotation.

3.3.1.16. *Storm Relative Helicity (SRH).* Discussed in detail earlier in the chapter, SRH can indicate the likelihood of tornadogenesis; helicity has been found to correlate strongly with the development of rotating updrafts. Helicity is very sensitive to storm motion; storms that encounter boundaries or slow down can have radically different helicities than the general environment. SRH is not a tornado predictor by itself; it's conditional on thunderstorm development. 0-3 km SRH values greater than 250 m^2 s^{-2} suggest an increased threat of tornadoes with supercells, and 0-3 km SRH values exceeding 300 m^2 s^{-2} are usually found in environments that produce violent tornadoes. At lower levels, at least 100 m^2 s^{-2} of 0-1 km SRH is needed for tornadogenesis.

3.3.1.17. *Surface Cross Totals (SCT).* Use SCT to predict severe potential for areas at high elevations.

3.3.1.18. *Thompson Index (TI).* Use TI to determine thunderstorm severity in mountainous regions, such as the Rockies.

3.3.1.19. *Total Totals (TT).* Use TT to forecast thunderstorm coverage and severity. This index is particularly good with cold air aloft. It may over- forecast severe weather when sufficient low-level moisture is not available. The TT index is the sum of the Vertical Totals and Cross Totals.

3.3.1.20. *Vertical Totals (VT).* Use VT in the western United States, the UK, and Western Europe to predict thunderstorm potential.

3.3.1.21. *Wet Bulb Zero Height (WBZ).* The WBZ is often a good indicator of hail and surface gusts greater than 50 knots when it lies between 5000 and 12,000 feet, and of tornadoes when it lies between 7000 and 9000 feet. It is not a good indicator in deep mT air masses, which naturally have high WBZs; hail or strong surface gusts rarely occur in these air masses outside the immediate vicinity of tornadoes. Multiple studies have indicated a strong correlation between the height of WBZ and the types of tornadoes that will occur; depending on the value, WBZ can help predict whether tornadoes will occur in isolated cases or form in groups.

3.3.2. Evaluation and Techniques. There are many data sources available to produce a forecast; atmospheric models and numerical analysis techniques, satellite, radar, conventional upper-air data, and a variety of software applications designed to help forecasters interpret these data. Deciding which tools and data to use in forecasting severe convective weather can be an overwhelming task; the following techniques can assist in the severe forecast process. Start with a knowledge of seasonal thunderstorm activity as described in regional climatology.

3.3.2.1. *Synoptic evaluation for potential severe weather.* Determine if the current and/or forecast weather pattern for the area of interest is favorable for severe convective weather pattern development. After initializing NWP model output, pay close attention to areas where favorable severe convective storm predictors stack with height. The more favorable conditions in a specific area, the greater the chance of development of severe thunderstorms. Use composite products to help stack significant features. When most predictors indicate strong potential for severe weather, seriously consider forecasting severe thunderstorms, tornadoes, strong winds, and/or hail. If predictors indicate weak potential, then consider forecasting non- severe thunderstorms. If indicators are mixed, consider forecasting non-severe thunderstorms with isolated or scattered severe thunderstorms. Finally, if low-level predictors are strong, weak upper-level diffluence is often sufficient to trigger severe weather, and if low-level predictors are marginal, strong upper-level diffluence is necessary to trigger severe convective storms. Incorporate local rules of thumb, forecast discussion bulletins, and various stability indices appropriate for the location into the decision-making process. Don't base a forecast on a single tool when many are available!

3.3.2.2. *Forecast products and techniques.* Begin with the nearest representative Skew-T, and use the techniques described in this document to analyze the sounding for indications of convective instability in the air mass. Determine if the air mass is absolutely or conditionally unstable. Next, analyze the upper-air and surface products; upper-air analyses are not as useful for forecasting airmass thunderstorms as they are for forecasting severe thunderstorms, but they can often help. Local area work charts can play a key role in severe weather analysis, since they're updated hourly; triggering mechanisms are often apparent on a shorter time scale. **Table 3.7** provides a guide on key features on the standard-level charts, and **Table 3.9** identifies key predictors to analyze, as well as their significance to severe weather occurrence.

3.3.2.3. *Identifying tornado features.* The first requirement for tornado prediction is a severe thunderstorm forecast; from there, a determination must be made whether tornadogenesis will occur. The magnitude of various parameters derived from the low-level wind and thermodynamic fields of the atmosphere are keys to tornado formation; the elements that contribute to tornadogenesis are strong storm- relative flow, strong vertical wind shear, strong low-level vorticity (i.e., strong low-level cyclonic circulation), potential for strong rotating updrafts and great instability or buoyancy. All of these elements are associated with supercells, which are known tornado producers. However, not all tornado-producing thunderstorms are supercells. Several tools are available for determining whether conditions exist for tornadogenesis; these are shown in **Table 3.5** with the parameters they measure, and what each tool is used to predict. The actual threshold values are listed in **Table 3.2, Table 3.3, and Table 3.4** Several of these tools indicate storm type rather than tornado type or strength; knowing the expected storm type can indicate where

tornadoes are likely to form within the storm, aiding severe storm METWATCH. Supercell tornadoes develop in the mesocyclone of classic and heavy precipitation supercells, and on the leading edge of the storm updraft in the vicinity of the wall cloud of low-precipitation supercells. Non-supercell tornadoes can occur in the flanking line of a supercell, during the growth stage in the updraft of "pulse" thunderstorms (strong, single-cell storms), along the gust front of multi-cell storms, and in strong updraft centers of multi-cell storms. Tornadoes in single cell and multi-cell storms are rare, and require exceptionally strong development to produce a tornado.

3.3.2.4. *Identifying bow echo features.* A bow echo is a line of storms that accelerates ahead of the main storm area; it forms from strong thunderstorms with a gust front. A strong downburst develops and the line echo wave pattern (LEWP) begins to "bow". A well-developed bow echo   or "spear head" is associated with the mature stage of the downburst; strong winds and tornadoes are possible near the bow. **Figure 3.13** shows the evolution of the bow echo in a LEWP. As the downburst weakens, the line forms a comma shape, with a mesocyclone often developing on the north end of the comma, evident by a "hook" in the radar echo. At this point, tornadoes may still occur in the area of the mesocyclone, but the winds are decreasing. Strong to severe straight-line winds are likely to exist if four specific characteristics of the bow echo are present (See **Figure 3.13** and **Figure 3.14**): the low-level echo configuration is concave downstream, weak echo channels exist, a strong reflectivity gradient along the leading edge of the concave-shaped echo exists, and the maximum echo top is over or ahead of the strong low-level reflectivity gradient.

Figure 3.13. Line echo wave pattern (LEWP) and bow echo evolution.
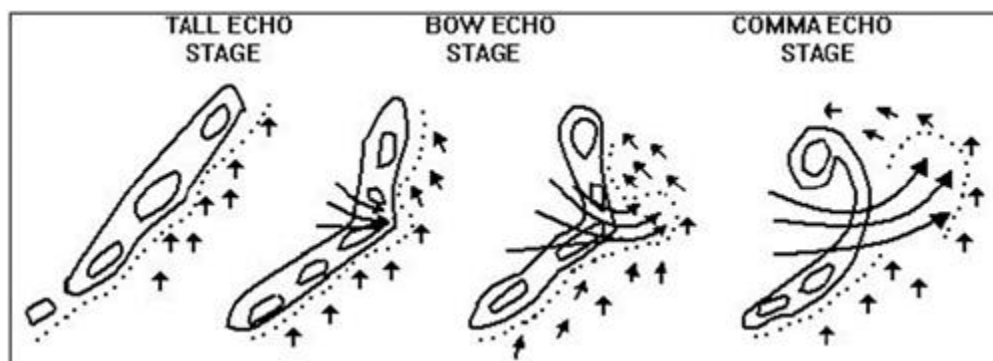
**Figure 3.14. Bow echo schematic and reflectivity example.**
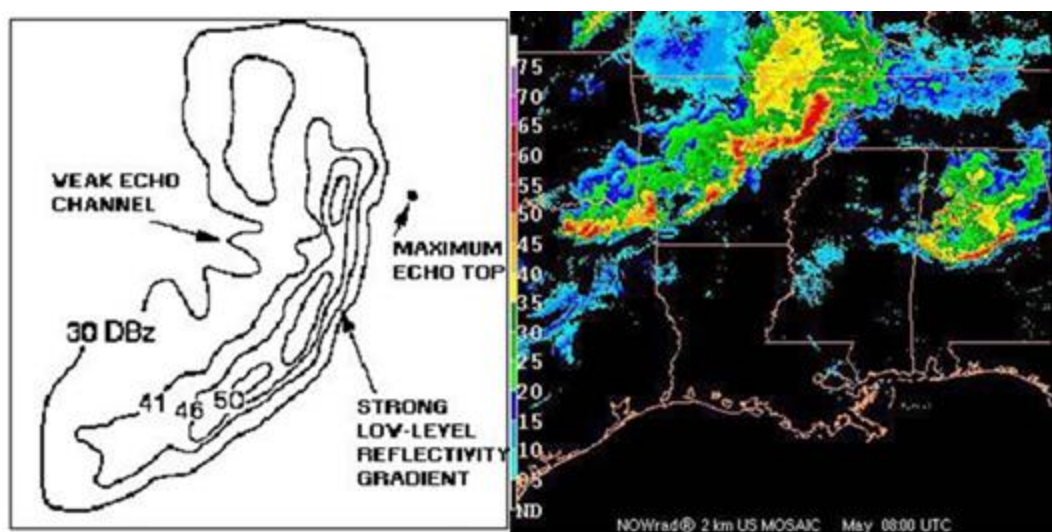
Table 3.7. Product analysis matrix and reasoning.

Charts	Feature to Analyze	Why (favorable/unfavorable; weak, moderate, strong chance for severe weather conditions.)	
200 mb/300 mb	Identify jet maximums.	• ≤55 knots	Weak
		• 56 to 85 knots	Moderate
		• ≥ 86 knots	Strong
	Streamline and identify diffluent areas.	Favorable for development.	
	Shade areas of horizontal wind speed shear.	Favorable for development.	
500 mb	Identify jet maximums.	• ≤ 35 kt	Weak
		• 36 to 49	Moderate
		• ≥ 50	Strong
	Streamline and identify diffluent areas.	Favorable for development.	
	Isopleth 12-hour height falls (Oct to Apr) or 24-hour height falls (May to Sep).	• ≤ 30 m	Weak
		• 31 to 60 m	Moderate
		• ≥ 61 m	Strong
	Perform 2°C isotherm analysis, color cold pools, identify thermal ridges and troughs.	Severe activity suppressed near and east of thermal ridge particularly when in phase with streamline ridge.	
	Identify areas of cold air advection.	The following temperatures are favorable:	
		• Dec to Feb:	-16°C or lower.
		• Mar, Apr, Oct, Nov:	-14°C or lower.
		• May, Jun:	-12°C or lower.
		• Jul to Sep:	-10°C or lower.
	Identify dew-point depressions of 6°C or less, moisture analysis.	Cut-off moisture sources indicate a short wave is present.	
	Identify areas of vorticity advection.	NVA: **Weak Or Not Favorable.**	
		Positive Vorticity isopleths crossing 500-mb height contours:	
		• ≤ 30°	Moderate
		• > 30°	Strong
		Storms develop on the periphery of the vorticity maximum and not directly below.	
700 mb	Perform 2° isotherm analysis, identify thermal troughs and ridges.	Good stacking of cold air here and at 500 mb is favorable for severe.	
	Indicate (12-hour) temperature no-change line.	Advancement of the temp. no-change line ahead of the 700-mb trough indicates the surface low will intensify.	
	Draw dew-point depression lines.	Moisture fields detached from the main moisture field indicate rising motions and a possible short wave in the area.	
	Mark dry line. The dry line can be placed where dew point is ≤ 0°C, the dew point depression is ≥ 7°C, or the RH is ≤ 50 percent.	Weak winds across the dry line: **Weak**	
		Winds 15 to 25 knots crossing between 10° and 40°: **Moderate**	
		Winds ≥ 26 knots crossing between 41° and 90°: **Strong**	
	Streamline and identify confluent areas.	Confluent areas are favorable for severe.	

Charts	Feature to Analyze	Why (favorable/unfavorable; weak, moderate, strong chance for severe weather conditions).
850 mb	Streamline and identify confluent zones.	The greater the angle of winds from dry to moist air, the more unstable.
	Identify wind speed maximums.	• ≤ 20 knots **Weak** • 21 to 34 knots **Moderate** • > 35 knots **Strong**
	Draw every 2°C isotherm starting with an isotherm that bisects the entire U.S. Mark thermal ridges.	Thermal ridge is often ahead of convergence zone. Cold air advection often found behind the main convergence zone, unless a dry line forms and moves out ahead of the cold advection. (Warm air is usually ahead of the main convergence zone).
	Draw isodrosotherms every 2°C starting at 6°C (43°F).	Dew point: • < 8°C (46°F) **Weak** • 9°C to 12°C (48 to 54°C) **Moderate** • ≥ 13°C (55°F) **Strong**

	Color in areas of significant moisture.	A diffuse moisture field is unfavorable for development of severe weather.
		      Thermal ridge east of moisture axis: **Weak**
		      Thermal ridge coincident with the moisture axis: **Moderate**
		      Thermal ridge west of the moisture axis: **Strong**

	Identify dry line.	Note the angle of winds crossing from dry to moist air, the greater the angle, the greater the instability. Where the dry line is intruding into moist areas is unstable.
Surface	2-mb isobar analysis	Surface pressure patterns indicate likely areas for severe weather: • > 1009 mb **Weak** • 1009 to 1005 mb **Moderate** • < 1005 **Strong**
	Isallobaric analysis (12-hour) identify areas of falling pressure.	Squall lines often develop in narrow troughs of falling pressure. A strong pressure rise/fall couplet is favorable for severe weather. The following values indicate probability of severe weather: • ≤ 1 mb **Weak** • 2 to 5 mb **Moderate** • > 6 mb **Strong**
	Identify areas of rapid temperature and dew point change	Favorable for development of severe weather
	2° isodrosotherm analysis starting at 50°F (10°C).	Areas of horizontal moisture convergence are favorable. The following dew point temperatures indicate probability of severe weather: • ≤ 50°F (10°C) **Severe Unlikely** • > 51 to 55°F (11 to 12°C) **Weak** • > 56 to 64°F (13 to 17°C) **Moderate** • > 65°F (18°C) **Strong**
	Identify confluent streamline areas.	Areas of strong winds converging with weak winds is favorable.
	Identify highs, lows, fronts, squall lines, and dry lines and mark their previous locations.	Any discontinuity line is a likely place for thunderstorm development. Intersecting discontinuity lines are highly probable locations for development. Use distance between past and current locations to extrapolate onset of thunderstorms.
1000/500 mb Thickness	Mark thickness ridge.	Probable area for squall line.
	Mark thickness no-change line (12-hour).	Indicates area of cold advection.

Table 3.8. Identifying features of airmass thunderstorm development on upper air charts.

Product	Feature to Analyze	Why (favorable/unfavorable for convective weather conditions.)
200 mb/300 mb	Streamline	Areas under diffluent flow aloft are favorable for thunderstorms; convergence strongly suppresses development.
500 mb	Ridge placement	Convection forms on the confluent side of the ridge axis.
	Vorticity advection	PVA is present, severe weather is possible. NVA or neutral, severe weather unlikely
	Short-wave troughs	Severe weather possible.
850 mb/925 mb	Streamline	Confluence.
	Gradient Winds	Use to forecast steering flow if stronger than forecast sea breeze.
Surface/LAWC	Streamline: Draw convergent asymptotes	Expect convection to begin along these lines when convective temperature is reached.
Composite Workchart	Satellite depiction Radar observations LAWC: streamlines	Identify cells/lines of convection. Identify intersecting boundaries as possible areas for severe winds, heavy rain, and possible hail.
	Mark past positions of significant features.	Use the time difference and distance between related weather features to forecast their future movement, and to forecast areas of intersecting boundaries and development.

3.3.2.5. *Identifying microburst features.* Microbursts are difficult to predict and detect, due to their small spatial scale (less than 4 km diameter), shallow vertical extent, and short life span. Ideal conditions for microburst formation occur when there is relatively warm and moist air in the low levels from the surface to the 700-600 mb (high theta-e), with relatively cool and dry air in the mid-levels from 600 mb to 400 mb (low theta-e). Microburst conditions also have relatively high CAPE values, (greater than 1000 J kg-1), although wet microbursts can occur with lower CAPE values as well. The following techniques can provide guidance on the potential for formation of microbursts.

3.3.2.5.1. Dry microburst forecast technique. Dry microbursts don't only occur from thunderstorms; they may occur from any cumuliform cloud of appreciable vertical extent on top of a mixed (PBL) layer with a dry adiabatic lapse rate. This technique is a rapid way to determine dry microburst potential.

3.3.2.5.1.1. Using a morning sounding, look for a radiational temperature inversion at the surface with a depth of 40-50 mb.

3.3.2.5.1.2. Look for a dry adiabatic layer above this inversion that extends up to a level between 600 mb and 500 mb.

3.3.2.5.1.3. Find the average mixing ratio below the convective condensation level (CCL) and determine if it is less than 5 g/kg.

3.3.2.5.1.4. Look for relative humidity $\geq$ 70% above the dry adiabatic layer (usually at or above 600 mb).

3.3.2.5.1.5. Determine if the convective temperature (CT) for the day will be reached by mixing down the 850 mb temperature dry adiabatically to the surface, or using a model forecast sounding. If the CT will be reached, dry microbursts are possible.

3.3.2.5.1.6. Find the strongest wind speed within the dry adiabatic layer; if all of the above conditions are met, this wind speed may descend to the surface as part of a dry microburst.

3.3.2.5.2. The Dry Microburst Index (DMI). The DMI objectively quantifies dry microburst potential using mid-level lapse rates, as well as the presence or lack of mid-level moisture. The DMI is given by: $\mathbf{DMI = \Gamma + (T - Td)_{700} - (T - Td)_{500}}$. Where Γ is the 700-500 mb lapse rate in °C/km, and T and Td are the 700 mb and 500 mb temperatures and dew points, respectively, in °C. Environments in which the DMI is greater than 6 and instability exists aloft (CAPE greater than 50 J/kg) are considered favorable for dry microbursts. Large DMI values occur in environments with steep mid-level lapse rates, dry 750-700 mb air, and moist 550-500 mb air. Precipitation originating near 500 mb will fall into the dry air below, evaporating and enhancing downdraft magnitude, which may reach the surface as a microburst. Negative buoyancy is further increased if mid-level lapse rates are sufficiently steep.

3.3.2.5.3. Wind Index (WINDEX). The WINDEX is useful to forecast maximum potential wind gusts when both wet and dry microbursts are possible. It is a weighted formula to derive microburst potential based on melting (freezing) level height, lapse rates, and mixing ratios. See **Table 3.9** for the equation for calculating the WINDEX.

Table 3.9. WINDEX Equation.

WINDEX Equation
$$WINDEX = 5\sqrt{[H_M R_Q(\Gamma^2 - 30 + Q_L - 2Q_M)]}$$
H_M = the height of the melting level in km AGL Q_L = the average mixing ratio (g/kg) in the lowest 1 km AGL $R_Q = Q_L/12$ (must be less than or equal to 1) Γ = the lapse rate in °C/km from the surface to the melting level Q_M = the mixing ratio at the melting level

3.3.2.5.3.1. From a sounding, determine the height of the melting level (H_M) in km AGL.

3.3.2.5.3.2. From the sounding, calculate the average mixing ratio (g/kg) in the lowest 1 km above the surface (Q_L).

3.3.2.5.3.3. Calculate the R_Q value (divide the Q_L value from step 2 by 12). If this value is greater than 1, use 1.

3.3.2.5.3.4. From the sounding, calculate the lapse rate (Γ) in °C/km from the surface to the melting level.

3.3.2.5.3.5. From the sounding, find the mixing ratio (g/kg) at the melting level (Q_M).

3.3.2.5.3.6. Plug these values into the WINDEX equation to determine the maximum potential wind gust from a microburst if thunderstorms develop.

3.3.2.5.4. Wet microburst potential using VIL and Echo Tops values. This technique can provide up to 40 minutes of lead time predicting maximum downburst winds from pulse-type (single cell) thunderstorms. In order for this method to be effective, there must be a source of dry (dew-point depression greater than 18°C), potentially cold air between 400 and 500 mb, along with reflectivity values 55 dBZ or greater (allowing for sufficient moisture for entrainment of the air parcel to produce negative buoyancy through evaporative cooling. To predict wind gust potential with this method, find the Echo Top and VIL values of the storm cell and refer to **Table 3.10** for the maximum downburst wind potential in knots. This technique won't work when VIL values are corrupted due to hail contamination, or when thunderstorms are too close to the radar, causing Echo Top estimates to be erroneously low. This technique also works poorly for thunderstorms over 125 NM away from the radar. The VIL and Echo Top method only works for pulse-type air-mass thunderstorms; it won't provide accurate estimates for multi-cell or supercell storms.

Table 3.10. Wet microburst potential table, using VIL and Echo Tops.

					T	O	P	S			
		250	300	350	400	450	500	550	600	650	700
	35	45	42	37	31	23					
	40	49	46	42	38	30	19				
	45	53	50	47	42	36	28	14			
V	50	57	55	51	46	41	34	24			
I	55	60	57	54	50	45	39	31	18		
L	60	63	61	57	54	50	44	37	27		
	65	66	64	61	58	53	48	42	33	21	
	70	69	67	64	61	57	53	46	39	29	
	75	72	70	67	64	60	56	50	44	35	22
	80	75	72	70	67	63	59	54	48	40	29

3.3.2.5.5. Wet microburst potential using the Atkins and Wakimoto (1991) method. Find the maximum equivalent potential temperature (theta-e) value (in degrees Kelvin) at the surface, then find the minimum equivalent potential temperature (theta-e) value (in degrees Kelvin) in the mid-levels, between 600 and 400 mb. Calculate the difference between the values; if the difference is greater than 20K, wet microbursts are likely. If the difference is less than 13K, wet microbursts are unlikely.

3.3.2.5.6. Wet microburst potential using the Microburst-Day Potential Index (MDPI). This method is not a tool for thunderstorm forecasting; it assumes that thunderstorms will develop on the day in question. Find the maximum theta-e value between the surface and 850 mb (in degrees Kelvin), then find the minimum theta-e value between 660 mb and 500 mb (in degrees Kelvin). Calculate the difference between the values and divide by 30; if the MDPI is greater than 1, wet microbursts are likely. If the value is less than 1, wet microbursts are unlikely.
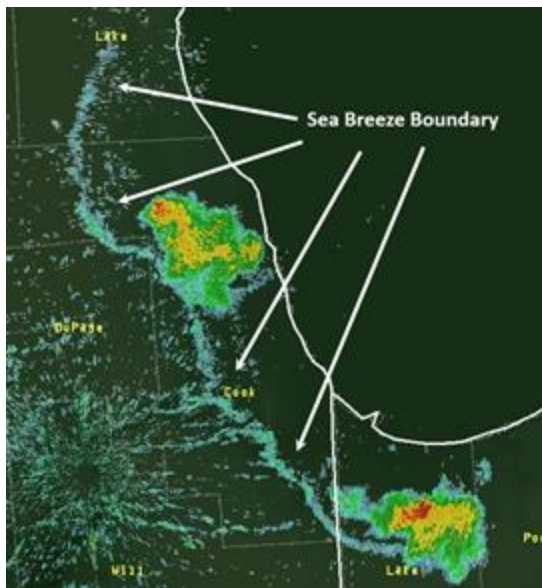
3.3.2.5.7. Wet microburst potential using the Wet Microburst Severity Index (WMSI). This index was developed by case studies of 35 wet microbursts in the eastern and central United States; it may need adjustment for other regions of the world. Find the maximum theta-e value at the surface (in degrees Kelvin), then find the minimum theta-e value (in degrees Kelvin) in the middle levels between 600 mb and 400 mb. Calculate the difference between these two values. Find a representative value of CAPE in the forecast area, multiply the CAPE value by the theta-e difference, then divide the result by 1000; this is the WMSI value. WMSI values between 10 and 49 indicate wind gusts less than 49 knots, WMSI values between 50 and 79 indicate wind gusts from 35-49 knots, and WMSI values greater than 80 equate to wind gusts greater than 50 knots.

3.3.2.6. *Boundaries and boundary interaction features.*

3.3.2.6.1. Satellite. As diurnal heating occurs, cumulus clouds will often form into cloud streets (over land) oriented with the gradient wind flow. Look for clear areas forming in the flow; these identify sea-breeze fronts, lake breezes, and outflow boundaries. The leading edge of these boundaries between clear areas and cloud streets is highly favorable for development. Similarly, the boundary between cloud-free areas and fog or stratus broken/overcast areas are prime for development as clouds burn off. When outflow boundaries intersect, convection is almost guaranteed if the air mass is unstable or conditionally unstable.

3.3.2.6.2. Radar (**Figure 3.15**). Sea breeze boundaries and other discontinuities in low-level flow can usually be identified on base reflectivity displays. The sea breeze will appear as a thin line of low intensity returns, parallel to coastlines. Convection is likely to form on these lines when the convective temperature is reached.

Figure 3.15. Sea breeze on a base reflectivity product.

3.3.2.6.3. Streamline analysis and sea breeze onset. Streamline analyses can be useful when combined with current satellite and radar analyses; create a composite product to identify locations of streamline-confluent asymptotes, sea/lake breezes, and outflow boundaries. Mark past locations of these boundaries, and determine speed and direction of boundary movement to project when and where these boundaries will intersect. The intersections are almost certain to result in air-mass thunderstorms. If thunderstorms are present along the boundaries already, severe weather (usually severe wind gusts) is possible. Tornadoes and hail are unlikely, unless strong upper-level support is evident.

3.3.2.7. *Severe thunderstorm checklist.* No two thunderstorm situations are alike; there are varying degrees of intensity for each parameter, and the combinations of parameters produce individual storm events. A foolproof, all-inclusive checklist for severe weather is impossible to create, so the steps below are an outline of the forecast reasoning process. Incorporate local rules of thumb and stability thresholds to fine-tune these steps for your individual location:

3.3.2.7.1. Identify the current weather regime and expected synoptic type (dryline, frontal, overrunning, cold core, squall line, or airmass thunderstorm).

3.3.2.7.2. Analyze available model data, and tailor the analysis.

3.3.2.7.3. Are elements for severe weather present? Refer to **Table 3.2, Table 3.3, Table 3.4, Table 3.5, Table 3.7,** and **Table 3.8** for features associated with severe weather elements.

3.3.2.7.4. Analyze current and forecast Skew-Ts and calculate stability indices appropriate for the weather pattern and station. Do they indicate severe weather potential?

3.3.2.7.5. Examine current and forecast hodographs; what types of storms can be expected from the wind shear pattern?

3.3.2.7.6. Based on the above steps, what type of severe weather can be expected, if any: winds, hail, or tornadoes?

3.3.2.8. *Forecasting convective wind gusts.* This section presents a variety of methods to forecast convective wind gusts; each technique is designed to forecast winds under different conditions. Each method requires a current or forecast Skew-T.

3.3.2.8.1. T1 gust computation – method 1. The T1 method is designed for scattered thunderstorms in the vicinity of the forecast location; method 1 applies when there's an inversion present within 150-200 mb of the surface and is not susceptible to breaking from surface heating.

3.3.2.8.1.1. Project the moist adiabat from the warmest point of the inversion to the 600 mb level.

3.3.2.8.1.2. Calculate the temperature difference (in °C) between the moist adiabat and the dry-bulb temperature trace at 600 mb. Label this point as T1.

3.3.2.8.1.3. Refer to **Table 3.11**; the value for T1 is considered to be the average gust speed. Add 1/3 of the lowest 5000 foot mean wind speed to the table value to find the maximum gust speed. Wind gust direction can be determined from the mean wind direction in the layer between 10,000 and 14,000 feet above the local terrain.

3.3.2.8.2. T1 gust computation – method 2. This method applies when there's no inversion present, or the inversion is relatively high (more than 200 mb above the surface).

3.3.2.8.2.1. Forecast the maximum surface temperature.

3.3.2.8.2.2. Project the moist adiabat from the maximum temperature to the 600 mb level.

3.3.2.8.2.3. Calculate the difference between the moist adiabat and the dry-bulb temperature trace at 600 mb. Label this point as T1.

3.3.2.8.2.4. Refer to **Table 3.11**; the value for T1 is considered to be the average gust speed. Add 1/3 of the lowest 5000 foot mean wind speed to the table value to find the maximum gust speed. Wind gust direction can be determined from the mean wind direction in the layer between 10,000 and 14,000 feet above the local terrain.

Table 3.11. T1 convective gust potential.

T1 values (°C)	Average Gust Speed (knots)	T1 values (°C)	Average Gust Speed (knots)
3	17	15	49
4	20	16	51
5	23	17	53
6	26	18	55
7	29	19	57
8	32	20	58
9	35	21	60
10	37	22	61
11	39	23	63
12	41	24	64
13	45	25	65
14	47		

3.3.2.8.3. T2 gust computation. The T2 method is designed to determine gust potential for intense squall lines or numerous thunderstorms.

3.3.2.8.3.1. Find the WBZ height – the point where the wet bulb curve crosses the 0°C isotherm.

3.3.2.8.3.2. Project the moist adiabat through the WBZ to the surface, and note the surface temperature in °C at that point.

3.3.2.8.3.3. Subtract the moist adiabat temperature from the surface dry bulb (or projected maximum) temperature; this is the T2 value.

3.3.2.8.3.4. Refer to **Figure 3.16**; follow the T2 value up to the intersection of the three curves. The first intersection point is the minimum gust, the middle intersection point is the average gust, and the upper intersection point is the maximum gust. Wind gust direction can be estimated from the mean wind direction between 10,000 and 14,000 feet.

3.3.2.8.4. Snyder method gust computation. The Snyder method is best used to forecast average wind gusts with airmass or "pulse" type thunderstorms.

3.3.2.8.4.1. Find the WBZ height.

3.3.2.8.4.2. Forecast maximum temperature at time of thunderstorm occurrence (in °F).
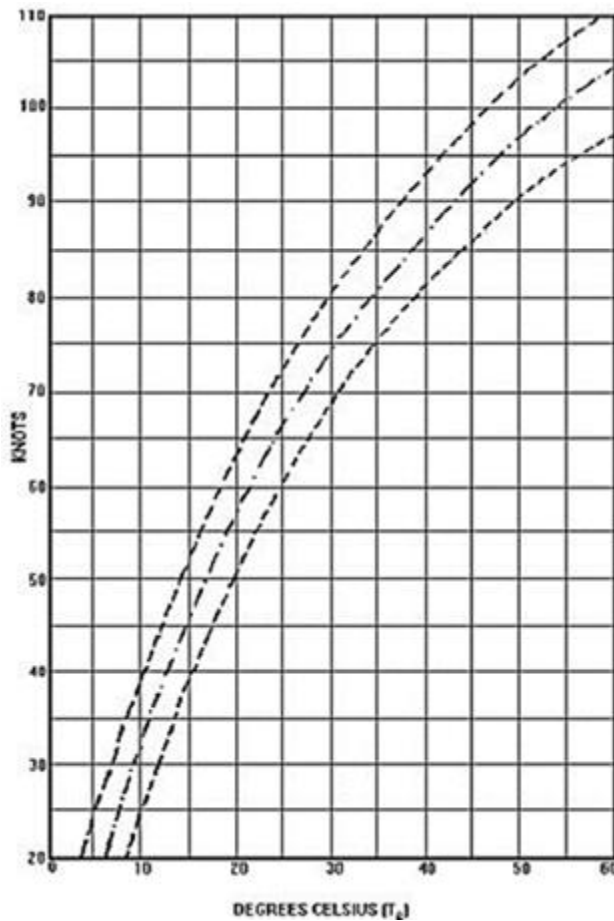
3.3.2.8.4.3. Lower the WBZ to the surface along the moist adiabat, and find the surface temperature (in °F) at the intersection point (the "down rush" temperature).

3.3.2.8.4.4. Subtract the step 3 value from the step 2 value (down rush temperature minus forecast max temperature).

3.3.2.8.4.5. Find half the average wind speed in the 10,000 foot layer centered on the WBZ height (5000 feet below the WBZ height to 5000 feet above the WBZ height).

3.3.2.8.4.6. Add the step 4 value to the step 5 value; this is the average gust potential for air-mass thunderstorms in the current environment.

Figure 3.16. T2 gust computation chart.

3.3.2.9. Hail forecasting. Hail is a common, microscale phenomenon associated with strong thunderstorms; the key factors to determine are whether or not the hail in a thunderstorm will reach the surface, and if so, what size hailstones will fall to the ground.
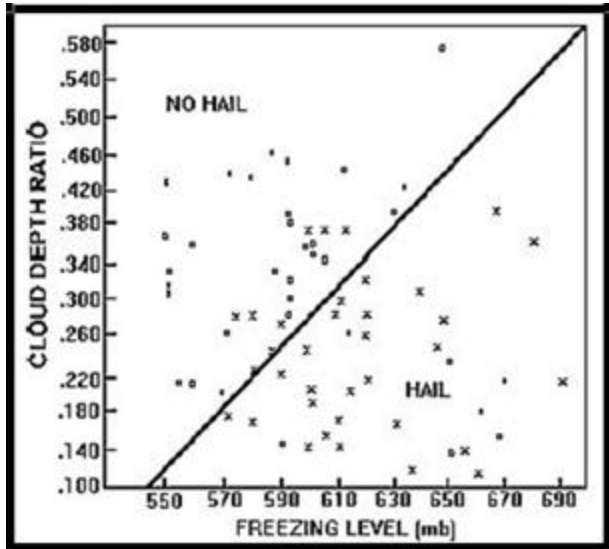
3.3.2.9.1. Forecasting hail occurrence. The first step in hail forecasting is to determine whether or not it will occur; this technique is an objective method derived from numerous case studies of severe thunderstorms over the Midwestern United States. The method determines the cloud depth ratio, and then correlates the ratio and freezing level to occurrence or non-occurrence of hail.

3.3.2.9.1.1. From a Skew-T diagram, calculate the Convective Condensation Level (CCL), Equilibrium Level (EL), and Freezing Level (FL).

3.3.2.9.1.2. Determine the cloud depth ratio using the following equation: **(CCL – FL)/(CCL – EL)**

3.3.2.9.1.3. Plot the cloud depth ratio and freezing level on **Figure 3.17**. If the plot is below the line, expect hail; if it's above the line, hail is not likely to occur.

Figure 3.17. Hail prediction chart, using cloud depth ratio and freezing level.

3.3.2.9.2. Forecasting hail size. If hail is likely to occur, this technique can assist in determining hail size potential.

3.3.2.9.2.1. From a Skew-T diagram, calculate the CCL, then follow the saturation mixing ratio line to its intersection with the temperature trace (**Figure 3.18**, point A).

3.3.2.9.2.2. The intersection of the -5°C isotherm and the sounding is point BH; note the pressure level where this intersection occurs.

3.3.2.9.2.3. From point A, follow the moist adiabat up to the point BH pressure level; this is point B' (**Figure 3.18**).

3.3.2.9.2.4. Calculate the temperature difference (in °C) between points BH and B'.

3.3.2.9.2.5. From point BH, follow the dry adiabat to the CCL; this is point H'. Calculate the temperature difference between BH and H'.

3.3.2.9.2.6. Refer to **Figure 3.19** to forecast preliminary hail size; find the BH-B' temperature difference on the x-axis, the BH-H' temperature difference on the y-axis, and plot the intersection – this will provide an initial estimate of hail size potential.

3.3.2.9.2.7. Find the WBZ height; if it's less than 10,500 feet, the preliminary hail size computed in step 6 will be the final hail size. If the WBZ height is above 10,500 feet, refer to **Figure 3.20** and use the preliminary hail size and WBZ height to determine final hail size potential.

Figure 3.18. Hail size parameters on the Skew-T diagram.
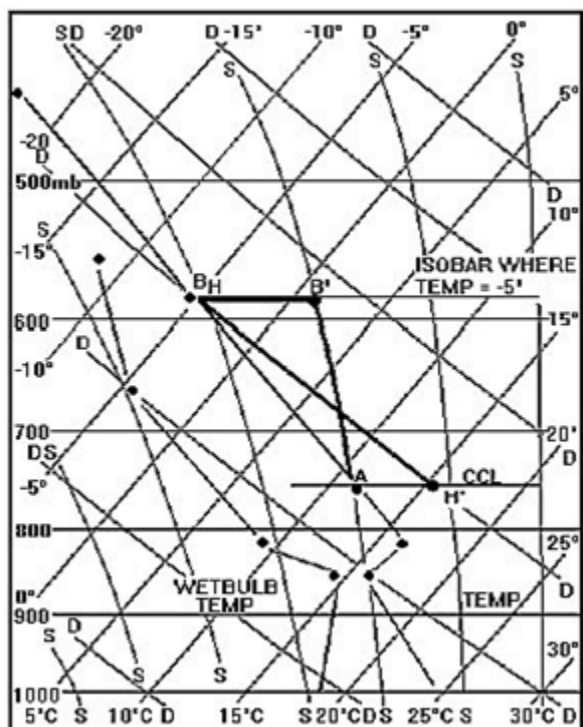
Figure 3.19. Preliminary hail size nomogram.
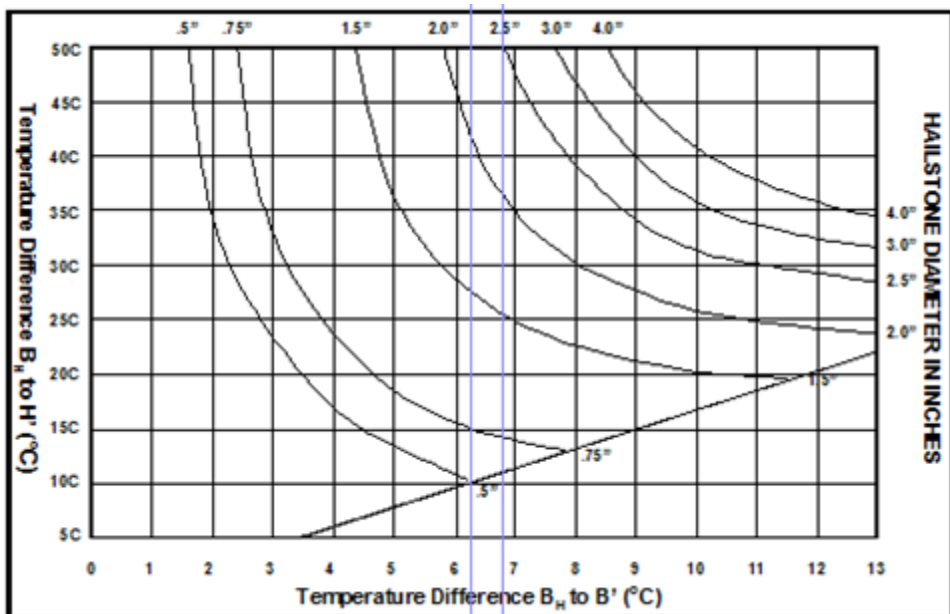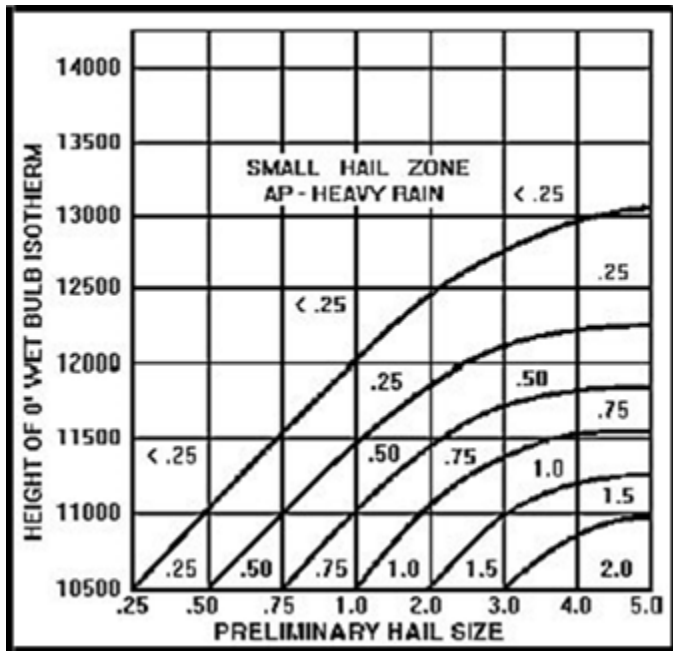
Figure 3.20. Final hail size nomogram – only use if WBZ height is above 10,500 feet.

3.3.2.9.3. Forecasting hail size using VIL density. VIL is a function of radar reflectivity data converted into an equivalent liquid water content value that is largely based on the sensed hydrometeor/target (rain drops, hail, snowflakes, etc.) size distribution. VIL is also a function of a "reflectivity factor" that has target diameter as its primary component (number of targets is a much smaller component). As target diameter increases, so does the reflectivity value. In fact, reflectivity increases exponentially as target diameter increases, so a small increase in target size results in a much more significant increase in the reflectivity value obtained. VIL values increase exponentially with increasing reflectivity, so large VIL values mean high reflectivity, which in turn often indicates the presence of large targets (i.e., hail) within the volume scan. However, VIL alone is not an adequate hail indicator because it is air mass dependent, neglects storm depth, and may be inaccurate for storms very close to or far away from the radar. VIL Density "normalizes" the VIL values using the height of the thunderstorm (i.e., echo top) as indicated by radar. This eliminates the air mass dependency of stand-alone VIL values, and is useful to identify high reflectivity thunderstorms relative to their height. This is important because hail growth is often a function of cloud height/depth. **Table 3.12** shows approximate relationships between VIL density and observed hail sizes; use the VIL density values from observed storms on radar to obtain a quick, real-time hail estimate. VIL Density has the following limitations:

3.3.2.9.3.1. VIL Density only indicates hail aloft. Hailstones that reach the surface may be much smaller than that indicated by the VIL Density values. Examining WBZ levels in tandem with VIL Density values is useful to mitigate this limitation. High VIL Density values and a WBZ Level between 5,000-11,000 feet indicate a higher potential of large hailstones reaching the surface.

3.3.2.9.3.2. VIL and VIL Density values will be quite accurate for slow moving thunderstorms with limited horizontal tilt such as found during the summer months in the mid-latitudes, but less accurate for fast-moving, tilted thunderstorms in environments of strong VWS. This may result in VIL values being averaged and lower than they actually are, resulting in smaller VIL Density values than reality.

3.3.2.9.3.3. Echo tops associated with reflectivity values greater than 18 dBZ may not be accurate because of scanning strategies chosen. In general, Volume Coverage Pattern (VCP) 11 does a better job of estimating VIL and echo top values than VCP 21.

Table 3.12. VIL density and hail size.

VIL Density	Hail Size
≥ 3.5 g/m^3	$\geq$ ¾ inch
≥ 4.0	≥ 1 inch
≥ 4.3	$\geq$ Golf ball size

3.3.2.10. Onset of typical thunderstorms. Predict thunderstorm onset at the time when the convective temperature is forecast, or maximum solar heating is expected. Predict formation along confluent streamline asymptotes and discontinuities in the flow such as sea breezes, outflow boundaries, and lake breezes.

3.3.2.11. Onset of severe thunderstorms. Hail, severe winds, and tornadoes are less common with air mass thunderstorms – for severe weather to occur, at least one of the following must be present:

3.3.2.11.1. Cold and/or dry air aloft.

3.3.2.11.2. Short-wave trough at 500 mb.

3.3.2.11.3. Positive vorticity advection (PVA).

MARK D. KELLY, Lt Gen, USAF
Deputy Chief of Staff, Operations

Attachment 1

GLOSSARY OF REFERENCES AND SUPPORTING INFORMATION

References

557th Weather Wing – Interactive Meteorological Techniques (**https://weather.af.mil/afwwebs_data/IMT/index.html**).

<u>**Visibility – Fog:**</u>

AFWA/TN-13/002: Forecasting Fog

AFWKC CBT: European Theater Weather Orientation 2C

AFWKC CBT: COMET - Customer Impacts: Forecasting Fog and Low Stratus

AFWKC CBT: COMET - Dynamically Forced Fog

AFWKC CBT: COMET - Fog and Stratus Forecasting Approaches

AFWKC CBT: COMET - Forecasting Radiation Fog

AFWKC CBT: SWA - Autumn Weather Forecasting

Cho, Y.-K., M.-O. Kim, and B.-C. Kim, 2000: Sea fog around the Korean Peninsula. J. Appl. Meteor., 39, 2473-2479.

Croft, P. J., R. L. Pfost, J. M. Medlin, and G. A. Johnson, 1997: Fog forecasting for the Southern Region: A conceptual model approach. Wea. Forecasting, 12, 545-556.

Gultepe, I., and Coauthors, 2007: Fog research: A review of past achievements and future perspectives. Pure Appl. Geophys., 164, 1121-1159.

Gurka, J. J., 1978: The role of inward mixing in the dissipation of fog and stratus. Mon. Wea. Rev., 106, 1633-1635.

Haeffelin, M., and Coauthors, 2010: PARISFOG: Shedding new light on fog physical processes. Bull. Amer. Meteor. Soc., 91, 767-783.

Koracin, D., J. Lewis, W. T. Thompson, C. E. Dorman, and J. A. Businger, 2001: Transition of stratus into fog along the California coast: Observations and modeling. J. Atmos. Sci., 58, 1714-1731.

Toth, G., and Coauthors, 2010: The Environment Canada Handbook on Fog and Fog Forecasting. 94 pp.

Westcott, N.E., 2007: Some aspects of dense fog in the Midwestern United States. Wea. Forecasting, 22, 457-465.

----------, and D. A. R. Kristovich, 2009: A climatology and case study of continental cold season dense fog associated with low clouds. J. Appl. Meteor. Climatol., 48, 2201-2214.

<u>**Visibility – Dust:**</u>

AWS/FM-100/021: Conditions for a Severe Duststorm and a Case Study for Iraq

AWS/TN--91/001: Dust and Sand Forecasting in Iraq and Adjoining Countries

AFWKC CBT: AMF Competencies: Forecasting Meteorological Phenomena

AFWKC CBT: COMET - Visible and Infrared Dust Detection Techniques

AFWKC CBT: COMET - Forecasting Dust Storms

AFWKC CBT: COMET - Dust Enhancement Techniques Using MODIS and SeaWiFS

AFWKC CBT: COMET - Forecasting Dust Storms

AFWKC CBT: SWA - Autumn Weather Forecasting

AFWKC CBT: SWA - Summer Weather Forecasting

COMET Program: Forecasting Dust Storms – Version 2.

Liu, M., D. L. Westphal, A. L. Walker, T. R. Holt, K. A. Richardson, and S. D. Miller, 2007: COAMPS real-time dust storm forecasting during Operation Iraqi Freedom. Wea. Forecasting, 22, 192-206.

Novlan, D. J., M. Hardiman, and T. E. Gill, 2007: A synoptic climatology of blowing dust events in El Paso, Texas from 1932-2005. Extended Abstract, 16th Conf. on Applied Climatology, San Antonio, TX, Amer. Meteor. Soc., J3.12.

Pauley, P. M., N. L. Baker, and E. H. Barker, 1995: An observational study of the "Interstate 5" dust storm case. Bull. Amer. Meteor. Soc., 77, 693-720.

Visibility – Haze:

Ball, R. J., and G. D. Robinson, 1982: The origin of haze in the central United States and its effect on solar radiation. J. Appl. Meteor, 21, 171-188.

Corfidi, S. F., 1993: Lost horizons. Weatherwise, 46, 12-17.

----------, 1996: Haze over the Central and Eastern United States. Nat. Wea. Dig., 20, 2-14.

Malm, W. C., 1992: Characteristics and origins of haze in the continental United States. Earth-Sci. Rev, 33, 1-36.

Wolff, G. T., N. A. Kelly, and M. A. Ferman, 1981: On the sources of summertime haze in the eastern United States. Science, 211, 703-705.

Visibility – Blowing Snow:

AFWA/TN-12/003: Forecasting Snow

AFWKC CBT: SWA - Winter Weather Forecasting

AFWKC CBT: SWA - Autumn Weather Forecasting

AFWKC CBT: 15 OWS Dual-Polarization Tutorials - Winter Weather Nowcasting

AFWKC CBT: COMET - Snowpack and its Assessment

AFWKC CBT: COMET - Avalanche Weather Forecasting

AFWKC CBT: AMF Competencies - Forecasting Meteorological Phenomena

Baggaley, D. G., and J. M. Hanesiak, 2005: An empirical blowing snow forecast technique for the Canadian Arctic and the Prairie Provinces. Wea. Forecasting, 20, 51-62.

COMET Program: Mesoscale Aspects of Winter Weather Forecasting: Blowing Snow, Baker Lake, Nunavut Canada, 04-10 February 2003.

Long, L., and J. W. Pomeroy, 1997: Estimates of threshold wind speeds for snow transport using meteorological data. J. Appl. Meteor., 36, 205-213.

Rasmussen, R. M., J. Vivekanandan, J. Cole, B. Myers, and C. Masters, 1999: The estimation of snowfall rate using visibility. J. Appl. Meteor., 38, 1542-1563.

Precipitation – Freezing Precipitation:

AFWA/TN-98/001: Freezing Precipitation

AFWKC CBT: SWA - Winter Weather Forecasting

AFWKC CBT: 15 OWS Dual-Polarization Tutorials - Winter Weather Nowcasting

Bourgouin, P., 2000: A method to determine precipitation types. Wea. Forecasting, 15, 583-592.

Cook, K., 2012: Dual-polarization storm of the month: Winter weather applications. WDTB storm of the month: December 2012.

Funk, T., n.d.: Precipitation type forecasting: A top-down approach to forecasting precipitation type. NWS Louisville, KY.

----------, n.d.: Determining winter precipitation type. NWS Louisville, KY.

Picca, J., 2012: 1/21/2012 Tri-State winter storm: Transitioning precipitation over Long Island. WDTB storm of the month: February 2012.

Rasmussen, R. M., I. Geresdi, G. Thompson, K. Manning, and E. Karplus, 2002: Freezing drizzle formation in stably stratified layer clouds: The role of radiative cooling of cloud droplets, cloud condensation nuclei, and ice initiation. J. Atmos. Sci., 59, 837-860.

Schlatter, P., 2011: Dual-pol applications: Winter weather nowcasting. Dual polarization radar operations course: Warning Decision Training Branch. [Available online at **http://www.wdtb.noaa.gov/courses/dualpol/Applications/WW/player.html**.]

Stewart, R. E., 1992: Precipitation types in the transition region of winter storms. Bull. Amer. Meteor. Soc., 73, 287-296.

Zerr, R. J., 1997: Freezing rain: An observational and theoretical study. J. Appl. Meteor., 36, 1647-1661.

Precipitation – Snow:

AFWA/TN-12/003: Forecasting Snow

AFWKC CBT: SWA - Winter Weather Forecasting

AFWKC CBT: SWA - Autumn Weather Forecasting

AFWKC CBT: 15 OWS Dual-Polarization Tutorials - Winter Weather Nowcasting

AFWKC CBT: COMET - Snowpack and its Assessment

AFWKC CBT: COMET - Avalanche Weather Forecasting

AFWKC CBT: AMF Competencies - Forecasting Meteorological Phenomena

Cook, B. J., 1980: A snow index using 200 mb warm advection. National Wea. Digest, 5, 29-40.

Garcia, C., Jr., 2000: Forecasting snowfall using mixing ratios on an isentropic surface: an update. NWS Technical Memorandum CR-166.

Jurewicz, M. L., Sr., and M. S. Evans, 2004: A comparison of two banded, heavy snowstorms with very different synoptic settings. Wea. Forecasting, 19, 1011-1028.

Roebber, P. J., S. L. Bruening, D. M. Schultz, and J. V. Cortinas, Jr., 2003: Improving snowfall forecasting by diagnosing snow density. Wea. Forecasting, 18, 264-287.

Schultz, D. M., and P. N. Schumacher, 1999: The use and misuse of conditional symmetric instability. Mon. Wea. Rev., 127, 2709-2732.

Stull, R. B., 2000: Meteorology for Scientists and Engineers. Brooks/Cole, Thomson Learning. 502 pp.

Wiesmueller, J. L., and S. M. Zubrick, 1998: Evaluation and application of conditional symmetric instability, equivalent potential vorticity, and frontogenetic forcing in an operational forecast environment. Wea. Forecasting, 13, 84-101.

Winds – Non-Convective:

Ashley, W. S., and A. W. Black, 2008: Fatalities associated with nonconvective high-wind events in the United States. J. Appl. Meteor. Climatol., 47, 717-725.

Browning, K. A., 2004: The sting at the end of the tail: Damaging winds associated with extratropical cyclones. Quart. J. Roy. Meteor. Soc., 130, 375-399.

Hultquist, T. R., M. R. Dutter, and D. J. Schwab, 2006: Reexamination of the 9-10 November 1975 "Edmund Fitzgerald" storm using today's technology. Bull. Amer. Meteor. Soc., 87, 607-622.

Knox, J., 2004: Non-convective windstorms in the Midwest United States: Surface and satellite climatologies. Preprints, 22nd Conference on Severe Local Storms, Hyannis, MA, Amer. Meteor. Soc., P5.3.

----------, J. D. Frye, J. D. Durkee, and C. M. Fuhrmann, 2011: Non-convective high winds associated with extratropical cyclones. Geogr.Compass, 5, 63-89.

Lacke, M. C., J. A. Knox, J. D. Frye, A. E. Stewart, J. D. Durkee, C. M. Fuhrmann, and S. M. Dillingham, 2007: A climatology of cold-season nonconvective wind events in the Great Lakes Region. J. Climate, 20, 6012-6022.

Niziol, T. A., and T. J. Paone, 2000: A climatology of non-convective high wind events in western New York State. NOAA Tech. Memo. NWS ER-91, 36 pp.

Orgill, M. M., J. D. Kincheloe, and R. A. Sutherland, 1992: Mesoscale influences on nocturnal valley drainage winds in western Colorado valleys. J. Appl. Meteor., 31, 121-141.

Schultz, D. M., and J. M. Sienkiewicz, 2013: Using frontogenesis to identify sting jets in extratropical cyclones. Wea. Forecasting, 28, 603-613.

Winds – Land and Sea Breeze:

AFWKC CBT: COMET - Sea Breezes

COMET Program: Thermally-forced circulation I: Sea Breezes.

COMET Program: Tropical Mesoscale and Local Circulations.

Kingsmill, D. E., 1995: Convection initiation associated with a sea-breeze front, a gust front, and their collision. Mon. Wea. Rev., 123, 2913-2933.

Temperature:

Dallavalle, P. J., and R. L. Cosgrove, 2005: GFS-based MOS guidance – The short-range alphanumeric messages from the 0000/1200 UTC forecast cycles. MDL Technical Procedures Bulletin No. 05-03, NOAA, U.S. Dept. of Commerce, 13 pp.

----------, and ----------, 2005: GFS-based MOS guidance – The short-range alphanumeric messages from the 0600/1800 UTC forecast cycles. MDL Technical Procedures Bulletin No. 05-04, NOAA, U.S. Dept. of Commerce, 13 pp.

Gilbert, K. K., R. L. Cosgrove, and J. Maloney, 2008: NAM-based MOS guidance – The 0000/1200 UTC alphanumeric messages. MDL Technical Procedure Bulletin No. 08-01, NOAA, U.S. Dept. of Commerce, 11 pp.

Glahn, B., K. Gilbert, R. Cosgrove, D. P. Ruth, and K. Sheets, 2009: The gridding of MOS. Wea. Forecasting, 24, 520-529.

Maloney, J. C., K. K. Gilbert, M. N. Baker, and P. E. Shafer, 2010: GFS-based MOS guidance – The extended range alphanumeric messages from the 0000/1200 UTC forecast cycles. MDL Technical Procedure Bulletin No. 2010-01, NOAA, U.S. Dept. of Commerce, 12 pp.

Mote, T. L., 2008: On the role of snow cover in depressing air temperature. J. Appl. Meteor. Climatol., 47, 2008-2022.

Pressure:

American Meteorological Society, cited 2013: Glossary of Meteorology.

Benjamin, S. G., and P. A. Miller, 1990: An alternative sea level pressure reduction and a statistical comparison of geostrophic wind estimates with observed surface winds. Mon. Wea. Rev., 118, 2099-2116.

Federal Aviation Administration, 2012: Aeronautical Information Manual, "Altimeter Setting Procedures".

Pauley, P. M., 1998: An example of uncertainty in sea level pressure reduction. Wea. Forecasting, 13, 833-850.

Clouds and Contrails:

AWS/TR-81/001: Forecasting Aircraft Condensation Trails

AWS/TR--93/001: New Techniques for Contrail Forecasting

NASA: Contrail Identification Chart and Formation Guide

Atlas, D., Z. Wang, and D. P. Duda, 2006: Contrails to cirrus - morphology, microphysics, and radiative properties. J. Appl. Meteor. Climatol., 45, 5-19.

Eastman, R., and S. G. Warren, 2014: Diurnal cycles of cumulus, cumulonimbus, stratus, stratocumulus, and fog from surface observations over land and ocean.

J. Climate. **http://dx.doi.org/10.1175/JCLI-D-13-00352.1**, in press.

Gierens, K., B. Kärcher, H. Mannstein, and B. Mayer, 2009: Aerodynamic contrails: Phenomenology and flow physics. J. Atmos. Sci., 66, 217-226.

Gurka, J. J., 1978: The role of inward mixing in the dissipation of fog and stratus. Mon. Wea. Rev., 106, 1633-1635.

Heymsfield, A., D. Baumgardner, P. DeMott, P. Forster, K. Gierens, and B. Kärcher, 2010: Contrail microphysics. Bull. Amer. Meteor. Soc., 91, 465-472.

Kärcher, B., B., Mayer, K. Gierens, U. Burkhardt, H. Mannstein, and R. Chatterjee, 2009: Aerodynamic contrails: Microphysics and optical properties. J. Atmos. Sci., 66, 227-243.

Koracin, D., J. Lewis, W. T. Thompson, C. E. Dorman, and J. A. Businger, 2001: Transition of stratus into fog along the California coast: Observations and modeling. J. Atmos. Sci., 58, 1714-1731.

Sassen, K., and J. R. Campbell, 2001: A midlatitude cirrus cloud climatology from the Facility for Atmospheric Remote Sensing: Part I: Macrophysical and synoptic properties. J. Atmos. Sci., 58, 481-496.

Schrader, M. L., 1997: Calculations of aircraft contrail formation critical temperatures. J. Appl. Meteor., 36, 1725-1729.

Wood, R., 2012: Review: Stratocumulus clouds. Mon. Wea. Rev., 140, 2373-2423.

World Meteorological Organization – International Cloud Atlas (**https://cloudatlas.wmo.int/home.html**).

Turbulence:

AFGWC/TN-79/001: Clear Air Turbulence

AFWA/TN-13/007: Turbulence Fundamentals

Brooks, G. R., and A. Oder, 2004: Low level turbulence algorithm testing at-or-below 10,000 ft. Preprints, 11th Conf. on Aviation, Range, and Aerospace Meteorology, Hyannis, MA, Amer. Meteor. Soc., P4.16.

Ellrod, G. P., 2000: Global climatology of clear air turbulence activity deduced from a numerical model index. Extended Abstract, 9th Conf. on Aviation, Range, and Aerospace Meteorology, Orlando, FL, Amer. Meteor. Soc., P1.14.

----------, and D. I. Knapp, 1992: An objective clear-air turbulence forecasting technique: Verification and operational use. Wea. Forecasting, 7, 150-165.

----------, and J. A. Knox, 2010: Improvements to an operational clear-air turbulence diagnostic index by additional of a divergence trend term. Wea. Forecasting, 25, 789-798.

Federal Aviation Administration, 2012: FAA Aeronautical Information Manual, Chapter 7.

Keller, D. L., 2011: The SLAT (index) as an indicator of vertically propagating mountain waves using WRF 15 km data, and its potential as a turbulence forecast product. Extended Abstract, 15th Conf. on Aviation, Range, and Aerospace Meteorology, Los Angeles, CA, Amer. Meteor. Soc., 3.3.

Lane, T. P., R. D. Sharman, T. L. Clark, and H. Hsu, 2003: An investigation of turbulence generation mechanisms above deep convection. J. Atmos. Sci., 60, 1297-1321.

----------, ----------, S. B. Trier, R. G. Fovell, and J. K. Williams, 2012: Recent advances in the understanding of near-cloud turbulence. Bull. Amer. Meteor. Soc., 93, 499-515.

Lee, D. R., R. S. Stull, and W. S. Irvine, 1984: Clear air turbulence forecasting techniques. Air Weather Service Tech. Note AFGWC/TN-79/001 (REV), Air Force Global Weather Central, Offutt AFB, NE. 85 pp.

Sinclair, P. C., and P. M. Kuhn, 1991: Infrared detection of high altitude clear air turbulence, NOARL Technical Note 205, 49 pp.

Stull, R. B., 1988: An Introduction to Boundary Layer Meteorology. Kluwer Academic Publishes, 673 pp.

----------, 2000: Meteorology for Scientists and Engineers. Brooks/Cole Thomson Learning, 502 pp.

Wolff, J. K., and R. D. Sharman, 2008: Climatology of upper-level turbulence over the contiguous United States. J. Appl. Meteor. Climatol., 47, 2198-2214.

Icing:

AFWA/TN-13/001: Forecasting Aircraft Icing

AFWA/TN-13/003: Dual-Polarization Radar

AWS/TR-80/001: Forecasters' Guide on Aircraft Icing

Federal Aviation Administration (FAA) Pilot Guide: Flight In Icing Conditions

AFWKC CBT: Forecasting Aviation Icing: Icing Type and Severity

Air Weather Service, 1980: Forecasters' guide on aircraft icing. AWS/TR-80/001, 60 pp.

Bernstein, B. C., T. A. Omeron, F. McDonough, and M. K. Politovich, 1997: The relationship between aircraft icing and synoptic scale weather conditions. Wea. Forecasting, 12, 742-762.

Cober, S. G., G. A. Isaac, and J. W. Strapp, 2001: Characterizations of aircraft icing environments that include supercooled large drops. J. Appl. Meteor., 40, 1984-2002.

COMET Program: Forecasting Aviation Icing: Icing Type and Severity.

Ellrod, G. P., and A. A. Bailey, 2012: Assessment of aircraft icing potential and maximum icing altitude from geostationary meteorological satellite data. Wea. Forecasting, 22, 160-174.

Sand, W. R., W. A. Cooper, M. K. Politovich, and D. L. Veal, 1984: Icing conditions encountered by a research aircraft. J. Climate and Appl. Meteor., 23, 1427-1440.

Schultz, P., and M. K. Politovich, 1992: Toward the improvement of aircraft-icing forecasts for the continental United States. Wea. Forecasting, 7, 491-500.

Zerr, R. J., 1997: Freezing rain: An observational and theoretical study. J. Appl. Meteor., 36, 1647-1661.

Electro-Optics:

AFWKC CBT: Introduction to Electro-Optical Systems

COMET Program: Introduction to Electromagnetic and Electro-Optic Propagation

Salby, Murry L., 1996: Fundamentals of Atmospheric Physics. Academic Press. 624 pp.

Stull, Roland B., 2000: Meteorology for Scientists and Engineers. Brooks/Cole Thomson Learning. 502 pp.

Volcanoes:

AFWKC CBT: Volcanic Ash

The COMET Program, 2013: Volcanic Ash: Introduction.

The COMET Program, 2013: Volcanic Ash: Volcanism.

The COMET Program, 2013: Volcanic Ash: Impacts to Aviation, Climate, Maritime Operations, and Society.

The COMET Program, 2013: Volcanic Ash: Observation Tools and Dispersion Models.

Neal, Christina et al., 1997: Volcanic Ash - Danger to Aircraft in the North Pacific. U.S. Geological Survey Fact Sheet 030-97. Online Version 1.0.

Nelson, Stephen, 2013: Volcanoes, Magma, and Volcanic Eruptions.

Newhall, C., Self, St., 2012: The Volcanic Explosivity Index.

Smith et al., 2010: Volcanic Ash. To Fly or Not to Fly? Institution of Mechanical Engineers Report, 24 pp.

United States Geological Survey, 2014: Volcanic Hazards Program Photo Glossary: More Volcanic Ash.

Convective Winds:

AFWA/TN-12/001: Forecasting Severe Convective Winds

Technical Report 200: Notes on Analysis and Severe-Storm Forecasting Procedures of the Air Force Global Weather Central

AFWKC CBT: SWA - Spring Weather Forecasting

Atkins, N. T., and R. M. Wakimoto, 1991: Wet microburst activity over the southeastern United States: Implications for forecasting. Wea. Forecasting, 6, 470-482.

Betts, A. K., and M. F. Silva Dias, 1979: Unsaturated downdraft thermodynamics in cumulonimbus. J. Atmos. Sci., 36, 1061-1071.

Doswell, C. A., 2001: Severe Convective Storms. Amer. Meteor. Soc., 570 pp.

Foster, D. S., 1958: Thunderstorm gusts compared with computed downdraft speeds. Mon. Wea. Rev., 86, 91-94.

Gilmore, M., and L. J. Wicker, 1998: The influence of midtropospheric dryness on supercell morphology and evolution. Mon. Wea. Rev., 126, 943-958.

Johns, R. H., and C. A. Doswell III, 1992: Severe Local Storms Forecasting. Wea. Forecasting, 7, 588-612.

Kuchera, E. L., and M. D. Parker, 2006: Severe convective wind environments. Wea. Forecasting, 21, 595-612. Kuhlman, C. J., 2006: Evaluation of Convective Wind Forecasting Methods during High Wind Events. Naval Postgraduate School Master's Thesis, 81 pp.

Pino, J. P., and J. T. Moore, 1989: An interactive method for estimating hailstone size and convectively-driven wind gusts from forecast soundings. Preprints, 12th Conf. Wea. Analysis and Forecasting, Monterey, California. Amer. Meteor. Soc., 103-106.

Srivastava, R. C., 1985: A simple model of evaporatively driven downdraft: Application to a microburst downdraft. J. Atmos. Sci., 42, 1004-1023.

----------, 1987: A model of intense downdrafts driven by the melting and evaporation of precipitation. J. Atmos. Sci., 44, 1752-1774.

Wakimoto, R. M., 1985: Forecasting dry microburst activity over the High Plains. Mon. Wea. Rev., 113, 1131-1143.

Hail:

AFWA/TN-12/002: Forecasting Hail

Technical Report 200: Notes on Analysis and Severe-Storm Forecasting Procedures of the Air Force Global Weather Central

AFWKC CBT: SWA - Spring Weather Forecasting

AFWKC CBT: 15 OWS Dual-Polarization Tutorials - Hail Detection

AFWKC CBT: Dual-Pol Radar Applications: Hail Detection

Amburn, Steven A., and Peter L. Wolf, 1997: VIL Density as a hail indicator. Wea. Forecasting, 12, 473-478.

Billet, J., M. DeLisi, and B. G. Smith, 1997: Use of regression techniques to predict hail size and the probability of large hail. Wea. Forecasting, 12, 154-164.

Doswell, C. A., 2001: Severe Convective Storms. Amer. Meteor. Soc., 570 pp.

Fawbush, E. J., and R. C. Miller, 1953: A method for forecasting hail size at the Earth's surface. Bull. of the Amer. Meteor. Soc., 35, 14-19.

Johns, R. H., and C. A. Doswell III, 1992: Severe local storms forecasting. Wea. Forecasting, 7, 588-612.

Knight, C. A., and P. Squires, Eds., 1981: Hailstorms of the Central High Plains, Vol. I: The National Hail Research Experiment. Colorado Associated University Press, 282 pp.

Miller, R. C., 1972: AFWA/TR-200, Notes on Analysis and Severe-Storm Forecasting Procedures of the Air Force Global Weather Central. 177 pp.

Heavy Rain:

AFWA/TN-13/004: Forecasting Heavy Rainfall

AFWKC CBT: 15 OWS Dual-Polarization Tutorials - Heavy Rain Forecasting

AFWKC CBT: Dual-Pol Radar Applications: Heavy Rain Detection

Atallah, E. H., L. F. Bosart, and A. R. Aiyyer, 2007: Precipitation distribution associated with landfalling tropical cyclones over the eastern United States. Mon. Wea. Rev., 135, 2185-2206.

Doswell, C. A., III, H. E. Brooks, and R. A. Maddox, 1996: Flash flood forecasting: An ingredients-based methodology. Wea. Forecasting, 11, 560-581.

Ebert, E. E., and Coauthors, 2011: Ensemble tropical rainfall potential (eTRaP) forecasts. Wea. Forecasting, 26, 213-224.

Funk, T. W., 1993: Heavy rainfall forecast techniques, CR technical attachment 93-06, 10 pp.

----------, 2004: Heavy convective rainfall forecasting: A comprehensive look at parameters, processes, patterns, and rules of thumb. Scientific training documents at NWS Louisville.

Glass, F. H., D. L. Ferry, J. T. Moore, and S. M. Nolan, 1995: Characteristics of heavy convective rainfall events across the mid-Mississippi valley during the warm season: Meteorological conditions and a conceptual model. Preprints, 14th Conf. on Weather Forecasting and Analysis, Dallas, TX, Amer. Meteor. Soc., 34-41.

Junker, N. W., R. S. Schneider, and S. L. Fauver, 1999: A study of heavy rainfall events during the great Midwest flood of 1993: Wea. Forecasting, 14, 701-712.

Maddox, R. A., C. F. Chappell, and L. R. Hoxit, 1979: Synoptic and meso-α scale aspects of flash flood events. Bull. Amer. Meteor. Soc., 60, 115-123.

Moore, J. T., F. H. Glass, C. E. Graves, S. M. Rochette, and M. J. Singer, 2003: The environment of warm-season elevated thunderstorms associated with heavy rainfall over the central United States. Wea. Forecasting, 18, 861-878.

Opitz, H. H., S. G. Summer, D. A. West, W. R. Snyder, R. J. Kane, R. H. Brady, P. M. Stokols, S. C. Kuhl, and G. M. Carter, 1995: The challenge of forecasting heavy rain and flooding throughout the eastern region of the National Weather Service. I: Forecast techniques and applications. Wea. Forecasting, 10, 91-104.

Roth, D., 2007: Tropical cyclone rainfall. Hydrometeorological Prediction Center.

Smith, J. A., M. L. Baeck, and Y. Zhang, 2001: Extreme rainfall and flooding from supercell thunderstorms. J. Hydrometeor., 2, 469-489.

Lightning:

AFWA/TN-13/006: Forecasting Lightning

Berdeklis, P., and R. List, 2001: The ice crystal-graupel collision charging mechanism of thunderstorm electrification. J. Atmos. Sci., 58, 2751-2770.

Christian, H. J., and Coauthors, 2003: Global frequency and distribution of lightning as observed from space by the Optical Transient Detector. J. Geophys. Res., 108 (D1), 4005, doi:10.1029/2002JD002347.

Livingston, E. S., J. W. Nielsen-Gammon, and R. E. Orville, 1996: A climatology, synoptic assessment, and thermodynamic evaluation for cloud-to-ground lightning Georgia: A study for the 1996 Summer Olympics. Bull. Amer. Meteor. Soc., 77, 1483-1495.

MacGorman, D. R., and W. D. Rust, 1998: The Electrical Nature of Storms. Oxford University Press, 422 pp.

----------, ----------, P. Krehbiel, W. Rison, E. Bruning, and K. Wiens, 2005: The electrical structure of two supercell storms during STEPS. Mon. Wea. Rev., 133, 2583-2607.

Orville, R. E., G. R. Huffines, W. R. Burrows, and K. L. Cummins, 2011: The North American Lightning Detection Network (NALDN) – Analysis of flash data: 2001-09. Mon. Wea. Rev., 139, 1305-1322.

Reynolds, S.E., M. Brook, and M. F. Gourley, 1957: Thunderstorm charge separation. J. Meteor., 14, 426-436.

Stolzenburg, M., W. D. Rust, and T. C. Marshall, 1998: Electrical structure in thunderstorm convective regions. Part 3: Synthesis. J. Geophys. Res., 103 (D12), 14 097-14 108.

Williams, E. R., 2001: The electrification of severe storms. Severe Convective Storms, Meteor. Monogr., No. 50, Amer. Meteor. Soc., 527-561.

Zajac, B. A., and S. A. Rutledge, 2001: Cloud-to-ground lightning activity in the contiguous United States from 1995 to 1999. Mon. Wea. Rev., 129, 999-1019.

Tornadoes:

AFWA/TN-13/005: Forecasting Tornadoes

Technical Report 200: Notes on Analysis and Severe-Storm Forecasting Procedures of the Air Force Global Weather Central

AFWKC CBT: 15 OWS Dual-Polarization Tutorials - Tornadic Debris Detection

AFWKC CBT: Dual-Pol: Operational Success Stories

Davies, J. M., and A. Fischer, 2009: Environmental characteristics associated with nighttime tornadoes. Electronic J. Operational Meteor., 10, 1-29.

Edwards, R., 2012: Tropical cyclone tornadoes: A review of knowledge in research and prediction. Electronic J. Severe Storms Meteor., 7, 1-61.

Falk, K., and W. Parker, 1998: Rotational shear nomogram for tornadoes. Extended Abstract, 19th Conf. on Severe Local Storms, Bloomington, MN, Amer. Meteor. Soc., P20.8.

Funk, T. W., 2002: Tornadogenesis in supercells: The three main ingredients. Scientific training documents at NWS Louisville.

Maddox, R. A., and C. A. Crisp, 1999: The Tinker AFB Tornadoes of March 1948. Wea. Forecasting, 14, 492-499.

Markowski, P. M., and Y. P. Richardson, 2009: Tornadogenesis: Our current understanding, forecasting considerations, and questions to guide future research. Atmos. Res., 93, 3-10.

Mead, C. M., and R. L. Thompson, 2011: Environmental characteristics associated with nocturnal significant-tornado events in the central and southern Great Plains. Electronic J. Severe Storms Meteor., 6, 1-35.

National Climatic Data Center, 2013: U. S. tornado climatology.

Rasmussen, E. N., 2003: Refined supercell and tornado forecast parameters. Wea. Forecasting, 18, 530-535.

Storm Prediction Center, cited 2013: Enhanced F Scale for tornado damage.

Thompson, R. L., B. T. Smith, J. S. Grams, A. R. Dean, and C. Broyles, 2012: Convective modes for significant severe thunderstorms in the contiguous United States. Part II: Supercell and QLCS tornado environments. Wea. Forecasting, 27, 1136-1154.

Trapp, R. J., S. A. Tessendorf, E. S. Godfrey, and H. E. Brooks, 2005: Tornadoes from squall lines and bow echoes. Part 1: Climatological distribution. Wea. Forecasting, 20, 23-34.

Van Den Broeke, M. S., J. M. Straka, and E. N. Rasmussen, 2008: Polarimetric radar observations at low levels during tornado life cycles in a small sample of classic southern plains supercells. J. Appl. Meteor., 47, 1232-1247.

Abbreviations and Acronyms

AC—Altocumulus

ACC—Altocumulus Castellanus

ACSL—Altocumulus Standing Lenticular

AFDIS—Air Force Dial-In Subsystems

AFH—Air Force Handbook

AFM—Air Force Manual

AIRMET—Airman's Meteorological Information

AGL—Above Ground Level

API—Antecedent Precipitation Index

AS—Altostratus

AWC—Aviation Weather Center

BKFG—Barokline Feucht (German NWP Model)

BRN—Bulk Richardson Number

BWER—Bounded Weak Echo Region

C—Celsius

CAA—Cold Air Advection

CAPE—Convective Available Potential Energy

CAT—Clear Air Turbulence (or Category)

CB—Cumulonimbus

CC—Cirrocumulus (or Conditional Climatology)

CCL—Convective Condensation Level

CI—Cirrus

CIG—Ceiling

CONTRAIL—Condensation Trail

CONUS—Continental United States

CP—Continental Polar Air Mass

CS—Cirrostratus

CT—Cross Totals

CU—Cumulus

DA—Density Altitude

DPD—Dew Point Depression

DOD—Department of Defense

EHI—Energy / Helicity Index

ESI—European Snow Index

EL—Equilibrium Level

ET—Echo Tops

F—Fahrenheit

FAA—Federal Aviation Administration

FBD—Formatted Binary Data

FE—Field Elevation

FMI—Fawbush-Miller Index

FITS—Fighter Index of Thermal Stress

FL—Flight Level

GALWEM—Global Air-Land Weather Exploitation Model

GMGO—German Military Geophysical Office

GMS—Geostationary Meteorological Satellite

GOES—Geostationary Operational Environmental Satellite

GSI—Gollehon Stability Index

HG—Mercury

IMC—Instrument Meteorological Conditions

IR—Infrared

ISMCS—International Station Meteorological Climate Summary

ITS—Index of Thermal Stress

JET—Joint Environmental Toolkit

KI—K Index

KM—Kilometer

KO—KO Index

KT—Knots

L—Light Turbulence

LAFP—Local Analysis and Forecast Program

LAWC—Local Area Work Chart

LC—Low Cloud

LCL—Lifted Condensation Level

LEWP—Line Echo Wave Pattern

LI—Lifted Index

LLJ—Low Level Jet

LLT—Low Level Thickness

LLWS—Low Level Wind Shear

M—Moderate Turbulence (or Meters)

MB—Millibars

MCC—Mesoscale Convective Complex

MCL—Mixing Condensation Level

MCS—Mesoscale Convective System

METEOSAT—Meteorological Satellite

METWATCH—Meteorological Watch

MLI—Modified Lifted Index

MODCURVES—Modeled Curves

MODCV—Modeled Ceiling and Visibility

MOGR—Moderate or Greater

MOS—Model Output Statistics

MP—Maritime Polar Air Mass

MT—Maritime Tropical Air Mass

MSI—Mean Storm Inflow

MSL—Mean Sea Level

MV—Mountain Wave Turbulence

MVMC—Marginal Visual Meteorological Conditions

MWA—Military Weather Advisory

NM—Nautical Miles

NCAR—National Center for Atmospheric Research

NCEP—National Center for Environmental Prediction

NESDIS—National Environmental Satellite Data and Information Service

NEXRAD—Next Generation Weather Radar

NOAA—National Oceanographic and Atmospheric Administration

NOGAPS—Naval Operational Global Atmospheric Prediction System

NS—Nimbostratus

NVA—Negative Vorticity Advection

NWP—Numerical Weather Prediction

NWS—National Weather Service

OVV—Omega Vertical Velocity

PA—Pressure Altitude

PGF—Pressure Gradient Force

PIREP—Pilot Report

PFJ—Polar Front Jet

PMSV—Pilot to Metro Service

POP—Probability of Precipitation

POPT—Probability of Precipitation Type

POR—Period of Record

POSA—Probability of Snow Accumulation

PVA—Positive Vorticity Advection

PWI—Precipitable Water Index

QFE—Station Pressure

QNE—Pressure Altitude

QNH—Altimeter Setting

QPF—Quantitative Precipitation Forecast

R—Base Reflectivity

RAOB—Radiosonde Observation

RAREP—Radar Report

RCS—Reflectivity Cross Section

RDA—Radar Data Acquisition

RH—Relative Humidity

RMS—Root Mean Square

RW—Rain Shower

S—Severe Turbulence

SBLI—Surface Based Lifted Index

SC—Stratocumulus

SCT—Surface Cross Totals

SFC—Surface

SHARP—Skew-T / Hodograph Analysis and Research Program

SIGMET—Significant Meteorological Information

SLD—Super-cooled Large Water Droplets

SLP—Sea Level Pressure

SOCS—Surface Observation Climatic Summary

SRDS—Storm Relative Directional Shear

SRH—Storm Relative Helicity

SSI—Showalter Stability Index

ST—Stratus

STJ—Subtropical Jet

SST—Sea Surface Temperature

SWEAT—Severe Weather Threat Index

T—Temperature

TAF—Terminal Aerodrome Forecast

TFRN—Terminal Forecast Reference Notebook

THI—Temperature Humidity Index

TI—Thompson Index

TRW—Thunderstorm / Rain Shower

TT—Total Totals Index

UGDF—Uniform Gridded Data Field

UK—United Kingdom

USAF—United States Air Force

USN—United States Navy

UTC—Universal Time Coordinate

VAD—Velocity Azimuth Display

VC—Vicinity

VCNTY—Vicinity

VIL—Vertically Integrated Liquid

VIS—Visibility (or Visible Satellite Imagery)

VMC—Visual Meteorological Conditions

VT—Vertical Totals Index

VWP—VAD Wind Profile

WAA—Warm Air Advection

WBGT—Wet Bulb Globe Temperature

WBZ—Wet Bulb Zero

WMO—World Meteorological Organization

WSR-88D—Weather Surveillance Radar-1988 Doppler

WV—Water Vapor Imagery

X—Extreme

Terms

Adiabatic Process—A thermodynamic change of state in a system in which there is no transfer of heat or mass across the boundaries of the system. An example of such a system is the concept of the air parcel. In an adiabatic process, compression always results in warming and expansion in cooling.

Advection—The horizontal transfer of an atmospheric property by the wind.

Ageostrophic Wind—The vector difference between the observed wind and the geostrophic wind.

Air Mass—A large body of air that is largely homogenous both horizontally and vertically in temperature and moisture.

Altimeter Setting—The station pressure reduced to sea level without compensating for temperature.

Apparent Temperature—What the air temperature "feels like" for various combinations of temperature and relative humidity.

Baroclinic—A state in which a constant-pressure surface intersects a constant density surface. In upper air products, can be seen where height lines intersect isotherms.

Barotropic—A state in which pressure gradients and the density gradients are parallel. In upper-air products, can be seen where height lines parallel isotherms.

Bora—Cold, dry, gale-force, gravity-assisted winds that blow down from mountains.

Bounded Weak Echo Region (BWER)—A radar signature within a thunderstorm characterized by a nearly vertical weak echo surrounded on the sides and top by significantly stronger echoes. This feature is associated with a strong updraft and is almost always found in the inflow region of a thunderstorm. It cannot be seen visually. See WER.

Boundary Layer—Also called Surface Boundary Layer and Friction Layer. The layer of air immediately adjacent to the earth's surface.

Bow Echo—A bow shaped line of convective cells that is often associated with swaths of damaging straight-line winds and small tornadoes.

Convective Available Potential Energy (CAPE)—The amount of energy available to create convection, with higher values indicating the possibility for severe weather.

Centripetal Force—The force that tends to keep an air parcel moving in a curved path, such as isobars.

Chinook—A warm and dry (sometimes very strong) wind that flows down the leeside of mountains.

Clear Icing—A layer or mass of ice which is relatively transparent because of its homogeneous structure and small number and size of air pockets. Clear icing is associated with freezing rain or drizzle and cumuliform cloud formations.

Cloud Streets—Rows of cumulus or cumulus-type clouds aligned parallel to the low-level flow. Cloud streets can sometimes be seen from the ground, but are best seen on satellite imagery.

Coalescence—Usually used to denote the growth of water drops by collision. The term is also used for the growth of an ice particle by collision with water drops.

Cold-Air Advection—The horizontal transport of colder air into a region by wind. See Warm-Air Advection.

Cold Front—Any non-occluded front, or portion thereof, that moves so that the colder air replaces the warmer air; that is, the leading edge of a relatively cold air mass.

Cold Low—At a given level in the atmosphere, any low that is generally characterized by colder air near its center than around its periphery. A significant case of the cold low is that of a cut-off low, characterized by a completely isolated pool of cold air.

Cold Pool—A region of relatively cold air, represented on a weather map analysis as a relative minimum in temperature surrounded by closed isotherms. Cold pools aloft represent regions of relatively low stability, while surface-based cold pools are regions of relatively stable air.

Comma Echo—A thunderstorm radar echo which has a comma-like shape. It often appears during latter stages in the life cycle of a bow echo.

Conditional Instability—Stable unsaturated air that results in instability in the event or on the condition that the air becomes saturated.

Condensation—The process in which a vapor is turned into a liquid, such as water vapor into water droplets. Condensation is the opposite of evaporation.

Confluence—A pattern of airflow in which wind direction converges along an axis oriented parallel to the flow. The opposite of diffluence. Confluence can be, but is not necessarily, mass convergence.

Convection—The mass motion within a fluid, resulting in the transport and mixing of the properties of that fluid. This could be the transport of heat and/or moisture. It is often used to imply only upward vertical motion; in this sense, it is the opposite of subsidence.

Convective Temperature—The ground temperature required for surface-based convection to develop. However, thunderstorms may develop well before or well after the convective temperature is reached (or may not develop at all) due to conditions other than heating. Convective temperature can be a useful parameter for forecasting the onset of convection.

Convergence—A contraction of a vector wind field; the opposite of divergence. Convergence in a horizontal wind field indicates that more air is entering a given area than is leaving at that level. To compensate for the resulting excess, vertical motion may result—upward forcing if convergence is at low levels or downward forcing (subsidence) if convergence is at high levels.

Convergent Asymptote—Any horizontal line along which horizontal convergence of the airflow is occurring. See Divergent Asymptote.

Coriolis Force—An apparent force due to the spinning earth that deflects an air parcel to the right of its motion in the Northern Hemisphere. The force deflects parcels to the left in the Southern Hemisphere.

Density Altitude—Density altitude is the pressure altitude corrected for temperature deviations from the standard atmosphere.

Derecho—A widespread, convectively-induced straight-line windstorm, usually consisting of a line of intense, fast-moving thunderstorms moving across a great distance. They are characterized by damaging straight-line winds over hundreds of miles.

Dew Point—The temperature to which air must be cooled to reach saturation (at constant pressure and water vapor content). Also called dew point temperature.

Diffluence—A pattern of air flow where wind direction spreads apart (or "fans out") along an axis oriented parallel to the flow – the opposite of confluence. Diffluence is not the same as divergence. In diffluent flow, winds normally decelerate as they move through the region of diffluence, resulting in speed convergence which offsets the apparent divergence of the diffluent flow.

Divergence—The expansion or spreading out of a vector wind field resulting in a net outflow of air from a particular region; usually said of horizontal winds. It is the opposite of convergence.

Divergence at upper levels of the atmosphere enhances upward motion, and hence the potential for thunderstorm development.

Divergent Asymptote—Any horizontal line along which horizontal divergence of the airflow is occurring.

Downburst—A strong, localized downdraft resulting in an outward burst of cool air creating damaging winds at or near the surface. Sometimes the damage resembles tornadic damage. Usually associated with thunderstorms, downbursts can occur with showers too weak to produce thunder. See Microburst.

Downdraft—A sudden descent of cool or cold column of air towards the ground, usually with precipitation, and associated with a thunderstorm or shower. See Updraft.

Drainage Wind—A wind directed down the slope of an incline caused by density differences.

Dry Line—The boundary between a dry air mass (e.g., from the desert southwest) and a moist air mass (e.g., from the Gulf of Mexico). The passage of a dry line results in a sharp decrease in humidity, clearing skies, and a wind shift from southeasterly or south to southwesterly or west. It usually lies north-south across the central and southern Plains states during spring and summer, and its presence influences severe weather development in the Great Plains.

Dry Microburst—A microburst with little or no precipitation reaching the ground; most common in semiarid regions. Dry microbursts may develop in an otherwise fair-weather pattern; visible signs may include a cumulus cloud or small cumulonimbus with a high base and high-level virga, or an orphan anvil from a dying rain shower. At the ground, the only visible sign might be a dust plume or a ring of blowing dust beneath a local area of virga. See Wet Microburst.

Dry Slot—An intrusion of dryer air into a region of moist air. Usually seen in the formation of comma clouds.

D-Value—The difference between the true altitude and the standard altitude of a pressure surface.

Empirical—Relying upon or gained from experiment or observation.

Equivalent Potential Temperature—The potential temperature a parcel of air would have if all its moisture were condensed out and the resultant latent heat was used to warm the parcel (condensation is a warming process).

Evaporation—The process in which a liquid is turned into a gas, such as liquid water turning into water vapor. Evaporation is the opposite of condensation.

Extrapolation—The technique of forecasting the position of a weather feature based solely upon recent past motion of that feature.

Fall Wind—Similar to a drainage wind, but with cold air on a much larger (and stronger) scale.

Fetch—The distance upstream of a measurement site or region of meteorological interest that is relatively uniform.

Flanking Line—A line of cumulus or towering cumulus clouds connected to and extending outward from the most active part of a supercell, normally on the southwest side. The line normally has a stair-step appearance, with the tallest clouds closest to the main storm, and generally coincides with the pseudo-cold front.

Flash Flood—A flood that rises and falls rapidly with little or no advance warning, usually because of intense rainfall over a relatively small area.

Foehn Wind—See Chinook Wind.

Fog—A hydrometeor consisting of visible water droplets suspended in the atmosphere near the earth's surface that restricts visibility below 1000 meters (0.62 miles). Fog can also be considered a cloud on the earth's surface.

Fog Index—An index derived from a formula that uses surface and 850 mb parameters to determine stability. The lower the index, the greater the likelihood of fog. Also called the fog stability index.

Forward-Flank Downdraft—The main region of downdraft in the forward, or leading, part of a supercell, where most of the heavy precipitation is. See Rear-Flank Downdraft.

Gale—In the Beaufort Wind Scale, a wind with speeds from 28 to 47 knots (32 to 54 miles per hour).

Geostrophic Wind—A wind that results from the balance of the Pressure Gradient Force and Coriolis Force; it's directed parallel to isobars with lower pressure to the left in the Northern Hemisphere (lower pressure to the right in the Southern Hemisphere).

Gradient Wind—The wind that results from the balance of the sum of the Coriolis Force, Pressure Gradient Force and Centripetal Force.

Gust Front—The leading edge of gusty surface winds from thunderstorm downdrafts; sometimes associated with a shelf cloud or roll cloud. See also Downburst, Outflow Boundary.

Haze—A lithometeor consisting of fine dust, salt, or pollutant particles dispersed through a portion of the atmosphere. The particles are so small they are not felt or individually seen with the naked eye.

Heat Index—An index that combines temperature and relative humidity to determine an apparent temperature. Heat index thresholds are used to indicate the effects of heat and humidity on the human body.

Helicity—A property of a moving fluid which represents the potential for helical flow (flow which follows a corkscrew pattern) to evolve. Helicity is proportional to the strength of the flow, the amount of vertical wind shear, and the amount of turning in the flow (vorticity). Atmospheric helicity is computed from the vertical wind profile in the lower part of the atmosphere (usually from the surface up to 3 km), and is measured relative to storm motion.

High Precipitation Supercell—A supercell thunderstorm in which heavy precipitation (often including hail) falls on the trailing side of the mesocyclone. Precipitation often totally envelops the region of rotation, making visual identification of any embedded tornadoes difficult and very dangerous. Unlike classic supercells, the region of rotation in these storms develops in the front-flank region of the storm. High precipitation supercells often produce extreme and prolonged downburst events, serious flash flooding, and very large damaging hail events.

Hodograph—A polar coordinate plot of wind vectors representing the vertical distribution of horizontal winds. Hodograph interpretation can help in forecasting the potential evolution of thunderstorms (squall line vs. supercells, splitting vs. non-splitting storms, tornadic vs. non-tornadic storms, etc.). Also, a method of analyzing a wind sounding. The individual wind vectors at selected levels are plotted head-to-tail on a polar coordinate diagram.

Hook (or Hook Echo)—A radar reflectivity pattern characterized by a hook-shaped extension of a thunderstorm echo, usually in the right-rear part of the storm (relative to its direction of motion). A hook often is associated with a mesocyclone, and indicates favorable conditions for tornado development.

Hydrometeors—Any substance produced by the condensation or deposition of water vapor in the air.

Insolation—The intensity at a specified time, or the amount in a specified period, of direct solar radiation incident on a unit of horizontal surface on or above the earth's surface.

Inflow Notch—A radar signature characterized by an indentation in the reflectivity pattern on the inflow side of the storm. The indentation often is V-shaped, but this term should not be confused with V-notch. Supercell thunderstorms often exhibit inflow notches, usually in the right quadrant of a classic supercell, but sometimes in the eastern part of an high precipitation supercell storm or in the rear part of a storm (rear inflow notch).

Instability—The state of equilibrium in which a parcel of air when displaced has a tendency to move further away from its original position (e.g., the tendency to accelerate upward after being lifted). It is a prerequisite condition of the atmosphere for spontaneous convection and severe weather to occur. For example, air parcels, when displaced upward, often accelerate forming cumulus clouds and possibly thunderstorms.

Inversion—A departure from the usual increase or decrease of an atmospheric property with altitude. It usually refers to an increase in temperature with increasing altitude, which is a departure from the usual decrease of temperature with height in the tropopause.

Isallobar—The line of equal change in atmospheric pressure during a certain time period. It marks the change in pressure tendency.

Isallotherm—A line of equal temperature change.

Isobar—A line connecting points of equal pressure.

Isochrone—A line drawn on a map in such a way as to join places at which a phenomenon is observed at the same time, i.e. lines indicating the places at which rain commences at a specified time.

Isodrosotherm—The line connecting points of equal dew point.

Isogon—Line connecting points of equal wind direction.

Isopleth—General term for a line connecting points of equal value of some quantity. Isobars and isotherms are examples of isopleths.

Isotach—A line connecting points of equal wind speed.

Isotherm—A line of equal temperature.

Jet Stream—An area of strong winds concentrated in a relatively narrow band in the middle latitudes and subtropical regions of the Northern and Southern Hemispheres. The most well-known is the polar jet stream flowing in a semi-continuous band around the globe from west to east, it is caused by the temperature gradient where cold polar air moving towards the equator meets warmer equatorial air moving poleward. It is marked by a strong temperature gradient and strong vertical wind shear. Various types of jet streams include arctic, low level, polar, and subtropical jets.

Kelvin-Helmholtz Instability—Instability arising from a strong vertical shear of wind through a narrow atmospheric layer across which there is a sharp gradient of temperature and density; e.g., at an inversion. A wave-like perturbation may be set up which gains energy at the expense of the large- scale flow.

Land Breeze—A breeze that blows from land to sea at night. Part of the land/sea breeze couplet.

Lapse Rate—The rate of change of temperature with height.

Lithometeor—The general term for dry atmospheric suspensoids, including dust, haze, smoke, and sand.

Line Echo Wave Pattern (LEWP)—A special configuration in a line of convective storms that indicates the presence of a low-pressure area and the possibility of damaging winds and tornadoes. In response to very strong outflow winds behind it, a portion of the line may bulge outward forming a bow echo.

Loess—Yellowish-brown, loamy soil deposited by wind.

Low-Level Jet—Strong winds that are concentrated in relatively narrow bands in the lower part of the atmosphere. It is often amplified at night. The strong southerly wind over the United States Plains states during spring and summer is a notable example. See Jet Stream.

Low-Precipitation Supercell—A supercell thunderstorm characterized by a relative lack of precipitation. Visually similar to a classic supercell, except without the heavy precipitation core. These storms often exhibit a striking appearance; the main tower often is bell-shaped, with a corkscrew appearance suggesting rotation. They are capable of producing tornadoes and very large hail. Radar identification often is difficult relative to other types of supercells, so visual reports are very important. They usually occur on or near the dry line, and thus are sometimes referred to as dry line storms.

Macroscale—The meteorological scale covering an area ranging from the size of a continent to the entire globe. Systems have a horizontal size greater than 1500 NM and duration from several days to over a week; e.g., long waves and semi-permanent pressure systems.

Maritime Air Mass—An air mass influenced by the sea. It is a secondary characteristic of an air mass classification, signified by the small "m" before the primary characteristic, which is based on source region. For example, mP is an air mass that is maritime polar in nature. Also known as a "marine air mass."

Mesoscale—Systems vary in size horizontally from 1 to 500 NM and duration from tens of minutes to several hours. This includes mesoscale convective complexes, mesoscale convective storms, and squall lines. Smaller phenomena are classified as microscale, while larger are classified as synoptic- scale.

Mesocyclone—A storm-scale region of rotation, typically 2 to 6 miles in diameter and often found in the right rear flank of a supercell (or often on the eastern, or front, flank of an HP supercell). The region of a mesocyclone is a known area for tornadogenesis. Mesocyclone, used as a radar term, is defined as a rotation signature on Doppler radar that meets specific criteria for magnitude, vertical depth, and duration.

Mesoscale Convective Complex (MCC)—A large, round or oval-shaped, mesoscale convective system (MCS), which is approximately 100,000 km2 in size and lasts at least 6 hours. Generally forms during the afternoon and evening, during which the threat of severe weather is the greatest. It normally reaches its peak intensity at night, when heavy rainfall and flooding become the primary threats. However, severe weather may occur anytime during its life cycle.

Mesoscale Convective System (MCS)—A large, organized convective weather system comprised of a number of individual thunderstorms. It normally persists for several hours and may be rounded or linear in shape. This term is often used to describe a cluster of thunderstorms that does not meet the criteria for a mesoscale convective complex (MCC).

Metamorphism—A pronounced change in internal structure due to pressure, heat, and water that results in a more compact and more highly crystalline condition, e.g., snow pack changing to ice.

Microburst—A severe localized wind from a collapsing thunderstorm. It covers an area less than 2.5 miles (4 km) in diameter and is of short duration, usually less than 5 minutes. See Downburst.

Microburst-Day Potential Index (MDPI)—Method of forecasting wet microburst potential that uses the difference in equivalent potential temperature between the surface and mid-levels; MDPI greater than 1 means that wet microbursts are likely.

Microscale—Systems having a horizontal size less than 1 NM and duration from a few seconds to a few minutes. These comprise the smallest weather systems.

Middle Latitudes—The latitude belt roughly between 35° and 65° North and South. Also referred to as the temperate region.

Mie Scattering—Scattering of energy predominantly in a forward direction from particles in the air.

Mixed Icing—A combination of clear and rime icing.

Mountain Breeze—A breeze that descends a mountain slope during the night. It is caused by surface cooling of an incline.

Mountain Waves—Atmospheric waves formed on the leeside (lee waves) of a mountain barrier, characterized by strong turbulence.

Nephanalysis—The analysis of a synoptic product in terms of the types and amount of clouds and/or precipitation.

Orographic—Related to, or caused by, physical geography such as mountains or sloping terrain.

Outflow Boundary—A storm-scale or mesoscale boundary separating thunderstorm-cooled air (outflow) from the surrounding air; similar in effect to a cold front, with passage marked by a wind shift and usually a drop in temperature. Outflow boundaries may persist for 24 hours or more after the thunderstorms that generated them dissipate, and may travel hundreds of miles from their area of origin. New thunderstorms often develop along outflow boundaries, especially near the point of intersection with another boundary (cold front, dry line, another outflow boundary, etc.).

Overrunning—Refers to an air mass moving over a denser surface air mass, such as warm air moving over a cold air mass in a warm front. Weather generally associated with this event includes cloudiness, cool temperatures, and steady rain.

Persistence—The tendency for a phenomenon to occur in the future, given it occurred in the immediate past. For example, if it rained the past two hours, persistence says it will rain during the next hour.

Potential Temperature—The temperature a parcel of air would have if it were moved dry adiabatically (i.e., with no heat transfer between the parcel and the environment) to the surface or to a reference pressure (often 1,000 mb).

Pressure Altitude—The height of a given level in the standard atmosphere above the level corresponding to a pressure of 1013.2 mb / 29.92 inches of Hg.

Pressure Gradient Force (PGF)—The primary force responsible for winds. It arises from spatial atmospheric pressure differences and acts in the direction from high to low pressure.

Pseudo-Cold Front—A boundary between a supercell's inflow region and the rear-flank downdraft. It extends outward from the mesocyclone center, usually toward the south or southwest (but occasionally bows outward to the east or southeast in the case of an occluded mesocyclone), and is characterized by advancing of the downdraft air toward the inflow region. It is a particular form of gust front.

Pulse Storm—A thunderstorm within which a brief period (pulse) of strong updraft occurs, during and immediately after which the storm produces a short episode of severe weather. These storms generally are not tornado producers, but often produce large hail and/or damaging winds.

Q-Vector—A measure of atmospheric motion that combines temperature advection and divergence due to changes in vorticity advection with height.

Rain—**Free Base**–A dark, horizontal cloud base with no visible precipitation beneath it. It typically marks the location of the thunderstorm updraft. Tornadoes may develop from wall clouds attached to the rain-free base, or from the rain-free base itself—especially when the rain-free base is on the south or southwest side of the main precipitation area.

Rear-Flank Downdraft (RFD)—Regions of dry air subsiding on the backside of, and wrapping around, a mesocyclone. It often is visible as a clear slot wrapping around the wall cloud. Scattered large precipitation particles (rain and hail) at the interface between the clear slot and wall cloud may show up on radar as a hook or pendant; thus the presence of a hook or pendant may indicate the presence of an RFD.

Relative Humidity—An indicator of moisture in the air, expressed as a percentage. It is the ratio of the actual mixing ratio to the saturation mixing ratio of the air.

Rime Icing—Deposit of white, rough ice crystals which form when supercooled water droplets of fog come into contact with a solid object (e.g., aircraft) at a temperature below 0° C.

Shear—The change in wind speed (speed shear) and/or direction (directional shear) over a short distance. It can occur vertically, such as a change with height (vertical wind shear), or horizontally. The term also is used in Doppler radar to describe changes in radial velocity over short horizontal distances.

Squall—A sudden onset of strong winds with speeds of 16 knots or higher, sustained for at least two minutes. The intensity and duration is longer than that of a gust.

Squall Line—A line of active, deep, moist convection frequently associated with thunder, either continuous or with breaks, including contiguous precipitation areas. A squall line is a type of Mesoscale Convective System, distinguished from other types by a larger length-to-width ratio (squall lines are long and narrow).

Stable/Stability—Occurs when a rising air parcel becomes denser than the surrounding air. It then returns to its original position. When the density of the air parcel remains the same as the surrounding air after being lifted, it is also considered stable, since it does not have the tendency to rise or sink further. Contrast with unstable air and instability.

Standard Atmosphere—The internationally-agreed upon vertical distribution of temperature, pressure, and density taken as representative of the atmosphere.

Storm Scale—Refers to weather systems with sizes on the order of individual thunderstorms. See Synoptic Scale, Mesoscale.

Straight-Line Winds—Any wind that is not associated with rotation - used mainly to differentiate from tornadic winds.

Streamline—A line whose tangent at any point in the flow is parallel to the horizontal velocity vector at a particular level at a particular instant in time.

Subsidence—A sinking or downward motion of air, often seen in anticyclones and most prevalent with cold, dense air aloft. It's often used to imply the opposite of atmospheric convection.

Supercell—A severe thunderstorm characterized by a rotating, long-lived, intense updraft. They produce severe weather including large hail, damaging straight-line winds, and tornadoes.

Suspensoid—A system composed of one substance dispersed throughout another substance, such as dust dispersed through the atmosphere.

Synoptic Scale (or Large Scale)—Size scale referring to weather systems with horizontal dimensions of several hundred miles or more. Most high and low pressure areas seen on weather maps are synoptic-scale systems. Systems vary in size horizontally from 500 NM to 1000 NM and duration from tens of hours to several days, e.g., migratory cyclones and frontal systems.

Thermal Ribbon—A band of closely-spaced isotherms.

Trajectory—The path in the atmosphere tracing the points successively occupied by an air parcel in motion.

Tropopause—The upper boundary of the troposphere, between the troposphere and the stratosphere, usually characterized by an abrupt change in lapse rate from positive (decreasing temperature with height) to neutral or negative (temperature constant or increasing with height).

Unstable/Instability—Occurs when a rising air parcel becomes less dense than the surrounding air. Since its temperature does not cool as rapidly as the surrounding environment, it continues to rise on its own.

Updraft—A small-scale current of rising air. If the air is sufficiently moist, then the moisture condenses to become a cumulus cloud or an individual tower of a towering cumulus or cumulonimbus. See Downdraft.

Valley Breeze—A wind that ascends a mountain slope during the day.

Virtual Temperature—In a given air mass, the temperature of dry air having the same density and pressure as the given air mass.

Visibility—The greatest distance in a given direction at which it is just possible to see and identify with the unaided eye: (1) in the daytime, a prominent dark object against the sky at the horizon, (2) at night, a preferably unfocused, moderately intense light source.

V-notch—A radar reflectivity signature seen as a V-shaped notch in the downwind part of a thunderstorm echo. The V-notch often is seen on supercells, and is thought to be a sign of diverging flow around the main storm updraft (and hence a very strong updraft). This term should not be confused with inflow notch or with enhanced V, although the latter is believed to form by a similar process.

Vorticity—A measure of the local rotation in a fluid flow. It usually refers to the vertical component of rotation (rotation about a vertical axis) and is used most often in reference to synoptic scale or mesoscale weather systems. By convention, positive values indicate cyclonic rotation.

Wall Cloud—A localized, persistent, often abrupt lowering from a rain-free cloud base. Wall clouds can range from a fraction of a mile to nearly 5 miles in diameter, and normally are found on the south or southwest (inflow) side of a thunderstorm. When seen from within several miles, many wall clouds exhibit rapid upward motion and cyclonic rotation. However, not all wall clouds rotate. Rotating wall clouds usually develop before strong or violent tornadoes, by anywhere from a few minutes up to nearly an hour. Wall clouds should be monitored visually for signs of persistent, sustained rotation, and/or rapid vertical motion.

Warm-Air Advection—The horizontal transport of warmer air into a region by wind. See Cold-Air Advection.

Warm Cloud-Top Rain—Rain that falls from clouds whose tops do not reach the freezing level. The coalescence process initiates such rain.

Weak Echo Region (WER)—Radar term for a region of relatively weak reflectivity at low levels on the inflow side of a thunderstorm echo, topped by stronger reflectivity in the form of an echo overhang directly above it. The WER is a sign of a strong updraft on the inflow side of a storm, within which precipitation is held aloft. When the area of low reflectivity extends upward into, and is surrounded by, the higher reflectivity aloft, it becomes a BWER.

Wet Microburst—A microburst accompanied by heavy precipitation at the surface. A "rain foot" may be a visible sign of a wet microburst. See Dry Microburst.

Wet Microburst Severity Index (WMSI)—Method of forecasting wet microburst potential that uses updraft strength (CAPE) and the difference in equivalent potential temperature between the surface and mid-levels.

Whiteout—An atmospheric optical phenomenon of the Polar Regions in which the observer appears to be engulfed in a uniformly white glow. Shadows, horizon, or clouds are indiscernible; sense of depth and orientation is lost; only very dark, nearby objects can be seen.